Informe Final

del Proyecto Interno HC-1304.1

Subcoordinación de Hidráulica Ambiental

Serge Tamari

Ariosto Aguilar Chávez

Víctor G. Mejía Astudillo

Diciembre de 2013

Tamari S., Aguilar Chávez A., Mejía Astudillo V. 2013. *Informe final del proyecto interno HC-1304.1.* Jiutepec (Mor.): Instituto Mexicano de Tecnología del Agua.

Índice

Resumen ejecutivo

1 Antecedentes

La problemática considerada en el Proyecto Interno HC-1304.1 se relaciona con la hidrometría; en este contexto, se trata de conocer mejor técnicas para estimar el gasto en grandes obras hidráulicas (tuberías a presión o canales abiertos). Más específicamente, se tuvo un especial interés en conocer mejor las dos siguientes técnicas de medición:

- *Método de Gibson* - Desde los 1980s, investigadores de varios países están evaluando el "método de Gibson", que se considera como un método primario [IEC 60041: 1991] para determinar el caudal en las tuberías a presión de las centrales hidroeléctricas. En este contexto, se ha realizado recientemente una evaluación de laboratorio en el IMTA [Tesis de Maestría de R. Briseno, 2011]. Los resultados obtenidos fueron bastante satisfactorios, en el caso de una tubería de diámetro pequeño (4 pulg.). Ahora, sería importante tratar de generalizar estos resultados a tuberías de mayor diámetro.

- *Método de la velocidad superficial con radar* - Desde hace 15 anos, se tiene un especial interés un utilizar radares de efecto Doppler para medir la velocidad superficial del agua en canales y ríos, y con esta información tratar de estimar el caudal. En este contexto, se han hecho en 2009 pruebas preliminares con un radar microonda en dos canales: el "canal largo" del IMTA y el canal principal "Las Estacas". Considerando los buenos resultados obtenidos, sería interesante seguir probando el radar en varios tipos de canales y ríos, sobre todo donde la velocidad del agua es muy alta (mayor a 3 m/s).

2 Objetivos del proyecto

Por lo anterior, los objetivos del Proyecto Interno HC-1304.1 fueron:

- *Evaluar el "método de Gibson" para las tuberías a presión de las centrales hidroeléctricas* - Al respecto, se considero que el uso de "experimentos numéricos" (es decir, la simulación de transitorios de presión en tuberías mediante CFD y un enfoque de Monte Carlo) era el enfoque más adecuado para tratar de alcanzar este objetivo.

- *Evaluar el "método de la velocidad superficial (con radar)" para los canales y ríos* - Al respecto, se considero que la realización de experimentos tanto en condiciones de laboratorio como en condiciones de campo era importante para tratar de alcanzar este objetivo.

3 Actividades realizadas

Las actividades realizadas en el marco del Proyecto Interno HC-1304.1 se pueden agrupar de la siguiente manera:

- *Evaluación del "método de Gibson"* - Tal como se había planeado, se desarrolló un conjunto de programas de computo para poder realizar experimentos numéricos y se utilizó dicho conjunto de programas para realizar un gran número de simulaciones. [ver **Anexo C.1**]

- *Evaluación del "método de la velocidad superficial con radar"* - Tal como se había planeado, se hicieron varias pruebas en condiciones de campo (perfiles de velocidad superficial en 10 canales) y de laboratorio (tratando de reproducir los principales factores que afectan la rugosidad del agua: turbulencia, viento y lluvia).

- *Otras actividades* - También se hicieron pruebas de laboratorio con un prototipo de picnómetro de gas (Helio), que es un aparato para determinar el volumen (y entonces la densidad) de materiales granulares; al respecto, se tuvo un especial interés en la caracterización de materiales con aplicaciones para la Ingeniería de Riego (muestras de suelo, rocas porosas) o el Tratamiento del agua (cárbono activado, madera). [ver **Anexo C.2**]

4 Resultados obtenidos

Los principales resultados obtenidos durante el desarrollo del Proyecto Interno HC-1304.1 fueron los siguientes:

- *Publicaciones formales* - Todavía se necesita analizar cuidadosamente una gran parte de los resultados obtenidos durante el desarrollo del Proyecto (sobre todo, los resultados sobre el método de Gibson), antes de saber si se podrán publicar formalmente. Sin embargo, se hicieron tres publicaciones formales en el marco del Proyecto Interno HC-1304.1; todas se relacionan con la evaluación del "método de la velocidad superficial con radar":

  - Un *artículo* en revista a comité de lectura. [ver **Anexo A.1**]

  - Un *libro* con ISBN que será editado por el IMTA. [ver **Anexo A.2**]

  - Un *cartel* que se presentó en un congreso internacional. [ver **Anexo A.3**]

- *Otros productos* - Finalmente, se adaptaron dos códigos fuente (para "Matlab vers. 2012") y se entregaron al área jurídica del IMTA para una cesasión de derechos:

  - Un *software* para determinar las fugas en edificios con tinaco. [ver **Anexo B.1**]

  - Un *software* para optimizar el diseño de un picnómetro de gas. [ver **Anexo B.2**]

Anexo A.1

Artículo aceptado
en una revista con comité de lectura

LA HOUILLE BLANCHE
Revue internationale de l'eau

Serge Tamari
IMTA (*Insituto Mexicano de Tecnología del Agua*)
Paseo Cuauhnáhuac 8532
Col. Progreso
Jiutepec, Mor. 62550 (Mexico)

Paris, le 26 novembre 2013

Objet : publication dans la Houille Blanche, revue internationale de l'eau

Monsieur,

Nous avons bien reçu votre projet d'article intitulé « HM-53- **Testing a handheld radar to measure the water velocity at the surface of open channels**»

,
par

S. Tamari (1), **F. García** (2), **J.I. Arciniega-Ambrocio** (3), **A. Porter** (4)

(1) IMTA, Paseo Cuauhnáhuac 8532, Jiutepec Mor. 62550, Mexico. (tamari@tlaloc.imta.mx)
(2) ENGEES, 1 quai Koch, 67070 Strasbourg, France.
(3) ITCh, Av. José Francisco Ruíz Massieu 5, Chilpancingo Gro. 39090, Mexico.
(4) MECOPAA, Miguel Lerdo de Tejada 118, Col. Guadalupe Inn, México DF 01020, Mexico.

Après examen par notre Comité de lecture et deux relecteurs, nous avons le plaisir de vous informer que votre article a été accepté pour publication dans notre revue.
Il sera publié dans le numéro 1 ou 2/2014.

Nous vous remercions pour votre proposition, et, nous vous prions d'agréer, Monsieur, nos sincères salutations.

Brigitte BITON

TESTING A HANDHELD RADAR TO MEASURE WATER VELOCITY AT THE SURFACE OF CHANNELS

S. Tamari [(1)], **F. García** [(2)], **J.I. Arciniega-Ambrocio** [(3)], **A. Porter** [(4)]

[(1)] IMTA, Paseo Cuauhnáhuac 8532, Jiutepec Mor. 62550, Mexico. (tamari@tlaloc.imta.mx)
[(2)] ENGEES, 1 quai Koch, 67070 Strasbourg, France.
[(3)] ITCh, Av. José Francisco Ruíz Massieu 5, Chilpancingo Gro. 39090, Mexico.
[(4)] MECOPAA, Miguel Lerdo de Tejada 118, Col. Guadalupe Inn, México DF 01020, Mexico.

Among the non-contact instruments to measure water velocity in open channels, two handheld radars are available on the market since ten years. Due to the lack of information about these instruments, one model was tested in the laboratory and in the field. The radar was able to estimate the velocity of a water surface within [p = 0.95] ± 0.3 m/s at medium velocities (from 0.3 to 3 m/s) and within ± 10 % of the measured value at large velocities (up to at least 6 m/s). Although this is not very accurate, the ease of using handheld radars still makes them attractive to quickly estimate discharge at gauging stations, safely determine water velocity during a flood and investigate how water flows under difficult access conditions. Nevertheless, the tested radar was tending to underestimate the water velocity, above all when it was looking downstream. More studies are necessary to know why.

Key words:

SVR (surface velocity radar), Doppler radar, microwave, water velocity, open channels, gauging.

Evaluation d'un radar portable pour mesurer la vitesse de l'eau à la surface des canaux

Parmi les instruments sans contact pour mesurer la vitesse de l'eau dans les canaux, deux radars portables sont disponibles sur le marché depuis une dizaine d'années. En raison du manque d'information sur ces instruments, l'un d'eux a été testé au laboratoire et sur le terrain. Le radar a permis d'estimer la vitesse à la surface de l'eau avec une incertitude [p = 0.95] de ± 0.3 m/s pour des vitesses moyennes (0.3 à 3 m/s) et ± 10 % de la valeur mesurée pour des vitesses plus élevées (jusqu'à au moins 6 m/s). Bien que ce ne soit pas très précis, la simplicité d'utilisation des radars portables les rend attractifs pour estimer rapidement le debit dans les stations de jaugeage, déterminer sans risque la vitesse de l'eau en cas de crue et savoir comment l'eau s'écoule dans des conditions difficiles d'accès. Néanmoins, le radar testé tendait à sous-estimer la vitesse de l'eau, surtout quand il pointait vers l'aval. Des études complémentaires sont nécessaires afin de savoir pourquoi.

Mots-clefs:

SVR, radar à effet Doppler, micro-ondes, vitesse de l'eau, canaux, jaugeage.

I INTRODUCTION

In Hydraulics, *current meters* are light instruments designed to measure the velocity of a small water volume (< 1 dm^3). They are useful in open channels to determine the discharge or investigate some certain hydrodynamic features. The most common instruments for field applications are [*e.g.* ISO 2007]: mechanical current meters (MCM), electromagnetic velocimeters (EMV) and acoustic Doppler velocimeters (ADV). Acoustic Doppler current profilers (ADCP) mounted on a floating platform can be used as well. When used properly, current meters can accurately determine water velocity: their uncertainty [p = 0.95] is better than ± 0.01 m/s for low velocities (below ≈ 0.5 m/s) and ± 2 % of the measured value for medium velocities (up to ≈ 3 m/s) [*e.g.* Hubbard *et al.* 2001;

ISO 2007]. Nonetheless, they must be inserted into water, which can be time-consuming and dangerous.

There is therefore an interest in developing instruments that can measure water velocity in open channels with no need to submerge them. For field applications, the two main techniques are image velocimetry (LSPIV/STIV) [*e.g.* Le Coz *et al.* 2010] and Doppler radar (considered in this study). Unfortunately, none of these is still operational to determine velocity below the water surface (*i.e.*, at a depth > 0.2 m). In this case, it is worth noting that measuring the water velocity only at the free surface -instead of measuring it at different depths- is still considered a reliable -although less accurate- method to estimate discharge in open channels [*e.g.* ISO 2007; Le Coz *et al.* 2010; Dramais *et al.* 2013].

Among the non-contact instruments to determine velocity in open channels under field conditions, two handheld radars are available on the market since ten years. Although they look attractive for their rather low cost (< 4,500 USD) and ease of use (Fig. 1), little is known about their performances. The goal of this study was therefore to test a handheld radar to determine the velocity at the surface of open channels.

II LITERATURE REVIEW

II.1 What is known about the handheld radars ?

Handheld radars look like a pistol (for this reason, they are often called *radar gun*). They can be defined as *monostatic* (the receiving antenna is near the emitting antenna) and *microwave* (they emit a signal in the microwave range) Doppler radar, designed to be easily transported by a walking person and operated from a steady position. Handheld radars were originally developed to determine the speed of cars. They have also become popular to determine the speed of animals and sporting balls. The idea of using similar instruments to determine water velocity in open channels was patented ten years ago [Smith *et al.* 2003]. There are currently two models of this type (called *surface velocity radar* by their manufacturers). Both look very similar for their shape and specifications; it is worth noting that their *(3 dB) beam width* is large in practice (12°) and that they emit a signal with a *circular polarization*.

Little has been published about the performances of handheld radars in the field of Hydraulics. First, the "SVR" model from Decatur Electronics [2011] has an operating frequency of 24 GHz (*K-band*). Its claimed uncertainty [$p = 0.95$] [(1)] is ± 10 % of the measurement for a range from 0.3 to 9 m/s. A few evaluations of this instrument [Song *et al.* 2006; Fulton & Ostrowski 2008; Zolezzi *et al.* 2011; Dramais *et al.* 2011, 2013] suggest that it can indeed estimate surface velocity within ± 10 % for medium to large velocities (≈ 0.5 - 5 m/s), but does not always operate at low velocities (< 0.5 m/s). Second, the "Stalker Pro II SVR" model from Stalker Radar [2008] has an operating frequency of 35 GHz (*Ka-band*). Its claimed uncertainty [$p = 0.95$] is ± 0.2 m/s for a range from 0.2 to 18 m/s. Compared to the previous radar model, its maximum operating velocity is therefore claimed to be larger (twice) and it is claimed to be more accurate at large velocities (> 2 m/s). Until now, there is no publication about the performances of the "Stalker Pro II SVR" radar; this model will be considered below.

(1) In the following, *any uncertainty that is reported by a manufacturer without specifying its confidence interval is assumed to be a standard uncertainty* [$p = 0.68$]. In this case, we report a twice larger uncertainty, considering a 95 % level of confidence [$p = 0.95$].

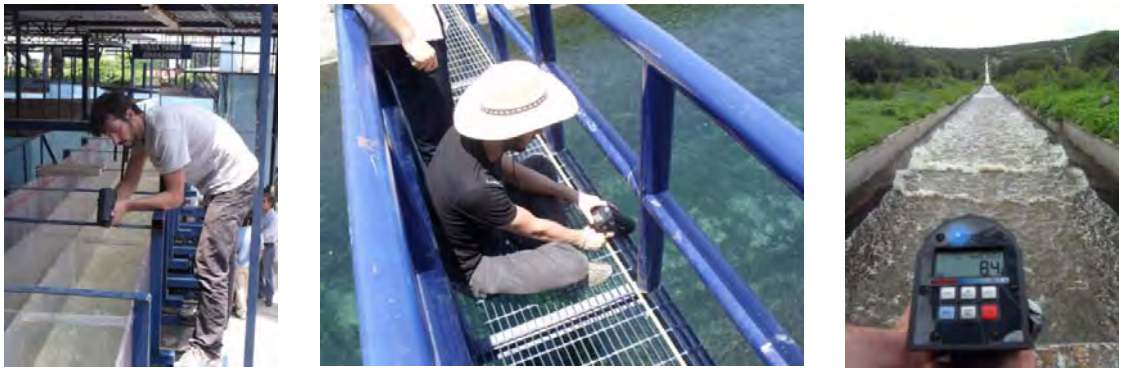

Fig. 1. Different types of sites where the radar was tested: (left) laboratory spillway, (middle) irrigation channel and (right) rapid with rolling waves.

II.2 Principle of operation of a handheld radar

A *radar* is a remote sensing system that sends an electromagnetic signal of a given frequency to a target and then measures some properties of the signal that is sent back (time delay, Doppler shift and/or intensity) in order to determine its distance, speed and/or texture.

As for any other fixed and monostatic Doppler radar, a handheld radar determines the velocity of a target by sending a signal of a given frequency (f_0, Hz) to the target, retrieving the backscattered signal and determining its frequency (f, Hz). The *Doppler effect* is used by the instrument to internally compute the *radial velocity* of the target, that is, the component of its velocity relative to the radar's line-of-sight (V_r, m/s):

$$V_r = -\frac{c_a}{2}\frac{\Delta f}{f_0} \quad (1)$$

where c_a is the speed of light through the air ($\approx 3 \times 10^8$ m/s) and $\Delta f = f_0 - f$ is the *Doppler shift* (negative when the target gets closer and positive when it goes away). So, unless the radar is placed exactly in front of a moving target, a trigonometric correction must be applied to estimate the velocity of the target in its main direction of movement. Consider a radar oriented in such a way (*e.g.* from a bridge) so that it looks in the main direction of a stream. Provided that the radar signal is backscattered (as discussed in Section II.4) and assuming that it is emitted as a narrow beam (as discussed in Tamari *et al.* 2013), the velocity of the water surface (V_s, m/s) can be estimated as:

$$V_s = \frac{V_r}{\sin\theta} \quad (2)$$

where V_r (m/s) is the radial velocity of the water surface and θ (^{o}) is the radar's incidence-angle relative to the water surface. At the scale of several metres, it can be usually assumed that the water surface of open channels is a horizontal plane: this is realistic (with a tolerance of $\pm$ 1 ^{o}) provided that the channel slope is gentle (< 0.017 m/m) and that there is no hydraulic jump. In this case, the angle θ of Eq. 2 is simply the *incidence angle* of the radar (θ_o), *i.e.* the angle between its line-of-sight and the vertical. Commercial handheld Doppler radars have a built-in inclinometer, so that they can automatically determine such an angle and use it to estimate the velocity of a horizontal water surface.

Next, the case of a plane but inclined water surface will be also considered. This situation occurs in steep artificial channels and in the middle part of some spillways. In this case, the angle of Eq. 2 is: $\theta = \theta_o - \beta$ for a radar looking upstream, and $\theta = \theta_o + \beta$ for a radar looking downstream, where β is the slope of the water surface ($0 \leq \beta < 90^o$). In practice, the water surface is often almost parallel

to the channel bottom and edges, which can be easily checked visually. If so, the angle β can be rapidly estimated by measuring the channel's slope with the built-in inclinometer of a handheld radar or any other inclinometer. Nevertheless, it becomes more difficult to determine the angle β when the water surface is curved; such a situation is out of the scope of this study.

II.3 Which incidence angle for the radar ?

To reduce the effect of the trigonometric correction (Eq. 2) as much as possible, a radar should be placed so that it looks at the water surface with a relative incidence angle as large as possible. Nonetheless, when a handheld radar looking at a water surface is oriented with a too large incidence angle, it becomes difficult in practice to know at what it is pointing. During this study, no attempt was made to use the handheld radar with a relative incidence angle larger than 70^o. Assuming that V_r and θ are normally-distributed and independent random variables, a simple model to estimate the uncertainty of V_s can be derived from Eq. 2:

$$U(V_s) = \sqrt{\frac{1}{\sin^2\theta}\,U^2(V_r) + \frac{V_s^2}{\tan^2\theta}\,U^2(\theta)} \quad (3)$$

where $U(\bullet)$ denotes the uncertainty of each variable (at a given confidence level); please note that the term $U(\theta)$ must be expressed in radians. Strictly speaking, the model does not agree with what is claimed by the manufacturers of handheld radars (Section II.1); in fact, it predicts that the uncertainty of the surface velocity ($U(V_s)$) is neither a constant value nor a fixed proportion of the measured value. In the case of the studied radar, assuming that its claimed uncertainty is for the radial velocity: $U(V_r) = 0.2$ m/s [$p = 0.95$] and considering that the claimed uncertainty of its built-in inclinometer is: $U(\theta) = 0.07$ rad (4^o) [$p = 0.95$], the expected uncertainty $U(V_s)$ can be computed using Eq. 3 for different scenarios (different values of V_s and θ). The results suggest that the radar should be oriented with an incidence angle $\theta > 45^o$, otherwise its uncertainty will rapidly increase (for more details, see Tamari *et al.* 2013).

II.4 Detection of a water surface by a microwave radar

To be able to determine the velocity of a water surface, a Doppler radar must first detect it: the signal sent by the instrument must be reflected by the water in such a way that it goes back to the instrument and can be processed. This phenomenon has been studied for 50 years in the laboratory and on the sea. Considering that the handheld radar emits microwaves, the backscattering of its signal by water (at least, for $20 \leq \theta \leq 70^o$) is currently described by the *Bragg / composite surface* theory [*e.g.* Plant and Keller 1990; Plant *et al.* 2004]. On the one hand, the theory considers that the microwaves are mostly backscattered by small water waves (traveling nearly in the plane of incidence, either toward the radar, either away from it), *i.e. ripples* with a wavelength $\Lambda_B \approx 6$ mm in the case of the studied radar (according to the *Bragg resonant condition*). In open channels, these ripples can be produced by external factors (the wind and the rain) and internal factors (the distortion of larger waves and the turbulence of water). On the other hand, the theory considers that the ripples backscattering the radar signal are mostly driven by larger water waves. In open channels, these larger waves (gravity-capillary waves and hydraulic boils) are due to the wind and turbulence of water. On average, they are assumed to move at the velocity of the water surface.

The above theory predicts that the tested radar will not work if there are virtually no ripples on a water surface, as it may occur under low water flow and clear weather conditions [*e.g.* Plant *et al.* 2005] or if there is an oil film on the water [*e.g.* Gade *et al.* 1998]. It also predicts that the raw data recorded by a radar (a time-series of Doppler shifts) are "noisy". The main reason for that is that each water wave (ripples and larger waves) tends to propagate in several directions. So, a radar should detect water waves that sometimes move faster than the average water surface (*advancing waves*) and that sometimes move slower (*receding waves*). Ideally, the histogram of the raw data

recorded by the radar (converted into surface velocities, according to Eqs. 1-2) should have two peaks: one corresponding to ($V_s + c_B$) and the other corresponding to ($V_s - c_B$), where c_B is the *phase speed* of the water waves that backscatter the radar signal. If so, processing the raw radar data simply consists in extracting the midway point between the two peaks. However, it is often difficult to discern this theoretical couple of peaks when working with a microwave radar. In this case, processing the raw radar data is not straightforward anymore. If data are not processed carefully, the estimated surface velocity (V_s) can be erroneous up to about $\pm c_B$ [Plant *et al.* 2005]. For the studied radar, $c_B \approx 0.3$ m/s [Tamari *et al.* 2013]; it is worth noting that the minimum expected uncertainty of the radar (computed from Eq. 3 with $\theta = 45^o$) is close to this value.

II.5 Difficulty in interpreting the velocity measured by a radar

Assuming that the data have been averaged over a sufficiently long period of time, the surface velocity determined by a Doppler radar (V_s) can be decomposed as an algebraic sum of four terms:

$$V_s = V + W + U_s + \upsilon \quad (4)$$

where V is the drift caused by the underlying current (m/s), W is the drift caused by the wind blowing in the direction of the radar's line-of-sight (m/s), U_s is the Stokes drift (m/s) and υ is an eventual bias due to the way a radar "sees" a water surface (m/s). Considering the goal in Hydraulics is to determine the underlying current (V), taking it to be equal to the surface velocity measured by a radar (V_s) may lead to three types of systematic errors:

- *Wind effect (W)* - During this study, the handheld radar was tested under low wind conditions, at most equivalent to a *gentle breeze* on the Beaufort scale. In this case, the wind effect was expected to be rather small ($W < 0.1$ m/s) [Tamari *et al.* 2013].
- *Stokes drift (U_s)* - The Stokes drift is accounted for by a Doppler radar (as well as by small surface drifters), but not by a conventional current meter that would be maintained at a fixed position and just below the water surface. Nevertheless, the Stokes drift was expected to be rather small for the studied channels ($U_s < 0.1$ m/s) [Tamari *et al.* 2013].
- *Bias term due to the radar (υ)* - Due to the specific motion of the water waves that backscatter the radar signal, there may be a systematic difference ($\upsilon \neq 0$) between the surface velocity determined by a Doppler radar and the true surface velocity for a number of reasons; this will be discussed further below (Section IV).

II.6 Experience with microwave radars in open channels

As shown, it is not so simple to use a radar to estimate the velocity of a water surface. In this context, microwave radars with different configurations have been tested over open channels over the last fifteen years. Above all, prototypes [Plant *et al.* 2005; Costa *et al.* 2006; Fulton & Ostrowski 2008] and commercial instruments [Song *et al.* 2006; Dramais *et al.* 2011, 2013; Sung-Kee *et al.* 2012] fixed to a bridge (radars looking in the direction of the main stream) have been tested. Prototypes [Plant *et al.* 2005; Costa *et al.* 2006] and commercial instruments [Sung-Kee *et al.* 2012] located at a channel bank have been also tested. Prototypes moved across a channel using a cableway or a helicopter have been tested as well [Plant *et al.* 2005]. It is worth noting that a radar with an operating frequency of 10 GHz (*X-band*) and a design very similar to that of the commercial handheld radars has been described and tested by Lee & Julien [2006]; nonetheless, it seems to have been forgotten for an unknown reason. All the mentioned field testing suggest that microwave radar can usually determine the surface velocity of open channels with an uncertainty [$p = 0.95$] of $\pm$ 0.2 m/s, which is consistent with that claimed by the manufacturers of handheld radars. Nevertheless, testing have been conducted in rivers but not in artificial channels (where the roughness of the water surface may be different) and only for water velocities ≤ 5 m/s.

III MATERIALS AND METHODS

III.1 Sites where the radar was tested

Based on the literature review, it was decided to test the handheld radar over a series of open channels:

- *Wide range of water velocities* - The radar was tested for the widest range of velocities as possible, *i.e.* from 0.3 to at least 6 m/s. To achieve this range, tests were performed not only over horizontal channels, but also over the plane part of inclined channels (slope as large as 28°). It was not sure whether the radar would work under clear weather conditions at low velocities (< 0.5 m/s), and the comparison with conventional current meters was quite challenging at large velocities (> 3 m/s).
- *Several types of open channels and flow conditions* - Compared to other radars designed to study open channels, the handheld radar can be very easily transported from one site to another, which makes it possible to rapidly test this instrument under several flow conditions. For this study, 18 sites were chosen for testing, with a special interest in artificial channels. The testing was performed in straight portions of narrow (*aspect ratio* ν as low as 1) and wide (ν as large as 40) channels, with different wall roughness (walls made of glass, acrylic, cement, concrete or earth and stones). Both subcritical (*Froude number Fr* as low as 0.2) and supercritical (*Fr* as high as 5) flow conditions were considered.
- *Clear weather conditions* - The radar was tested in the laboratory (13 sites) and in the field (5 sites). In the field, testing was made under low wind (not more than a gentle breeze) and no rain conditions. Although these conditions are convenient for the user and should ensure that the water surface is mostly driven by the underlying current, they are known to be challenging for the radar when water flows slowly. The water surface may indeed be too smooth to produce a significant backscattering of the radar signal [Plant *et al.* 2005].
- *No oil at the water surface* - The radar was tested over channels with clear, turbid and very turbid water, but *not* in channels contaminated by gasoline or detergent, where the presence of an oil film could prevent the radar from detecting the water surface [*e.g.* Gade *et al.* 1998].

III.2 Conditions for using the tested radar

The only parameter for configuring the tested radar was its "power output", which was set at 20 mW (as recommended by the manufacturer for taking data close to a water surface). After that, taking a measurement with the tested radar was easy: once oriented in the main direction of a stream, its built-in inclinometer was used to incline the radar to a desired incidence angle ($\theta_o = 90° - \phi_o$, where ϕ_o is the *grazing angle* that was actually displayed by the radar); the radar was then maintained in the same position and its trigger was pressed. About 30 s later, the radar was usually displaying a symbol saying whether water was moving forward or downward and an average velocity data (V_s^*); because the radar has been designed to be used over horizontal channels, this data is a projection in an horizontal plane of the determined radial-velocity ($V_r = V_s^* \times \sin \theta_o$). During testing, the radar was operated as follows:

- *Radar oriented in the main-stream direction* - The radar was always oriented in the main-stream direction. So, field testing was made from bridges of gauging stations. No attempt was made to use the radar from a channel edge; in this case, there was no need to correct the radar data for the azimuthal angle relative to the channel direction (as done by Lee & Julien 2006) and there was no concern with secondary or cross currents (as discussed by Plant *et al*. 2005).

- *Radar looking upstream / downstream* - Each time, a measurement was taken with the radar looking upstream and another with the radar looking downstream. In the laboratory, special attention was paid to locate the radar so that it was pointing at the same part of a channel. While this was not possible in the field, the studied channels were long and uniform enough to reasonably assume that the transversal velocity-profile was the same along the section where the measurements were taken.

- *Radar located as close as possible to the water surface* - As a first approximation, the tested radar should "see" an area at the water surface *(footprint*), which is an ellipse with a transversal diameter: $D_T \approx 0.2 \times L$, where L (m) is the distance to the surface in the line-of-sight direction [Tamari *et al.* 2013]. It must be recognized that this relation applies only if the distance L is larger than a certain value, which is: $L_f = 0.6$ m for the studied radar (according to the *far field condition*). In the field, the radar was located at $3 \leq L \leq 10$ m, resulting in $0.6 \leq D_T \leq 2$ m. In the laboratory, it was empirically located at $0.1 \leq L \leq 0.3$ m; this is smaller than L_f, resulting in $D_T <$ 0.12 m. Thus, it was felt that the area sampled by the radar was not too large, so that the radar data could be used on channels with a width $b \geq 0.3$ m and so that its data could be compared to the data provided by current meters.

- *Measurements taken rather quickly* - Once a first value for the average velocity was displayed by the radar, the instrument was left to take more data and average them during ≈ 20 - 40 s. This duration was usually sufficient to achieve repeatable data with a tolerance of ± 0.15 m/s.

- *Intermediate incidence angle* - Based on the results of a preliminary testing [Tamari *et al.* 2013], the radar was used with its handle downward and a relative incidence angle (θ) between 45 to 50° for moderately inclined channels (slope $\beta \leq 10°$) and between 50 to 60° for steeper channels.

- *Radar's inclinometer considered as unbiased* - The radar's built-in inclinometer has a claimed uncertainty [$p = 0.95$] of ± 4 °. This was checked in the laboratory against a comparison with an external inclinometer with a tolerance < 1 ° (model "MTi", Xsens Technologies, Enschede, The Netherlands). Although systematic differences were found, their magnitude was always < 2.6 ° (Fig. 2).

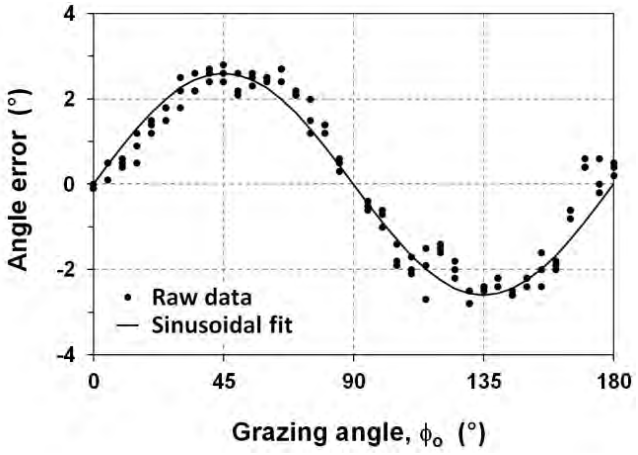

Fig. 2. Laboratory verification of the radar's built-in inclinometer. The error is the difference between the angle displayed by the radar and the actual angle. Please, note that the radar displays the *grazing angle* (ϕ_o), *i.e.* the angle between its line-of-sight and the horizontal.

III.3 Reference techniques for testing the radar

Most of the radar testing was conducted taking an ADV (model "FlowTracker", Sontek/YSI) as the reference at low to medium velocities (< 2.5 m/s) and a Pitot tube (model "630", Lambrecht) as the reference at larger velocities. To estimate the surface velocity in open channels, these meters were located as close as possible to the water surface (sensor top at ≈ 2 cm below the surface), with special care to avoid cavitation around them during the measurements. The ADV was expected to be several times more accurate than the studied radar at low to medium water velocities, whereas the Pitot tube was expected to be much more accurate at large velocities [Tamari *et al.* 2013]. In addition, an MCM (model "Price AA", Rossbach) was taken as the reference for testing the radar in a river and a simple PIV technique was used as the reference in a field channel where water was flowing very rapidly [Tamari *et al.* 2013].

IV RESULTS AND DISCUSSION

IV.1 Global performances of the tested radar

When tested in the laboratory and looking upstream, the handheld radar was found (Fig. 3) to estimate water velocity at the surface of open channels from 0.3 to 6 m/s with an uncertainty slightly better [$p > 0.95$] than what was expected at the beginning of this study (Section II.3); please note that the uncertainty of the reference techniques has been neglected because it was *a priori* several times lower than that of the radar. Roughly, it corresponds to: $U(V_s) \approx 0.3$ m/s at medium velocities (from 0.3 to 3 m/s) and $U(V_s) \approx 0.1 \times V_s$ at large velocities. Such an uncertainty is similar to that previously reported for the other model of handheld radar (Section II.1) and slightly larger than that previously reported for other types of microwave Doppler radars that have been tested in rivers (Section II.6).

When tested in the laboratory and looking downstream, the radar was found to estimate water velocity with an uncertainty still [$p = 0.95$] consistent with what was expected at the beginning. It could be argued that the laboratory results underestimate the usual performances of the radar, because it has been tested very close to the water surface (Section III.2). However, the radar data obtained in the field were consistent with those obtained in the laboratory (Fig. 3).

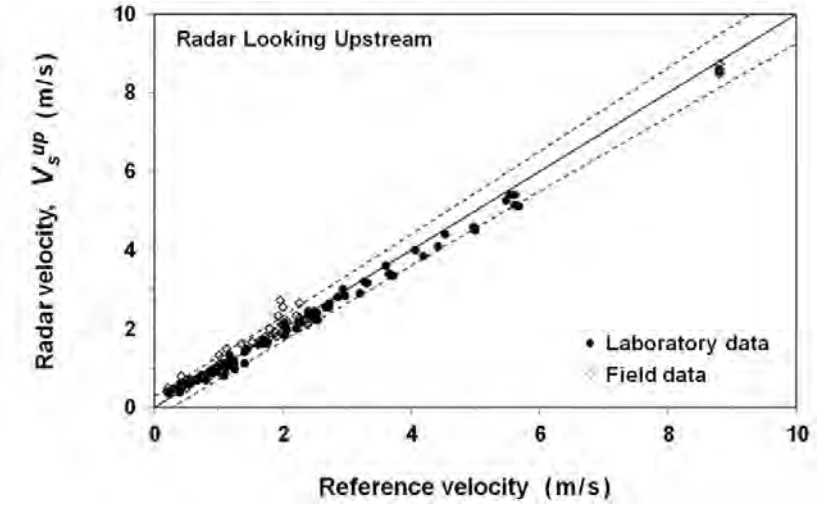

Fig. 3. Velocity measured by the radar looking upstream (V_s^{up}) vs. velocity measured by reference techniques. The dashed lines show the expected radar uncertainty [$p = 0.95$].

IV.2 Underestimation of the reference velocities

Although the performances of the tested radar were consistent with what was expected at the beginning, two biases were found during this study. This will be discussed in this section and in the next one. According to a regression analysis, the radar data were significantly different from the reference data: on the average, the radar data were lower by ≈ 5 % of the value when the radar was looking upstream, and lower by ≈ 8 % of the value when the radar was looking downstream. This trend is still unexplained:

- *A bias of the radar's inclinometer ?* - Contrary to what has been reported for the other commercial model of handheld radar [Dramais *et al.* 2013], the trend cannot be explained by the bias of the radar's inclinometer: in a preliminary attempt to correct for this bias (Fig. 2), no significant improvement of the radar's performances was obtained.
- *A bad choice of the reference techniques ?* - It could be argued that the current meters used as a reference for testing the radar (Section III.3) may have underestimated the velocity at the surface of narrow (*i.e.* aspect ratio < 5) and rectangular channels, due to the *dip phenomenon*. However, the radar was also tested in the central part of wide rectangular channels and of trapezoidal channels, where the dip phenomenon should not occur [Tominaga *et al.* 1989].

IV.3 Radar looking downstream vs. looking upstream

The radar was found to usually estimate a lower velocity when looking downstream (V_s^{down}) instead of upstream (V_s^{up}). Roughly, the velocity difference ($\Delta V_s = V_s^{up} - V_s^{down}$) was increasing as a function of water velocity, when it was larger than ≈ 1 m/s (Fig. 4). No clear trend was found in ΔV_s as a function of other quantitative (Froude number, aspect ratio, channel slope) or qualitative (laboratory or field testing) variables. It is still difficult to know why:

- *A wind effect ?* - The histogram of the raw data recorded by a microwave Doppler radar (converted into surface velocities) is often skewed. Many studies performed in water tanks [*e.g.* Gade *et al.* 1998; Plant *et al.* 2004] and on the sea [*e.g.* Plant and Keller 1990] have shown that this can be due to the wind (even a light air, with a speed as low as ≈ 0.3 m/s), unless it is blowing perpendicularly to the radar's line-of-sight. If a radar is looking upwind, it should record a histogram with a larger peak corresponding to the advancing water waves ($V_s + c_B$). On the opposite, if the radar is looking downwind, it should record a histogram with a larger peak corresponding to the receding waves ($V_s - c_B$). Under those circumstances, if the radar does not process carefully the raw data (*i.e.* if it does not extract the midway point between the two theoretical peaks of the histogram, but computes an average value, or -even worse- takes the mode), the absolute value of ΔV_s could be as large as ≈ $2 \times c_B$, which is ≈ 0.6 m/s for the studied radar (Section II.4). Since most of the observed values of ΔV_s were within ± 0.6 m/s (Fig. 4), they could be due to a wind effect and to an inaccurate data processing.
- *An hydrodynamic effect ?* - If the observed values of ΔV_s were due to the wind, the fact that they were usually positive would mean that the wind was usually blowing from upstream in the studied channels. Although, the wind direction and speed have not been systematically measured during this study, it seems that the observed values of ΔV_s were not always due to the wind: in the field, larger values of ΔV_s were obtained in some specific parts of channels where the water surface was more irregular due to turbulence, even under a light air condition or a light breeze coming from downstream [Tamari *et al.* 2013]. More studies are necessary to know if this is a general feature of microwave Doppler radars when used in open channels under clear weather conditions or an imperfection of the studied radar (unfortunately, its data processing algorithm is a "black box").

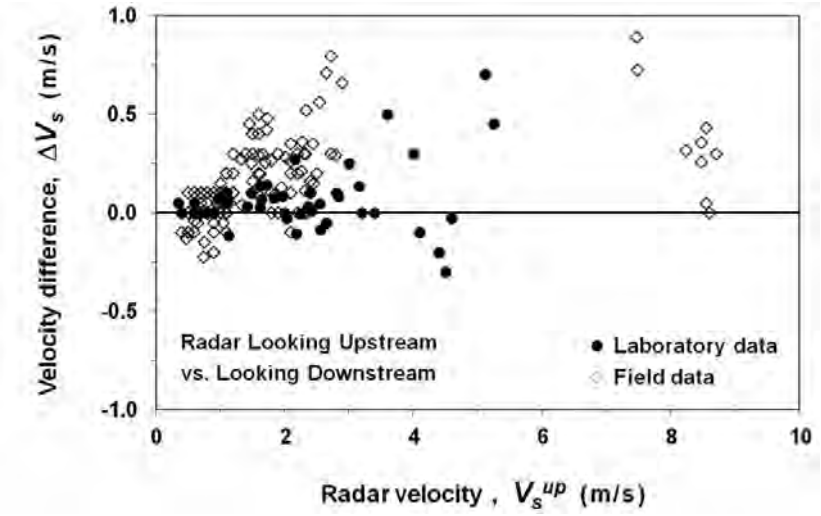

Fig. 4. Difference in velocity between the radar looking upstream and downstream (ΔV_s) as a function of the velocity measured by the radar looking upstream (V_s^{up}).

V CONCLUSION

Over the last fifteen years, a growing number of studies have shown that Doppler radar technology is a promising tool to estimate water velocity at the surface of open channels. In this context, a commercial handheld radar was tested. The testing covered a broad range of velocities (from 0.3 to at least 6 m/s) and channel types (including inclined channels). The radar was able to estimate the water velocity within [p = 0.95] ± 0.3 m/s at medium velocities (from 0.3 to 3 m/s) and ± 10 % of the measured value at large velocities. Although this is not very accurate, the ease of using handheld radars still makes them attractive to quickly estimate discharge at gauging stations and to investigate how water flows under difficult access conditions. Nonetheless, the tested radar was tending to underestimate the water velocity, above all when it was looking downstream. More studies are necessary to know if this is due to a wind effect and an imperfection of the tested radar or if this is a general feature of microwave Doppler radars when used in open channels under clear weather conditions. Meanwhile, it is a good precaution to compare -whenever possible- the velocities obtained with a radar looking upstream and downstream.

VI ACKNOWLEDGMENTS

This paper is a short version of a small book edited by the Mexican Institute of Water Technology (IMTA). Thank you to Bertrand Chapron (IFREMER) and to two anonymous reviewers for their comments about an earlier version of the paper.

VII REFERENCES

Chapron B., Collard F., Ardhuin F. (2005). – Direct measurements of ocean surface velocity from space: Interpretation and validation. *J. Geophysical Res.*, **110**: paper C07008.

Costa J.E., Cheng, R.T., Haeni F.P., Melcher N., Spicer K.R., Hayes E., Plant W., Hayes K., Teague C., Barrick D. (2006). – Use of radars to monitor stream discharge by noncontact methods. *Water Resour. Res.*, **42:** paper W07422.

Decatur Electronics (2011). – *SVR (Surface Velocity Radar) - User's Manual (Rev. 02/08/2011).* Decatur Electronics Europe Inc., Kokkola (Finland). 45 p.

Dramais G., Le Coz J., Gallavardin A., Duby P., Hauet A., Laronne J. (2011). – Mesures sans contact des débits de crue : avancées et perspectives. *In*: Mono M.O. (ed.), *Proc. "ECOTECHS' 2011 (CEMAGREF)"*, Montoldre (France), October 17-18, 2011.

Dramais G., Le Coz J., Le Boursicaud R., Hauet A., Lagouy M. (2013). – Jaugeage para radar mobile: protocole et résultats [paper HM-044]. *In*: Biton B. (ed.), *Proc. "Hydrométrie 2013 (SHF)"*, Paris (France), May 15-16, 2013. [ISBN 978-2-906831-94-0]

Fulton J., Ostrowski J. (2008). – Measuring real-time streamflow using emerging technologies: radar, hydroacoustics, and the probability concept. *J. Hydrol.*, **357 (1-2):** 1-10.

Gade M., Alpers W., Ermakov S.A., Huehnerfuss H., Lange P.A. (1998). – Wind wave tank measurements of bound and freely propagating short gravity-capillary waves. *J. Geophys. Res.*, **103**: 21697-21710.

Hubbard E.F., Schwarz G.E., Thibodeaux K.G., Turcios L.M. (2001). – Price current-meter standard rating development by the U.S. Geological Survey. *J. Hydraul. Eng.*, **127 (4):** 250–257.

ISO (2007). – *Hydrometry - Measurement of liquid flow in open channels using current-meters or floats (ISO 748: 2007).* International Organization for Standardization (ISO), Genève.

Le Coz J., Hauet A., Dramais G., Pierrefeu G. (2010). – Performance of image-based velocimetry (LSPIV) applied to flash-flood discharge measurements in Mediterranean rivers. *J. Hydrol.*, **394 (1-2):** 42-52.

Lee J.S., Julien P.Y. (2006). – Electromagnetic wave surface velocimetry. *J. Hydraul. Eng.*, **132 (2):** 146-153.

Plant W. J., Keller W.C. (1990). – Evidence of Bragg scattering in microwave Doppler spectra of sea return. *J. Geophys. Res.*, **95 (C9):** 16299-16310.

Plant W.J., Dahl P.H., Giovanangeli J.P., Branger H. (2004). – Bound and free surface waves in a large wind-wave tank. *J. Geophys. Res.*, **109 (C10):** paper C10002.

Plant W.J., Keller W.C., Hayes K. (2005). – Measurement of river surface currents with coherent microwave systems. *IEEE Trans. Geosci. and Remote Sensing*, **43:** 1242-1257.

Smith K.J., Janson S.D., Smith K.T. (2003). – *Radar device for measuring water surface velocity.* US Patent 2003/0058158.

Song H.S., Zhang L.Z., Liu W. 2006. Comparing test and analysis on flow velocity measurement with handheld radar current meter. [*Chinese*] *Automation in Water Resources and Hydrology*, **1:** 30-32.

Stalker Radar (2008). – *Stalker Pro II SVR - Operator Manual (document 011-0098-00 Rev. C).* Stalker Radar / Applied Concepts Inc., Plano (TX). 23 p.

Sung-Kee Y., Dong-Su K., Kwon-Kyu Y., Meyong-Su K., Woo-Yul J., Jun-Ho L., Yong-Seok K., Ho-Jun Y. (2012). – Comparison of flood discharge and velocity measurements in a mountain stream using electromagnetic wave and surface image. [*Korean*] *J. Environ. Sci.*, **21 (6):** 739-747. [doi: 10.5322/JES.2012.21.6.739]

Tamari S., Garcia F., Arciniega-Ambrocio J.I., Porter A. (2013). – *Laboratory and field testing of a handheld radar to measure the water velocity at the surface of open channels*. Jiutepec, Mor. (Mexico): IMTA. [ISBN 978-607-7563-80-8]

Tominaga A., Nezu I., Ezaki K., Nakagawa H. (1989) . – Three-dimensional turbulent structure in straight open channel flows. *J. Hydraul. Res.*, **27 (1):** 149-173.

Zolezzi G., Zamler D., Laronne J.B., Salvaro M., Piazza F., Le Coz J., Welber M., Dramais G. (2011). – A systematic test of surface velocity radar (SVR) to improve flood discharge prediction (Poster H51I-1332). *In: "AGU Fall Meeting"*, San Francisco (CA), December 5-9, 2011. [only the abstract is available]

Anexo A.2

Libro con ISBN
que será editado por el IMTA

LABORATORY AND FIELD TESTING OF A HANDHELD RADAR TO MEASURE THE WATER VELOCITY AT THE SURFACE OF OPEN CHANNELS

S. Tamari

F. García

J. I. Arciniega-Ambrocio

A. Porter

LABORATORY AND FIELD TESTING OF A HANDHELD RADAR TO MEASURE THE WATER VELOCITY AT THE SURFACE OF OPEN CHANNELS

S. Tamari

IMTA, Paseo Cuauhnáhuac 8532, Jiutepec Mor. 62550, Mexico (tamari@tlaloc.imta.mx)

F. García

ENGEES, 1 quai Koch, 67070 Strasbourg, France

J. I. Arciniega-Ambrocio

ITCh, Av. José Francisco Ruíz Massieu 5, Chilpancingo Gro. 39090, Mexico

A. Porter

MECOPAA, Miguel Lerdo de Tejada 118, Col. Guadalupe Inn, México DF 01020, Mexico

December 2013

Tamari, Serge

Laboratory and field testing of a handheld radar to measure the water velocity at the surface of open channels / S. Tamari, F. García, J. I. Arciniega-Ambrocio, A. Porter -- Jiutepec, Mor.: Instituto Mexicano de Tecnología del Agua, © 2013. (Colección Avances del Conocimiento)
76 p.

ISBN 978-607-7563-80-8

1. Surface Velocity Radar (SVR) 2. Doppler radar 3. Microwave 4. Water velocity 5. Open channels 6. Gauging

Content

Abstract

Among the non-contact instruments to measure water velocity in open channels, two handheld radars are available on the market since ten years. Due to the lack of information about these instruments, one model was tested in the laboratory and in the field. The radar was able to estimate the velocity of a water surface within [p = 0.95] ± 0.3 m/s at medium velocities (from 0.3 to 3 m/s) and within ± 10 % of the measured value at large velocities (up to at least 6 m/s). Although this is not very accurate, the ease of using handheld radars still makes them attractive to quickly estimate discharge at some gauging stations, safely determine maximum water velocity during a flood and investigate how water flows under difficult access conditions (*e.g.* very shallow channels or the straight part of some spillways).

Even though the tested radar has provided velocity data in the range of what was expected *a priori*, some biases were found. On the one hand, the radar was not working well at too low incidence angles and it was tending to underestimate the reference data, which could be due to the rather large beam width of the handheld radar. On the other hand, the radar was tending to estimate a lower velocity when looking downstream instead of upstream. More studies are necessary to know if this is due to an inaccurate data processing algorithm of the tested instrument or if this is a general feature of microwave Doppler radars when used in open channels under clear weather conditions. Meanwhile, it is a good precaution to compare -whenever possible- the velocities obtained with a radar looking upstream and downstream.

Keywords: Surface Velocity Radar (SVR); Doppler radar; microwave; water velocity; open channels; gauging.

Acknowledgements

The first author acknowledges the financial support of IMTA (Mexican Institute of Water Technology). Any reference to a commercial model and its manufacturer is for identification purposes only, and does not represent an endorsement of the product.

Thank you to colleagues from IMTA (Patricia Navarro, Verónica Vargas, Marco Antonio Mijangos), CONAGUA (Isaac Villaseñor, Juan Chávez, Aurelio Díaz, Agustín Gamboa, Rosalio Sánchez, Gabriel Barrios) and CFE (Federico Ochoa, Elisabeth González) for their help during testing.

Thank you also to Bertrand Chapron (IFREMER) and to two anonymous reviewers for their comments about an earlier version of this document.

1. Introduction

In Hydraulics, *current meters* are light instruments (< 10 kg) designed to measure the velocity of a small water volume (< 1 dm^3). They are useful in open channels (artificial channels and rivers) to determine the discharge or investigate some certain hydrodynamic features. The most common instruments for field applications are [ISO 2007, Rantz & Col. 1982, Turnipseed & Sauer 2010]: mechanical current meters (MCM), electromagnetic velocimeters (EMV) and acoustic Doppler velocimeters (ADV). Acoustic Doppler current profilers (ADCP) mounted on a floating platform can be used as well [*e.g.* Costa *et al.* 2006, Szupiany *et al.* 2007].

When used properly, current meters can accurately determine water velocity: their uncertainty [$p = 0.95$] is better than ± 0.01 m/s for low velocities (below ≈ 0.5 m/s) and ± 2 % of the measured value for medium velocities (up to ≈ 3 m/s) [*e.g.* Hubbard *et al.* 2001, ISO 2007]. Nonetheless, they must be inserted into water, which is not always practical under field conditions, since it can be time-consuming (because the operator must get close to the water surface and then control the immersion depth of the meter), dangerous (especially in case of fast flow, floating debris or crocodiles), unhealthy (when a meter has to be immersed into waste water) and costly (a meter repeatedly immersed into water can get damaged due to corrosion, incrustation, clogging or fouling).

There is therefore an interest in developing instruments that can measure water velocity in open channels with no need to submerge them. Such an interest is not new: forty years ago, an optical current meter (OCM) was developed to measure velocity at the surface of open channels [Rantz & Col. 1982], but this stroboscopic device with a telescope is no longer popular. Now, other non-contact techniques for open channels are emerging. For field applications, the two main techniques are image velocimetry (LSPIV/STIV) [*e.g.* Fujita *et al.* 2007, Le Coz *et al.* 2010] and Doppler radar (considered in this study). Unfortunately, none of these is still operational to determine velocity below the water surface (*i.e.* at a depth > 0.2 m). In this case, it is worth noting that measuring the water velocity only at the free surface -instead of measuring it at different depths- is still considered a reliable -although less accurate- method to estimate discharge in open channels [Rantz *& Col.* 1982, ISO 2007]; several researchers are currently testing [*e.g.* Costa *et al.* 2006, Lee & Julien 2006, Dramais *et al.* 2013] and trying to improve [*e.g.* Le Coz *et al.* 2010, Negrel *et al.* 2011] this method.

Among the non-contact instruments to determine velocity in open channels under field conditions, two handheld radars are available on the market since ten years. Although they look attractive for their rather low cost (< 4,500 USD) and ease of use (**Fig. 1**), little is known about their performances. The goal of this study was therefore to test a handheld radar to determine the velocity at the surface of open channels.

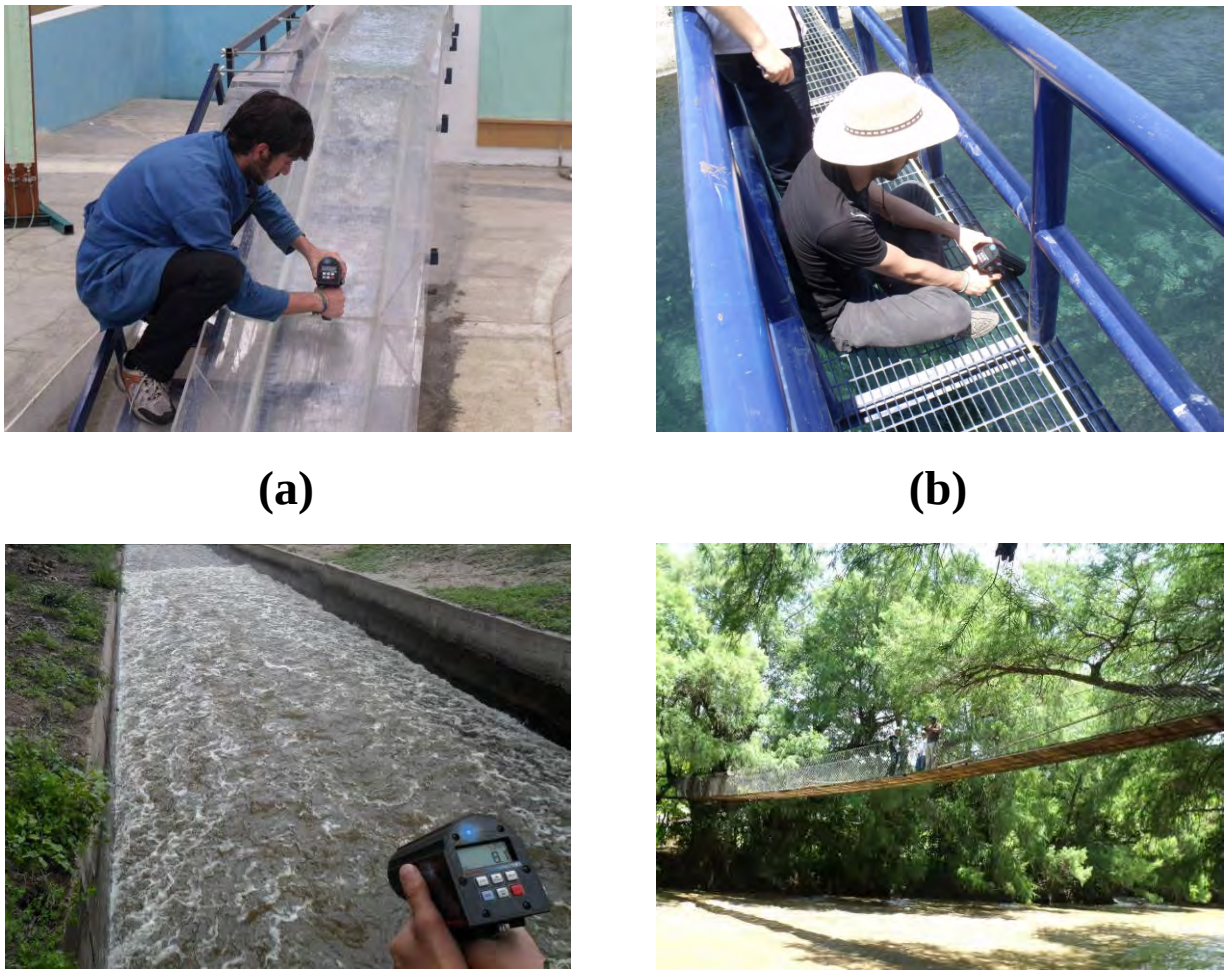

Fig. 1. Different types of sites where the handheld radar was tested:
(a) plane part of a laboratory spillway (case "L.9" of **Table 1**), (b) irrigation channel (case "F.1"), (c) rapid with rolling waves (case "F.4") and (d) river with breaking waves (case "F.5").

2. Background

2.1. What is known about the handheld radars ?

A *radar* is a remote sensing system that sends an electromagnetic signal of a given frequency to a target and then measures some properties of the signal that is sent back (time delay, Doppler shift and/or intensity) in order to determine its distance, speed and/or texture. [(1)] There are radars of different signal frequencies and designs, depending on their purpose and level of sophistication [*e.g.* Ulaby *et al.* 1981]. In particular, the *Doppler radars* are designed to determine the speed of a target.

Handheld radars look like a pistol (for this reason, they are often called *radar gun*). They can be defined as *monostatic* (the receiving antenna is near the emitting antenna) and *microwave* (they emit a signal in the microwave range) Doppler radar, designed to be easily transported by a walking person and operated from a steady position. The current instruments of this type are *Continuous Wave* (a low cost technology that does not allow the instrument to measure the distance to a target) and *K-band* (operating frequency between 18 and 27 GHz) or *Ka-band* (operating frequency between 27 and 40 GHz) radar.

(1) The purpose of the first radars was to determine the distance to a target. For this reason, the word "radar" is an acronym for "RAdio Detection And Ranging". Nonetheless, the word "radar" is now used in a more general sense.

Handheld radars were originally developed to determine the speed of cars [*e.g.* Jendzurski & Paulter 2008]. They have also become popular to determine the speed of animals and sporting balls [*e.g.* Newton & McEvoy 1994]. The idea of using similar instruments to determine water velocity in open channels was patented ten years ago [Smith *et al.* 2003]. However, determining the velocity of a water surface is not the same as determining the speed of a single solid object, in terms of data acquisition and processing. This emphasizes the need to test handheld radars designed to measure water velocity. There are currently two models of this type (called *surface velocity radar* by their manufacturers). Both look very similar for their shape and specifications; it is worth noting that their *(3 dB) beam width* is large in practice (12°) and that they emit a signal with a *circular polarization* (whereas the other radars for studying water usually use linear polarization: HH and/or VV). Although some authors seem to use handheld radars routinely to estimate discharge in rivers [*e.g.* Corato *et al.* 2011], little has been published about their performances:

- First, the "SVR" model from Decatur Electronics [2011] has an operating frequency of 24 GHz (*K-band*). Its claimed uncertainty [$p = 0.95$] [(2)] is ± 10 % of the measurement for a range from 0.3 to 9 m/s. A few evaluations of this instrument [Song *et al.* 2006, Fulton & Ostrowski 2008, Zolezzi *et al.* 2011, Dramais *et al.* 2011, 2013] suggest that it can indeed estimate surface velocity within ± 10 % for medium to large velocities (≈ 0.5 - 5 m/s), but does not always operate at low velocities (< 0.5 m/s).

[(2)] In the following, *any uncertainty that is reported by a manufacturer without specifying its confidence interval is assumed to be a standard uncertainty* [$p = 0.68$]. In this case, we report a twice larger uncertainty, considering a 95 % level of confidence [$p = 0.95$].

- Second, the "Stalker Pro II SVR" model from Stalker Radar [2008] has an operating frequency of 35 GHz (*Ka-band*). Its claimed uncertainty [p = 0.95] is ± 0.2 m/s for a range from 0.2 to 18 m/s. Compared to the previous radar model, its maximum operating velocity is therefore claimed to be larger (twice) and it is claimed to be more accurate at large velocities (> 2 m/s). In addition, it can measure incidence angles smaller than 40° (which can be useful for studying steep channels). Until now, there is no publication about the performances of the "Stalker Pro II SVR" radar; this model will be considered below.

Due to the lack of information about the performances of handheld radars in the field of Hydraulics, some concepts about the Doppler radar are reviewed in the next section, in order to better know what can be expected from these instruments.

2.2. Principle of operation of a handheld radar

As for any other fixed and monostatic Doppler radar, a handheld radar determines the velocity of a target by sending a signal of a given frequency (f_0, Hz) to the target, retrieving the backscattered signal and determining its frequency (f, Hz). The *Doppler effect* is used by the instrument to internally compute the *radial velocity* of the target, that is, the component of its velocity relative to the radar's line-of-sight (V_r, m/s):

$$V_r = -\frac{c_a}{2}\frac{\Delta f}{f_0} \quad (1)$$

where c_a is the speed of light through the air ($\approx 3 \times 10^8$ m/s) and $\Delta f = f_0 - f$ is the *Doppler shift* (negative when the target gets closer and positive when it goes away). So, unless the radar is placed exactly in front of a moving target, a trigonometric correction must be applied to estimate the velocity of the target in its main direction of movement.

Consider a radar oriented in such a way (*e.g.* from a bridge) so that it looks in the main direction of a stream (**Fig. 2**). Provided that the radar signal is backscattered (as discussed in **Section 2.4**) and assuming that it is emitted as a narrow beam (as discussed in **Section 5.1**), the velocity of the water surface (V_s, m/s) can be estimated as:

$$V_s = \frac{V_r}{\sin\theta} \quad (2)$$

where V_r (m/s) is the radial velocity of the water surface and θ (°) is the radar's incidence-angle relative to the water surface. At the scale of several metres, it can be usually assumed that the water surface of open channels is a horizontal plane: this is realistic (with a tolerance of ± 1°) provided that the channel slope is gentle (< 0.017 m/m) and that there is no hydraulic jump. In this case, the angle θ of **Eq. 2** is simply the *incidence angle* of the radar (θ_o), *i.e.* the angle

between its line-of-sight and the vertical. Commercial handheld Doppler radars have a built-in inclinometer, so that they can automatically determine such an angle and use it to estimate the velocity of a horizontal water surface [Smith *et al.* 2003].

Next, the case of a plane but inclined water surface will be also considered. This situation occurs in steep artificial channels and in the middle part of some spillways. In this case, the angle of **Eq. 2** is: $\theta = \theta_o - \beta$ for a radar looking upstream, and $\theta = \theta_o + \beta$ for a radar looking downstream, where β is the slope of the water surface ($0 \leq \beta < 90°$). In practice, the water surface is often almost parallel to the channel bottom and edges, which can be easily checked visually. If so, the angle β can be rapidly estimated by measuring the channel's slope with the built-in inclinometer of a handheld radar or any other inclinometer. Nevertheless, it becomes more difficult to determine the angle β when the water surface is curved (as it occurs over many spillways); such a situation is out of the scope of this study.

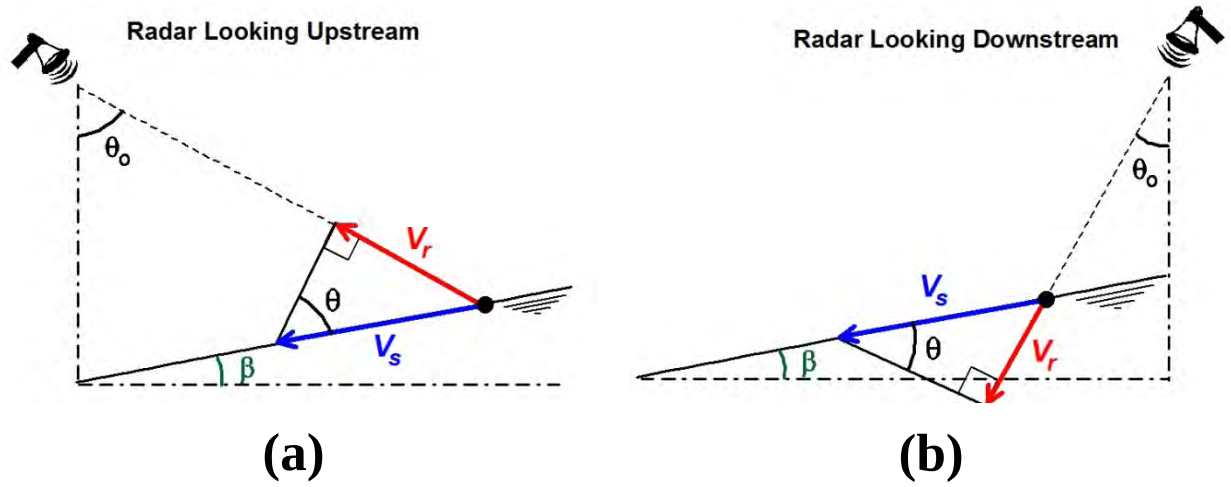

Fig. 2. Geometrical framework considered to determine the velocity of a free water surface using the radar (symbols are explained in **Section 2.2**): the instrument is placed above water and is looking (a) upstream or (b) downstream. The water surface is assumed to be a plane, that can be inclined ($0 \leq \beta < 90°$).

2.3. Which incidence angle for the radar ?

To reduce the effect of the trigonometric correction (**Eq. 2**) as much as possible, a radar should be placed so that it looks at the water surface with a relative incidence angle as large as possible ($\theta \rightarrow 90°$, so that $\sin\theta \rightarrow 1$). Nonetheless, when a handheld radar looking at a water surface is oriented with a too large incidence angle, it becomes difficult in practice to know at what it is pointing. During this study, no attempt was made to use the handheld radar with a relative incidence angle larger than 70°.

Assuming that V_r and θ are normally-distributed and independent random variables [JCGM 2008], a simple model to estimate the uncertainty of V_s can be derived from **Eq. 2**; this model is slightly more rigorous than the one proposed by Fulton & Ostrowski [2008]:

$$U(V_s) = \sqrt{\frac{1}{\sin^2\theta}\,U^2(V_r) + \frac{V_s^2}{\tan^2\theta}\,U^2(\theta)} \qquad (3)$$

where $U(\bullet)$ denotes the uncertainty of each variable (at a given confidence level); please note that the term $U(\theta)$ must be expressed in radians. Strictly speaking, the model does not agree with what is claimed by the manufacturers of handheld radars (**Section 2.1**); in fact, it predicts that the uncertainty of the surface velocity $U(V_s)$ is neither a constant value nor a fixed proportion of the measured value. In the case of the studied radar, assuming that its claimed uncertainty is for the radial velocity: $U(V_r)$ = 0.2 m/s [p = 0.95] and considering that the claimed uncertainty of its built-in inclinometer is: $U(\theta)$ = 0.07 rad (4°) [p = 0.95] [Stalker Radar 2008], the expected uncertainty $U(V_s)$ can be computed using **Eq. 3** for different scenarios (different values of V_s and θ). The results (**Fig. 3)** suggest that the radar should be oriented with an incidence angle $\theta > 45°$, otherwise its uncertainty will rapidly increase.

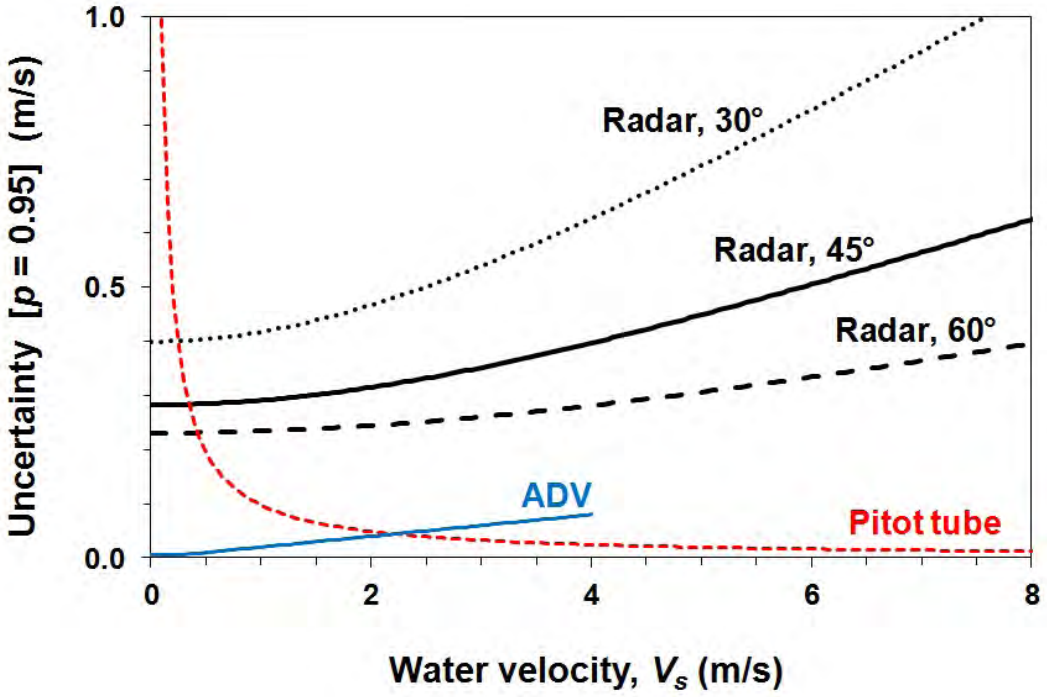

Fig. 3. Expected uncertainty of the tested radar (see **Section 2.3**) as a function of water velocity (V_s) for three local incidence angles (θ = 30, 45 and 60°).

The expected uncertainty of two current meters used as a reference is also shown: an ADV and a Pitot tube (see **Section 3.3**).

2.4. Detection of a water surface by a microwave radar

To be able to determine the velocity of a water surface, a Doppler radar must first detect it: the signal sent by the instrument must be reflected by the water in such a way that it goes back to the instrument and can be processed. This phenomenon has been studied for 50 years in the laboratory and on the sea (for more details, see **Section A.1**). Considering that the handheld radar emits microwaves, the backscattering of its signal by water (at least, for intermediate incidence angles: $20 \leq \theta \leq 70°$) is currently described by the *Bragg / composite surface* theory [*e.g.* Hasselmann *et al.* 1985, Plant & Keller 1990, Plant *et al.* 2004]. On the one hand, the theory considers that the microwaves are mostly backscattered by small water waves (traveling nearly in the plane of incidence, either toward the radar, either away from it), *i.e. ripples* with a wavelength $\Lambda_B \approx 6$ mm in the case of the studied radar (for more details, see **Section A.2**). In open channels, these ripples can be produced by external factors (the wind and the rain) and internal factors (the distortion of larger waves and the turbulence of water). On the other hand, the theory considers that the ripples backscattering the radar signal are mostly driven by larger water waves (for more details, see **Section A.3**). In open channels, these larger waves (gravity-capillary waves and hydraulic boils) are due to the wind and turbulence of water. On average, they are assumed to move at the velocity of the water surface.

The above theory predicts that the tested radar will not work if there are virtually no ripples on a water surface, as it may occur under low water flow and clear weather conditions [*e.g.* Plant *et al.* 2005] or if there is an oil film on the water [*e.g.* Gade *et al.* 1998]. It also predicts that the raw data recorded by a radar (a time-series of Doppler shifts) are "noisy". The main reason for that is that each water wave (ripples and larger waves) tends to propagate in several directions. So, a radar should detect water waves that sometimes move faster than the average water surface ("advancing waves") and that sometimes move slower ("receding waves"). Ideally, the histogram of the raw data recorded by the radar (converted into surface velocities, according to **Eqs. 1-2**) should have two peaks: one corresponding to ($V_s + c_B$) and the other corresponding to ($V_s - c_B$), where c_B is the *phase speed* of the water waves that backscatter the radar signal. If so, processing

the raw radar data simply consists in extracting the midway point between the two peaks. However, it is often difficult to discern this theoretical couple of peaks with a microwave radar (for more details, see **Section A.3**). In this case, processing the raw radar data is not straightforward anymore. If data are not processed carefully, the estimated surface velocity (V_s) can be erroneous up to ± c_B [Plant *et al.* 2005]. For the studied radar, $c_B \approx 0.3$ m/s (**Section B.1**); it is worth noting that the minimum expected uncertainty of the radar (computed from **Eq. 3** with $\theta = 45°$) is close to this value (**Fig. 3**).

2.5. Difficulty in interpreting the velocity measured by a radar

Assuming that the data have been averaged over a sufficiently long period of time, the surface velocity determined by a Doppler radar (V_s) can be decomposed as an algebraic sum of four terms (**Fig. 4**):

$$V_s = V + W + U_s + \upsilon \qquad (4)$$

where V is the drift caused by the underlying current (m/s), W is the drift caused by the wind blowing in the direction of the radar's line-of-sight, U_s is the Stokes drift (m/s) and υ is an eventual bias due to the way a radar "sees" a water surface (m/s). Considering the goal in Hydraulics is to determine the underlying current (V), taking it to be equal to the surface velocity measured by a radar (V_s) may lead to three types of systematic errors:

- *Wind effect (W)* - In practice, the drift of a water surface caused by the wind can be roughly estimated as [*e.g.* Plant *et al.* 2005]: $W \approx 0.02 \times W_{10}$, where W_{10} (m/s) is wind speed measured at 10 m above the surface. During this study, the handheld radar was tested under low wind conditions, at most equivalent to a *gentle breeze* on the Beaufort scale ($W_{10} < 5.5$ m/s); the wind effect was therefore expected to be rather small ($W < 0.1$ m/s).

- *Stokes drift (U_s)* - The Stokes drift is accounted for by a Doppler radar (as well as by small surface drifters), but not by a conventional current meter that would be maintained at a fixed position and just below the water surface [*e.g.* Monismith & Fong 2004]. So, this could be a cause of systematic difference between the radar and a conventional estimation of water velocity. Nevertheless, the Stokes drift was expected to be rather small for most of the studied channels: $U_s \leq 0.14$ m/s, at least in the laboratory (see **Section B.2**).

- *Bias term due to the radar (υ)* - Due to the specific motion of the water waves that backscatter the radar signal, there may be a systematic difference ($\upsilon \neq 0$) between the surface velocity determined by a Doppler radar and the true surface velocity for a number of reasons; this will be discussed further below (**Section 4**).

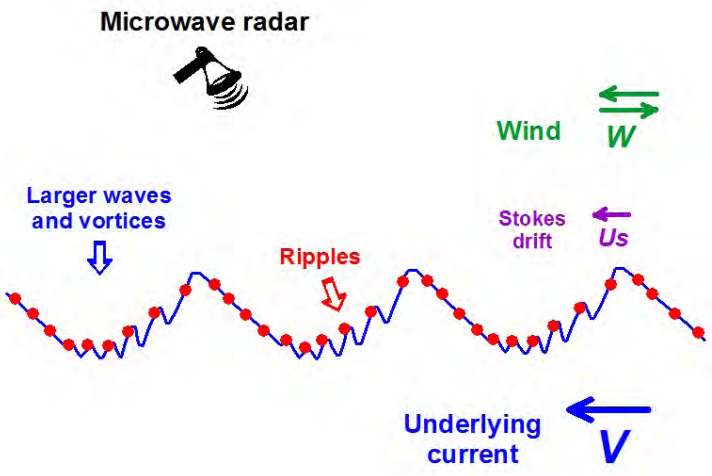

Fig. 4. Diagram showing which details of a water surface should be "seen" by the tested radar (see **Section 2.4**): most of the radar signal is expected to be backscattered by some parts (points on the diagram) of small water waves (ripples), which should be driven by larger waves. Although the water waves tend to move in several directions at their own phase speed, on the average they are assumed to be advected by the underlying current (the drift caused by the wind was expected to be small for the studied channels); in this case, the Stokes drift should be in the direction of the current.

2.6. Experience with microwave radars in open channels

As shown, it is not so simple to use a radar to estimate the velocity of a water surface. In this context, microwave radars with different configurations have been tested over open channels over the last fifteen years. Above all, prototypes [Contreras & Plant 2004, Costa *et al.* 2006, Plant *et al.* 2005, Fulton & Ostrowski 2008] and commercial instruments [Song *et al.* 2006, Dramais *et al.* 2011, 2013, Sung-Kee *et al.* 2012] fixed to a bridge (radar looking in the direction of the main stream) have been tested. Prototypes [Costa *et al.* 2006, Plant *et al.* 2005] and commercial instruments [Sung-Kee *et al.* 2012] located at a channel bank have been also tested. Prototypes moved across a channel using a cableway [Costa *et al.* 2006, Plant *et al.* 2005] or a helicopter [Plant *et al.* 2005] have been tested as well. It is worth noting that a radar with an operating frequency of 10 GHz (*X-band*) and a design very similar to that of the commercial handheld radars has been described and tested by Lee & Julien [2006]; nonetheless, it seems to have been forgotten for an unknown reason.

All the mentioned field testing suggest that microwave radar can usually determine the surface velocity of open channels with an uncertainty [$p = 0.95$] of ± 0.2 m/s, which is consistent with that claimed by the manufacturers of handheld radars. Nevertheless, testing have been conducted in rivers but not in artificial channels (where the roughness of the water surface may be different due to different turbulence conditions) and only for water velocities ≤ 5 m/s.

3. Materials and methods

3.1. Sites where the radar was tested

Based on the literature review (**Section 2**), it was decided to test the handheld radar over a series of open channels (**Table 1**):

- *Wide range of water velocities* - The radar was tested for the widest range of velocities as possible, *i.e.* from 0.3 up to at least 6 m/s. To achieve this range, tests were performed not only over horizontal channels, but also over the plane part of inclined channels (slope as large as 28°). It was not sure whether the radar would work under clear weather conditions at low velocities (< 0.5 m/s), and the comparison with conventional current meters was quite challenging at large velocities (> 3 m/s).

- *Several types of open channels and flow conditions* - Compared to other radars designed to study open channels, the handheld radar can be very easily transported from one site to another, which makes it possible to rapidly test this instrument under several flow conditions. For this study, 18 sites were chosen for testing, with a special interest in artificial channels. The testing was performed in straight portions of wide (*aspect ratio* $\nu > 5$) and narrow ($\nu < 5$) channels, with different wall roughness (walls made of glass, acrylic, cement, concrete or earth and stones). Both subcritical (*Froude number* $Fr < 1$) and supercritical ($Fr > 1$) flow conditions were considered.

- *Clear weather conditions* - The radar was tested in the laboratory (13 sites) and in the field (5 sites). In the field, testing was made under low wind (not more than a gentle breeze) and no rain conditions. Although these conditions are convenient for the user and should ensure that the water surface is mostly driven by the underlying current, they are known to be challenging for the radar when water flows slowly. The water surface may indeed be too smooth to produce a significant backscattering of the radar signal [*e.g.* Plant *et al.* 2005].

- *No oil at the water surface* - The radar was tested over channels with clear (laboratory channels and case "F.1" in **Table 1**), turbid (cases "F.3" and "F.4") and very turbid (cases "F.2" and "F5") water, but *not* in channels contaminated by gasoline or detergent (where the presence of an oil film could prevent the radar from detecting the water surface) [*e.g.* Gade *et al.* 1998].

3.2. Conditions for using the tested radar

The only parameter for configuring the tested radar was its "power output", which was set at 20 mW (as recommended by the manufacturer for taking data close to a water surface). After that, taking a measurement with the tested radar was easy: once oriented in the main direction of a stream, its built-in inclinometer was used to incline the radar to a desired incidence angle (θ_o = 90° - ϕ_o, where ϕ_o is the *grazing angle* that was actually displayed by the radar); the radar was then maintained in the same position and its trigger was pressed. About 30 s later, the radar was usually displaying a symbol saying whether water was moving forward or downward and an average velocity data (V_s^m); because the radar has been designed to be used over horizontal channels, this data is a projection in an horizontal plane of the determined radial-velocity ($V_r = V_s^m \times \sin\theta_o$).

During testing, the radar was operated as follows:

- *Radar oriented in the main-stream direction* - The radar was always oriented in the main-stream direction. So, field testing was made from bridges of gauging stations. No attempt was made to use the radar from a channel edge; in this case, there was no need to correct the radar data for the azimuth angle relative to the channel direction (as done by Lee & Julien [2006]) and there was no concern with secondary or cross currents (as discussed by Plant *et al.* [2005]).

- *Radar looking upstream / downstream* - Each time, a measurement was taken with the radar looking upstream and another with the radar looking downstream. In the laboratory, special attention was paid to locate the radar so that it was pointing at the same part of a channel. While this was not possible in the field, the studied channels were long and uniform enough to reasonably assume that the transversal velocity-profile was the same along the section where the measurements were taken.

- *Radar located as close as possible to the water surface* - As a first approximation **(Section A.5**), the tested radar should "see" an area at the water surface *(footprint*), which is an ellipse with a transversal diameter: $D_T \approx 0.2 \times L$, where L (m) is the distance to the surface in the line-of-sight direction. It must be recognized that this relation applies only if the distance L is larger than a certain value, which is: $L_f = 0.6$ m for the studied radar **(Section A.4**). In the field, the radar was located at $3 \leq L \leq 10$ m, resulting in $0.6 \leq D_T \leq 2$ m. In the laboratory, it was empirically [(3)] located at $0.1 \leq L \leq 0.3$ m; D this is smaller than L_f, resulting in $D_T < 0.12$ m. Thus, it was felt that the area sampled by the radar was not too large (so that the radar data could be used on channels with a width $b \geq 0.3$ m and so that its data could be compared to the data provided by current meters).

[(3)] We relied on the recommendation of a manufacturer [Decatur Electronics 2011], saying: "*The radar gun makes the best measurements, when it is as close to the water surface as possible*".

- *Measurements taken rather quickly* - Once a first value for the average velocity was displayed by the radar, the instrument was left to take more data and average them during ≈ 20 - 40 s. This duration was usually sufficient to achieve repeatable data with a tolerance of ± 0.15 m/s. [(4)]

- *Radar's inclinometer considered as unbiased* - According to its manufacturer [Stalker Radar 2008], the radar's built-in inclinometer has an uncertainty [p = 0.95] of ± 4°. This was checked against a comparison with an external inclinometer with a tolerance < 1° (model "MTi", Xsens Technologies, Enschede, The Netherlands). Although systematic differences were found, their magnitude was always < 2.6° (**Fig. 5**).

- *Radar always oriented with its handle downward* - At the beginning of the study, some preliminary tests were performed to see how the handheld radar responds to different orientations: First, it was found that the instrument provides unreliable incidence angles if its handle is not in a vertical plane (roll angle ≠ 0); an interpretation would be that the radar's inclinometer measures the pitch only, but not the roll. Second, it was found that the tested radar must be oriented with its handle downward: for unknown reasons, the instrument provides unreliable velocity data if its handle is upward.

- *Intermediate incidence angle* - The radar was oriented with a relative incidence angle (θ) between 45 and 60° during normal operation. This will be discussed more in detail further below (**Section 4.2**).

[(4)] During laboratory and field testing, two replicates were performed with the radar most of the time: one measurement was taken before using reference techniques (**Section 3.3**) and the other was taken after. A mean value was computed from the result of these two measurements.

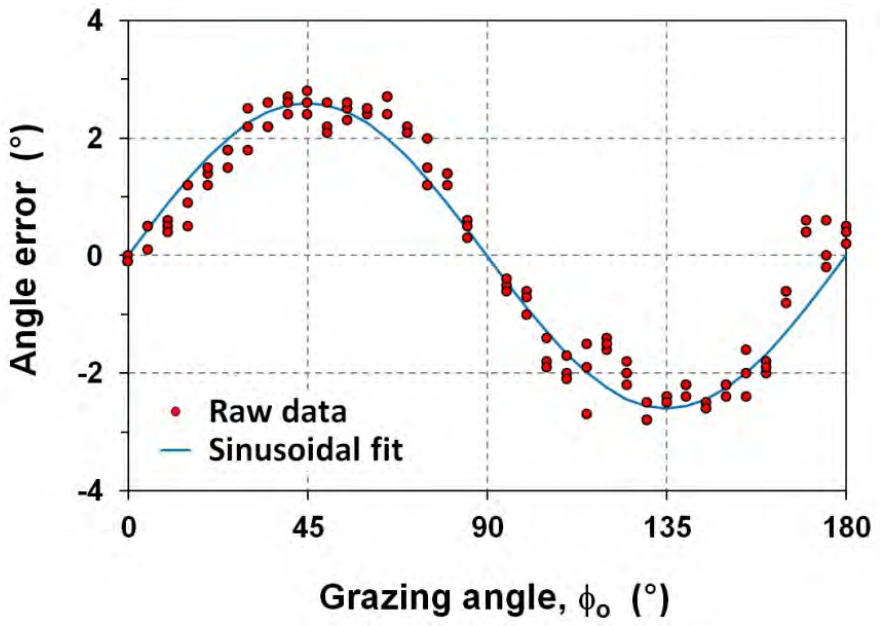

Fig. 5. Laboratory verification of the radar's built-in inclinometer.
The error is the difference between the angle displayed by the radar and the actual angle.

Please, note that the radar displays the *grazing angle* (ϕ_o),
i.e. the angle between its line-of-sight and the horizontal.

3.3. Reference techniques for testing the radar

The handheld radar was compared with five other techniques of velocimetry (**Table 2**):

- *Reference techniques in the laboratory* - In the laboratory, three types of current meters were considered as a reference: an EMV (model "Flo-Mate", Marsh-McBirney), an ADV (model "FlowTracker, Sontek/YSI) and a Pitot tube (model "630", Lambrecht). To estimate the surface velocity in open channels, these meters were located as close as possible to the water surface (sensor top at ≈ 2 cm below the surface), with special care to avoid cavitation around them during the measurements (if cavitation was observed, the meter was taken out and immersed again; if cavitation persisted, the meter's data were discarded). If working properly, the EMV and the ADV were expected to be several times more accurate than the studied radar at low to medium water velocities, whereas the Pitot tube was expected to be much more accurate at large velocities (**Fig. 3**). However, an inter-comparison performed at medium velocities showed that the EMV data were often in disagreement with the ADV and the Pitot tube data (**Fig. 6**); since this was occurring when the water level was low (< 8 cm), it was concluded that the EMV is not suitable for studying very shallow open channels (which could be due to the fact that its sensing part is three times higher than that of both the ADV and the Pitot tube). Therefore, most of the laboratory testing was conducted taking the ADV as the reference at low to medium velocities (< 2.5 m/s) and the Pitot tube as the reference at large velocities.

- *Reference techniques in the field* - The above mentioned ADV ("FlowTracker") was used in the field as the reference wherever it was possible to immerse it using a wading rod: low to medium water velocity (< 2.5 m/s) and water surface close to the bottom of a bridge (< 3 m). When the velocity was not too large but the water surface was too low (case "F.5" of **Table 1**), an MCM connected to a cable with a sounding weight was used as the reference. And when water was flowing very rapidly (case "F.4"), a simple PIV technique was used (**Appendix C.2**).

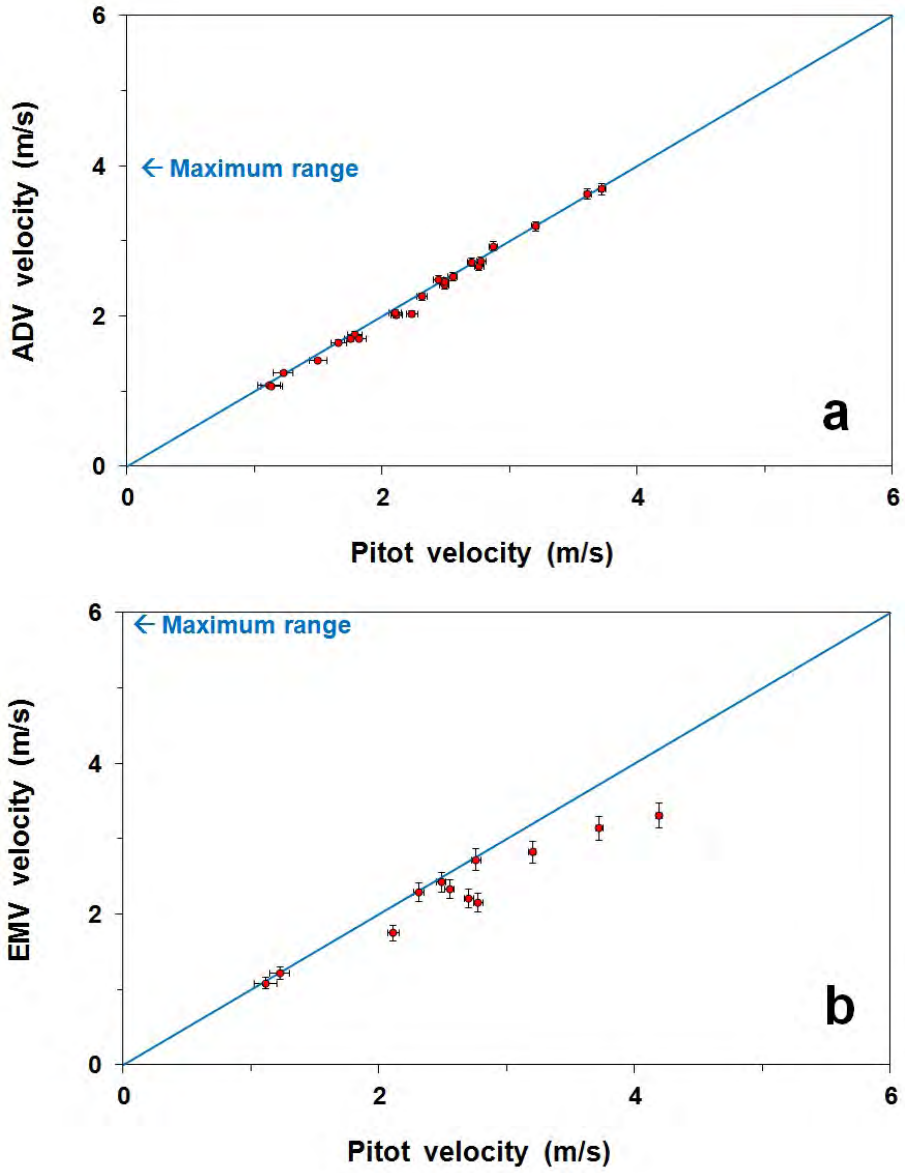

Fig. 6. Laboratory inter-comparison of three conventional current meters used during this study: (a) ADV ("FlowTracker") vs. Pitot tube; (b) EMV ("Flo-Mate") vs. Pitot tube. Bars show the expected uncertainty [p = 0.95] of each meter (see **Table 2**).

Please note that the meters were intended to be used to estimate the velocity of a water surface, therefore the top of their sensing part was located ≈ 2 cm below the surface.

4. Results and discussion

4.1. Global performances of the radar

In this section, only the global results obtained with the handheld radar during normal operation (*i.e.* with a relative incidence angle between 45 and 60°) are shown. When tested in the laboratory and looking upstream, the handheld radar was found (**Fig. 7a**) to estimate water velocity at the surface of open channels from 0.3 to at least 6 m/s with an uncertainty slightly better [$p > 0.95$] than what was expected at the beginning of this study (**Section 2.3**). [(5)] Roughly, it corresponds to: $U(V_s) \approx 0.3$ m/s at medium velocities (from 0.3 to 3 m/s) and $U(V_s) \approx 0.1 \times V_s$ at large velocities. Such an uncertainty is similar to that previously reported for the other commercial model of handheld radar (**Section 2.1**) and slightly larger than that previously reported for other types of microwave Doppler radars that have been tested in rivers (**Section 2.6**). Nevertheless, it is worth noting that the handheld radar was tested over a large set of water velocities (including > 4 m/s) and channel types (including inclined channels). [(6)]

[(5)] Please note that the uncertainty of the reference techniques has been neglected because it was *a priori* several times lower than that of the radar (see **Fig. 3**).

[(6)] Also worth noting is that the radar was satisfactorily tested over a channel covered by an acrylic sheet (case "L.11"): if the signal emitted by a radar can pass through a solid material, its frequency will indeed remain the same (contrary to its speed) and the instrument will therefore be able to properly determine the velocity of a water surface.

More in details, it must be recognized from a regression analysis that the radar data were significantly lower than the reference data (this will be discussed in **Section 4.3**).

When tested in the laboratory and looking downstream, the radar was found (**Fig. 7b**) to estimate water velocity with an uncertainty still [p = 0.95] consistent with what was expected at the beginning. Nonetheless, the radar tended to estimate a lower velocity when looking downstream instead of upstream. It was also working less well over steep channels. On the one hand, it was often taking more time before displaying a velocity data. And on the other hand, it was more sensitive to its relative incidence angle: unrealistic (too low) velocity data were determined when θ was not large enough (see **Section 4.2**); this could explain why a velocity data taken with a rather low incidence angle ($\theta \approx 53°$) over a very steep channel (case "L.13b") is significantly low (see the oval in **Fig. 7b**).

It could be argued that the laboratory results underestimate the usual performances of the radar, because it has been tested very close to the water surface (**Section 3.2**). However, when tested in the field, the radar data (**Figs. 7-8**) were found to be consistent with those obtained in the laboratory. In particular, for four cases (**Fig. 8c-f**) it was observed that the radar clearly estimated a lower velocity when looking downstream instead of upstream.

Summarizing, even though the handheld radar has provided velocity data in the range of what was expected *a priori*, three biases (to be discussed further below) were found during this study:

- *The tested radar does not work well at too low incidence angles*.

- *The radar underestimates the reference data*.

- *The radar estimates a lower velocity when looking downstream instead of upstream*.

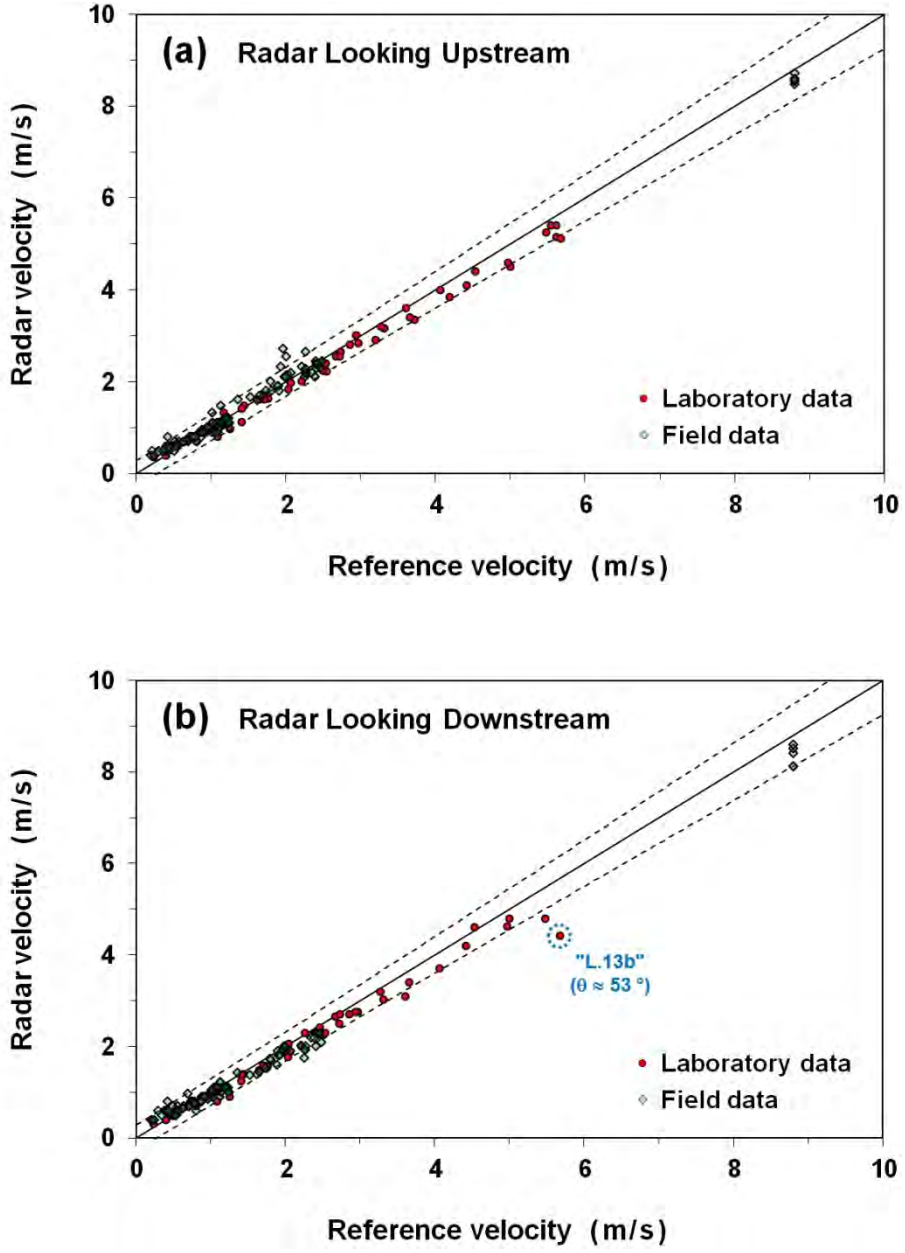

Fig. 7. Laboratory and field testing of the handheld radar:
radar vs. reference techniques (see **Section 3.5**).

The results are shown for all the channels listed in **Table 1**.
The dashed lines show the expected uncertainty of the radar [p = 0.95].

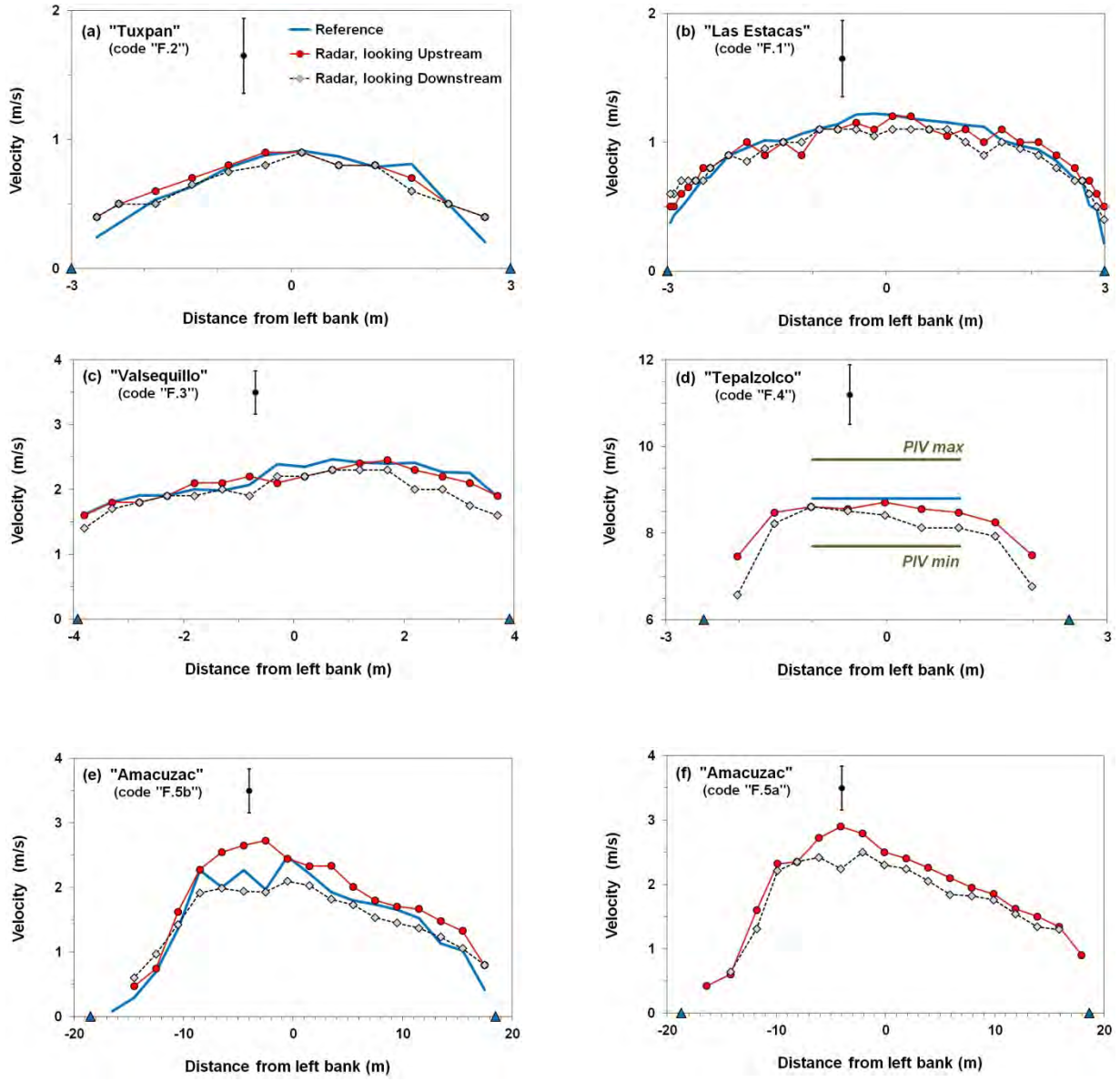

Fig. 8. Field testing of the handheld radar: horizontal velocity profiles obtained at the water surface with the radar and with others techniques chosen as a reference.

The results are shown for all the field channels listed in **Table 1**.

The vertical line on each plot shows the maximum expected radar uncertainty [p = 0.95]. The triangles at the bottom of each plot show the channel edges.

4.2. Effect of the radar' s incidence angle

Some preliminary tests were performed in the laboratory to see the range of relative incidence angles (θ) for which the radar provides reliable velocity data: measurements were taken with the radar oriented at different incidence angles, and the consistency of the radar data was evaluated. In all cases, the slope of the water surface (β) was assumed to be the slope of the channel, which was measured using an external inclinometer ("MTi"). Whereas the radar was expected to work in the range $20 \leq \theta \leq 70°$ (**Section 2.4**), the obtained results (**Fig. 9**) suggest that it only provides realistic data if its relative incidence angle is large enough: $\theta \geq 40°$ for moderately inclined channels (slope $\beta \leq 10°$) and $\theta \geq 50°$ for steep channels ($\beta > 10°$).

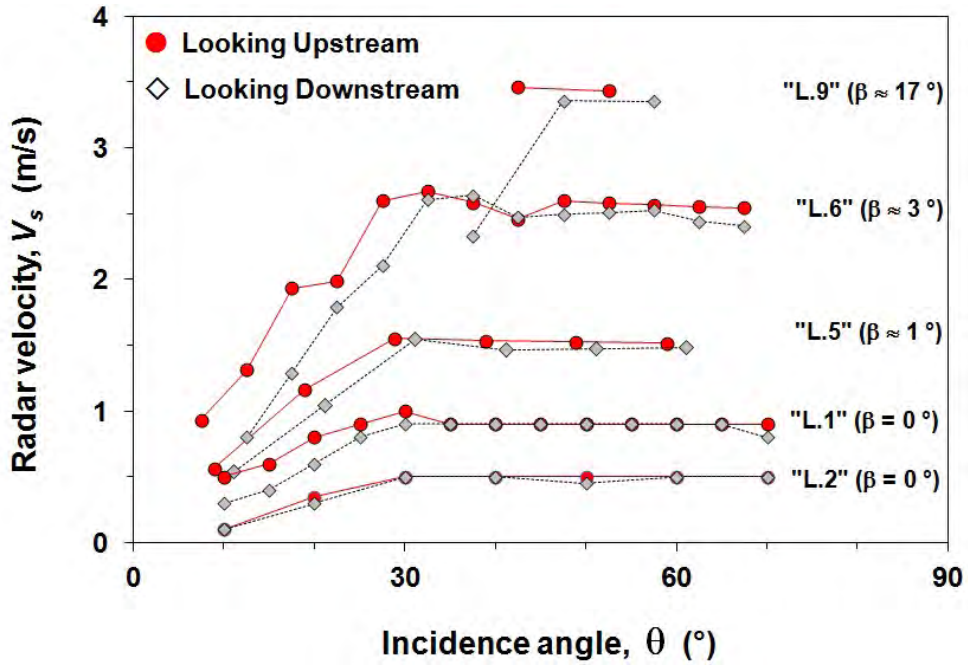

Fig. 9. Laboratory testing of the handheld radar: effect of the local incidence angle (θ) on the water velocity (V_s) estimated by the radar, when it is looking upstream (circles) or downstream (diamonds). The results are shown for five laboratory channels (codes refer to the list in **Table 1**) with different slopes (β).

The radar was found to increasingly underestimate water velocity as its relative incidence angle decreases from $\theta \approx 35$ ° in horizontal channels and $\theta \approx 45°$ in steep channels (**Fig. 9**). This trend was not expected, but rather, it was thought that the radar would still work satisfactorily for a relative incidence angle as low as $\theta \approx 20°$.

- *A bias of the radar's inclinometer ?* - The trend cannot be explained by the bias of the radar's inclinometer (**Fig. 5**): in a preliminary attempt to correct for this bias, no significant improvement of the radar's performances was obtained.

- *An effect of the radar's beam width ?* - The trend could be due to the rather large beam width (12°) of the studied radar [Anonymous 2013, personal communication]. An inclined radar with a non-zero beam width should be indeed more sensitive at incidence angles lower than the nominal one (θ). In this case, the water velocity (V_s) should be estimated from the measured radial velocity (V_r) using an incidence angle smaller than the nominal one. Otherwise, the water velocity will be underestimated (see **Eq. 2**). However, this effect is pronounced only for radars with a large beam width (as the tested one) and for small incidence angles (*i.e.* as $\sin\theta \rightarrow 0$). In this context, it was empirically found that the experimental results shown on **Fig. 9** can be roughly explained (**Fig. 10**) by assuming that the *effective* radar's incidence angle (θ^e) is lower by 4° than the nominal incidence angle (θ). [(7)]

Based on the results of the preliminary testing, the radar was further tested with a relative incidence angle (θ) between 45 to 50° for moderately inclined channels ($\beta \leq 10°$) and between 50 to 60° for steep channels.

[(7)] Due to the lack of knowledge, it was not possible to analyze more in details the effect of the radar's beam width (as a radar's expert could).

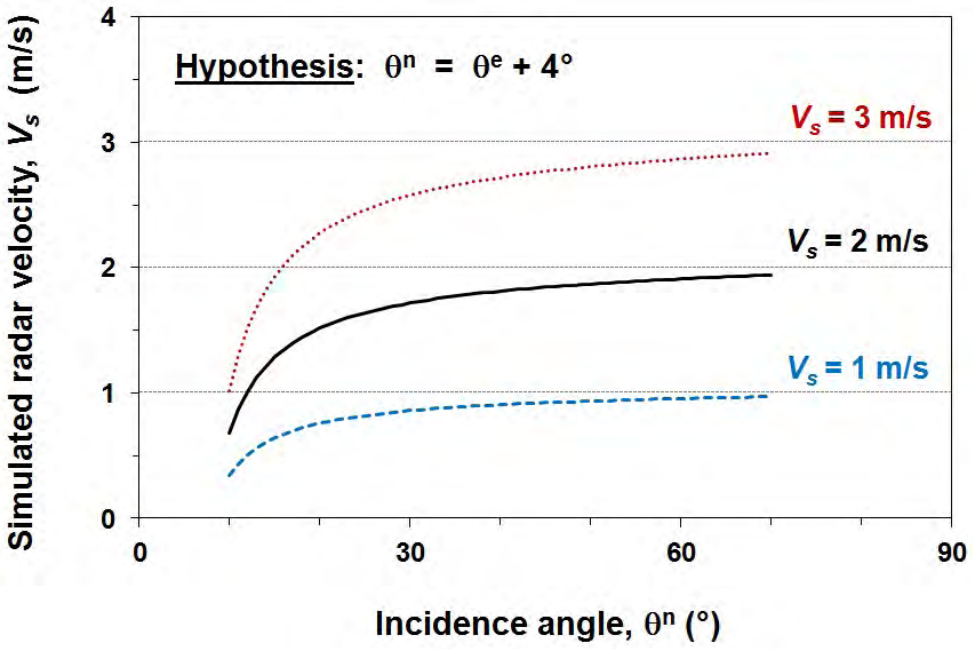

Fig. 10. A simple simulation of the water velocity (V_s) estimated by the radar, based on the assumption that its *effective* incidence angle (θ^e) is lower by 4° than the nominal incidence angle (θ). Three cases of surface velocity (1, 2 and 3 m/s) are shown.

4.3. Underestimation of the reference velocities

According to a regression analysis, the radar data were significantly different from the reference data: on the average, the radar data were lower by ≈ 5 % of the value when the radar was looking upstream (**Fig. 11a**), and lower by ≈ 8 % of the value when the radar was looking downstream (**Fig. 11b**). This trend was not expected:

- *A bad choice of the reference techniques ?* - It could be argued that the current meters used as a reference for testing the radar (**Section 3.3**) may have underestimated the velocity at the surface of narrow (*i.e.* aspect ratio < 5) and rectangular channels, due to the dip phenomenon. However, the radar was also tested at the central part of trapezoidal channels and of wide rectangular channels, where the dip phenomenon should not occur [Tominaga *et al.* 1989].

- *An effect of the Stokes drift ?* - There could be a difference between the radar and the reference data due to the Stokes drift, because it is accounted for by a Doppler radar, but not by the conventional current meters (*i.e.* MCC, EMV, ADV and Pitot tube). Nevertheless, the Stokes drift should be in the direction where the larger water waves propagate. Considering that the wind was small (see **Section 2.5**), these waves should have been mostly driven by the underlying current. In this case, the Stokes drift should have been in the direction of the current: it cannot therefore explain why the radar data were lower than the reference data.

- *A bias of the radar's inclinometer ?* - Contrary to what has been reported for the other commercial model of handheld radar [Dramais *et al.* 2013], the trend cannot be explained by the bias of the radar's inclinometer (**Fig. 5**): in a preliminary attempt to correct for this bias, no significant improvement of the radar's performances was obtained.

- *An effect of the radar's beam width ?* - Although we are not able to analyze in details the effect of the radar's beam, the underestimation of the reference velocities is rather well explained (**Fig. 11c-d**) by the simple hypothesis (**Section 4.2**) of an overestimation (by 4°) of the radar's *effective* incidence angle (θ^e).

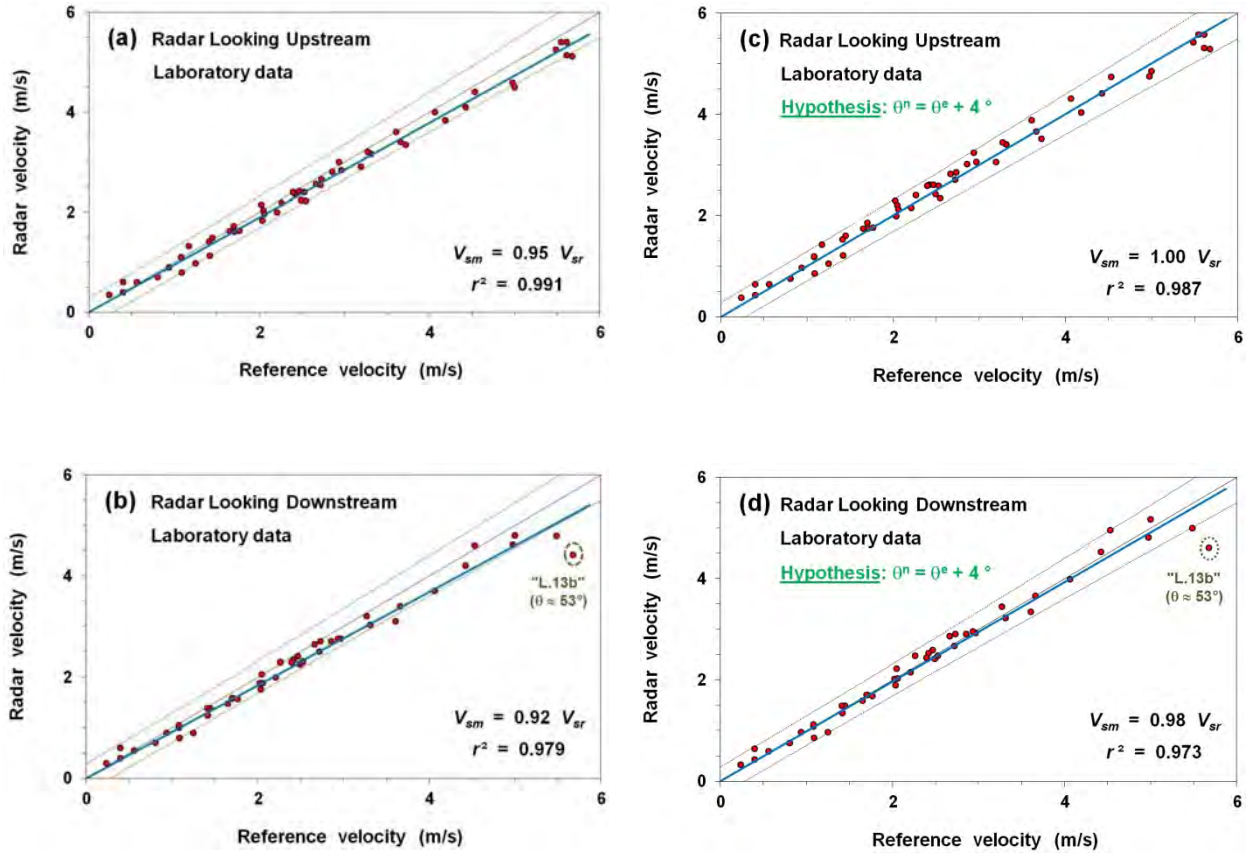

Fig. 11. Laboratory testing of the handheld radar:
radar vs. conventional current meters located at ≈ 2 cm below the water surface (see **Section 3.5**).

The results are shown for all the laboratory channels listed in **Table 1**.
The dashed lines show the expected uncertainty of the radar [p = 0.95].
The results shown on the plots of the right column are based on the assumption that the radar's *effective* incidence angle (θ^e) is lower by 4° than the nominal incidence angle (θ).

4.4. Radar looking downstream vs. looking upstream

The radar was found to usually estimate a lower velocity when looking downstream (V_s^{down}) instead of upstream (V_s^{up}). Roughly, the velocity difference ($\Delta V_s = V_s^{up} - V_s^{down}$) was increasing as a function of water velocity, when it was larger than ≈ 1 m/s (**Fig. 12**). No clear trend was found in ΔV_s as a function of other quantitative (Froude number, aspect ratio, channel slope) or qualitative (laboratory or field testing) variables listed in **Table 1** (results not shown).

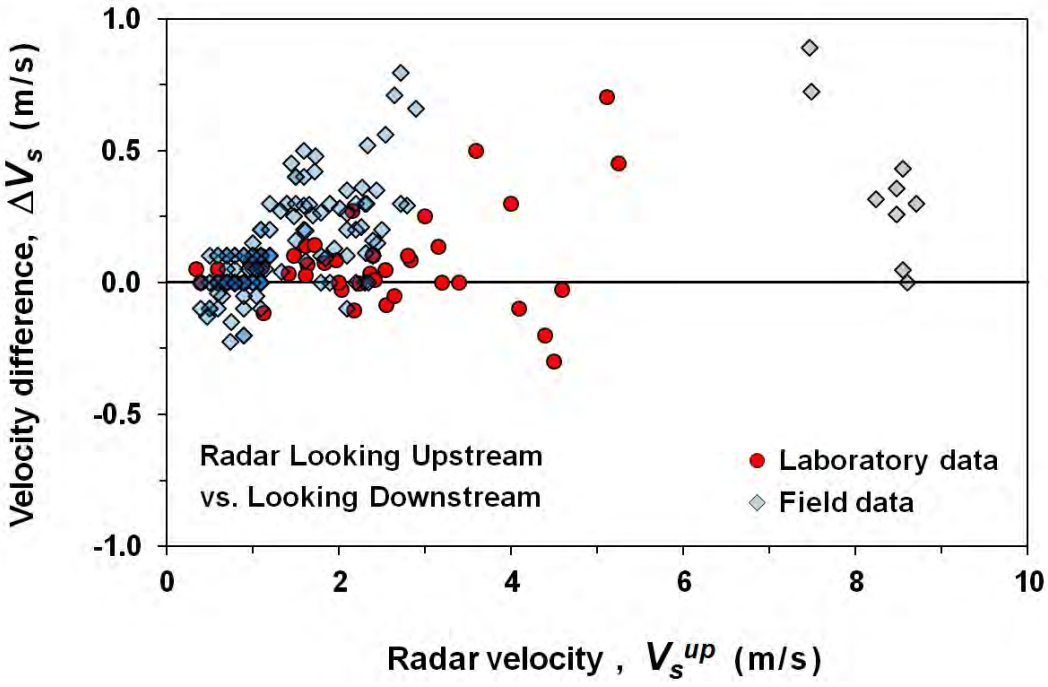

Fig. 12. Difference in velocity between the radar looking upstream and downstream (ΔV_s) as a function of the velocity measured by the radar looking upstream (V_s^{up}).

It is still difficult to know why the radar was tending to estimate a lower velocity when looking downstream instead of upstream: [8]

- *A wind effect (and an inaccurate data processing) ?* - The histogram of the raw data recorded by a microwave Doppler radar (converted into surface velocities) is often skewed. Many studies performed in water tanks [e.g. Gade *et al.* 1998, Plant *et al.* 2004] and on the sea [e.g. Plant & Keller 1990] have shown that this can be due to the wind (even a light air, with a speed as low as ≈ 0.3 m/s), which produces an asymmetry in the roughness at the water surface (unless the wind is blowing perpendicularly to the radar's line-of-sight): (1) if a radar is looking *upwind*, it should record a histogram with a larger peak corresponding to the advancing ripples ($V_s + c_B$); (2) on the opposite, if the radar is looking *downwind*, it should record a histogram with a larger peak corresponding to the receding ripples ($V_s - c_B$) and (3) under those circumstances, if the radar does not process carefully the raw data (*i.e.* if it does not extract the midway point between the two theoretical peaks of the histogram, but computes an average value, or -even worse- takes the mode), the absolute value of ΔV_s could be as large as $\approx 2 \times c_B$, which is ≈ 0.6 m/s for the studied radar (**Section 2.4**).

  Since most of the observed values of ΔV_s were within ± 0.6 m/s (**Fig. 12**), they could be due to a wind effect and to an inaccurate data processing.

[8] The hypothesis that the radar's *effective* incidence angle is overestimated (**Sections 4.2-3**) cannot explain the trend, because it is not related to the fact that the radar is looking upstream or downstream.

- *A hydrodynamic effect ?* - Unfortunately, the wind direction and speed have not been systematically measured during this study. However, if the observed values of ΔV_s were due to the wind, the fact that they were usually positive would mean that the wind was blowing most of the time from upstream in the studied channels. A few field observations suggest that this was not always true: above all, the observed values of ΔV_s were usually positive at the "Las Estacas" channel (**Fig. 8b**) although a light breeze was coming from downstream. In addition, larger values of ΔV_s were obtained twice at the same specific part of the "Amacuzac" river (**Fig. 8d-f**), although a light air with changing direction was blowing during testing (for more details, see **Section D.1**).

  So, it can be argued that some of the observed values of ΔV_s were not due to a wind effect but to a hydrodynamic effect. However, still little is known about how a microwave Doppler radar responds to a rough water surface produced by the turbulence (for more details, see **Section A.3**):

  ❖ *A hydrodynamic effect and an inaccurate data processing ?* - The observed values of ΔV_s could be due to an asymmetry in the roughness at the water surface produced by the underlying current (instead of the wind) and to an inaccurate data processing by the radar: (1) the radar looking *upstream* would record a histogram of raw data with a larger peak corresponding to the advancing ripples; (2) the radar looking *downstream* would record a histogram with a larger peak corresponding to the receding ripples and (3) the radar would not be able to properly extract the midway point between the two theoretical peaks of the histogram.

  ❖ *A hydrodynamic effect only ?* - Finally, if the tested radar properly processes the raw data, the question arises if the observed values of ΔV_s are a general feature of microwave Doppler radars when used in open channels under clear weather conditions. For instance, a hypothesis based on the distortion of the larger water waves is proposed in **Section D.2** to qualitatively explain the positive values of ΔV_s. More studies are necessary to verify this hypothesis.

5. Conclusion

Over the last fifteen years, a growing number of studies have shown that Doppler radar technology is a promising tool to estimate water velocity at the surface of open channels. In this context, a commercial handheld radar was tested. The testing covered a broad range of velocities (from 0.3 to 6 m/s) and channel types (including inclined channels). The radar was able to estimate the water velocity within [p = 0.95] ± 0.3 m/s at medium velocities (from 0.3 to 3 m/s) and ± 10 % of the measured value at large velocities. Although this is not very accurate, the ease of using handheld radars still makes them attractive to quickly estimate discharge at some gauging stations and to investigate how water flows under difficult access conditions.

Even though the tested handheld radar has provided velocity data in the range of what was expected *a priori*, some biases were found during this study. On the one hand, the fact that the radar does not work well at too low incidence angles and that it underestimates the reference data could be due to the rather large radar's beam width. On the other hand, the fact that the radar was usually estimating a lower velocity when looking downstream instead of upstream is still difficult to explain.

It would be useful to go on testing radars in open channels in order to see if the trends observed during this study on a single commercial instrument (with an unknown data processing algorithm) are reproducible or not. If they are, more investigations conducted by experts would be necessary to improve the estimation of water velocity at the surface of open channels by microwave Doppler radars: currently, little is known about how these instruments respond to a rough water surface, when the roughness is due to the underlying current.

Appendix A - Some details about radar

A.1. Doppler radars to study water bodies

Doppler radars have been used in Oceanography for fifty years, to estimate either the wind above the ocean either the superficial currents [*e.g.* Hasselmann *et al.* 1985, Lipa & Barrick 1986, Chapron *et al.* 2005]. In the last fifteen years, a growing number of studies have shown that Doppler radars can also determine the surface velocity of rivers [*e.g.* Plant *et al.* 2005, Costa *et al.* 2006]; different types of instruments have been developed for this purpose and some are now commercially available (*e.g.* "RiverSonde" from Codar Ocean Sensors, "Flo-Dar" from Marsh-McBirney, "RQ-30" from Sommer GmbH).

Two broad categories of radar must be distinguished according to their signal frequency:

- *HF radar* - On the one hand, the *HF radar* [*e.g.* Lipa & Barrick 1986] sends a signal in the HF/VHF/UHF range ($f_0 \approx$ 3 to 3000 MHz), which corresponds to a wavelength λ_0 between ≈ 0.1 and 100 m ($\lambda_0 = c_a / f_0$, with $c_a \approx 3 \times 10^8$ m/s); this signal is scattered by rather large (gravity) water waves.

- *Microwave radar* - On the other hand, the *microwave radar* [*e.g.* Plant & Keller 1990] sends a signal in the SHF/EHF range ($f_0 \approx$ 3 to 300 GHz), which corresponds to a wavelength λ_0 between ≈ 0.001 and 0.1 m; this signal is scattered by small (capillary-gravity) water waves.

A.2. Bragg resonant condition

The theory of how a radar signal is backscattered by a water surface is not straightforward [*e.g.* Hasselmann *et al.* 1985, Plant & Keller 1990, Elfouhaily & Guérin 2004, Plant *et al.* 2004]. On the one hand, it is considered that the radar signal barely penetrates the water (not more than a few cm for a microwave signal) [*e.g.* Ulaby *et al.* 1986, Plant *et al.* 2005]. On the other hand, and for a moderately inclined radar ($20 \leq \theta \leq 70°$), the theory considers that most of the signal backscattering will be produced by periodic water waves traveling in front of the radar (either toward the radar, either away from it) and with a specific wavelength (Λ_B, m), which depends on two radar characteristics: the wavelength of the radar signal (λ_0, m) and the incidence angle (θ,°). The relation is known as the *Bragg resonant condition* (**Fig. A.1**):

$$\Lambda_B = \frac{\lambda_0}{2 \sin\theta} \qquad \text{(A.1)}$$

Of course, the real shape of an agitated water surface is quite irregular. In this case, it is considered that it can be decomposed in a superposition of periodic waves, each one having a specific wave length. For instance, the frequency of the signal emitted by the studied handheld radar is f_0 = 34.7 GHz [Stalker Radar 2008], which corresponds to a wavelength of λ_0 = 9 mm. If such a radar is oriented with an incidence angle $\theta \approx 45°$, the water waves expected to backscatter its signal should have a wavelength $\Lambda_B \approx 6$ mm. In Hydraulics, these small waves ($\Lambda_B < 17$ mm; see **Section B.1**) are called *ripples* (or *capillary waves*).

A consequence of the above theory is that the raw data obtained by a Doppler radar (a time-series of Doppler shifts) above a water surface are "noisy": the water waves that backscatter the radar signal do not travel exactly at the mean velocity of the surface (V_s), because they also tend to move forward and backward at their own *phase speed* (c_B; see **Section B.1**). So, the histogram of the raw data recorded by a radar looking at a moving water surface (converted into surface velocities, according to **Eqs. 1-2**) should ideally show two marked peaks (not necessarily of the same amplitude): one for the advancing water waves ($V_s + c_B$) and the other for the receding ones ($V_s - c_B$). In this case, the basic operation of a Doppler radar consists in [*e.g.* Lipa & Barrick 1986, Plant *et al.* 2005]: (1) recording velocity data for a sufficiently long integration time, (2) identifying the two largest peaks in the histogram of the velocity data and (3) estimating the average velocity (V_s) as the midway point between these two peaks.

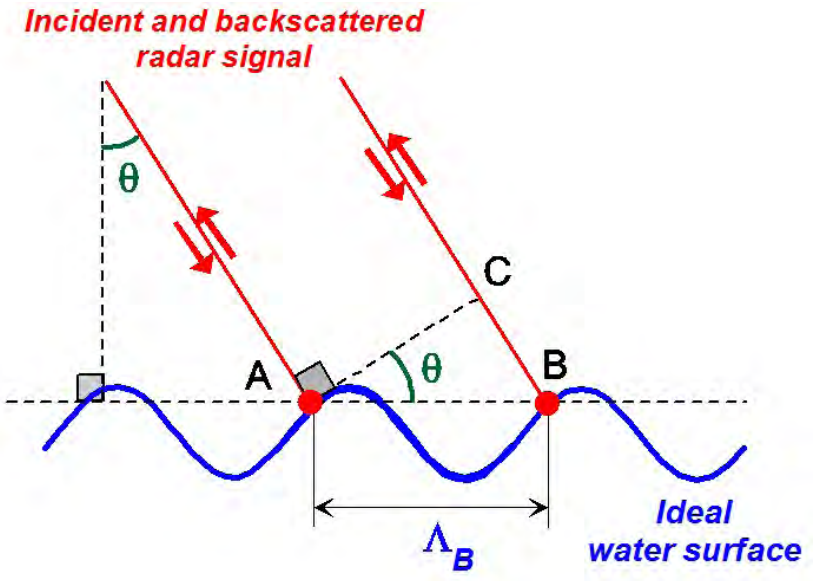

Fig. A.1. Diagram of the Bragg resonant condition in case of a monostatic radar.

The resonance occurs if the distance CB ($= \Lambda_B \times \sin\theta$)
is half the wavelength of the radar signal (λ_0).

A.3. Composite surface theory (for microwave radar)

Compared to a HF radar, the histogram of the raw data recorded by a microwave radar unfortunately does not always show two marked peaks. This is mostly explained by the *composite surface theory* [*e.g.* Hasselmann *et al.* 1985], which basically considers that the small water waves (ripples) that backscatter microwaves (**Section A.2**) are advected by larger waves:

- *The two peaks of the histogram can be mingled into a single one due to advection by larger waves* - Advection of ripples by larger water waves produces a broadening in the histogram of the raw radar data for two reasons: (1) the larger water waves travel at a variety of speeds (depending on their own phase speed) and (2) they tilt the ripples (producing variations in the local incidence angle of the radar). In cases where this broadening is not too severe, two peaks can still be detected in the histogram of the raw radar data. However, severe broadening causes the two peaks to be mingled into a single broad one [*e.g.* Contreras & Plant 2004, Plant *et al.* 2005].

- *One of the two peaks of the histogram can be sometimes difficult to discern* - Under certain circumstances, it may be difficult to discern one of the two theoretical peaks in the histogram of the raw radar data. Above all, many studies performed in water tanks [*e.g.* Gade *et al.* 1998, Plant *et al.* 2004] and on the sea [*e.g.* Plant & Keller 1990] have shown that this can be due to the wind (even a light air, with a speed as low as ≈ 0.3 m/s), which produces an asymmetry in the roughness at the water surface (unless the wind is blowing perpendicularly to the radar's line-of-sight): (1) if a radar is looking upwind, it should record a histogram with a larger peak corresponding to the advancing ripples ($V_s + c_B$); (2) on the opposite, if the radar is looking downwind, it should record a histogram with a larger peak corresponding to the receding ripples ($V_s - c_B$).

For the above reasons, complex algorithms can be necessary to properly estimate an average velocity (V_s) from the histogram of raw data recorded by a microwave radar: if data are not processed carefully (*i.e.* if the midway point between the two theoretical peaks of the histogram is not extracted), the estimated surface velocity (V_s) can be erroneous up to $\pm\ c_B$, where c_B is the phase speed of the water waves (ripples) that backscatter the radar signal [Plant *et al.* 2005].

It is worth noting that the composite surface theory has been extensively verified when the roughness at a water surface is due to the wind, but not so much when it is due to water turbulence:

- *Roughness due to the wind* - The effect of a roughness caused by the wind has been investigated in the sea [*e.g.* Plant & Keller 1990] and in water tanks exposed to a blower [*e.g.* Plant *et al.* 2004]. As said, the wind can produce a skewed histogram of the raw radar data. [(9)]

- *Roughness due to the distortion of larger water waves* - The effect of a roughness due to the distortion of larger water waves (*i.e.* the production of the so-called *bound waves*) has been also investigated in the sea [*e.g.* Plant 2003] and in water tanks exposed to a mechanical agitation [*e.g.* Gade *et al.* 1998] or to a blower [*e.g.* Plant *et al.* 2004]. In this case, the effect of the distortion of larger waves on the response of microwave radars was found to be quite similar to the effect of the wind [Plant *et al.* 2005].

[(9)] An extreme situation is when the wind is blowing nearly in front or behind the radar (under no rain conditions): in this case, the smaller peak in the histogram of the raw radar's data can be so small (in fact, it can disappear into the noise baseline), that it becomes very difficult to properly process the radar data, unless the wind direction is known [Plant *et al.* 2005].

- *Roughness due to the rain* - Rain drops falling on a water surface typically produces ring waves. In this case, the two theoretical peaks in the histogram of the raw radar data can be easily identified [*e.g.* Contreras & Plant 2004, Plant *et al.* 2005].

- *Roughness due to the turbulence* - The effect of a roughness due to the water turbulence still has not been investigated extensively. Although some recent studies have been performed in rivers in the last fifteen years, some experts [Plant *et al.* 2005] consider that "*when the short waves are produced by turbulence, the azimuth angle dependence of their intensity has not been well established to date*". In this context, it is worth noting that we could not find in the literature a study about Doppler radar performed in laboratory channels with flowing water.

A.4. Far field condition

From a theoretical point of view, the data obtained with a radar are more difficult to interpret if the distance between its antenna and a target (L) is too small [Ulaby *et al.* 1981]. For this reason, radars are usually operated according to the *far field condition*, *i.e.* so that the distance L is larger than a minimum value (L_F); for a circular antenna (as the one of the studied radar), it is:

$$L_F = \frac{2\ D^2}{\lambda_0} \qquad \text{(A.2)}$$

where D is the antenna diameter (m) and λ_0 is the wavelength of the radar signal (m). For the studied radar, λ_0 = 9 mm (f_0 = 34.7 GHz) and $D \approx$ 50 mm (diameter of the front part), which gives: $L_F \approx$ 0.6 m. So, it must be recognized that the radar has not been operated according to the far field condition during laboratory testing (**Section 3.2**); rather, it has been located at a distance to the water surface between 0.1 and 0.3 m, which corresponds to the so-called *Fresnel zone* [Ulaby *et al.* 1981].

A.5. Footprint of the studied radar

Under the far field condition (**Section A.4**), the area "seen" by a radar (*footprint*) can be estimated with simple geometrical calculations (**Fig. A.2**). Assuming that the signal is sent as a cone, this area should be an ellipse with the following longitudinal (D_L) and transversal (D_T) diameters:

$$D_L = L \cos(\theta) \left[\tan\left(\theta + \frac{\gamma}{2} \right) - \tan\left(\theta - \frac{\gamma}{2} \right) \right] \quad \text{(A.3a)}$$

$$D_T = 2 L \tan\left(\frac{\gamma}{2} \right) \quad \text{(A.3b)}$$

where L (m) is the distance between the radar and the water surface in the line-of-sight direction, θ (°) is the local incidence angle and γ (°) is the aperture of the cone containing most of the radar signal (*3 dB beam width*). Considering γ = 12° (Stalker Radar 2008) and θ ≈ 45° (the typical incidence angle of the radar used during this study), it gives $D_T \approx 0.2 \times L$ and $D_L \approx 0.3 \times L$.

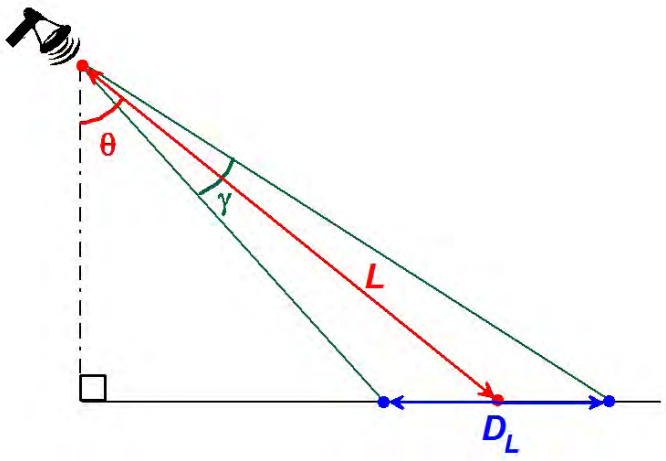

Fig. A.2. Diagram of the radar footprint, in the plane of incidence (assuming that the radar is operated according to the *far field condition*).

Appendix B - Some details about water waves

B.1. Phase speed

The *phase speed* of a water wave is the velocity at which its shape (crests and troughs) moves along the water surface. For a deep open channel (water depth h large enough, so that: $k \times h >> 1$), the phase speed of a (gravity - capillary) water wave is [*e.g.* Ulaby *et al.* 1986]:

$$c = \sqrt{\frac{g}{k} + \frac{\sigma_w \, k}{\rho_w}} \qquad \text{(B.1)}$$

where $k = 2 \times \pi / \Lambda$ is the angular wavenumber (m^{-1}), Λ is the water wavelength (m), σ_w is the water's surface tension ($\approx 73 \times 10^{-3}$ N/m), ρ_w is the water density (≈ 1000 kg/m^3) and g is the acceleration of gravity (≈ 9.8 m/s^2). [(10)] For instance, the water waves expected to backscatter the signal of the studied radar should have a wavelength $\Lambda_B \approx 6$ mm (**Section A.2**); in this case, their phase speed should be $c_B \approx 0.3$ m/s.

[(10)] According to **Eq. B.1**, the phase speed of water waves must have a minimum value ($c_{min} \approx 0.23$ m/s) at one particular wavelength, which is: $\Lambda_{min} \approx 17$ mm. The properties of water waves with a wavelength larger than Λ_{min} are mostly controlled by the acceleration of gravity (*i.e.*, the first term of **Eq. B.1**): this is the *gravity wave regime*. On the opposite, the properties of water waves with a wavelength smaller than Λ_{min} are mostly controlled by the surface tension (*i.e.*, the second term of **Eq. B.1**): this is the *capillary wave regime*.

B.2. Stokes drift

The *Stokes drift* is a displacement of a water surface produced by the water waves themselves. Due to this phenomenon, a water surface moves faster than what advects it (the combined effect of the wind and the underlying current). This is because: (1) water particles rotate into the waves (*orbital motion*) in the direction of what advects the surface and (2) the speed of particles at the crests of a water wave is forward and slightly larger than the speed at the troughs, which is backward. For gravity water waves ($\Lambda >> 17$ mm), the Stokes drift at the water surface is [*e.g.* Monismith & Fong 2004]:

$$U_s = (a\,k)^2 \; c_{GW} \; \frac{\cosh(2\,k\,h)}{2\,\sinh^2(k\,h)} \tag{B.2a}$$

$$c_{GW} = \sqrt{\frac{g\,\tanh(k\,h)}{k}} \tag{B.2b}$$

where $k = 2 \times \pi / \Lambda$ is the wavenumber (m^{-1}), Λ is the wavelength (m), a is the wave amplitude (m), h is the water depth (m) and g is the acceleration of gravity (≈ 9.8 m/s^2). Two situations must be distinguished for the studied channels (**Table 1**):

- *Laboratory channels* - Considering: $h \geq 0.03$ m, $\Lambda \leq 0.2$ m and the fact that there was no breaking waves (that is: $a \leq 0.072 \times \Lambda$ [*e.g.* Gemmrich 2005]), a rather small Stokes drift was expected in the laboratory: $U_s \leq 0.14$ m/s.

- *Field channels* - Considering: $h \geq 0.25$ m and $\Lambda \leq 1$ m, the Stokes drift may have been sometimes large in the field: $U_s \leq 0.27$ m/s, even in the case of non-breaking waves.

B.3. Froude number

Considering a channel with shallow water waves and a trapezoidal cross section, the *Froude number* (*Fr*) was computed as:

$$Fr \approx \frac{V_m}{\sqrt{g\left(\frac{B+b}{2B}\right)h}} \quad \text{(B.3)}$$

where V_m is the mean water velocity in the channel (m/s), h is the water depth (m), b is the channel width at the bottom (m), B is the channel width at the surface (m) and g is the acceleration of gravity (≈ 9.8 m/s^2). The mean velocity was estimated as: $V_m = \kappa \times V_s$, where V_s is the surface velocity (m/s) measured at the center of a channel and κ is a coefficient (-). Considering that most of the studied channels were wide (*aspect ratio* $\nu > 5$), we took $\kappa \approx 0.85^2 \approx 0.72$ [*e.g.* ISO 2007, Le Coz *et al.* 2010].

Appendix C - Some details about current meters

C.1. Pitot tube

The Pitot tube is a current meter often taken for granted today (Brown 2003). Although often used in Aerodynamics (*e.g.* to determine the speed of an airplane), it is not anymore commonly used in Hydraulics. However, the Pitot tube is still attractive to measure large water velocities, at least in the laboratory.

A commercial Pitot tube (model 630, Lambrecht, Germany) connected to two water manometers was used to determine the velocity in laboratory channels (**Fig. C.1**). In this case, the water velocity was computed as:

$$V = \sqrt{2\ g\ \Delta h} \tag{C.1}$$

where Δh is the measured difference in level between the two manometers (m) and g is the acceleration of gravity (= 9.78 m/s^2 in Cuernavaca, Mexico). The theoretical uncertainty of the Pitot tube is deduced from the previous equation [JCGM 2008]:

$$U(V) = \sqrt{\frac{g}{2\ \Delta h}}\ \times\ U(\Delta h) \tag{C.2}$$

where $U(\Delta h)$ is the uncertainty of the measured difference in level; during this study, an uncertainty [p = 0.95] of ± 0.01 m was easily achieved.

(a) **(b)** **(c)**

Fig. C.1. Pitot tube: (a) instrument, (b) water manometers and (c) laboratory testing.

C.2. Particle image velocimetry

To estimate the surface velocity at the "Tepalzolco" rapid (**Fig. 1c**), a simple PIV technique was used: (1) some marks were left on the channel edges (spacing = 1 m), (2) a video camera placed in the center of the channel was used to film the water surface (upstream and then downstream, speed of recording = 30 frames/s), (3) assuming that the camera's objective was not producing too much distortion, the recorded images were digitally processed so that a grid was drawn over the plane corresponding to the water surface and (4) the number of image-frames necessary for a floating object (whitecap) to travel over a given distance was manually counted. A single velocity data was then estimated as:

$$V = \Delta L / \Delta t \tag{C.3}$$

where ΔL is the travelled distance (m) and Δt is the measured duration (s). The theoretical uncertainty of the technique is deduced from the previous equation [JCGM 2008]:

$$U(V) = V \times \sqrt{\left(\frac{U(\Delta L)}{\Delta L} \right)^2 + \left(\frac{U(\Delta t)}{\Delta t} \right)^2} \tag{C.4}$$

At the "Tepalzolco" rapid, the water velocity was $V \approx 9$ m/s and the observable distance was ΔL = 3 m, which gives $\Delta t \approx 0.3$ s. Considering $U(\Delta L) = 0.05$ m and $U(\Delta t) = 0.016$ s (*i.e.* half a video frame), the uncertainty [$p = 0.95$] for a single velocity estimation was expected to be $U(V) = 0.5$ m/s. Because this is not accurate, 30 replicates were made, which should give the following uncertainty for the average: $U(V^{\bullet}) = U(V) / \sqrt{30} = 0.1$ m/s. It is worth noting that a classical LSPIV algorithm [*e.g.* Le Coz *et al.* 2010] would have been difficult to use at the "Tepalzolco" rapid, because the flow field was not steady at a short time scale due to rolling waves passing every ≈ 6 seconds. In this case, the simple PIV technique was used to estimate three surface velocity data: in front, at the crest and behind the rolling waves. After that, a mean value was computed from these data (**Table C.1**).

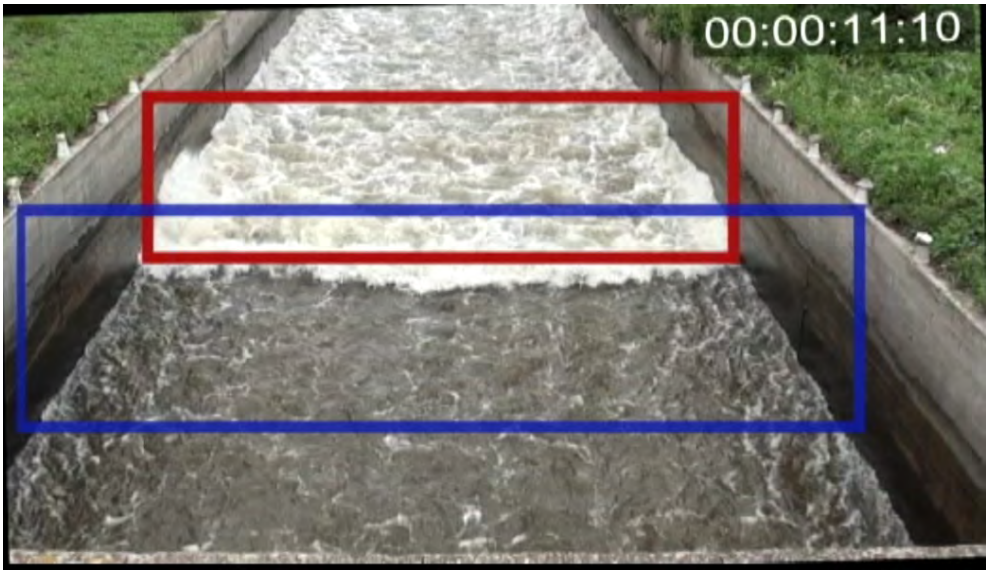

Fig. C.2. PIV at the "Tepalzolco" rapid: digitized image.

Table C.1. Surface velocities estimated by a simple PIV technique at the middle part of the "Tepalzolco" rapid (code "F.4" of **Table 1**).

Camera orientation	Estimated velocity (m/s) [(a)]			
	In front of the rolling waves	At the crest of rolling waves	Behind the rolling waves	Mean value
Looking Upstream	8.0 (0.3)	9.5 (0.3)	9.1 (0.3)	8.9
Looking Downstream	7.7 (0.6)	9.7 (0.6)	9.1 (0.5)	8.8

[(a)] The mean and the standard deviation of 30 replicates are shown.

Appendix D - Some details about field testing

D.1. Wind conditions during field testing

Except at the "Valsequillo" channel (case "F.3") where the wind was blowing more than usual (**Fig. B.1a**), we have unfortunately not measured the wind speed during the testing of the handheld radar. However, some qualitative observations -based on human sensations and the observation of trees- about the wind direction and intensity have been made in the field (**Table D.1**). These observations suggest that the hypothesis of a wind effect (**Section 4.4**) is not sufficient to explain the observed velocity differences between the radar looking upstream and downstream (ΔV_s):

- *"Valsequillo" channel (case "F.3")* - It must be recognized that the wind was coming from upstream during testing at the "Valsequillo" channel. Nonetheless, the velocity difference ΔV_s was larger *at a specific part* of the channel, *i.e.* near the right bank (**Fig. 8c**). This could be due to more turbulent flow conditions (**Fig. D.1b**), caused by a channel curvature located upstream.

- *"Tepalzolco" rapid (case "F.4")* - Although no attempt was made to determine the wind speed and direction very close to the water surface, there was virtually no wind ≈ 2 m above the surface during testing at the "Tepalzolco" rapid. In this case, the velocity difference ΔV_s (**Fig. 8d**) could be due to the passing of rolling waves (**Fig. D.1c**).

- *"Amacuzac" river (cases "F.5a" and "F.5b")* - During testing at the "Amacuzac" river, the velocity difference ΔV_s was larger *at a specific part* of the river, *i.e.* between the middle and the left bank (**Figs. 8e-f**). This could be due to more turbulent flow conditions with water waves breaking downward (**Fig. D.1d**), probably caused by a rocky bottom located upstream.

- *"Las Estacas" channel (case "F.1")* - Although the wind was coming from downstream during testing at the "Las Estacas" channel, there was no evidence of negative velocity differences ΔV_s (**Fig. 8b**), as one would expect in case of a wind effect (**Section 4.4**).

Table D.1. Wind conditions during the field testing of the studied radar.

Code	Site	Wind [(a)]		Comment about the water surface at the studied channels
		Intensity	Coming from	
F.1	*Las Estacas* (29/12/2011)	Light breeze	Downstream	Some boils at the middle part of the channel
F.2	*Tuxpan* (07/06/2011)	Calm	*n.a.*	Low agitated water surface
F.3	*Valsequillo* (20/06/2012)	Gentle breeze	Upstream	More turbulence (and foam) near the right bank
F.4	*Tepalzolco* (21/06/2012)	Calm	*n.a.*	Rapid with rolling waves
F.5a	*Amacuzac* (15/08/2012)	Light air	Changing direction	River with breaking waves between the middle part and the left bank
F.5b	*Amacuzac* (21/08/2012)			

[(a)] According to the human sensations and the observation of trees.

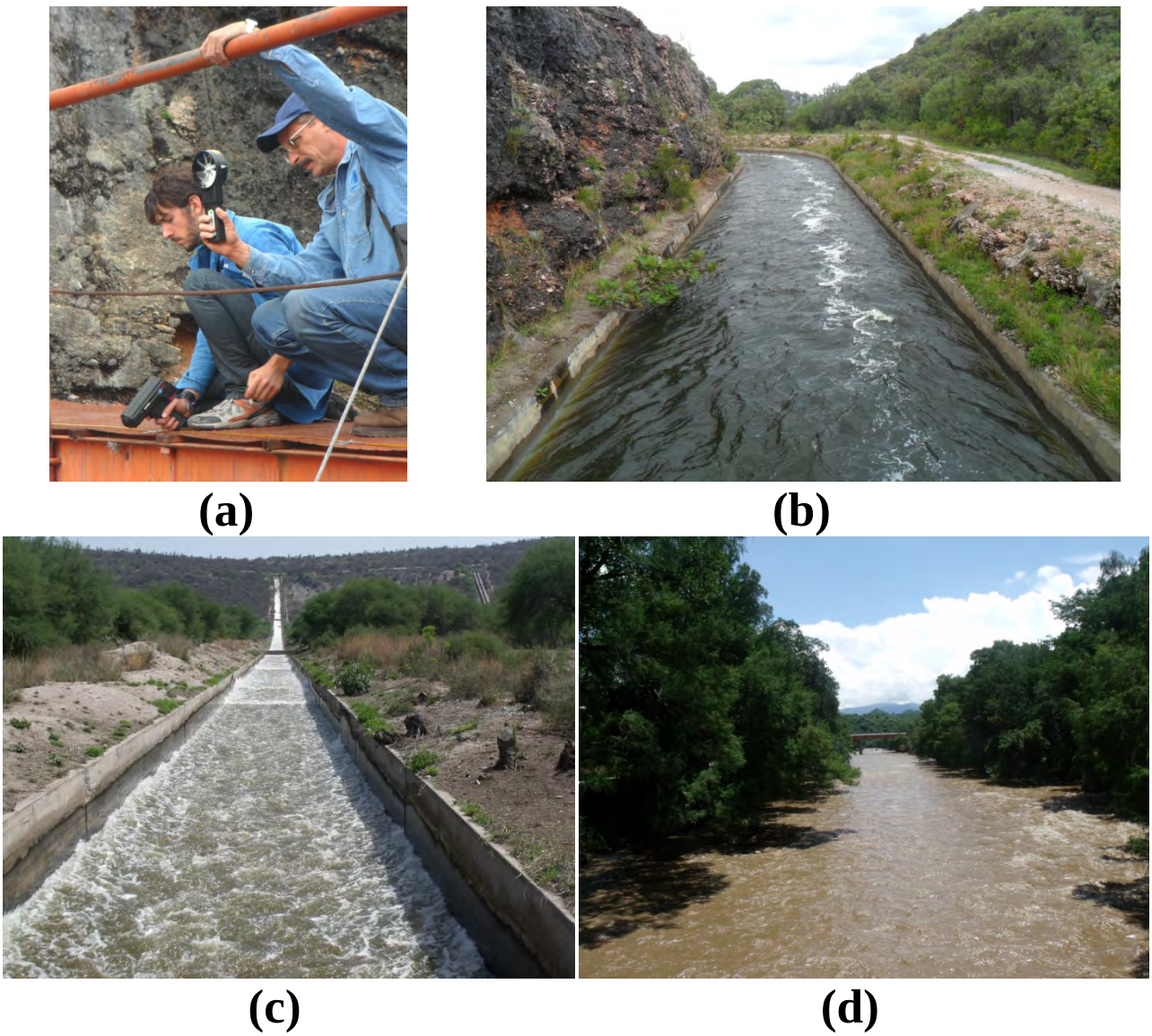

Fig. D.2. Water surface at some channels where the radar was tested:
(a) "Valsequillo" channel (code "F.3") where the maximum wind intensity (a gentle breeze) was observed, (b) "Valsequillo" channel (code "F.3") seen from upstream and with more turbulence (and foam) near the right bank, (c) "Tepalzolco" rapid (code "F.4") seen from downstream and with rolling waves and (d) "Amacuzac" river (code "F.5") seen from downstream and with breaking waves near the left bank.

D.2. A hypothesis about microwave radars under clear weather

The fact that the tested radar does not provide the same average velocity data when looking downstream or upstream (**Section 4.4**) could be due to a *combination* of two phenomena:

- *Orbital motion into water waves* - Due to the orbital motion into waves, a water surface does not move only horizontally, but also vertically. A Doppler radar should be sensitive to this vertical movement [*e.g.* Romeiser & Thompson 2000, Plant *et al.* 2004, Chapron *et al.* 2005]. Nevertheless, if the water waves that backscatter its signal (*i.e.* ripples for a microwave radar) cover the entire water surface, this phenomenon should only broaden the histogram of velocities recorded by the radar, but not affect the average velocity computed from this histogram (unless the averaging time is short; [*e.g.* Romeiser & Thompson 2000]).

- *Uneven spatial distribution of ripples* - Under clear weather conditions (no rain drops or wind blowing), the ripples that backscatter microwaves (at least those emitted by a *Ka-band* radar, as the tested one) are however probably not evenly distributed over the water surface. Many of these are indeed produced by the distortion of steep larger waves, and in this case, several theoretical [*e.g.* Hung & Tsai 2009] and laboratory [*e.g.* Gade *et al.* 1998, Plant *et al.* 2004] studies have shown that their distribution depends on the wavelength of the carrier waves (Λ_C): although ripples tend to be located over the whole surface of small carrier waves ($\Lambda_C \leq$ 0.05 m), they tend to be located only at the forward part of intermediate waves ($0.05 \leq \Lambda_C \leq$ 0.3 m; due to wave distortion) [(11)] and at the crest of the largest ones ($\Lambda_C \geq$ 0.3 m; due to micro-breaking).

[(11)] In this case, the wavelength of ripples is larger near the crest of larger waves and smaller further from the crest.

So, if a microwave radar only detects ripples located on a very specific part of larger waves, the histogram of the recorded radial velocities should be shifted by a quantity that is the projection of the velocity vector at this specific part ($\vec{V_{GW}}$) over the radar line-of-sight. In this case, the average velocity computed from the histogram of radial velocities would depend on the radar incidence angle. Given this argumentation, the fact that the studied radar estimated a lower water velocity when looking downstream instead of when looking upstream could be qualitatively explained if the ripples that backscatter its signal are located at the forward and bottom part of larger water waves, because $\vec{V_{GW}}$ is oriented upward and backward in this case (**Fig. D.3**).

So, the question is open to know if the trend observed during this study is due to an imperfection in the studied radar or to a general feature of microwave Doppler radars when used in open channels under clear weather conditions. If this is a general feature, the question that follows would be to know if the trends can be corrected with an appropriate data processing algorithm (see **Section A.3**); unfortunately, the one used by the studied radar is a "black box" and it is not possible to retrieve the raw radar data (*i.e.* a time-series of Doppler shifts recorded during one velocity determination) in order to guess how they are processed.

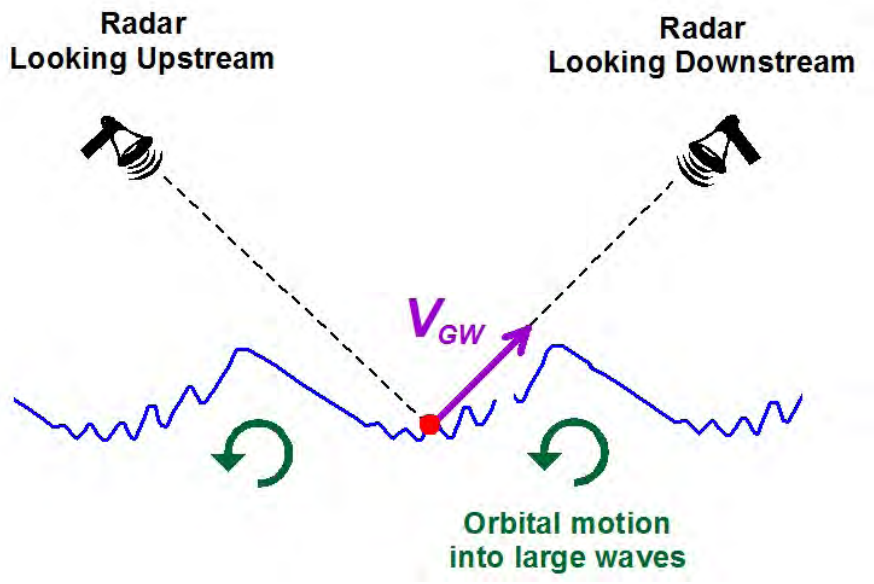

Fig. D.3. Hypothesis for qualitatively explaining why the tested radar was usually estimating a lower velocity when looking downstream instead of upstream: under clear weather conditions, the ripples that backscatter the radar signal would be located only at the forward and bottom part of larger waves, where the surface velocity vector ($\vec{V}_{GW}$) is oriented upward and backward.

References

Brown GO. (2003). – Henry Darcy's perfection of the Pitot tube. *In*: Brown GO, Garbrecht JD & Hager WH (ed.), *Henry PG Darcy and other pioneers in hydraulics: contributions in celebration of the 200th birthday of Henry Philibert Gaspard Darcy*. ASAE, Reston (VA). pp. 14-23.

Chapron B, Collard F, Ardhuin F. (2005). – Direct measurements of ocean surface velocity from space: Interpretation and validation. *J. Geophysical Res.* **110**: paper C07008.

Contreras RF, Plant WJ. (2004). – Ku-band backscatter from the Cowltiz River: Bragg scattering with and without rain. *IEEE Trans. Geosci. Rem. Sensing* **42 (7):** 1444-1449.

Corato G, Moramarco T, Tucciarelli T. (2011). – Combining flow routing modelling and direct velocity measurement for optimal discharge estimation. *Hydrol. Earth Syst. Sci. Discuss.* **8:** 2699–2738.

Costa JE, Cheng, RT, Haeni FP, Melcher N, Spicer KR, Hayes E, Plant W, Hayes K, Teague C, Barrick D. (2006). – Use of radars to monitor stream discharge by noncontact methods. *Water Resour. Res.* **42:** paper W07422.

Decatur Electronics. (2011). – *SVR (Surface Velocity Radar) - User's Manual (Rev. 02/08/2011)*. Decatur Electronics Europe Inc., Kokkola (Finland). 45 p.

Dramais G, Le Coz J, Gallavardin A, Duby P, Hauet A, Laronne J. (2011). – Mesures sans contact des débits de crue: avancées et perspectives. *In*: Mono M. O. (ed.), *Proc. ECOTECHS' 2011 (Capteurs et Systèmes de Mesures pour les applications environnementales)*, CEMAGREF, 17-18 October 2011, Montoldre (France).

Dramais G., Le Coz J., Le Boursicaud R., Hauet A., Lagouy M. (2013). – Jaugeage para radar mobile: protocole et résultats [paper HM-044]. *In*: Biton B. (ed.), *Proc. "Hydrométrie 2013 (SHF)"*, Paris, 15-16 May 2013. [ISBN 978-2-906831-94-0]

Elfouhaily TM, Guérin CA. (2004). – A critical survey of approximate scattering wave theories from random rough surfaces. *Waves in Random and Complex Media* **14:** 1–40.

Fujita I, Watanabe H, Tsubaki R. (2007). – Development of a non-intrusive and efficient flow monitoring technique: the space-time image velocimetry (STIV). *Int. J. River Basin Management* **5 (2):** 105-114.

Fulton J, Ostrowski J. (2008). – Measuring real-time streamflow using emerging technologies: radar, hydroacoustics, and the probability concept. *J. Hydrol.* **357:** 1-10.

Gade M, Alpers W, Ermakov SA, Huehnerfuss H, Lange PA. (1998). – Wind wave tank measurements of bound and freely propagating short gravity-capillary waves. *J. Geophys. Res.* **103**: 21697-21710.

Gemmrich J (2005). – On the occurrence of wave breaking. *In*: Muller P. & Henderson D. (ed.), *Proc. 4th Aha Huliko'a Hawaian Winter Workshop on Rogue Waves*, Univ. Hawaii, School of Ocean and Earth Science and Technology, 24-28 January 2005. pp 123-130.

Hasselmann K, Raney RK, Plant WJ, Alpers W, Shuchman RA, Lyzenga RA, Rufenach CL, Tucker MJ. (1985). – Theory of SAR ocean wave imaging: a MARSEN view. *J. Geophys. Res.* **90**: 4659-4686.

Hubbard EF, Schwarz GE, Thibodeaux KG, Turcios LM. (2001). – Price current-meter standard rating development by the U.S. Geological Survey. *J. Hydraul. Eng.* **127:** 250–257.

Hung LP, Tsai WT. (2009). – The formation of parasitic capillary ripples on gravity–capillary waves and the underlying vortical structures. *J. Physical Oceanography* **39**: 263-289.

ISO. (2007). – *Hydrometry - Measurement of liquid flow in open channels using current-meters or floats (ISO 748: 2007).* International Organization for Standardization (ISO), Genève.

JCGM. (2008). – *Evaluation of measurement data — Guide to the expression of uncertainty in measurement (JCGM 100:2008).* Working Group 1 of the Joint Committee for Guides in Metrology (JCGM/WG1), Paris.

Jendzurski J, Paulter NJ. (2008). – Calibration of speed enforcement down-the-road radars. *J. Res. Natl. Inst. Stand. Technol.* **114:** 137-148.

Le Coz J, Hauet A, Dramais G, Pierrefeu G. (2010). – Performance of image-based velocimetry (LSPIV) applied to flash-flood discharge measurements in Mediterranean rivers. *J. Hydrol.* **394:** 42-52.

Lee JS, Julien PY. (2006). – Electromagnetic wave surface velocimetry. *J. Hydraul. Eng.* **132:** 146-153.

Lipa BJ, Barrick DF. (1986). – Extraction of sea state from HF radar sea echo. *Radio Sci.* **21**: 81-100.

Monismith SG, Fong DA. (2004). – A note on the potential transport of scalars and organisms by surface waves. *Limnology and Oceanography* **49:** 1214-1217.

Negrel J, Kosuth P, Bercher N. (2011). – Estimating river discharge from earth observation measurements of river surface hydraulic variables. *Hydrol. Earth Syst. Sci.* **15**: 2049–2058.

Newton RU, McEvoy KI. (1994). – Baseball throwing velocity: a comparison of medicine ball training and weight training. *J. Strength & Conditioning Res.* **8:** 198-203.

Plant WJ. (2003). – A new interpretation of sea-surface slope probability density functions. *J. Geophys. Res.* **108 (C9):** 3295.

Plant WJ, Keller WC. (1990). – Evidence of Bragg scattering in microwave Doppler spectra of sea return. *J. Geophys. Res.* **95 (C9):** 16299-16310.

Plant WJ, Dahl PH, Giovanangeli JP, Branger H. (2004). – Bound and free surface waves in a large wind-wave tank. *J. Geophys. Res.* **109**: Paper C10002.

Plant WJ, Keller WC, Hayes K. (2005). – Measurement of river surface currents with coherent microwave systems. *IEEE Transactions on Geoscience and Remote Sensing* **43:** 1242-1257.

Rantz SE & Col. (1982). – *Measurement and computation of streamflow: Volume 1 - Measurement of stage and discharge (USGS Water Supply Paper 2175)*. US Government Printing Office, Wahsington DC. 284 p.

Romeiser R, Thompson DR. (2000). – Numerical study on the along-track interferometric radar imaging mechanism of oceanic surface currents. *IEEE Trans. on Geosci. and Remote Sensing* **38**: 446-458.

Smith KJ, Janson SD, Smith KT. (2003). – *Radar device for measuring water surface velocity.* US Patent 2003/0058158.

Song HS, Zhang LZ, Liu W. (2006). – Comparing test and analysis on flow velocity measurement with handheld radar current meter. *[Chinese] Automation in Water Resources and Hydrology* **1:** 30-32.

Stalker Radar. (2008). – *Stalker Pro II SVR - Operator Manual (document 011-0098-00 Rev. C).* Stalker Radar / Applied Concepts Inc., Plano (TX). 23 p.

Sung-Kee Y, Dong-Su K, Kwon-Kyu Y, Meyong-Su K, Woo-Yul J, Jun-Ho L, Yong-Seok K, Ho-Jun Y. (2012). – Comparison of flood discharge and velocity measurements in a mountain stream using electromagnetic wave and surface image. *[Korean] Journal of the Environmental Sciences* **21:** 739-747.

Szupiany RN, Amsler ML, Best JL, Parsons DR. (2007). – Comparison of fixed-and moving-vessel flow measurements with an aDp in a large river. *J. Hydraul. Eng.* **133 (12):** 1299-1309.

Tominaga A, Nezu I, Ezaki K, Nakagawa H. (1989). – Three-dimensional turbulent structure in straight open channel flows. *J. Hydraul. Res.* **27 (1):** 149-173.

Turnipseed DP, Sauer VB. (2010). – *Discharge measurements at gaging stations ("U. S. Geological Survey techniques and methods", Book 3, Section A, Chapter 8).* USGS, Denver (CO).

Ulaby FT, Moore RK, Fung AK. (1981). – *Microwave remote sensing: active and passive, Vol. I - Fundamentals and radiometry*. Addison-Wesley, Advanced Book Program, Reading, Norwood (MA).

Ulaby FT, Moore RK, Fung AK. (1986). – *Microwave remote sensing: active and passive, Vol. III - From theory to applications*. Addison-Wesley, Advanced Book Program, Reading, Norwood (MA).

Zolezzi G, Zamler D, Laronne JB, Salvaro M, Piazza F, Le Coz J, Welber M, Dramais G. (2011). – A systematic test of surface velocity radar (SVR) to improve flood discharge prediction (Poster H51I-1332). *In*: *AGU Fall Meeting 2011*, AGU, San Francisco (CA), 5-9 December 2011. [only the abstract is available]

Table 1. Sites where the handheld radar has been tested.

Code	Location	Name	Channel type	Shape	Channel walls	Length of the straight part (m)	Channel slope (β, °)	Bottom width (b, m)	Surface width (b_s, m)	Water level (h, m)	*Aspect ratio* ($\nu = b/h$)	Surface velocity (V_s, m/s) [a]	*Froude number* (Fr) [b]	Reference techniques [c]	No. of data
L.1	IMTA Laboratory	*Canal Largo*	Horizontal	Rectangular	Glass	50	0.0	1.0	1.0	0.15 - 0.30	3 - 7	0.4 - 1.2	0.2 - 0.4	ADV, EMV, Pitot	7
L.2	"	Outlet of *Coyotes*	"	"	Cement	10	0.0	1.0	1.0	≈ 0.40	≈ 2	0.4	≈ 0.2	EMV	1
L.3	"	Outlet of *Hervidero*	"	"	"	8	0.0	0.8	0.8	0.28	3	0.25	0.2	ADV, Pitot, EMV	1
L.4	"	Outlet of *Naranjos*	"	Trapezoidal	Acrylic	1	0.0	0.7	0.8	0.03	26	2.7	3.6	ADV, Pitot, EMV	1
L.5	"	Inlet of *Vista Hermosa*	"	"	"	2	1.1	0.3	0.4	0.25	1	1.2	0.7	EMV	1
L.6	"	Spillway of *Coyotes*	Inclined	"	Cement	6	2.9	0.4	0.5	0.07 - 0.08	5 - 6	2.3 - 2.7	1.9 - 2.3	ADV, Pitot, EMV	3
L.7	"	Spillway of *Hervidero*	"	"	Acrylic	5	5.4	0.3	0.4	0.05 - 0.07	5 - 7	2.4 - 3.3	2.3 - 3.4	ADV, EMV	3
L.8	"	Spillway of *Naranjos*	"	"	"	3	7.2	0.7	0.8	0.03 - 0.04	22 - 26	2.1 - 2.7	2.7 - 3.4	ADV, Pitot, EMV	2
L.9	"	Spillway of *Vista Hermosa*	"	"	"	3	17.9	0.3	0.3	0.03 - 0.06	5 - 11	2.5 - 4.2	2.2 - 5.3	Pitot, ADV, EMV	4 [d]
L.10	"	*Canal Inclinable*	Tilting	Rectangular	Glass	18	0.2 - 1.0	0.6	0.6	0.08 - 0.24	3 - 7	1.4 - 2.1	0.6 - 2.2	ADV, Pitot	14
L.11	CFE Laboratory	*Fondo (Yesca)*	Covered	"	Acrylic	5	0.0	0.6	0.6	≈ 0.30	≈ 2	2.2 - 4.5	≈ 0.8 - 1.7	Pitot	9
L.12	"	Inlet of *Aeradores (Yesca)*	Horizontal	"	"	≈ 5	0.0	0.3	0.3	0.25	1	3.6	1.7	Pitot, ADV	1
L.13a	"	Spillway MI of *Aeradores (Yesca)*	Inclined	"	"	≈ 4	27.6	0.3	0.3	0.20	1.5	5.5 - 5.6	2.7 - 2.8	Pitot	3 [4]
L.13b	"	Spillway C of *Aeradores (Yesca)*	Inclined	"	"	≈ 5	27.6	0.3	0.3	0.05 - 0.14	2 - 7	5.0 - 5.7	3.2 - 5.0	Pitot	3
F.1	18° 43' 24.10" N 99° 6' 42.60" W	*Las Estacas* (29/12/2011)	Irrigation	Trapezoidal	Concrete	300	0.0	1.7	6.0	1.65	2	1.2	0.3	ADV, EMV	31
F.2	19° 32' 22.20" N 100° 29' 13.10" W	*Tuxpan* (07/06/2011)	"	Rectangular	"	200	0.0	6.0	6.0	0.98	6	0.9	0.2	ADV	12
F.3	18° 54' 42.21" N 98° 5' 55.35" W	*Valsequillo* (20/06/2012)	"	"	"	50	0.0	8.0	8.0	2.82	3	2.4	0.3	ADV	16
F.4	18° 40' 55.50" N 97° 43' 28.00" W	*Tepalzolco* (21/06/2012)	Rapid with rolling waves	"	"	950	2.0	5.0	5.0	≈ 0.25	≈ 20	≈ 8.7	≈ 4.0	PIV	11
F.5a	18° 35' 59.65" N 99° 22' 29.47" W	*Amacuzac* (15/08/2012)	River with breaking waves	Irregular	Earth and stones	50	0.0	≈ 38	38	1.00	40	2.5	0.6	*n.a.*	16
F.5b	"	*Amacuzac* (21/08/2012)	"	"	"	"	"	"	38	0.98	40	2.5	0.6	MCM	17

Table 2. Techniques used as a reference for estimating the velocity at the surface of open channels.

Type of meter	Model (manufacturer)	Conditions for use	Maximum velocity (m/s)	Height of the sensing part (m)	Depth at which the top of the sensing part was immersed (m)	Measuring duration (s)	Expected uncertainty (m/s) [$p = 0.95$]
EMV (electromagnetic velocimeter)	"Flo-Mate" (Marsh-McBirney, Frederick, Maryland)	The sensing part must be oriented in front of the main stream	6 (claimed)	0.03	≈ 0.02	40	Claimed by the manufacturer: $U(V) = 0.034 + 0.04 \times V$ (m/s)
ADV (acoustic Doppler velocimeter)	"FlowTracker" [(a)] (Sontek/YSI, San Diego, California)	The sensing part must be placed at ≈ 0.12 m at one side from where the velocity is measured	4 (claimed)	0.01	"	60	Claimed by the manufacturer: $U(V) = 0.005$ (m/s), if $V \leq 0.5$ m/s; $U(V) = 0.02 \times V$ (m/s), if $V \geq 0.5$ m/s
Pitot tube (connected to water manometers)	"Model 630" (Lambrecht, Goettingen, Germany)	Velocity computed from: **Eq. C.1**	No theoretical limit	"	"	≈ 240	Theoretical: **Eq. C.2** with $U(\Delta h) = 0.01$ m
MCM (mechanical current meter)	"Price AA" [(b)] (Rossbach, Mexico)	Meter connected to a cable with a sounding weight of 7 kg	≈ 3.5 (nominal)	0.10	≈ 0.20	60	Nominal: $U(V) = 0.01$ (m/s), if $V \leq 0.5$ m/s; $U(V) = 0.02 \times V$ (m/s), if $V \geq 0.5$ m/s
PIV (particle image velocimetry)	"Handycam HDR-CX110" (Sony, Mexico)	Velocity computed from: **Eq. C.3**	No theoretical limit	*n.a.*	Water surface is filmed	≈ 300 (filmation)	Theoretical: **Eq. C.4**

[(a)] Firmware vers. 2.5

[(b)] Meter rated at IMTA

Anexo A.3

Cartel presentado en un congreso internacional

SHF Hydrométrie 2013
Mesures et incertitudes
Paris, 15-16 Mai 2013
CONTRÔLES RADAR FRÉQUENTS

TESTING A HANDHELD RADAR TO MEASURE THE WATER VELOCITY AT THE SURFACE OF CHANNELS

S. Tamari, F. García, J. I. Arciniega-Ambrocio, A. Porter

e-mail: tamari@tlaloc.imta.mx

IMTA Instituto Mexicano de Tecnología del Agua

ABSTRACT – *The ability of a handheld radar to measure water velocity at the surface of open channels was tested. When looking upstream, the radar was estimating water velocity within ± 0.3 m/s at medium velocities (from 0.3 to 3 m/s) and ± 10 % of the measured value at larger velocities. When looking downstream, the radar was tending to underestimate water velocity; is it a feature of microwave radars when used in open channels under clear weather conditions ?*

1. INTRODUCTION

Among the non-contact instruments to measure water velocity in open channels, two handheld radars are available on the market since ten years. Due to the lack of information about these instruments, one model was tested in the laboratory and in the field.

The handheld radar can be easily transported from one site to another, which makes it possible to rapidly test it under several flow conditions.






2. MATERIALS AND METHODS

2a. Sites for testing

- *Wide range of velocities* (from 0.3 to > 6 m/s)
- *Several types of open channels and flow conditions* -The radar was tested in the laboratory (13 sites) and in the field (5 sites).
- *Clear weather conditions* - Low wind (not more than a gentle breeze) and no rain.
- *No oil at the water surface.*

2b. Protocol for using the radar

- *Radar oriented in the main-stream direction*
- *Radar looking upstream / downstream*
- *Radar as close as possible to the surface*
- *Intermediate incidence angle* - Relative incidence angle (θ) between 45 to 50° for moderately inclined channels (β ≤ 10°) and between 50 to 60° for steeper channels.
- *Measurements taken rather quickly* (≈ 40 s).

2c. Reference techniques

- An "*ADV*" (sensor top at ≈ 2 cm below the surface) was usually taken as the reference at low to medium velocities (< 2.5 m/s).
- A "*Pitot tube*" (top at ≈ 2 cm below surface) was usually taken as the reference at larger velocities (up to ≈ 6 m/s).
- A "*Price AA*" was taken as the reference for testing in a river.
- A simple "*PIV*" technique was taken as the reference for testing in a rapid.


3. RESULTS AND DISCUSSION

The radar was estimating water velocity with an uncertainty similar to what was expected at the beginning of the study, and slightly larger than that reported for other microwave radars that have been tested in rivers. Nevertheless, the radar was tested over a large set of water velocities (including > 4 m/s) and channel types.

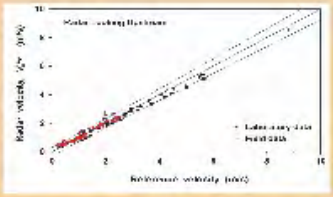

The radar was usually estimating a lower velocity when looking downstream instead of upstream. The difference was larger where the water surface was more irregular (due to breaking or rolling waves). This trend could have a physical meaning [Tamari *et al.* 2013, submitted]...

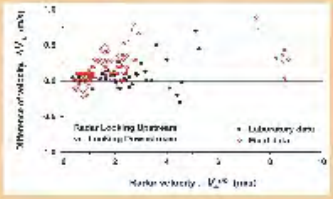

4. CONCLUSION

The tested radar estimates water velocity with an uncertainty consistent with what was expected. Although not very accurate, this type of instrument is easy to use: it makes it attractive to quickly estimate discharge and safely investigate how water flows during a flood or others difficult access conditions.

More studies are necessary to know how microwave radars work in open channels and under clear weather. Meanwhile, it is a good precaution to compare -whenever possible- the velocities obtained with a radar looking upstream and downstream.

Anexo B.1

Software para determinar las fugas en edificios con tinaco

"CLIC"

SOFTWARE PARA DETERMINAR
LAS FUGAS DE AGUA EN EDIFICIOS CON TINACO

CÓDIGO FUENTE

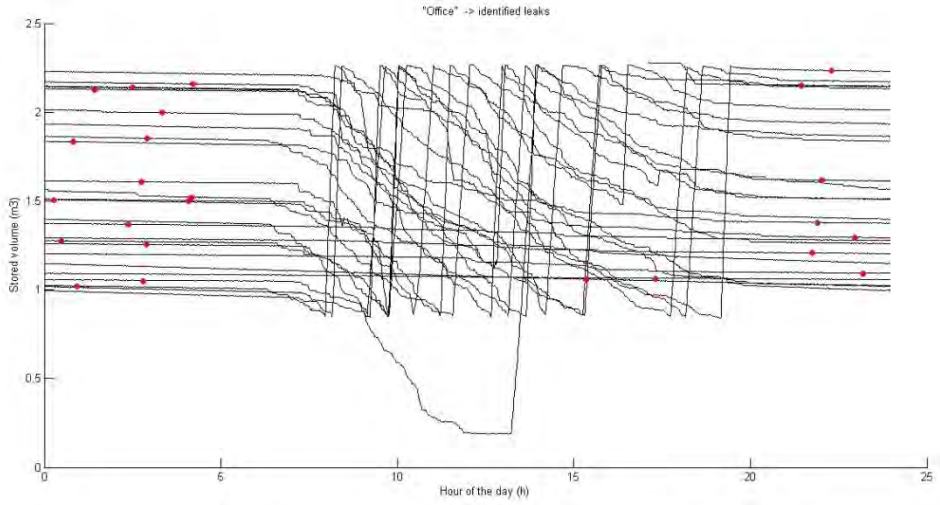

S. Tamari

Diciembre de 2013

Tamari S. 2013. "CLIC": software para determinar las fugas de agua en edificios con tinaco (código fuente). Jiutepec, Mor.: Instituto Mexicano de Tecnología del Agua.

```
% ************************************************************************
% Objectivo:  Programa (Matlab) para determinar las fugas de agua en un
%             edificio con tinaco, mediante un análisis de los cambios
%             de tirante en el tinaco medidos durante varios dias.
%
% Referencia: Tamari S & Ploquet J. (2012). Determination of
%             leakage inside buildings with a roof tank.
%             Urban Water J., Vol. 9(5), pp. 287-303.
%
% Datos:   1. El programa lee un archivo de texto con 2 columnas:
%             + Columna 1 = Tiempo acumulado              (dias)
%             + Columna 2 = Tirante medido en el tinaco   (m)
%
%          2. El nombre del archivo de datos crudo y el valor de los
%             parametros para realizar los calculos se definen al
%             inicio de este programa, en la sección 'menu' (donde se
%             pueden agregar casos).
%
% Notas:   1. Con la opción 'klis = 1', el programa busca automaticamente
%             los extrema locales (es decir, los tirantes minima y maxima)
%             en los datos de tirante medidos en el tinaco; para hacerlo,
%             el programa utiliza 2 parametros: 'tolhini' y 'tolhfin'.
%
%             Con la opción 'klis = -1', el programa utiliza una lista
%             de índices pre-definida para los extrema locales:
%             minima ('imin') y maxima ('imax').
%
%          2. El programa utiliza un parametro ('tolh') para extraer los
%             cambios de tirante en el tinaco que se consideran como
%             significativos.
%
%          3. Después de haber determinado la fuga de agua de algun dia,
%             el programa realiza dos pruebas estadisticas para saber si
%             este valor de fuga es confiable o dudoso.
%
%          4. Las unidades que maneja internamente el programa son:
%             horas, metros y litros.
%
% Funciones:  'trilis.m' = Funcion para suavizar los datos
%             'stati.m'  = Funcion para calcular percentiles
%             'hansen.m' = Test estadistico de Hansen (1992)
%
% Autor:      Serge Tamari (tamari@tlaloc.imta.mx)
%             Vers. 19 de diciembre de 2013 (para 'Matlab 2012')
% ************************************************************************


% Lee la tabla de datos crudos y define los parametros para los calculos
% ======================================================================
```

```
disp(' ')
disp(' ')
disp(' ***********************************************')
disp(' *              FUGAS DE AGUA                  *')
disp(' *         EN EDIFICIOS CON TINACO             *')
disp(' ***********************************************')
disp(' ')
disp([' Fecha de los calculos : ' date ])
disp(' ')

disp(' [1] Monitoreo en casa privada           ')
disp(' [2] Monitoreo en edificio del gobierno  ')
disp(' [3] Monitoreo en edificio privado       ')

nrep = input(' No prueba deseada -> ' );
disp(' ')

if (nrep == 1)

% ---------------------------------------------------------------------
  disp(' Lugar    : Tinaco de casa particular               ')
  disp(' Tinaco   : Cilíndrico - capacidad de 450 L         ')
  disp(' Inicio   : Domingo 9 de septiembre 2007 a las 14:31 ')
  disp(' Final    : Miercoles 3 de octubre 2007 a las 8:01   ')
  disp(' Datos    : 34,162 registros [una lectura / min.]    ')
  disp(' ')

  % Notas: [1] Baño que fuga durante 2 fines de semana (dias 7-8/21-23)
  %        [2] Periodo normal de trabajo
  %        [3] El tinaco se llena aprox. 98 veces (conteo manual)

  % Archivo de datos crudos
    code  = ' Occupied house '  ;
    eval(['load ' 'TI_casa.txt' ' -ascii'])
    datos     = TI_casa   ;
    toffset   =   14.50   ;  % Hora de inicio de la prueba (h)

  % Area del tinaco (m2)
    pi        = 3.1416 ;
    perimetro =   2.700    ;  % Perimetro externo del tinaco (m)
    espesor   =   0.005    ;  % Espesor de la pared del tinaco (m)
    diame     = perimetro / pi ;
    diami     = diame - 2. * espesor ;
    area      = pi * diami^2 / 4.    ;

  % Parametros de calculo
     tolh      =   0.0025  ; % Cambio significativo de tirante (m)
     tolhini   =  -0.00001 ; % Cambio maximo cuando no hay bomba (m)
     tolhfin   =   0.00050 ; % Cambio mínimo cuando arranca la bomba (m)
     klis      =   0       ; % Codigo para suavizar antes de buscar picos
     imin_manual = [ ]     ; % Lista manual de minima (para: klis = -1)
```

```
    imax_manual = [ ]     ; % Lista manual de maxima (para: klis = -1)
% ------------------------------------------------------------------

elseif (nrep == 2)

% ------------------------------------------------------------------
  disp(' Lugar    : Tinaco de un edificio del gobierno          ')
  disp(' Tinaco   : Cilíndrico - capacidad de hasta 2,500 L     ')
  disp(' Inicio   : Lunes 17 de marzo 2008 a las 16:45 [aprox.] ')
  disp(' Final    : Viernes 11 de abril 2008 a las 10:32        ')
  disp(' Datos    : 36,720 registros [una lectura / min.]       ')
  disp(' ')

  % Notas: [1] Vacaciones de Semana Santa (del al 23 de marzo)
  %        [2] El tinaco se rellena aprox. 22 veces (conteo manual)

  % Archivo de datos crudos
    code  = ' "Office" ' ;
    eval(['load ' 'TI_work.txt' ' -ascii'])
    datos     = TI_work   ;
    toffset   =   17.117 ;  % Hora de inicio de la prueba (h)

  % Area del tinaco (m2)
    pi        = 3.1416 ;
    perimetro =   5.000    ;  % Perimetro externo del tinaco (m)
    espesor   =   0.008    ;  % Espesor de la pared del tinaco (m)
    diame     = perimetro / pi ;
    diami     = diame - 2. * espesor ;
    area      = pi * diami^2 / 4.    ;

   % Parametros de calculo
     tolh      =   0.0034  ; % Cambio significativo de tirante (m)
     tolhini   =  -0.00001 ; % Cambio maximo cuando no hay bomba (m)
     tolhfin   =   0.00400 ; % Cambio mínimo cuando arranca la bomba (m)
     klis      =   0       ; % Codigo para suavizar antes de buscar picos
     imin_manual = [ ]     ; % Lista manual de minima (para: klis = -1)
     imax_manual = [ ]     ; % Lista manual de maxima (para: klis = -1)
% ------------------------------------------------------------------

elseif (nrep == 3)

% ------------------------------------------------------------------
  disp(' Lugar    : Edificio privado                            ')
  disp(' Tinaco   : Rectangular - capacidad mayor a 16,000 L    ')
  disp(' Inicio   : Domingo 24 de Agosto 2008 a las 19:12       ')
  disp(' Final    : Domingo 28 de Septiembre 2008 a las 14:30   ')
  disp(' Datos    : 54,492 registros [una lectura / min.]       ')
  disp(' ')

  % Notas: [1] Regreso a clases el 24 de agosto
  %        [2] Día nacional el 16 de septiembre
```

```
      % Archivo de datos crudos
        code  = '  "Building" ' ;
        eval(['load ' 'TI_build.txt' ' -ascii'])
        datos     = TI_build    ;
        toffset   =   19.200    ;  % Hora de inicio de la prueba (h)

      % Area del tinaco (m2)
        largo     =   5.050   ;  % Largo externo del tinaco (m)
        ancho     =   2.700   ;  % Ancho externo del tinaco (m)
        espesor   =   0.190   ;  % Espesor de la pared del tinaco (m)
        area      = (largo-2*espesor) * (ancho-2*espesor) ;

       % Parametros de calculo
         tolh      =   0.0045  ; % Cambio significativo de tirante (m)
         tolhini   =   0.00000 ; % Cambio maximo cuando no hay bomba (m)
         tolhfin   =   0.00010 ; % Cambio mínimo cuando arranca la bomba (m)
         klis      =   3       ; % Codigo para suavizar antes de buscar picos
         imin_manual = [ ]     ; % Lista manual de minima (para: klis = -1)
         imax_manual = [ ]     ; % Lista manual de maxima (para: klis = -1)
    % ------------------------------------------------------------------

    else

    % ------------------------------------------------------------------
        disp( ' Elegir una opcion valida !... ')
        return
    % ------------------------------------------------------------------

    end


% Otros parametros para realizar los calculos
% ===========================================

%- 'Cero' numérico
    epsilon = 1e-10   ;

 %- Criterio para definir los tirantes pequeños (= tinaco vacío)
 %  que seran eliminados del archivo de datos crudos
    hsmall = 0.000    ;  % Umbral para tirantes pequeños (m)

%- Criterios para apreciar la bondad de las estimaciones de fuga
    tolLc   =  1.20   ;  % Criterio para la prueba de Hansen (1992)
    tolR    = -0.90   ;  % Criterio para el coef. de correlacion lineal


% Despliega en pantalla los parametros de calculo
% ===============================================

     disp(' ')
```

```
    disp(' ')
    disp(' PARAMETROS DE CALCULO ')
    disp(' ===================== ')
    disp(' ')
    disp([ ' Criterio <Tolh> (m)    = ' num2str(tolh)    ])
    disp(' ')
    disp([ ' Criterio <Klis>        = ' int2str(klis)    ])
    if (klis >= 0)
      disp([ ' Criterio <Tolhini> (m) = ' num2str(tolhini) ])
      disp([ ' Criterio <Tolhfin> (m) = ' num2str(tolhfin) ])
    end
    disp(' ')
    disp([ ' Criterio <hsmall> (m)  = ' num2str(hsmall)   ])
    disp([ ' Criterio <TolLc>       = ' num2str(tolLc)    ])
    disp([ ' Criterio <TolR>        = ' num2str(tolR)     ])
    disp(' ')


% ************************************************************************

    disp(' ')
    disp(' ')
    disp(' PROCESA LOS DATOS CRUDOS ')
    disp(' ======================== ')


%  Procesa los datos crudos: (1) Extrae los datos crudos
% ======================================================

  %- Dimensiones de la tabla de datos
    [n0 ncol] = size(datos)     ;

    if ( ncol ~= 2 )
       disp(' ')
       error(' - FATAL ! No hay dos columnas de datos.')
    end

  %- Define los vectores de datos crudos
    t0 = datos(:,1)            ; % Tiempo acumulado (dias)
    h0 = datos(:,2)            ; % Tirante en el tinaco (m)

    if ( t0(1) ~= 0 )
       firstday  =  floor(t0(1))            ;
       firsthour =  24 * (t0(1) - firstday)  ;
       disp(' ')
       disp(' - WARNING ! Los tiempos no empiezan desde cero.')
       disp('   Verificar que <toffset> esta bien definido !')
       disp(' ')
       disp(['   Dia  de inicio <archivo> = ' num2str(firstday)  ])
       disp(['   Hora de inicio <archivo> = ' num2str(firsthour) ])
       disp(['   Hora de inicio <toffset> = ' num2str(toffset)   ])
```

```
   end

   disp(' ')
   disp([' Numero total de datos crudos = ' int2str(n0) ])

%- Elimina los datos de tirante pequeños (cf: cuando el tinaco se vacia)
   t0     = t0(h0 >= hsmall)  ; % Tiempo acumulado (dias)
   h0     = h0(h0 >= hsmall)  ; % Tirante en el tinaco (m)
   nsmall = length(h0)        ;

   if ( nsmall ~= n0 )
      disp(' ')
      disp(' - WARNING ! Se eliminan datos de tirante pequeños.')
      disp([' Numero de datos eliminados  = ' int2str(n0-nsmall) ])
      n0 = nsmall ;
      disp(' ')
      disp([' Numero total de datos crudos = ' int2str(n0) ])
   end


%  Procesa los datos crudos: (2) transforma los datos crudos
% ==========================================================

%- Cambio de unidades para los datos crudos
   t0     = t0 - t0(1)               ; % Empieza a 'cero'
   t0     = t0 + (toffset/24.)       ; % Agrega hora de inicio
   t0     = t0 * 24.                 ; % Convierte tiempo en horas
   tdia0  = t0 - 24. * floor(t0/24.) ; % Hora del dia (0-24 h)

%- Calcula los Volumenes de agua en el tinaco
   v0     = h0 * area                ; % Volumenes (m3)
   v0     = v0 * 1000.               ; % Volumenes (L)

%- Determina la duracion total de la prueba
   ttotal = max(t0) - min(t0)        ; % Duracion de la prueba (h)

   if ( ttotal ~= t0(n0)-t0(1) )
      disp(' ')
      error(' - FATAL ! Error en los datos de tiempo.')
   end

   disp(' ')
   disp([' Duracion total de prueba (h) = ' num2str(ttotal) ' <<<'  ])


%- Revisa los intervalos de muestreo
   dt0    = t0(2:n0) - t0(1:(n0-1))   ; % Intervalos de tiempo (h)
   dtraw  = mean(dt0)                 ; % Valor promedio (h)
   fdt0   = abs(dt0-dtraw) > (5/3600) ; % Tolerancia de 5 segundos
   ndt0   = sum(fdt0)                 ; % Busca valores estraños
```

```
     disp(' ')
     disp([' Intervalo de muestreo    (s) = ' num2str(dtraw*3600) ' <<<' ])

     if (ndt0 > 0)
        disp(' ')
        disp([' - WARNING ! Hay ' int2str(ndt0) ' intervalos raros...' ])
        disp([' - Intervalo mini  (s) = ' num2str(min(dt0)*3600) ])
        disp([' - Intervalo maxi  (s) = ' num2str(max(dt0)*3600) ])
     end


% ************************************************************************

     disp(' ')
     disp(' ')
     disp(' BUSCA LOS MINIMA Y MAXIMA LOCALES ')
     disp(' ================================= ')

% Busca los extrema locales: (1) inicializa el filtro
% ===================================================

  %- Código para el filtro de los cambios de tirantes
  %  0 : dato descartado
  %  1 : mínimo local
  %  2 : máximo local
  %  3 : dato de consumo guardado
  %  4 : dato de llenado guardado
     f = 0 * ones(n0,1)      ; % Inicializa el filtro


% Busca los extrema locales: (1) busqueda AUTOMATICA
% xxxxxxxxxxxxxxxxxxxxxxxxxxxxxxxxxxxxxxxxxxxxxxxxx

  if (klis >= 0)

        disp(' ')
        disp(' Busqueda automatica de extrema locales...')

% Busca los extrema locales: (1a) busca los 'minimos locales'
% ===========================================================

  %- Suaviza eventualmente los datos, antes de buscar los minimos
     if klis == 0
        hh0 = h0             ; % No suaviza los datos
     else
        hh0 = trilis(h0')    ; % Suaviza una primera vez
        for i = 1 : (klis-1) ; % Suaviza 'klis-1' veces
           hh0 = trilis(hh0) ;
        end
        hh0 = hh0'           ;
     end
```

```
  %- Busca 'aumentos abruptos' (cf: cuando se prende la bomba)
     for i = 4 : (n0-2)

        condi1 = hh0(i-3)-hh0(i-2) > tolhini ; % Sin bomba: h decrece
        condi2 = hh0(i-2)-hh0(i-1) > tolhini ; % Sin bomba: h decrece
        condi3 = hh0(i-1)-hh0(i)   > tolhini ; % Sin bomba: h decrece
        condi  = condi1 | condi2 | condi3    ; % Uno de los tres...

        condf1 = hh0(i+1)-hh0(i)   > 0       ; % Con bomba: h aumenta
        condf2 = hh0(i+2)-hh0(i+1) > tolhfin ; % Con bomba: h aumenta
        condf  = condf1 & condf2             ; % Los dos a la vez...

        conda1 = f(i-3) ~= 1                 ; % Evita un "doble minimo"
        conda2 = f(i-2) ~= 1                 ; % Evita un "doble minimo"
        conda3 = f(i-1) ~= 1                 ; % Evita un "doble minimo"
        conda  = conda1 & conda2 & conda3    ; % Los tres a la vez...

        if (condi & condf & conda)
           f(i) = 1                          ;  % Minimo encontrado
        end

     end

  %- Lista 'provisional' de los minima locales
     f(1)  = 1             ; % Clasifica 'a priori' el primer dato
     f(n0) = 1             ; % Clasifica 'a priori' el ultimo dato
     imin  = find(f == 1)  ; % Indices de minima locales
     nmin  = length(imin)  ; % Numero de minima locales


% Busca los extrema locales: (1b) busca los 'maximos locales'
% ===========================================================

  %- Se define el "maximo local" como siendo el maximo entre dos minimos
     for i = 1 : nmin-1

        n1 = imin(i)   + 1    ; % Inicio de un llenado
        n2 = imin(i+1) - 1    ; % Inicio del siguiente llenado
        xh = h0(n1:n2)        ; % Datos entre dos llenados
        xm = max(xh)          ; % Maximo local entre dos llenados
        k  = find(xh == xm)   ; % Indice de (de los) maxima local(es)
        k  = k(1)             ; % Guarda una sola solucion

        f(n1+k-1) = 2         ; % Maximo encontrado

     end

  %- Lista 'provisional' de los maxima locales
     imax = find(f == 2)   ; % Indices de maxima locales
     nmax = length(imax)   ; % Numero de maxima locales
```

```
% Busca los extrema locales: (1c) busca los 'minimos locales'
% ============================================================
% Es una nueva busqueda, porque se cometen pequeños errores
% cuando se suavizan los datos...

  %- Borra la lista anterior de minima locales
     for i = 1 : n0
        if (f(i) == 1)
           f(i) = 0 ;
        end
     end

  %- Se define el "minimo local" como siendo el minimo entre dos maximos
     for i = 1 : nmax-1
        n1 = imax(i)   + 1    ; % Inicio de un llenado
        n2 = imax(i+1) - 1    ; % Inicio del siguiente llenado
        xh = h0(n1:n2)        ; % Datos entre dos llenados
        xm = min(xh)          ; % Maximo local entre dos llenados
        k  = find(xh == xm)   ; % Indice de (de los) minima local(es)
        k  = k(1)             ; % Guarda una sola solucion
        f(n1+k-1) = 1         ; % Minimo encontrado
     end

  %- Lista 'provisional' de los minima locales
     imin = find(f == 1)   ; % Indices de maxima locales
     nmin = length(imin)   ; % Numero de maxima locales


% Busca los extrema locales: (1d) clasifica primer dato y ultimo dato
% ===================================================================

     f(1)  = 1             ; % Clasifica 'a priori' el primer dato
     f(n0) = 1             ; % Clasifica 'a priori' el ultimo dato

  %- Vuelve a clasificar el primer y el ultimo dato del archivo
     if ( h0(1) > h0(imax(1)) )
        f(1)         = 2      ; % Primer dato = cambio a 'maximo'
        f(imax(1))   = 0      ; % Reemplaza el dato
     end

     if ( h0(n0) > h0(imax(nmax)) )
        f(n0)         = 2     ; % Ultimo dato = cambio a 'maximo'
        f(imax(nmax)) = 0     ; % Reemplaza el dato
     end


% Busca los extrema locales: (2) definicion MANUAL de los extremas
% xxxxxxxxxxxxxxxxxxxxxxxxxxxxxxxxxxxxxxxxxxxxxxxxxxxxxxxxxxxxxxx
```

```
 elseif (klis == -1)

        disp(' ')
        disp(' Se utiliza una lista pre-definida de extrema locales...')

% Busca los extrema locales: (2a) datos pre-definidos
% ===================================================
%- Los vectores que contienen los indices de los minima (imin) y
%  maxima (imax) locales deben de estar pre-definidos: esto se logra
% graficando los datos crudos ('plot(i:n0,h0)') y utilizando 'ginput'...

        imin = imin_manual  ;
        imax = imax_manual  ;
        nmin = length(imin) ;
        nmax = length(imax) ;

   %- Verifica las listas de minima y maxima
        if (nmin == 0) |(nmax == 0)
           disp(' ')
           error(' FATAL - No hay una lista pre-definida de extrema')
        end

        if (abs(nmin-nmax) > 1)
           disp(' ')
           error(' FATAL - Numeros de minima y maxima incompatibles')
        end

   %- Define los valores del filtro 'f' (1= minimo 2= maximo)
        for k = 1:nmin
           f( imin(k) ) = 1 ;
        end

        for k = 1:nmax
           f( imax(k) ) = 2 ;
        end

% Busca los extrema locales: (2b) clasifica los primer y ultimo datos
% ===================================================================

  %- Verifica que el primer y el ultimo dato aun no son clasificados !
     if (imin(1) <= 1) | (imax(1) <= 1)
        disp(' ')
        errror(' FATAL - No clasificar manualmente el primer dato !')
     end

     if (imin(nmin) >= n0) | (imax(nmax) >= n0)
        disp(' ')
        errror(' FATAL - No clasificar manualmente el ultimo dato !')
     end

  %- Clasifica el primer y el ultimo dato del archivo
```

```
     if ( imin(1) < imax(1) )
        f(1)          = 2       ; % Primer dato = 'maximo'
     else
        f(1)          = 1       ; % Primer dato = 'minimo'
     end

     if ( imin(nmin) > imax(nmax) )
        f(n0)         = 2       ; % Ultimo dato = 'maximo'
     else
        f(n0)         = 1       ; % Ultimo dato = 'minimo'
     end

 else
   disp(' ')
   disp(' FATAL - valor de <klis> mal definido ...')
 end


% Busca los extrema locales: (3) lista definitiva
% ===============================================

  %- Lista 'definitiva' de los minima y maxima locales
     imin = find(f == 1)       ; % Indices de minima locales
     nmin = length(imin)       ; % Numero de minima locales
     imax = find(f == 2)       ; % Indices de maxima locales
     nmax = length(imax)       ; % Numero de maxima locales


% Busca los extrema locales: (4) clasifica el archivo de datos
% ============================================================

  %- Verifica los numeros de minima y maxima
     if ( abs(nmax-nmin) > 1 )
        disp(' ')
        error( ' - FATAL ! Error en el conteo de extrema.')
     end

     disp(' ')
     disp([' Numero de minimos locales = ' int2str(nmin) ' <<< ' ])
     disp([' Numero de maximos locales = ' int2str(nmax) ])

  %- Clasifica el archivo de datos en 4 categorias (variable "kdata")
  %- y define indices para buscar cambios significativos
     if (f(1) == 1) & (f(n0) == 1)

        kdata = 1 ; % Empieza con minimo, termina con minimo
        kneg  = 0 ;
        dneg  = 1 ;
        kpos  = 1 ;
        dpos  = 0 ;
```

```
    elseif (f(1) == 2) & (f(n0) == 2)

       kdata = 2 ; % Empieza con maximo, termina con maximo
       kneg  = 1 ;
       dneg  = 0 ;
       kpos  = 0 ;
       dpos  = 1 ;

    elseif (f(1) == 1) & (f(n0) == 2)

       kdata = 3 ; % Empieza con minimo, termina con maximo
       kneg  = 1 ;
       dneg  = 1 ;
       kpos  = 0 ;
       dpos  = 0 ;

    elseif (f(1) == 2) & (f(n0) == 1)

       kdata = 4 ; % Empieza con maximo, termina con minimo
       kneg  = 0 ;
       dneg  = 0 ;
       kpos  = 1 ;
       dpos  = 1 ;

    else
       disp(' ')
       error( ' - FATAL ! Error al inicio o al final del archivo.')
    end


% ************************************************************************

    disp(' ')
    disp(' ')
    disp(' CONSUMO PROMEDIO ESTIMADO CON LOS EXTREMOS LOCALES ')
    disp(' ================================================= ')

% Busca los decrementos de volumen desde un maximo hasta un minimo
% ================================================================

  %- Busqueda de los indices de los extrema para hacer el calculo
    if (kdata == 1)        ; % Empieza con minimo, termina con minimo
       ipicmax = imax(1 : nmax)   ;
       ipicmin = imin(2 : nmin)   ;
    elseif (kdata == 2)    ; % Empieza con maximo, termina con maximo
       ipicmax = imax(1 : nmax-1) ;
       ipicmin = imin(1 : nmin)   ;
    elseif (kdata == 3)    ; % Empieza con minimo, termina con maximo
       ipicmax = imax(1 : nmax-1) ;
       ipicmin = imin(2 : nmin)   ;
    elseif (kdata == 4)    ; % Empieza con maximo, termina con minimo
```

```
        ipicmax = imax(1 : nmax)   ;
        ipicmin = imin(1 : nmin)   ;
     else
        disp(' ')
        error(' FATAL - Error en la clasificacion del archivo')
     end

  %- Calculo de "pico a pico"
     sumdv   =  sum( v0(ipicmax) - v0(ipicmin) ) ;
     sumdt   =  sum( t0(ipicmax) - t0(ipicmin) ) ;
     Qmean0  = - sumdv / sumdt ;

  %- Calculo eliminando los picos (porque pueden ser mal estimados)
     sumdv   =  sum( v0(ipicmax+1) - v0(ipicmin-1) ) ;
     sumdt   =  sum( t0(ipicmax+1) - t0(ipicmin-1) ) ;
     Qmean1  = - sumdv / sumdt ;

     disp(' ')
     disp(' Consumo promedio durante la prueba [usando extrema locales] ')
     disp(' ')
     disp(['  - Consumo [pico a pico]  (L/h) = ' num2str(Qmean0) ' <<<' ])
     disp(['  - Consumo [fuera de pico](L/h) = ' num2str(Qmean1) ' <<<' ])


% ************************************************************************

     disp(' ')
     disp(' ')
     disp(' EXTRAE LOS DATOS ')
     disp(' ================ ')

% Extrae los datos: (1) busca decrementos significativos ('consumos')
% ====================================================================

  %- Algoritmo de busqueda
     for k = 1 : (nmax-kneg)

        i     = imax(k)           ; % Inicia desde un maximo local
        j     = i + 1             ; % Inicializa 'j'
        jstop = imin(k+dneg) - 1  ; % Termina antes de un minimo

        while (j < jstop) & (j < (n0-1))

            tolhh = tolh          ; % Inicializa criterio estadistico

            while ((h0(i)-h0(j)) < tolhh) & (j < jstop)

               j = j + 1          ; % No hay cambio

             %-------------------------------------------------------
             %- SE VUELVE 'MAS ESTRICTO' PARA LOS FLUJOS PEQUEÑOS
```

```
            %- PORQUE LOS DATOS YA NO SON 'BIEN' AUTO-CORRELACIONADOS
            %- CUANDO EL INTERVALO DE TIEMPO ES MAYOR A 2 h
              if ( (t0(j)-t0(i)) > 2.) & ( (t0(j)-t0(i)) <= 6.)
                 tolhh = 1.5 * tolh    ;
              elseif ( (t0(j)-t0(i)) > 6.)
                 tolhh = 2.0 * tolh    ;
              end
            %-------------------------------------------------------

           end

           f(j) = 3              ; % Punto encontrado

          if ( h0(j)-h0(jstop) < tolhh)
              f(j)  = 0          ; % Elimina eventualmente ultimo
          end

          i    = j               ; % Cambio de indice
          j    = i + 1           ; % Cambio de indice

       end

    end

  %- Lista de los indices encontrados
    ineg = find(f==3)            ; % Indices de consumos (-)
    nneg = length(ineg)          ; % Numero de  consumos (-)


% Extrae los datos: (2) busca incrementos significativos ('suministros')
% ======================================================================

  %- Algoritmo de busqueda

    for k = 1 : (nmin-kpos)

       i     = imin(k)           ; % Inicia desde un minimo local
       j     = i + 1             ; % Inicializa 'j'
       jstop = imax(k+dpos) - 1  ; % Termina antes de un maximo


       while (j < jstop) & (j < (n0-1))

           tolhh = tolh          ; % Inicializa criterio estadistico

           while ((h0(j)-h0(i)) < tolhh) & (j < jstop)

              j = j + 1          ; % No hay cambio

            %-------------------------------------------------------
            %- SE VUELVE 'MAS ESTRICTO' PARA LOS FLUJOS PEQUEÑOS
```

```
            %- PORQUE LOS DATOS YA NO SON 'BIEN' AUTO-CORRELACIONADOS
            %- CUANDO EL INTERVALO DE TIEMPO ES MAYOR A 2 h
              if ( (t0(j)-t0(i)) > 2.) & ( (t0(j)-t0(i)) <= 6.)
                 tolhh = 1.5 * tolh    ;
              elseif ( (t0(j)-t0(i)) > 6.)
                 tolhh = 2.0 * tolh    ;
              end
            %-------------------------------------------------------

           end

           f(j) = 4              ; % Punto encontrado

          if ((h0(jstop)-h0(j)) < tolhh)
              f(j)  = 0          ; % Elimina eventualmente ultimo
          end

          i    = j               ; % Cambio de indice
          j    = i + 1           ; % Cambio de indice

       end

    end

  %- Lista de los indices encontrados
     ipos = find(f==4)           ; % Indices de rellenos (+)
     npos = length(ipos)         ; % Numero de  rellenos (+)


% Extrae los datos: (3) filtro de los datos guardados
% ===================================================

     fg    = f(f>0)              ; % Codigos guardados (1,2,3,4)
     ng    = length(fg)          ; % Numero de valores guardados
     tg    = t0(f>0)             ; % Fechas guardadas (h)
     tdiag = tdia0(f>0)          ; % Horas del dia guardadas
     hg    = h0(f>0)             ; % Tirantes guardados (m)
     vg    = v0(f>0)             ; % Volumenes guardados (L)

     disp(' ')
     disp([' Numero de valores extraidos   = ' int2str(ng)      ])
     disp([' Proporcion de datos extraidos = ' num2str(ng/n0,2) ' <<< ' ])


% Extrae los datos: (4) duracion de los consumos / suministros
% ============================================================

     disp(' ')
     disp(' ')
     disp(' ANALIZA LA DURACION DE LOS CONSUMOS Y SUMINISTROS ')
     disp(' ================================================ ')
```

```
     tgmin = tg(fg==1)     ; % Fechas de los minimos (h)
     ngmin = length(tgmin) ; % Numero de valores
     tgmax = tg(fg==2)     ; % Fechas de los maximos (h)
     ngmax = length(tgmax) ; % Numero de valores

     if ( (ngmin ~= nmin) | (ngmax ~= nmax) )
        disp(' ')
        error(' - FATAL ! Problema en num. de extremos locales')
     end

     if (kdata == 1)      % Empieza con minimo, termina con minimo
        dtgs  = tgmax(1:ngmax)  - tgmin(1:(ngmin-1))  ;
        dtgc  = tgmin(2:ngmin)  - tgmax(1:ngmax)      ;
     elseif (kdata == 2)  % Empieza con maximo, termina con maximo
        dtgs  = tgmax(2:ngmax)  - tgmin(1:ngmin)      ;
        dtgc  = tgmin(1:ngmin)  - tgmax(1:(ngmax-1))  ;
     elseif (kdata == 3)  % Empieza con minimo, termina con maximo
        dtgs  = tgmax(1:ngmax) - tgmin(1:ngmin)      ;
        dtgc  = tgmin(2:ngmin) - tgmax(1:(ngmax-1))  ;
     elseif (kdata == 4)  % Empieza con maximo, termina con minimo
        dtgs  = tgmax(2:ngmax) - tgmin(1:(ngmin-1))  ;
        dtgc  = tgmin(1:ngmin) - tgmax(1:ngmax)      ;
     end

     tgs     = sum(dtgs)   ;
     tgc     = sum(dtgc)   ;
     tgtotal = tgs + tgc   ;

     if ( (tgtotal-ttotal) > epsilon ) ; % Valores numericamente iguales
        disp(' ')
        error(' - FATAL ! Problema en duracion de la prueba')
     end

    disp(' ')
    disp([' - Duracion de los consumos    (h)  = ' num2str(tgc) ' <<<'   ])
    disp(['   Proporcion temporal         (-)  = ' num2str(tgc/ttotal,2) ])
    disp(' ')
    disp([' - Duracion de los suministros (h)  = ' num2str(tgs)  ' <<<'  ])
    disp(['   Proporcion temporal         (-)  = ' num2str(tgs/ttotal,2) ])


% ************************************************************************

     disp(' ')
     disp(' ')
     disp(' ANALIZA LOS CAMBIOS SIGNFICATIVOS ')
     disp(' ================================= ')

% Analiza los cambios: (1) calcula los cambios significativos
% ===========================================================
```

```
% Flujos: positivo para 'consumo', negativo para 'suministro'

     nx    =  ng-1                          ; % Numero datos interpolados
     tx    = (tg(2:ng)+tg(1:(ng-1)))/2.     ; % Fechas interpoladas (h)
     tdiax = tx - 24. * floor(tx/24.)       ; % Hora del dia (0-24 h)
     hx    = (hg(2:ng)+hg(1:(ng-1)))/2.     ; % Tirantes interpolados (m)
     vx    = (vg(2:ng)+vg(1:(ng-1)))/2.     ; % Volumenes interpolados (L)
     dtx   = tg(2:ng) - tg(1:(ng-1))        ; % Intervalos de tiempo (h)
     dhx   = hg(2:ng) - hg(1:(ng-1))        ; % Cambios de tirante (m)
     dvx   = vg(2:ng) - vg(1:(ng-1))        ; % Cambio de volumen (L)

     tasax = - dhx ./ dtx                   ; % Tasa cambio tirante (m/h)
     phix  = - dvx ./ dtx                   ; % Flujos calculados (L/h)
     fx    =   (phix >= 0)                  ; % Filtro de los consumos


% Analiza los cambios: (2) estadistica sobre los intervalos de tiempo
% ====================================================================

     disp(' ')
     disp(' Estadistica sobre los intervalos de tiempo (h)   ')
     disp(' ')
     disp(['  - Promedio            = ' num2str( mean(dtx) )       ])
     disp(['  - Desviacion estándar = ' num2str( std(dtx)  )       ])
     disp(' ')
     disp(['  - Minimo              = ' num2str( stati(dtx,0) )   ])
     disp(['  - Primer cuartil      = ' num2str( stati(dtx,25) )  ])
     disp(['  - Mediana             = ' num2str( stati(dtx,50) )  ])
     disp(['  - Tercer cuartil      = ' num2str( stati(dtx,75) )  ])
     disp(['  - Maximo              = ' num2str( stati(dtx,100) ) ])
     disp(' ')
     disp(['  - Intervalos > 1 hora = ' num2str(sum(dtx>1.))       ])
     disp(['    CANTIDAD            = ' num2str(sum(dtx>1.),1)     ])
     disp(['    Proporción          = ' num2str(sum(dtx>1.)/nx,2)  ])
     disp(' ')
     disp(['  - Intervalos > 2 hora = ' num2str(sum(dtx>2.))       ])
     disp(['    CANTIDAD            = ' num2str(sum(dtx>2.),1)     ])
     disp(['    Proporción          = ' num2str(sum(dtx>2.)/nx,2)  ])
     disp(' ')
     disp(['  - Intervalos > 4 hora = ' num2str(sum(dtx>4.))       ])
     disp(['    CANTIDAD            = ' num2str(sum(dtx>4.),1)     ])
     disp(['    Proporción          = ' num2str(sum(dtx>4.)/nx,2)  ])
     disp(' ')
     disp(['  - Intervalos > 8 hora = ' num2str(sum(dtx>8.))       ])
     disp(['    CANTIDAD            = ' num2str(sum(dtx>8.),1)     ])
     disp(['    Proporción          = ' num2str(sum(dtx>8.)/nx,2)  ])


% Analiza los cambios: (3) Cambios de volumen, tirante...
% ======================================================
```

```
    wtotalc  = - sum( dvx(fx) )      ; % Total de consumos    (L)
    wdiarioc =   wtotalc/tgc         ; % Consumo promedio horario (L/h)

    wtotals  =   sum( dvx(~fx) )     ; % Total de suministros (L)
    wdiarios =   wtotals/tgs         ; % Suministro promedio horario (L/h)

    wdiff    =   sum(dvx)            ; % Balance absoluto (L)
    wrel     =   wdiff / wtotalc     ; % Balance relativo a consumos (-)

    disp(' ')
    disp(' Consumos durante la prueba [usando cambios significativos] ')
    disp(' ')
    disp([' - Consumos detectados     (m3) = ' num2str(wtotalc/1000) ])
    disp([' - Consumo promedio       (L/h) = ' num2str(wdiarioc) ' <<<' ])
    disp(' ')
    disp([' - Cambio tirante max. (mm/min) = ' num2str( max(tasax(fx))       *1000/60 )↙
])
    disp([' - Cambio tirante <99% (mm/min) = ' num2str( stati(tasax(fx),99) *1000/60 )↙
])
    disp([' - Cambio tirante <95% (mm/min) = ' num2str( stati(tasax(fx),95) *1000/60 )↙
])
    disp([' - Cambio tirante <90% (mm/min) = ' num2str( stati(tasax(fx),90) *1000/60 )↙
])
    disp([' - Cambio tirante medio(mm/min) = ' num2str( mean(tasax(fx))      *1000/60 )↙
])
    disp([' - Cambio tirante min. (mm/min) = ' num2str( min(tasax(fx))       *1000/60 )↙
])

    disp(' ')
    disp(' ')
    disp(' Suministros durante la prueba [usando cambios significativos] ')
    disp(' ')
    disp([' - Suministros detectados  (m3) = ' num2str(wtotals/1000) ])
    disp([' - Suministro promedio    (L/h) = ' num2str(wdiarios) ' <<<' ])
    disp(' ')
    disp([' - Cambio tirante max. (mm/min) = ' num2str( max(-tasax(~fx))       *1000/60↙
) ])
    disp([' - Cambio tirante <99% (mm/min) = ' num2str( stati(-tasax(~fx),99) *1000/60↙
) ])
    disp([' - Cambio tirante <95% (mm/min) = ' num2str( stati(-tasax(~fx),95) *1000/60↙
) ])
    disp([' - Cambio tirante <90% (mm/min) = ' num2str( stati(-tasax(~fx),90) *1000/60↙
) ])
    disp([' - Cambio tirante medio(mm/min) = ' num2str( mean(-tasax(~fx))      *1000/60↙
) ])
    disp([' - Cambio tirante min. (mm/min) = ' num2str( min(-tasax(~fx))       *1000/60↙
) ])

    disp(' ')
    disp(' ')
    disp(' Balance entre consumos y suministros durante la prueba ')
```

```
     disp(' ')
     disp(['  - Diferencia absoluta          (L) = ' num2str(wdiff )     ])
     disp(['    Dif. relativa a los consumos (-) = ' num2str(wrel,2) ' <<<' ])


% ************************************************************************

     disp(' ')
     disp(' ')
     disp(' ANALIZA LOS FLUJOS ')
     disp(' ================== ')

% Analiza los cambios: (1) Flujos
% ===============================
%- Flujos: positivos = consumos / negativos = suministros

     phic = phix(fx)  ;
     phis = phix(~fx) ;

     disp(' ')
     disp(' Estadistica sobre los flujos positivos = vaciados (L/h) ')
     disp(' ')
     disp(['  - Promedio            = ' num2str( mean(phic) )       ])
     disp(['  - Desviacion estándar = ' num2str( std(phic)  )       ])
     disp(' ')
     disp(['  - Minimo              = ' num2str( stati(phic,0) )   ])
     disp(['  - Maximo              = ' num2str( stati(phic,100) ) ])

     disp(' ')
     disp(' Estadistica sobre los flujos negativos = llenados (L/h) ')
     disp(' ')
     disp(['  - Promedio            = ' num2str(-mean(phis) )       ])
     disp(['  - Desviacion estándar = ' num2str( std(phis)  )       ])
     disp(' ')
     disp(['  - Minimo              = ' num2str(-stati(phis,0) )   ])
     disp(['  - Maximo              = ' num2str(-stati(phis,100) ) ])


% Analiza los cambios: (2) intensidades de (micro)fugas
% =====================================================

     disp(' ')
     disp(' ')
     disp(' ANALIZA LAS FUGAS [= FLUJOS MAS PEQUEÑOS] ')
     disp(' ========================================= ')

  %- Criterios para considerar una posible fuga
     ffuga = fx                          ; % Flujo positivo

  %- Lista de los periodos de la prueba
  %- La funcion 'floor' redondea hacia 'abajo'
```

```
    disp(' ')
    disp(' Se determina una fuga por cada periodo de 24 h ...')

    dti    = 24.                          ; % Periodo (24 h)
    txi    = dti * floor(tx/dti)          ; % Fechas redondeadas (h)
    tiini  = min(txi) + dti               ; % Primer periodo
    tifin  = max(txi) - dti               ; % Ultimo perido
    tilist = ( tiini : dti : tifin )      ; % Lista de periodos
    nlist  = length(tilist)               ; % Numero de intervalos

%- Busqueda de las fugas, periodo por periodo
    statf  = NaN * ones(nlist,9)          ; % Inicializa  %%% FUGAS %%%
    zmin   = NaN                          ;

    for i = 1 : nlist                     ; % quita un periodo @@@

       fti    = ffuga & (txi==tilist(i))  ; % Filtro por periodo
       z      = phix(fti)                 ; % Flujos guardados
       nz     = length(z)                 ; % Numero de valores
       zmin   = min(z)                    ; % Flujo minimo

       if (zmin == NaN)

          disp(' ')
          disp(' - WARNING - No se encontro fuga durante un periodo...')

       else

          indmin = find((phix==zmin)&fti) ; % Indice del minimo

          if (isempty(indmin))         ; % Ningun dato encontrado
             indmin = NaN                  ;
             zmin   = NaN                  ;
             disp(' ')
             disp(' - WARNING - Problema en la busqueda de fugas !...')
          elseif (length(indmin) > 1)     ; % En caso de duplicados
             indmin = indmin(1)            ; % Decision arbitraria
             disp(' ')
             disp(' - WARNING - Mas de un minima por dia...')
          end

          %-----------------------------------------------------------------
          % VERIFICA LA BONDAD DE LAS ESTIMACIONES DE FUGA, VERIFICANDO
          % QUE EL VOLUMEN EN EL TINACO DECRECE LINEALMENTE CON EL TIEMPO

          %- Vuelve a los datos crudos
            tbeg  = tx(indmin) - dtx(indmin)/2 ;
            tend  = tx(indmin) + dtx(indmin)/2 ;
            flin  = (t0 >= tbeg) & (t0 <= tend) ;
            tlin    = t0(flin)     ;
            vlin    = v0(flin)     ;
```

```
            nlin    = length(tlin) ;
            tdialin = tdia0(flin)  ;
            hlin    = h0(flin)     ;

          %- Criterio 1 - Estadistica 'Lc' de Hansen (1992)
             dat = [ vlin tlin ones(nlin,1) ]   ;

             [ Lc , Li , R2 , b ] = hansen(dat) ; % b(1)=slope  b(2)=origin

           %- Criterio 2 - Coeficiente de correlacion lineal
             coefR    = corrcoef(tlin,vlin)     ;
             coefR    = coefR(2)                ;

           %- DETERMINA LAS ESTIMACIONES DE FUGA MAS CONFIABLES
             if (Lc < tolLc) & (coefR < tolR)
                  statf(i,9) = 1               ; % DATO CONFIABLE
             else
                  statf(i,9) = 0               ; % DATO DUDOSO
             end
           %---------------------------------------------------------------

           statf(i,1)  =  tilist(i)         ; % Inicio del periodo (h)
           statf(i,2)  =  indmin            ; % Indice del minimo
           statf(i,3)  =  zmin              ; % Valor del minimo
           statf(i,6)  =  nz                ; % Numero de valores
           statf(i,7)  =  coefR             ; % Coef. Correl. Linear
           statf(i,8)  =  Lc                ; % Coef. de Hansen(1992)

        end

        if (length(z) >= 2)                 ; % Varias 'fugas'

           statf(i,4) = stati(z,1)          ; % Percentil 1%
           statf(i,5) = stati(z,2)          ; % Percentil 2%

        end

     end


 %- Procesa todas las estimaciones de fuga
     ileak = statf(:,2)              ; % Indice temporal de la fuga
     leak  = statf(:,3)              ; % Fuga (flujo minimo de cada dia)
     ileak = ileak(~isnan(leak))     ; % Elimina datos faltantes
     leak  = leak(~isnan(leak))      ; % Elimina datos faltantes

     disp(' ')
     disp(' Estimaciones de fuga = FLUJO MAS PEQUEÑO DEL DIA (L/h)    ')
     disp(' ')
     disp(['  - Numero de datos     = ' num2str(length(leak))    ])
     disp(' ')
```

```
    disp(['  - Promedio            = ' num2str(mean(leak)     ) ])
    disp(['  - Desviacion estándar = ' num2str(std(leak)      ) ])
    disp(' ')
    disp(['  - Minimo              = ' num2str(min(leak)      ) ])
    disp(['  - Maximo              = ' num2str(max(leak)      ) ])


 %- Procesa las estimaciones de fuga mas confiables
    fleak = statf(:,9) ;
    LEAK  = statf( logical(fleak) ,3 )         ; % Fugas mas confiables

    disp(' ')
    disp(' Estimaciones de fuga = DATOS MAS CONFIABLES (L/h)   ')
    disp(' ')
    disp(['  - Numero de datos     = ' num2str(length(LEAK))   ' <<< ' ])
    disp(' ')
    disp(['  - Promedio            = ' num2str(mean(LEAK)     ) ' <<< ' ])
    disp(['  - Desviacion estándar = ' num2str(std(LEAK)      ) ' <<< ' ])
    disp(' ')
    disp(['  - Minimo              = ' num2str(min(LEAK)      ) ' <<< ' ])
    disp(['  - Maximo              = ' num2str(max(LEAK)      ) ' <<< ' ])


 %- Síntesis sobre las estimaciones de fuga

    disp(' ')
    disp(' Evolucion temporal de las fugas = flujos más pequeños (L/h)   ')
    disp(' ')
    disp('    ------------------------------------------------------------------- ')
    disp('    Hora    Indice  FUGA    Flujo   Flujo   Numero  Coef.   Coef.  Fiable')
    disp('    (h)             (L/h)   perc.1% perc.2% valores   R     Hansen    ?  ')
    disp('    ------------------------------------------------------------------- ')

    fmt  = ' %7i %7i %7.2f %7.2f %7.2f %7i %7.3f %7.2f %7i  \n' ;
    fprintf( fmt , statf' )


% ************************************************************************

% Grafica (1): Tirantes, en función del tiempo
% ============================================

    %- Resetea el grafico
       nfig = 1             ;
       hfig = figure(nfig)  ;
       close(hfig)          ;
       figure(nfig)         ;
       hold on              ;

      %- Grafica los datos crudos (tiempo - tirante)
       plot(t0/24,h0,'k-','LineWidth',1.2)
```

```
     %- Grafica los extremos encontrados
        plot(t0(imin)/24,h0(imin),'r+','LineWidth',1.6,'Markersize',6.0)
        plot(t0(imax)/24,h0(imax),'go','LineWidth',2.2,'Markersize',3.0)

     %- Titulos de la grafica
        title( [ code ' -> identified extrema'] )
        xlabel( 'Time (d)' )
        ylabel( 'Water level (m)' )


% Grafica (2): Tirantes, en función del tiempo
% ============================================

     %- Resetea el grafico
        nfig = 2             ;
        hfig = figure(nfig)  ;
        close(hfig)          ;
        figure(nfig)         ;
        hold on              ;

     %- Grafica los datos crudos (tiempo - tirante)
     %- DATOS INTERPOLADOS = un poco distintos de los originales !
        plot(tx/24,hx,'k-','LineWidth',1.2)

     %- Ubica las fugas encontradas
        plot(tx(ileak)/24,hx(ileak),'ro','LineWidth',2.0,'Markersize',5.0)

        title( [ code ' -> identified leaks'] )
        xlabel( 'Time (d)' )
        ylabel( 'Water level (m)' )


% Grafica (3): Volumen, en funcion de la hora
% ===========================================

     %- Resetea el grafico
        nfig = 3             ;
        hfig = figure(nfig)  ;
        close(hfig)          ;
        figure(nfig)         ;
        hold on              ;

     %- Grafica los volumenes de agua en el tinaco
     %- Elimina unos datos 'para que no se crucen lineas' !
     %- DATOS ORIGINALES = un poco distintos a los interpolados !
        v00 = v0    ;
        dtu = 2. * dtraw ; % Umbral para eliminar datos
        for i = 1 : n0
           if (tdia0(i) < dtu) || (tdia0(i) > (24-dtu))
              v00(i) = NaN ;
```

```
            end
         end
         plot(tdia0,v00/1000,'k-','LineWidth',1.2)

      %- Ubica las fugas encontradas
         plot(tdiax(ileak),vx(ileak)/1000,'ro','LineWidth',3.5,'Markersize',3.0)

      %- Titulos de la grafica
         title( [ code ' -> identified leaks'] )
         xlabel( 'Hour of the day (h)' )
         ylabel( 'Stored volume (m3)' )


% Grafica (4): Fugas, en funcion del tiempo
% =========================================

      %- Resetea el grafico
         nfig = 4             ;
         hfig = figure(nfig)  ;
         close(hfig)          ;
         figure(nfig)         ;
         hold on              ;

      %- Grafica todas las fugas estimadas
         idia   = statf(:,1) / 24 ;
         fuga   = statf(:,3)      ; % Fuga del dia
         bar(idia,fuga)

      %- Ubica las estimaciones de fuga mas confiables
         fu  = statf(:,9)      ; % Filtro para las fugas 'confiables'
         plot(idia(logical(fu)),fuga(logical(fu)),'ro','LineWidth',4.0,'Markersize',5.0)

      %- Titulos de la grafica
         title( [ code ' -> reliable leaks in [red] '] )
         xlabel( 'Time (d)' )
         ylabel( 'Leak (L/h)' )

% ************************************************************************
   disp(' ')
   disp(' Fin del programa');
   disp(' ')
% ************************************************************************
```

```
function [ lj , li , r2 , b ] = hansen(dat)
%%%%%%%%%%%%%%%%%%%%%%%%%%%%%%%%%%%%%%%%%%%%%%%%%%%%%%%%%%%%%%%%%%%%%%%%%%%%%%%
% This Matlab function calculates the 'LC test' as reported in:
%
%          Hansen BE (1992)- Testing for parameter instability in linear
%          models. J. Policy Modeling, Vol.14, pp. 517-533.
%
% Input:   The matrix "dat" is a nx(k+1) matrix, with the dependent
%          (y) variable in the first colume, and the independent (x)
%          variables in the remaining columes.  If a constant is desired
%          in the regression, it should be included in the dat matrix.
%          The vector "datname" is a (k+1)x1 list of variable names,
%          for the columes of "dat".
%
% Author:  Bruce E. Hansen, Department of Economics
%          University of Wisconsin, Madison, WI 53706-1393
%          email: bhansen@ssc.wisc.edu
%          web:   http://www.ssc.wisc.edu/~bhansen/
%
% Version: Serge Tamari (30/04/2011) [slightly adapted from the original]
%%%%%%%%%%%%%%%%%%%%%%%%%%%%%%%%%%%%%%%%%%%%%%%%%%%%%%%%%%%%%%%%%%%%%%%%%%%%%%%

   n    = length( dat(:,1) )      ;
   k    = length( dat(1,:) ) - 1  ;
   y    = dat(:,1)                ;
   x    = dat(:,2:k+1)            ;
   m    = inv( x' * x )           ;
   b    = m * ( x' * y )          ;
   e    = y - x * b               ;

   xe   = x .* ( e * ones(1,length(x(1,:))) ) ;

   e2   = e.^2                    ;
   sig2 = mean(e2)'               ;
   e2m  = e2 - sig2               ;

   se   = [ sqrt(diag(m*xe'*xe*m)) ; sqrt(mean(e2m.^2)/n) ] ;

   r2   = 1 - sum(e2) / sum((y-mean(y)).^2) ;

   f    = [xe , e2m]              ;
   s    = cumsum(f)               ;
   v    = f' * f                  ;

   lj   = sum( sum(s.*(s*inv(v)))' )' / n  ;
   li   = sum(s.^2)' ./ diag(v) / n        ;
%%%%%%%%%%%%%%%%%%%%%%%%%%%%%%%%%%%%%%%%%%%%%%%%%%%%%%%%%%%%%%%%%%%%%%%%%%%%%%%
```

```
function [y] = stati(x,i)
% ------------------------------------------------------------------
% Funcion:    stati.m
%
% Objectivo:  Funcion que hace calculos estadisticos basicos
%
%             Se calculan los percentiles de un vector 'x'
%             El parametro 'i' es el percentil (0 - 100)
%             i =   0 -> Minimo
%             i =  25 -> primer cuartil
%             i =  50 -> segundo cuartil (mediana)
%             i =  75 -> tercer cuartil
%             i = 100 -> Maximo
%
% Nota:       La funcion devuelve un valor indefinido ('NaN')
%             si hay menos de 2 valores en el vector 'x'
%             o si este vector contiene valores indefinidos
%
% Referencia: - Función 'median' de la biblioteca Matlab
%
% Autor:      Serge Tmari (vers. 20/03/2008)
% ------------------------------------------------------------------

%  Dimensiones del vector de entrada
%  =================================

   [m,n] = size(x);

%  Verificaciones preliminares
%  ===========================

   %- Verifica que i es un entero
      if (i ~= round(i) )
         error(' STATIS - Error = i debe de ser un entero...')
      end

   %- Verifica que el valor de i es congruente
      if (i < 0) | (i > 100)
         error(' STATIS - Error = i debe de ser entre 0 y 100 % ...')
      end

   %- Verifica que x es un vector
      if (n ~= 1)
         disp(' STATIS - Error = x no es un vector = columna...')
      end

   %- Verifica que x contiene por lo menos 2 datos
      if (m < 2)
         disp(' STATIS - Error = x contiene menos de 2 datos...')
      end
```

```
   %- Verifica que x no contiene datos indefinidos
      if ( sum(isnan(x)) ~= 0 )
         disp(' STATIS - Error = x contiene datos indefinidos...')
      end

%  Calculos
%  ========

   if (n == 1) & (m > 1) & (sum(isnan(x)) == 0)

      %- Ordena los valores de x
         x = sort(x);

      %- Determina el valor más cerca del indice buscado
         kz =  (i/100.)*(m-1) + 1 ;

      %- Determina la 'porcion fraccional' de k
         f = kz - floor(kz) ;

      %- Redondea k hacia 'menos infinito'
         k = floor(kz) ;

      %- Encuentra el valor del percentil (mediante una interpolacion)
         if (f == 0) ;
            y = x(k) ;
         else
            y = x(k) + f*( x(k+1) - x(k) ) ;
         end

   else
      %- Calculo imposible
         y = NaN ;
   end
% ---------------------------------------------------------------------
```

```
function [y] = trilis(x)
% ---------------------------------------------------------------------
%  Objectivo:   Funcion que suaviza una serie de datos
%
%  Input:       n  : numero de valores de 'x'
%               x  : datos de referencia
%
%  Output:      y  : datos ajustados
%
%  Referencia: "triangular smoothing" con 5 puntos
%              [http://www.wam.umd.edu/~toh/spectrum/Smoothing.html]
%
%  Nota:    1. La lista 'x' debe contener > 5 valores
%
%           2. El algoritmo puede usarse aun si hay datos indefinidos ('NaN')
%
%  Autor:      Serge Tamari, 09/02/2009 (MATLAB)
% ---------------------------------------------------------------------

% Verifica que 'x' contiene mas de 5 valores
  n = length(x) ;
  if n <= 5
     error('No hay suficientes datos')
  end

% Algoritmo
  y  = NaN * x ;

  z = [ NaN*ones(1,2) x NaN*ones(1,2) ] ;
  m = length(z) ;

  y = ( z(1:m-4) + 2*z(2:m-3) + 3*z(3:m-2) + 2*z(4:m-1) + z(5:m) ) / 9 ;

% Suaviza (¡como puede!) los primeros y últimos datos
  y(1)   =   x(1)   ;
  y(2)   = ( x(1) + 2*x(2)   + x(3)   ) / 4 ;

  y(n-1) = ( x(n) + 2*x(n-1) + x(n-2) ) / 4 ;
  y(n)   =   x(n)   ;

  end
%---------------------------------------------------------------------
```

Anexo B.2

Software para optimizar el diseño de un picnómetro de Helio

"CVPIC"

A CODE TO COMPUTE
THE THEORETICAL UNCERTAINTY
OF A CONSTANT-VOLUME GAS PYCNOMETER

USER'S MANUAL AND SOURCE CODE

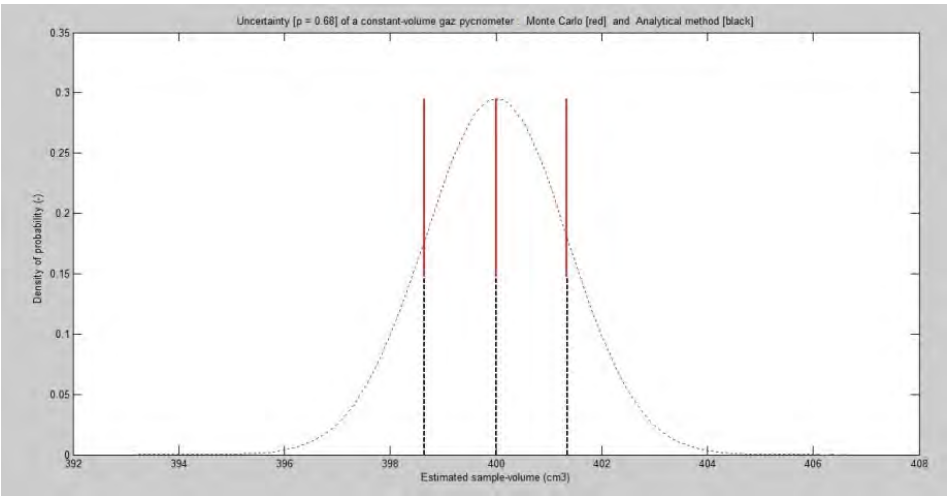

S. Tamari

December 2013

Tamari S. 2013. "CVPIC": a code to compute the theoretical uncertainty of a constant-volume gas pycnometer (user's manual and source code). Jiutepec, Mor.: Instituto Mexicano de Tecnología del Agua.

Content

Abstract

Gas pycnometry has been used widely to determine the volume (and thus the density) of many types of granular materials. This document describes "CVPIC", *i.e.* a simple Matlab code to compute the theoretical uncertainty of a (constant-volume) gas pycnometer. Such an uncertainty is computed in two different ways: using a first-order analytical approach and using an *a priori* more robust Monte Carlo approach. The "CVPIC" code can be used to compare both approaches and investigate the optimum design of any (constant-volume) gas pycnometer.

Keywords: gas pycnometer, volume determination, particle density, GUM, uncertainty analysis, Monte Carlo

1. Introduction

Determining the volume (and thus the density) of granular materials by *liquid pycnometry* (*e.g.*, using water) can be difficult (*e.g.*, Tamari *et al.* 2005) and even impossible (*e.g.*, if the material dissolves into the liquid).

As an alternative, *gas pycnometry* is based on Boyle-Mariotte's law of volume-pressure relationships. It has been used widely to determine the volume (and thus the density) of many types of granular materials (Tamari 2004). Among the three different kinds of gas pycnometers, the so-called "constant-volume" gas pycnometer is the most widely used (Tamari & Aguilar-Chávez 2005).

This user's manual describes a Matlab code "CVPIC" that computes the theoretical uncertainty of a constant-volume gas pycnometer in two different ways (JCGM 2008): (1) a first-order analytical approach and (2) an *a priori* more robust Monte Carlo simulation.

The "CVPIC" code can be used to: (1) compare the first-order analytical approach to the Monte Carlo approach (it will be find that there are consistent in practice, unless very large uncertainties are considered) and (2) investigate the optimum design of a constant-volume gas pycnometer (as done by Tamari 2004).

2. Background

2.1. Principle of operation of a constant-volume gas pycnometer

2.1.1. Theoretical description of the gas pycnometer

A constant-volume gas pycnometer (**figure 1**) is made of a sample chamber with a screw cap, a tank and an absolute pressure transducer. The chamber and the tank can be connected pneumatically through a tube with a coupling valve ("Z"). The tank is also connected to the pressure transducer and can be connected to a gas supply through a tube with a main coupling valve ("M"). The pycnometer is placed into a thermostatically controlled enclosure.

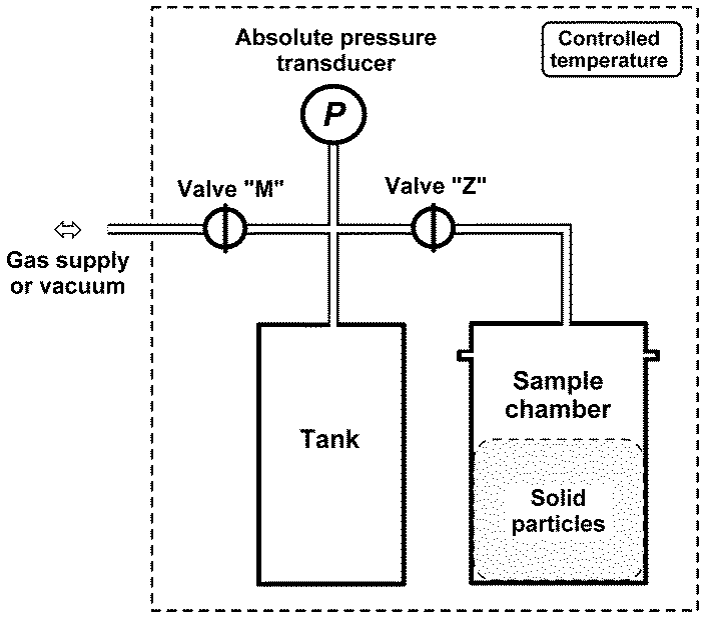

Fig. 1. Diagram of a constant-volume gas pycnometer.

2.1.2. Determination of a sample volume

To procedure to determine the volume of a sample is:

1. The sample is placed into the chamber.
2. Valves "Z" and "M" are opened and the pycnometer is filled with gas.
3. Valve "M" is closed and the absolute pressure transducer is used to measure the initial gas pressure in the pycnometer (P_i).
4. Valve "Z" is closed to isolate the sample-chamber.
5. Valve "M" is opened and some gas is introduced into the tank (or removed from it).
6. Valve "M" is closed again and the gas pressure into the tank is measured (P_j).
7. Valve "Z" is opened so that the gas can expand from the tank to the sample-chamber (or vice versa).
8. The final gas pressure is measured (P_f) when the gas expansion is finished.

2.1.3. Hypotheses

The (classical) following hypotheses are made:

1. The gas inside the pycnometer behaves ideally.
2. The sample and the pycnometer's components are rigid.
3. The pycnometer is gas tight and the expanding gas quickly reaches a static equilibrium.
4. Gas temperature is constant.
5. The decrease of internal volume of valve "Z" is small.

2.1.4. Pycnometer's equation

The (classical) equation of the constant-volume gas pycnometer is (Tamari 2004):

$$V_s = V_c + V_t \tau \qquad (1a)$$

$$\tau = \left(\frac{P_f - P_j}{P_f - P_i} \right) \qquad (1b)$$

where:

- P_i is the initial gas pressure in the sample-chamber (Pa)
- P_j is the initial gas pressure in the tank (Pa)
- P_f is the final gas pressure in the pycnometer (Pa)

- $V_s^{\bullet}$ is the sample volume (m^3)
- V_c is the sample-chamber volume (m^3)
- V_t is the tank volume (m^3)

- T_i, T_j and T_f are the gas temperatures (K) when P_i, P_j and P_f are measured ($T_i \approx T_j \approx T_f$).

Equation (1) shows that the sample-volume estimation (V_s) depends linearily on an experimental coefficient (τ). The slope (V_t) and origin (V_c) of this relation are estimates of the tank and sample-chamber volumes, respectively. Usually, V_t and V_c are determined by mean of a calibration procedure.

2.1.5. Adimensional coefficients

The design of a constant-volume gas pycnometer can be described using three adimensional coefficients (Tamari 2004):

$$\phi = \frac{V_s}{V_c} \quad (2)$$

$$\lambda = \frac{V_t}{V_c} \quad (3)$$

$$\nu = \frac{P_{\max}}{P_{\min}} \quad (4)$$

with: $P_{max} = \text{Max}(P_i, P_j)$

$P_{min} = \text{Min}(P_i, P_j)$

- ϕ = *filling factor* ($0 \leq \phi < 1$)
- λ = *geometric factor* ($\lambda > 0$)
- ν = *pressure factor* ($\nu > 1$)

The pycnometer's designer can select the value he desires for the *geometric factor* ($\lambda > 0$). It can also select the value he desires for the *pressure factor* ($\nu > 1$). However, it must consider a range of possible values for the *filling factor*: the range $0.40 \leq \phi \leq 0.70$ was thus thought to be realistic for a sample-chamber filled with as many solid particles as practical (Tamari 2004).

2.2. Principle of the uncertainty analysis

2.2.1. Sources of error

The sources of error on sample-volume estimation (V_s) can be classified as:

1. Non-ideal gas behaviour
2. Deformation of pycnometer's components
3. Pycnometer's calibration
4. Gas leakage and transient effects
5. **Gas pressure measurements**
6. **Non isothermy**
7. **Handling of pycnometer's components**

The first three sources of error were discarded from this study, for the reasons given in Tamari (2004). The fourth sources of error must be studied experimentally (*e.g.* Tamari *et al.* 2012). So, only the consequence of the last three sources of error is analyzed in the following:

- *Uncertainty of gas pressure measurements.* Any uncertainty of the gas pressures measured during a pycnometric test (P_i, P_j and P_f) contributes to the uncertainty of V_s.

- *Non isothermy.* Any change of gas temperature at the middle ($T_j \neq T_i$) or end ($T_f \neq T_i$) of a test contributes to the uncertainty of V_s.

- *Errors due to pycnometer's handling.* The sample chamber must be opened for introducing a sample and closed after that. Chamber handling is a source of random error for V_c, which contributes to the uncertainty of V_s.

2.2.2. General method for the uncertainty analysis of the gas pycnometer

For the reasons discussed in the previous section, the following variables were thought to be the ones contributing significantly to the uncertainty of sample-volume estimation (V_s):

$$X_i \quad = \quad \{ \; P_i \; , \; P_j \; , \; P_f \; , \; T_j \; , \; T_f \; , \; V_c \; \}$$

In the lack of any other information, the X_i were assumed to be:

- Independent random-functions
- Normally distributed random-functions
- With a small relative standard uncertainty (*for the first-order approach only*)

2.2.3. First-order analytical approach

The above assumptions make it possible the use of the so-called "*law of propagation of uncertainty*" (JCGM 2008), which states that:

$$u(V_s) \approx \sqrt{\sum_i \left(\frac{\partial V_s}{\partial X_i} \right)^2 u^2(X_i)} \qquad (5)$$

where $u(V_s)$ is the (combined) standard uncertainty of V_s and $u(X_i)$ are the individual standard uncertainty of the X_i.

> Note: According to the manufacturers of most commercial pressure transducers, their uncertainty is a constant value which is expressed as a fraction of the highest pressure that the tranducer is adjusted to measure (P_{FS}). In the following, it is assumed that a gas pycnometer is operated so that its maximum pressure P_{max} = Max(P_i, P_j) matches P_{FS}.

The partial derivatives $\partial V_s/\partial X_i$ of **Eq. 5** (*i.e.*, the so-called "*sensitivities*") were computed to derive a general analytical formula that predicts the relative standard uncertainty of V_s (Tamari 2004). This formula is implemented into the "CVPIC" code.

2.2.4. Monte Carlo approach

Because it is based on a first-order Taylor series approximation (JCGM 2008), it is convenient to check the numerical accuracy of the analytical approach using a Monte Carlo approach.

In addition, the Monte Carlo approach is more versatile. In particular, it can be used even if the uncertainty of the input variables is large.

In the "CVPIC" code, a random number generator (*i.e.*, the function "randn.m" from Matlab) is used to simulate the effect of uncertainties in pressure measurements, gas temperature and sample-chamber volume on V_s for some hypothetical pycnometer's configurations.

3. Using the "CVPIC" code

3.1. Install and run the code

Installing and running the "CVPIC" code is easy:

- Copy the following codes into a given directory: "cvpic.m" (main code) and "statis.m" (a function to compute the percentiles of a data list).

- Open Matlab and use the command "addpath" to add the directory containing the "cvpic.m" code.

  Note: the code "cvpic.m" calls the function "randn.m" from "Matlab to generate (normally distributed) random numbers; this built-in function has the same name since since 1994. However, it does not generate random numbers in the same way from one Matlab version to the other. It is worth noting that the "rng.m" function can be used to initialize this random number generator for the "Matlab 2012" version, but that functions with another name were used for this purpose in earlier Matlab versions.

- Run "cvpic.m": the main data are input from the from the Matlab command window.

  Note: by pressing the key "Enter", a default value is stored for each input.

3.2. Data input

The "cvpic.m" code needs nine basic data to perform its computations:

- V_t = Volume of the pycnometer's tank (default: 25 cm^3)
- V_c = Volume of the pycnometer's sample chamber (default: 50 cm^3)
- V_s = Sample volume (default: 20 cm^3)

- P_i = Initial (absolute) pressure into the sample chamber (default: 1,000 Pa)
- P_j = Initial (absolute) pressure into the tank (default: 100,000 Pa)
- T_i = Initial (absolute) temperature of the pycnometer (default: 295 K)

- $u(P)$ = Standard uncertainty of the pressure transducer (default: 20 Pa)
- $u(V_c)$ = Standard uncertainty on the sample-chamber volume (default: 0.002 cm3)
- $u(T)$ = Standard uncertainty of the pycnometer's temperature (default: 0.02 K)

Three parameters are also internally defined (for the Monte Carlo simulations), but their value can be modified if desired:

- *seed* = Initialization parameter for the random numbers (any positive integer)
- *nsim* = Number of replicates for the Monte Carlo simulations (default: 500,000)
- *nhist* = Number of divisions to plot an histogram (default: 100)

Note: the parameter "*nhist*" must be a divider of the parameter "*nsim*", otherwise an error occurs during the graphical display of the results.

3.3. Data output

First, the "cvpic.m" code computes and displays on the screen all the values related to the chosen configuration of a gas pycnometer, especially:

- P_f = Final (absolute) pressure into the pycnometer

- ϕ = Filling factor
- λ = Geometric factor
- ν = Pressure factor

- $u_r(P)$ = Relative standard uncertainty of the pressure transducer (i.e., $u(P) / P_{max}$)
- $u_r(V_c)$ = Relative standard uncertainty on the sample-chamber volume
- $u_r(T)$ = Relative standard uncertainty of the pycnometer's temperature

After that, the "cvpic.m" code computes and displays the results about the standard [p = 0.68] uncertainty of the sample volume to be estimated using the considered gas pycnometer:

- $u^A(V_s)$ = Standard uncertainty of the sample volume, based on the analytical approach
- $u^M(V_s)$ = Standard uncertainty of the sample volume, based on Monte Carlo

- $u_r^A(V_s)$ = Relative standard uncertainty of the sample volume (analytical approach)
- $u_r^M(V_s)$ = Relative standard uncertainty of the sample volume (Monte Carlo)

The "cvpic.m" code also displays the confidence intervals [p = 0.68] for the sample volume:

- On the one hand, the analytical approach considers that the "true" sample volume is estimated with no bias. In this case, the confidence interval is simply:

$$V_s \qquad [\quad V_s - u(V_s) \quad ; \quad V_s + u(V_s) \quad]$$

- On the other hand, the Monte Carlo approach does not make any assumption about the probability distribution of the variable V_s. In this case, the confidence interval is:

$$V_s^{med} \qquad [\quad V_s^{low} \quad ; \quad V_s^{sup} \quad]$$

  where V_s^{low}, V_s^{med} and V_s^{sup} are the 16%, 50% (median) and 84% percentiles of the probability distribution of the simulated V_s values.

The "cvpic.m" code also displays on the screen the *uncertainty budget*, based on the analytical approach (JCGM 2008):

- The *sensitivities* are the partial derivatives $\partial V_s/\partial X_i$ of **Eq. 5**. They show how the uncertainty of each input parameter (*i.e.*, $u(P)$, $u(V_c)$ and $u(T)$) is weighted in the computation of the uncertainty of the sample volume (*i.e.*, $u^A(V_s)$).

- The *(relative) contributions to the variance* are computed as: $c_r(X_i) = \left(\frac{\partial V_s}{\partial X_i} \times \frac{u(X_i)/X_i}{u(V_s)/V_s} \right)^2$. They show which variable (*i.e.*, P, V_c or T) has the major effect onto the uncertainty of the sample volume.

Finally, the "cvpic.m" code displays a plot with the following components:

- Histogram of the probability distribution of V_s simulated with Monte Carlo (*i.e.*, all the possible values for an estimation of the sample volume, with their density of probability).

- Confidence interval [p = 0.68] for the sample volume, according to the Monte Carlo approach: vertical continuous lines (in red) at the top of the plot.

- Confidence interval [p = 0.68] for the sample volume, according to the first-order analytical approach: vertical dashed lines (in red) at the bottom of the plot.

  Note: the difference between the confidences intervals computed using the analytical and the Monte Carlo approaches can be seen using the "zoom" option of the Matlab graphical interface.

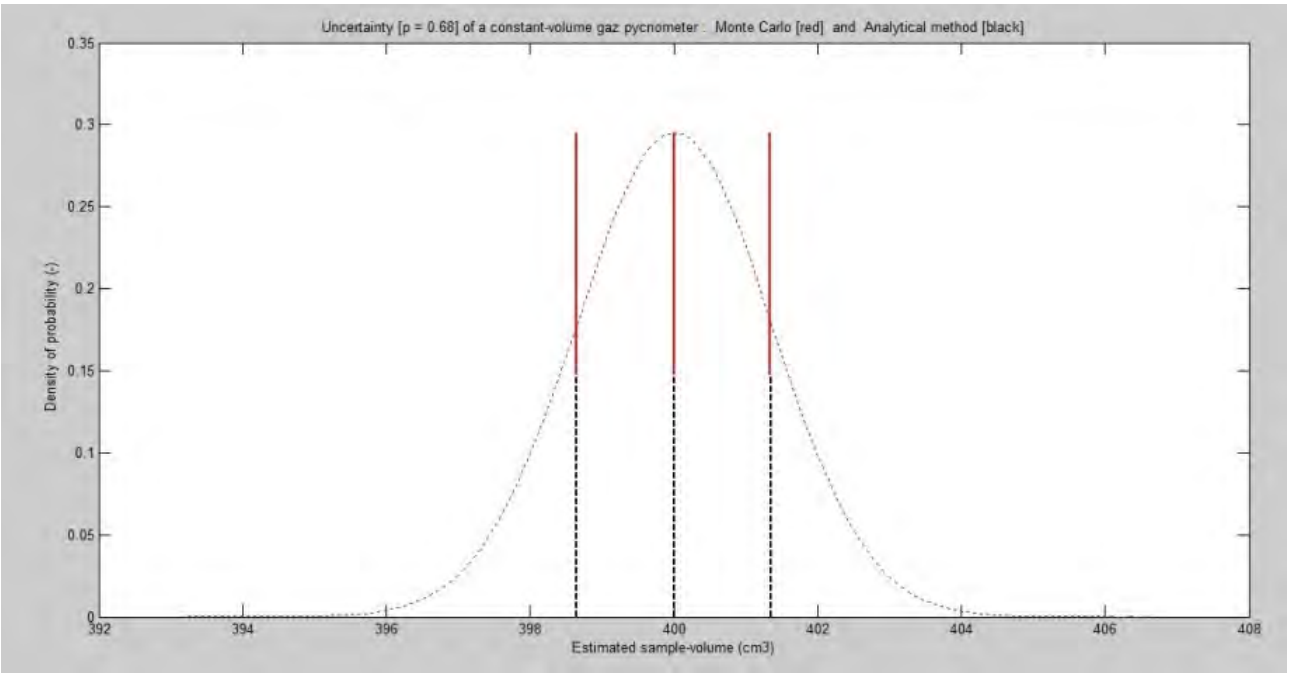

Fig. 2. Graphical output of the "CVPIC" code.

3.4. Examples

3.4.1. Case of a well-designed gas pycnometer

A well-designed gas pycnometer which has been properly filled with a sample (according to Tamari 2004) is first considered (**Table 1**):

- Rather large filling factor: ϕ = 0.4
- Adequate geometric factor λ = 0.5
- Large pressure factor ν = 100
- Very accurate pressure transducer $u_r(P)$ = 0.02%
- Good control of the pycnometer's sample chamber $u_r(V_c)$ = 0.00%
- Good control of temperature $u_r(T)$ = 0.01%

In this case, the sample volume should be estimated accurately, *i.e.* with a relative standard uncertainty of ≈ 0.15% (**Table 1**).

And as expected (since small relative uncertainties are propagated), both the analytical and the Monte Carlo approaches produce virtually the same results (**Fig. 3**).

Table 1. Case of a well-designed gas pycnometer.

```
**********************************************************************
*            CHARACTERISTICS OF THE SIMULATION                       *
**********************************************************************

* PYCNOMETER CONFIGURATION

  Tank volume                  (cm3)  =     25.000
  Sample-chamber volume        (cm3)  =     50.000
  Sample volume                (cm3)  =     20.000

  Initial Cell Pressure         (Pa)  =      1000
  Initial Tank Pressure         (Pa)  =    100000
  Final System Pressure         (Pa)  =     46000

  Coefficient Tau               (-)   =   -1.2000

  Geometric factor              (-)   =     0.500
  Filling ratio                 (-)   =     0.400
  Pressure factor               (-)   =   100.000

* INPUT UNCERTAINTIES (STANDARD AND RELATIVE)

  Std uncert. on pressure       (Pa)  =    20.000
  Std uncert. on chamber volume (cm3) =     0.002
  Std uncert. on temperature    (K)   =     0.020

  Rel. uncert. on pressure        (%) =      0.02
  Rel. uncert. on chamber volume  (%) =      0.00
  Rel. uncert. on temperature     (%) =      0.01

**********************************************************************
*                  RESULTS OF THE SIMULATION                         *
**********************************************************************

* ESTIMATED UNCERTAINTY ON THE SAMPLE VOLUME

  Std uncert.  < Analytical  > (cm3)  =      0.031
  Std uncert.  < Monte Carlo > (cm3)  =      0.030

  Rel. uncert. < Analytical  >  (%)  =      0.15
  Rel. uncert. < Monte Carlo >  (%)  =      0.15

* SAMPLE VOLUME (cm3) AND ITS CONFIDENCE INTERVAL [p = 0.68]

  < Analytical  >   20.000 [  19.969 -   20.031]
  < Monte Carlo >   20.000 [  19.970 -   20.030]

* UNCERTAINTY BUDGET [Analytical method]

  Variable        Sensitivity   Contrib. variance (%%)
  -----------     -----------   ----------------------
  Presure             7.49          96.49
  Temperature         3.95           3.08
  Chamber vol.        2.50           0.43

**********************************************************************
*                     END OF THE PROGRAM                             *
**********************************************************************
```

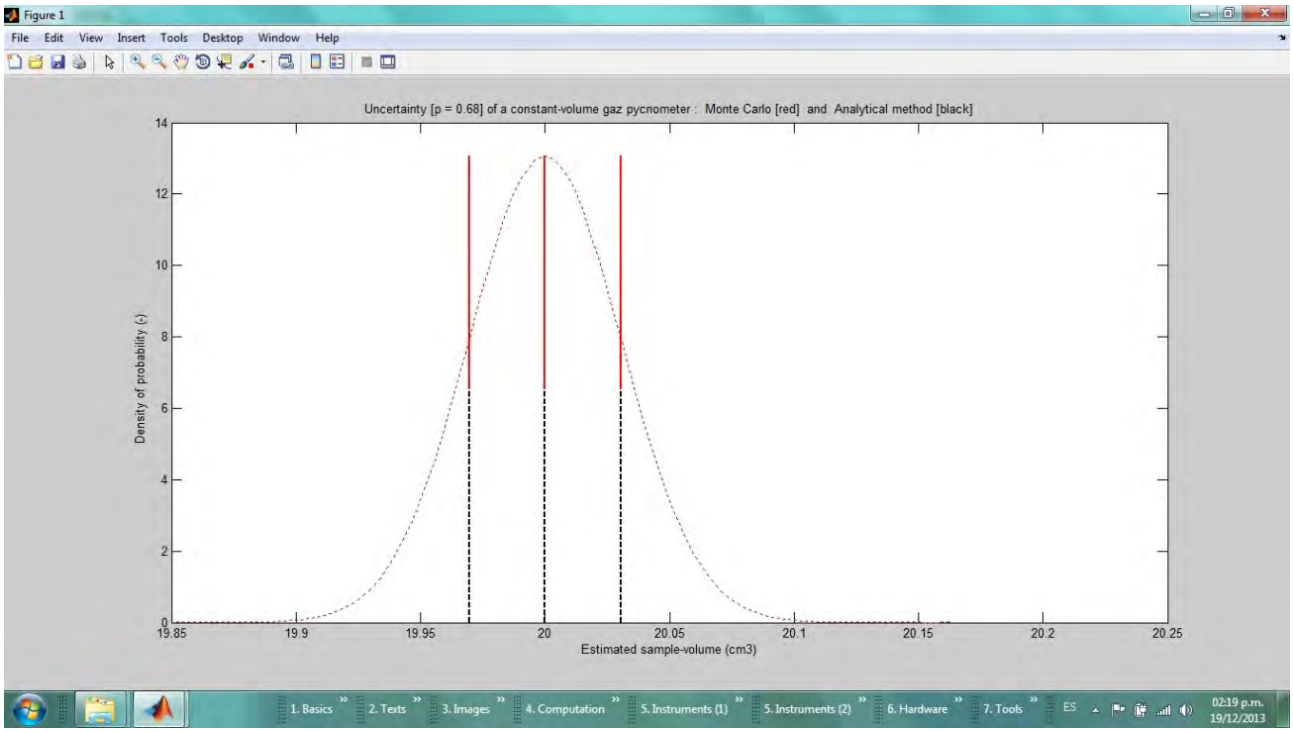

Fig. 3. Theoretical uncertainty of a well-designed gas pycnometer.

3.4.2. Case of a badly-designed gas pycnometer

In this example, a "badly-designed" gas pycnometer which has been poorly filled with a sample (according to Tamari 2004) is considered (**Table 2**):

- Rather low filling factor: ϕ = 0.2
- Too low geometric factor λ = 0.1
- Very low pressure factor ν = 1.2
- Unaccurate pressure transducer $u_r(P)$ = 0.17%
- Bad control of the pycnometer's sample chamber $u_r(V_c)$ = 0.40%
- Bad control of temperature $u_r(T)$ = 0.17%

In this case, the sample volume should be estimated inaccurately, *i.e.* with a relative standard uncertainty of ≈ 65% (**Table 2**) !

And since larger relative uncertainties are propagated (compared to the previous example), it is found that the first-order analytical approach starts to deviate notably from the Monte Carlo approaches (**Fig. 4**): in fact, the Monte Carlo approach predicts a probability distribution which is obviously skewed (*i.e.*, not anymore a normal distribution, as considered in the analytical approach).

> Note: In this example (**Table 2**), the median of the probability distribution (*i.e.*, V_s^{med}) is surprisingly very close to the "true" value for the sample volume (*i.e.*, V_s), in spite of the skewed probability distribution.

Table 2. Case of a badly-designed gas pycnometer.

```
*********************************************************************
*           CHARACTERISTICS OF THE SIMULATION                       *
*********************************************************************

* PYCNOMETER CONFIGURATION

  Tank volume                  (cm3)  =      5.000
  Sample-chamber volume        (cm3)  =     50.000
  Sample volume                (cm3)  =     10.000

  Initial Cell Pressure         (Pa)  =     100000
  Initial Tank Pressure         (Pa)  =     120000
  Final System Pressure         (Pa)  =     102222

  Coefficient Tau               (-)   =    -8.0000

  Geometric factor              (-)   =      0.100
  Filling ratio                 (-)   =      0.200
  Pressure factor               (-)   =      1.200

* INPUT UNCERTAINTIES (STANDARD AND RELATIVE)

  Std uncert. on pressure       (Pa)  =    200.000
  Std uncert. on chamber volume (cm3) =      0.200
  Std uncert. on temperature    (K)   =      0.500

  Rel. uncert. on pressure        (%) =       0.17
  Rel. uncert. on chamber volume  (%) =       0.40
  Rel. uncert. on temperature     (%) =       0.17

*********************************************************************
*                 RESULTS OF THE SIMULATION                         *
*********************************************************************

* ESTIMATED UNCERTAINTY ON THE SAMPLE VOLUME

  Std uncert.  < Analytical  > (cm3)  =      6.490
  Std uncert.  < Monte Carlo > (cm3)  =      6.606

  Rel. uncert. < Analytical  >  (%)   =      64.90
  Rel. uncert. < Monte Carlo >  (%)   =      66.05

* SAMPLE VOLUME (cm3) AND ITS CONFIDENCE INTERVAL [p = 0.68]

  < Analytical  >   10.000 [   3.510 -   16.490]
  < Monte Carlo >   10.000 [   2.411 -   15.623]

* UNCERTAINTY BUDGET [Analytical method]

  Variable        Sensitivity   Contrib. variance (%%)
  -----------     -----------   ----------------------
  Presure           326.24           70.19
  Temperature       208.75           29.72
  Chamber vol.        5.00            0.09

*********************************************************************
*                    END OF THE PROGRAM                             *
*********************************************************************
```

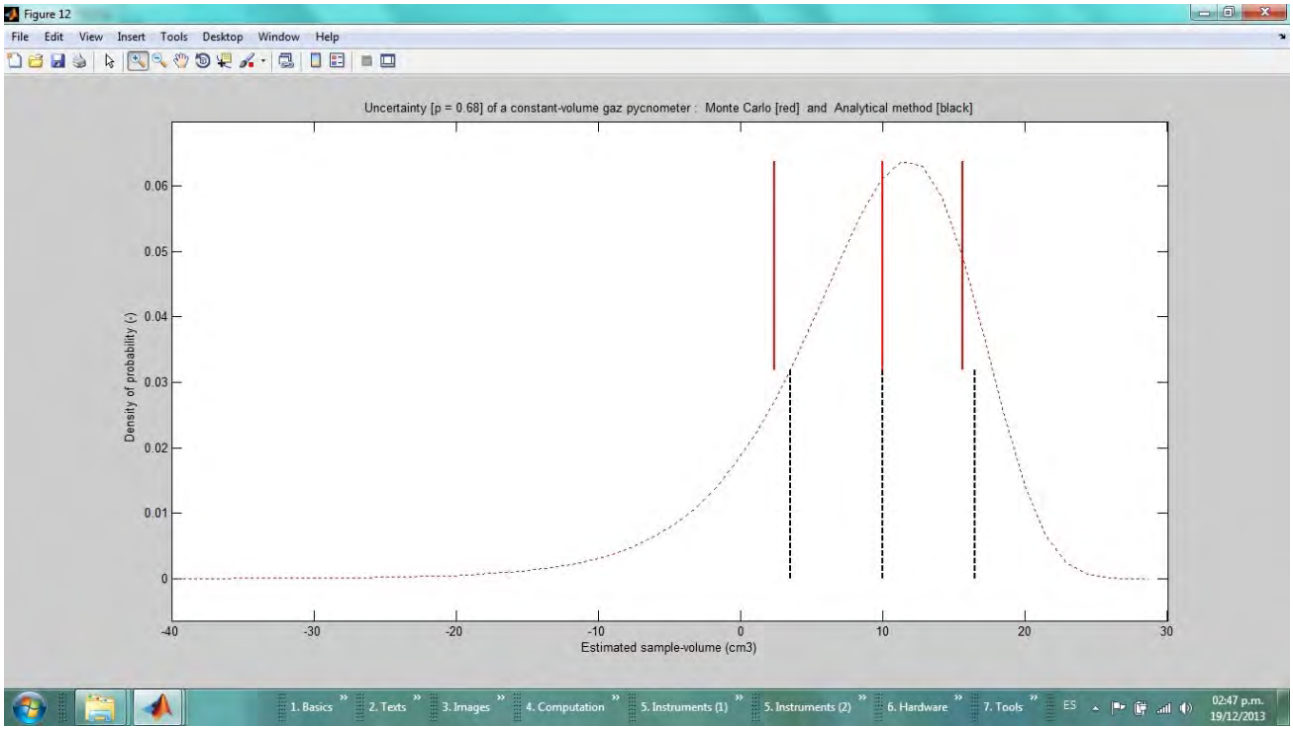

Fig. 4. Theoretical uncertainty of a badly-designed gas pycnometer.

References

JCGM. (2008).- *Evaluation of measurement data — Guide to the expression of uncertainty in measurement (JCGM 100:2008)*. Working Group 1 of the Joint Committee for Guides in Metrology (JCGM/WG1), Paris.

Tamari S. (2004).- Optimum design of the constant-volume gas pycnometer for determining the volume of solid particles. *Meas. Sci. Technol.,* **Vol. 15:** pp. 549-558.

Tamari S., Aguilar-Chávez A. (2005).- Optimum design of gas pycnometers for determining the volume of solid particles. *J. Testing and Evaluation,* **Vol. 33:** pp. 135-138

Tamari S., Samaniego-Martínez D., Bandala E.R., Bonola I., Ordaz-Chaparro V. (2005).- Particle density of volcanic scoria (tezontle) determined by water pycnometry. *Geotechnical Testing J.*, **Vol. 28:** pp. 321-327.

Tamari S., Zisa J. M., Albarrán A. (2012).- The problem of water vapor outgassing in gas (Helium) pycnometry. *In*: Becerra L.O. et al. (ed.), *Proc. "Simposio de Metrología 2012"* (Querétaro, Qro., 8–12 October 2012). CENAM (publ.), 5 p.

```
% ========================================================================
%
%      Objective of the program
%      ========================
%      This Matlab program computes the theoretical uncertainty
%      of a constant-volume gas pycnometer.
%
%      The uncertainty is estimated in two different ways:
%      1. First-order analytical approximation
%      2. Monte Carlo simulation
%
%      Physical hypotheses
%      ===================
%      1. The gas inside the pycnometer behaves ideally
%      2. The pycnometer temperature is constant
%      3. The pycnometer is gas-tight
%      4. The pycnometer has been perfectly calibrated
%      5. The internal volume of valves does not change during operation
%
%      Statistical hypotheses
%      ======================
%      1. Input data are normally-distributed random-variables
%      2. Input data are uncorrelated random-variables
%
%      References
%      ==========
%      [1] Tamari S. (2004). Optimum design of the constant-volume gas
%          pycnometer for determining the volume of solid particles.
%          Meas. Sci. Technol., Vol. 15: pp. 549-558.
%      [2] JCGM. (2008). Evaluation of measurement data — Guide to the
%          expression of uncertainty in measurement (JCGM 100:2008).
%          Working Group 1 of the Joint Committee for Guides in Metrology
%         (JCGM/WG1), Paris.
%
%      Details of the program
%      ======================
%      Matlab version     :  2012
%      External function  :  'statis.m'
%
%      Contact
%      =======
%      Author             :  Serge Tamari (tamari@tlaloc.imta.mx)
%      Program version    :  December 18, 2013
%
% ========================================================================

disp(' ')
disp(' ')
disp(' ***************************************************************')
disp(' *                                                             *')
disp(' *                  THEORETICAL UNCERTAINTY                    *')
```

```
disp(' *              OF A CONSTANT-VOLUME GAS PYCNOMETER               *')
disp(' *                                                                *')
disp(' ******************************************************************')
disp(' ')
disp(['  Date : ' date ])
disp(' ')
disp('   > Press <Enter> to select a default value... ')


% ------------------------------------------------------------------------
% epsil  = Small number (numerically)
% ------------------------------------------------------------------------

  epsil = 1e-12 ;


% ========================================================================
% DATA INPUT:  (1) PYCNOMETER CONFIGURATION
% ========================================================================

disp(' ')
disp(' * PYCNOMETER GEOMETRY ')
% ------------------------------------------------------------------------
% Vc     = Volume of the sample chamber (cm3)
% Vt     = Volume of the pycnometer's tank (cm3)
% Vs     = Volume of the sample inside the pycnometer (cm3)
% ------------------------------------------------------------------------

  Vt = input('   Volume of the pycnometer tank (eg, 25 cm3) .......... ' );

     if (Vt < 0)
        error('   > Incorrect value ! ') ;
     elseif isempty(Vt)
        Vt  = 25 ;
     end

  Vc = input('   Volume of the sample chamber (eg, 50 cm3) ........... ' );

     if (Vc < 0)
        error('   > Incorrect value ! ') ;
     elseif isempty(Vc)
        Vc  = 50 ;
     end

  Vs = input('   Volume of the sample (eg, 20 cm3) ................... ' );

     if (Vs < 0) | (Vs > Vc)
        error('   > Incorrect value ! ') ;
     elseif isempty(Vs)
        Vs  = 20 ;
     end
```

```
disp(' ')
disp(' * PYCNOMETER OPERATING CONDITIONS ')
% ------------------------------------------------------------------------
% Pi     = Initial gas pressure into the pycnometer's sample chamber (Pa)
% Pj     = Initial gas pressure into the pycnometer's tank (Pa)
% Ti     = Initial gas temperature into the sample chamber (K)
% ------------------------------------------------------------------------

  Pi = input('   Absolute pressure in sample chamber (eg, 1000 Pa) ... ' );

     if (Pi < 0)
        error('   > Incorrect value ! ') ;
    elseif isempty(Pi)
        Pi  =  1000 ;
     end

  Pj = input('   Absolute pressure in the tank (eg, 100000 Pa) ..... ' );

     if (Pj < 0)
        error('   > Incorrect value ! ') ;
     elseif isempty(Pj)
        Pj  =  100000 ;
     end

  Ti = input('   Absolute temperature of pycnometer (eg, 295 K) ..... ' );

     if (Ti < 0)
        error('   > Incorrect value... ') ;
     elseif isempty(Ti)
        Ti  =  295 ;
     end


% ========================================================================
% DATA INPUT:  (2) PARAMETERS TO COMPUTE THE PYCNOMETER UNCERTAINTY
% ========================================================================

disp(' ')
disp(' * STANDARD UNCERTAINTY OF THE MEASUREMENTS ')
% ------------------------------------------------------------------------
% uP   = Standard uncertainty of the pressure transducer (Pa)
% uVc  = Standard uncertainty of the sample-chamber volume (cm3)
% uT   = Standard uncertainty of the pycnometer temperature (K)
% ------------------------------------------------------------------------

  uP = input('   Std uncertainty of pressure transducer (eg, 20 Pa) .. ' );

     if (uP < 0)
        error('   > Incorrect value ! ') ;
     elseif isempty(uP)
```

```
      uP  =  20 ;
   end

  uVc = input('   Std uncertainty on chamber volume (eg, 0.002 cm3) ... ' );

   if (uVc < 0)
      error('   > Incorrect value ! ') ;
   elseif isempty(uVc)
      uVc  =  0.002 ;
   end

  uT = input('   Std uncertainty of temperature (eg, 0.02 K) ......... ' );

   if (uT < 0)
      error('   > Incorrect value ! ') ;
   elseif isempty(uT)
      uT  =  0.02 ;
   end


disp(' ')
disp(' * PARAMETERS FOR THE MONTE CARLO SIMULATION [INTERNALLY DEFINED] ')
% ------------------------------------------------------------------------
% seed   = Positive integer (to initialize the generator of random numbers)
% nsim   = Number of replicates for the Monte Carlo simulations (-)
% nhist  = Number of divisions to plot an histogram (= divider of 'nsim')
% ------------------------------------------------------------------------

  seed = 1 ;

  nsim   = 5000000 ;
  nhist  =     100 ;

  if ( abs( nsim/nhist - round(nsim/nhist) ) > epsil )
     error('   > Check the Monte Carlo parameters [internally defined] ') ;
  end


% ========================================================================
% COMPUTATION:  (1) PRELIMINARY DATA
% ========================================================================

% ------------------------------------------------------------------------
% Tj     = Initial gas temperature into the tank (K)  [Tj = Ti]
% Tf     = Final temperature into the pycnometer (K)  [Tf = Ti]
% Pf     = Final gas presure into the pycnometer (Pa)
% Tau    = Experimental coefficient determined from a pycnometric test (-)
% Vss    = Computed 'true' sample volume (cm3) [for check]
% ------------------------------------------------------------------------

  Tj     = Ti ;
```

```
  Tf     = Ti ;

  Pf     = Tf * ( (Pi/Ti)*(Vc-Vs) + (Pj/Tj)*Vt ) / (Vc-Vs+Vt) ;

  Tau    = (Pf-Pj) / (Pf-Pi) ;

     Vss   = Vc  +  Vt * Tau ;

     if ( abs(Vs-Vss)/Vs > epsil )
        error('   > There is an error in the computation of Vs ! ') ;
     end

% ------------------------------------------------------------------------
% Lambda = Geometric factor (Lambda =  Vt/Vc)
% Phi    = Filling factor   (Phi    =  Vs/Vc)
% Nu     = Pressure factor  (Nu     =  Pmax/Pmin > 1)
% ------------------------------------------------------------------------

  Lambda  =  Vt / Vc ;
  Phi     =  Vs / Vc ;
  Nu      =  max(Pi,Pj) / min(Pi,Pj) ;

% ------------------------------------------------------------------------
% urP    = Relative uncertainty of the pressure transducer
% urT    = Relative uncertainty of the pycnometer temperature
% urVc   = Relative uncertainty of the sample-chamber volume
% ------------------------------------------------------------------------

  urP  = uP  / max(Pi,Pj) ;
  urT  = uT  / Ti         ;
  urVc = uVc / Vc         ;

  if (urP > 0.01) || (urVc > 0.01) || (urT > 0.01)
     disp('   > WARNING: analytical computation can be unaccurate ! ') ;
  end


% ========================================================================
% COMPUTATION:  (2) UNCERTAINTY BASED ON THE ANALYTICAL METHOD
% ========================================================================

% ------------------------------------------------------------------------
% FctP   = Sensitivity to the pressure data (Pi, Pj, Pf)
% FctVc  = Sensitivity to the volume data   (Vc)
% FctT   = Sensitivity to the temperature   (Ti, Tj, Tf)
% ------------------------------------------------------------------------

  k      = sqrt(2) * (Nu/(Nu-1)) * (1-Phi+Lambda)/(Lambda*Phi) ;

  FctP   = k * sqrt( Lambda^2 + (1-Phi)*Lambda + (1-Phi)^2 ) ;
  FctT   = k * sqrt( Lambda^2 + (1-Phi)*Lambda/Nu + (1-Phi)^2/(2*Nu^2) ) ;
```

```
  FctVc  = 1 / Phi ;

% ------------------------------------------------------------------------
% VarP   = Contribution to variance of the pressure data (Pi, Pj, Pf)
% VarVc  = Contribution to variance of the volume data   (Vc)
% VarT   = Contribution to variance of the temperature   (Ti, Tj, Tf)
% VarVs  = Relative variance of the sample volume
% ------------------------------------------------------------------------

  VarP   = ( FctP  * urP  )^2 ;
  VarT   = ( FctT  * urT  )^2 ;
  VarVc  = ( FctVc * urVc )^2 ;

  VarVs  = VarP + VarVc + VarT ;

% ------------------------------------------------------------------------
% urVs   = Relative standard uncertainty of the sample volume (-)
% uVs    = Standard uncertainty of the sample volume (cm3)
% ------------------------------------------------------------------------

  urVs   = sqrt( VarVs ) ;

  uVs    = Vs * urVs ;


% ========================================================================
% COMPUTATION: (3) UNCERTAINTY BASED ON MONTE CARLO
% ========================================================================

% ------------------------------------------------------------------------
% Initialize the generator of random numbers
% ------------------------------------------------------------------------

  rng( seed ) ;

% ------------------------------------------------------------------------
% Tjn    = Corrupted temperature at the beginning of a test (K)
% Tfn    = Corrupted temperature at the end of a test (K)
% Vcn    = Corrupted sample-chamber volume (cm3)
% Vtn    = Tank volume (cm3)  [Dummy data]
% Pin    = Initially "measured" pressure into the sample chamber (Pa)
% Pjn    = Initially "measured" pressure into the tank (Pa)
% Pfcon  = "True" final pressure, according the perfect gas law (Pa)
% Pfn    = "Measured" final pressure into the pycnometer (Pa)
% Taun   = Experimental coefficient (-)
% Vsn    = Simulated sample-volume data (cm3)
% ------------------------------------------------------------------------

  Tjn    = Ti + (randn(nsim,1)) * uT  ;
  Tfn    = Ti + (randn(nsim,1)) * uT  ;
```

```
  Vcn    = Vc + (randn(nsim,1)) * uVc ;
  Vtn    = Vt ;

  Pin    = Pi + (randn(nsim,1)) * uP  ;
  Pjn    = Pj + (randn(nsim,1)) * uP  ;

  Pfcon  = Tfn .* ( (Pi/Ti).*(Vcn-Vs) + (Pj./Tjn).*Vtn ) ./ (Vcn-Vs+Vtn) ;
  Pfn    = Pfcon +  (randn(nsim,1))* uP ;

  Taun   = (Pfn - Pjn) ./ (Pfn - Pin) ;

  Vsn    = Vc  +  Vt * Taun ;

% ------------------------------------------------------------------------
% VsnMed  = Median of the simulated sample-volume data (cm3)
% VsnLow  = Low bound  [p = 0.68] of the sample-volume data (cm3)
% VsnSup  = High bound [p = 0.68] of the sample-volume data (cm3)
% uVsn    = Uncertainty [p = 0.68] of the sample-volume data (cm3)
% urVsn   = Relative uncertainty [p = 0.68] of the sample-volume data (-)
% ------------------------------------------------------------------------

  [ VsnMed , kerrM ] =  statis( Vsn , 50 )  ;

  [ VsnLow , kerrL ] =  statis( Vsn , 50 - 68/2 ) ;
  [ VsnSup , kerrS ] =  statis( Vsn , 50 + 68/2 ) ;

   if ( kerrM < 0 ) | ( kerrL < 0 ) | ( kerrS < 0 )
        error('   > There is a problem with the function statis.m ! ') ;
     end

  uVsn    = ( VsnSup - VsnLow ) / 2 ;

  urVsn   = uVsn / VsnMed ;


% ========================================================================
% DATA OUTPUT:  (1) TABLE OF DATA
% ========================================================================

disp(' ')
disp(' ')
disp(' ************************************************************************')
disp(' *            CHARACTERISTICS OF THE SIMULATION                         *')
disp(' ************************************************************************')

disp(' ')
disp(' * PYCNOMETER CONFIGURATION ')

disp(' ')
fprintf('   Tank volume                 (cm3)  = %10.3f \n', Vt     )
fprintf('   Sample-chamber volume       (cm3)  = %10.3f \n', Vc     )
```

```
fprintf('   Sample volume                (cm3)  = %10.3f \n', Vs     )

disp(' ')
fprintf('   Initial Cell Pressure         (Pa)  = %10.0f \n', Pi     )
fprintf('   Initial Tank Pressure         (Pa)  = %10.0f \n', Pj     )
fprintf('   Final System Pressure         (Pa)  = %10.0f \n', Pf     )

disp(' ')
fprintf('   Coefficient Tau               (-)   = %10.4f \n', Tau    )

disp(' ')
fprintf('   Geometric factor              (-)   = %10.3f \n', Lambda )
fprintf('   Filling ratio                 (-)   = %10.3f \n', Phi    )
fprintf('   Pressure factor               (-)   = %10.3f \n', Nu     )

disp(' ')
disp(' * INPUT UNCERTAINTIES (STANDARD AND RELATIVE) ')

disp(' ')
fprintf('   Std uncert. on pressure       (Pa)  = %10.3f \n', uP   )
fprintf('   Std uncert. on chamber volume (cm3) = %10.3f \n', uVc  )
fprintf('   Std uncert. on temperature    (K)   = %10.3f \n', uT   )

disp(' ')
fprintf('   Rel. uncert. on pressure        (%%) = %10.2f \n', 100*urP  )
fprintf('   Rel. uncert. on chamber volume  (%%) = %10.2f \n', 100*urVc )
fprintf('   Rel. uncert. on temperature     (%%) = %10.2f \n', 100*urT  )


disp(' ')
disp(' ')
disp(' ***************************************************************')
disp(' *                  RESULTS OF THE SIMULATION                  *')
disp(' ***************************************************************')

disp(' ')
disp(' * ESTIMATED UNCERTAINTY ON THE SAMPLE VOLUME ')

disp(' ')
fprintf('   Std uncert.  < Analytical  > (cm3)  = %10.3f \n', uVs  )
fprintf('   Std uncert.  < Monte Carlo > (cm3)  = %10.3f \n', uVsn )

disp(' ')
fprintf('   Rel. uncert. < Analytical  >  (%%)  = %10.2f \n', 100*urVs  )
fprintf('   Rel. uncert. < Monte Carlo >  (%%)  = %10.2f \n', 100*urVsn )

disp(' ')
disp(' * SAMPLE VOLUME (cm3) AND ITS CONFIDENCE INTERVAL [p = 0.68] ')

disp(' ')
fprintf('   < Analytical  > %8.3f [%8.3f - %8.3f]\n', Vs , Vs-uVs , Vs+uVs)
```

```
fprintf('   < Monte Carlo > %8.3f [%8.3f - %8.3f]\n', VsnMed,VsnLow,VsnSup)

disp(' ')
disp(' * UNCERTAINTY BUDGET [Analytical method] ')

disp(' ')
disp('   Variable        Sensitivity   Contrib. variance (%%) ')
disp('   -----------     -----------   --------------------- ')
fprintf('   Presure         %8.2f       %8.2f \n', FctP,  100*VarP/VarVs  )
fprintf('   Temperature     %8.2f       %8.2f \n', FctT,  100*VarT/VarVs  )
fprintf('   Chamber vol.    %8.2f       %8.2f \n', FctVc, 100*VarVc/VarVs )


% ========================================================================
% DATA OUTPUT:  (2) GRAPHICAL OUTPUT
% ========================================================================

% ------------------------------------------------------------------------
% Density of probability of the sample-volume data simulated by Monte Carlo
% ------------------------------------------------------------------------

  [ contn , valn ] = hist( Vsn , nhist ) ;

  dvaln   = valn(2) - valn(1) ;
  frecn   = contn / nsim      ;
  densn   = frecn / dvaln     ;

  if ( abs(sum(frecn) - 1) > epsil )
     error('   > There is an error in the computation of frecuencies ! ') ;
  end

% ------------------------------------------------------------------------
% Plot the histogram of the sample-volume data simulated by Monte Carlo
% ------------------------------------------------------------------------

  figure() ;
  clf reset ;
  plot( valn , densn , 'r:' , 'LineWidth',1.2 ) ;
  hold on

  dmax = max( densn ) ;

  plot( [VsnMed VsnMed] , [0.5*dmax dmax] ,'r-' , 'LineWidth',1.5 )

  plot( [VsnLow VsnLow] , [0.5*dmax dmax] ,'r-' , 'LineWidth',1.5 )
  plot( [VsnSup VsnSup] , [0.5*dmax dmax] ,'r-' , 'LineWidth',1.5 )

% ------------------------------------------------------------------------
% Add the results obtained with the analytical method
% ------------------------------------------------------------------------
```

```
  plot( [Vs Vs] , [0 0.5*dmax] , 'k--' , 'LineWidth',1.5 )

  plot( [(Vs-uVs) (Vs-uVs)] , [0 0.5*dmax] , 'k--' ,'LineWidth',1.5 )
  plot( [(Vs+uVs) (Vs+uVs)] , [0 0.5*dmax] , 'k--' ,'LineWidth',1.5 )

% ------------------------------------------------------------------------
% Add a legend to the plot
% ------------------------------------------------------------------------

  tita = 'Uncertainty [p = 0.68] of a constant-volume gaz pycnometer :  ' ;
  titb = 'Monte Carlo [red]  and  Analytical method [black]'              ;
  title( [ tita titb ] ) ;

  xlabel( 'Estimated sample-volume (cm3)' ) ;
  ylabel( 'Density of probability (-)   ' ) ;

% ------------------------------------------------------------------------
% Final banner
% ------------------------------------------------------------------------

disp(' ')
disp(' ************************************************************************')
disp(' *                      END OF THE PROGRAM                              *')
disp(' ************************************************************************')
disp(' ')
```

```
function [ xval , kerr ] = statis( xlist , iperc )

% ========================================================================
%      Objective of the program
%      ========================
%      This  function extracts a percentil (iperc) from a list (xlist)
%      and returns the corresponding value (xval). The percentil must be
%      expressed in percents (%), for instance:
%
%      Input 'iperc'       Output 'xval'
%      -------------       -------------------
%           0              Minimum
%          25              1st cuartil
%          50              2nd cuartil (median)
%          75              3rd cuartil
%         100              Maximum
%
%      The error codes (kerr) are:
%
%      'kerr'    'xval'    Comment
%      ------    ------    ---------------------------------------------
%        -2       NaN      Problem: the list contains 'NaN' data
%        -1       NaN      Problem: the list contains less than 2 data
%         0       yes      No problem to extract the percentil
%         1       yes      Percentil extracted by a linear extrapolation
%
%      References
%      ==========
%      [1] Function 'median' of the Matlab library.
%
%      Details of the program
%      ======================
%      Matlab version     :  2012
%      External function  :  none
%
%      Contact
%      =======
%      Author             :  Serge Tamari (tamari@tlaloc.imta.mx)
%      Program version    :  December 18, 2013%
% ========================================================================

% Initialization and checks
% =========================

% Initialize the error code
  kerr  =  0  ;

% Length of the data list
  [ nlig , ncol ]  =  size( xlist ) ;
```

```
% Check that 'iperc' is an integer, between 0 and 100 %
  if ( iperc ~= round(iperc) )
     error(' STATIS - iperc must be an integer ! ')
  elseif ( iperc < 0 ) | ( iperc > 100 )
     error(' STATIS - iperc must be between 0 and 100 %% ! ')
  end

% Checks that 'xlist' is a list (or a vector, which is then transposed)
  if ( nlig > 1 ) & ( ncol > 1 )
     error(' STATIS - xlist should not be a table ! ')
  elseif ( ncol ~= 1 )
     xlist =  xlist' ;
     nlig  =  ncol   ;
  end

% Check that 'xlist' contains > 2 data
  if ( nlig < 2 )
     kerr  = -1      ;
  end

% Check that 'xlist' does not contain 'NaN' data
  if ( sum(isnan(xlist)) ~= 0 )
     kerr  = -2      ;
  end

%  Computation
%  ===========

   if ( kerr >= 0 )

      %- Sort the list (xlist) in ascending order
         xlist = sort(xlist);

      %- Determine the index of the list just below the required percentil
         idatax =  (iperc/100.)*(nlig-1) + 1 ;
         frac   =  idatax - floor(idatax) ;

      %- Determine the value (xval) corresponding to the percentil (iperc)
         if (frac == 0) ;
            xval = xlist(idatax) ;
         else
            kerr  = 1  ;
            idata = floor(idatax) ;
            xval  = xlist(idata) + frac*( xlist(idata+1) - xlist(idata) ) ;
         end

   else
         xval = NaN ;
   end
% ======================================================================
```

Anexo C.1

Informe de una orden de servicio sobre el método de Gibson

PUESTA EN OPERACIÓN DE UN SIMULADOR NUMERICO PARA PODER EVALUAR EL MÉTODO DE GIBSON

INFORME FINAL

SOLICITADO POR:

INSTITUTO MEXICANO DE TECNOLOGÍA DEL AGUA

ELABORADO POR:

CONSULTORES Y PROYECTOS DEL SUR, S.A. DE C.V.

mayo de 2013

ÍNDICE

I. INTRODUCCIÓN

I.1. ANTECEDANTES

Desde los años 80s, investigadores de varios países están evaluando el método de Gibson (1923), que la norma internacional IEC-60041 (1991) considera como un método primario para determinar el caudal en las tuberías a presión de las centrales hidroeléctrica. En este contexto, el personal del Instituto Mexicano de Tecnología del Agua (IMTA) pretende evaluar el método de Gibson mediante experimentos numéricos, por lo cual se necesita contar con un conjunto de programas de cómputo:

1. Simulador de transitorios en tuberías a presión - Dicho simulador se utilizará para simular una serie de casos típicos que servirán como referencia (benchmark).

2. Simulador de tipo Monte Carlo - Dicho simulador se utilizará para corromper en forma aleatoria los datos generados por el simulador de transitorios.

3. Algoritmo para determinar el caudal según el método de Gibson - Dicho algoritmo se utilizará para determinar el caudal de acuerdo con lo especificado en la norma IEC-60041 (1991), y comparar los resultados obtenidos con los datos de referencia.

I.2. OBJETIVO DEL SERVICIO

Por lo que el objetivo del servicio será brindar apoyo en lo siguiente:

1. Simulador de transitorios en tuberías a presión - Apoyo en el desarrollo y la ejecución de un programa numérico en el ambiente Matlab (vers. 6 o superior) que permita simular transitorios de presión en una tubería horizontal con las siguientes opciones: posibilidad de definir las características de la tubería (diámetro, tipo de material y espesor, carga en la entrada) y del cierre progresivo de compuerta aguas abajo (función de cierre no lineal).

2. Simulador de tipo Monte Carlo - Apoyo en el desarrollo y la ejecución de un programa numérico en el ambiente Matlab que permita leer los datos generados por el simulador de transitorios de presión y corromperlos con las siguientes opciones: posibilidad de simular un tiempo de retraso (con una constante de tiempo arbitraria) y/o un desfase del cero (variable aleatoria normal con una magnitud arbitraria) y/o un ruido (variable aleatoria normal con una proporción arbitraria de la escala de medición).

3. Algoritmo para determinar el caudal según el método de Gibson - Apoyo en el desarrollo y la ejecución de un programa numérico (iterativo) en el ambiente Matlab que permita leer los datos generados por el simulador de Monte Carlo y procesarlos de conformidad con el algoritmo de Gibson descrito en la norma IEC-60041 (1991), con las siguientes opciones: posibilidad de definir los parámetros de los cálculos (tiempos considerados para estimar las pérdidas por fricción, criterio de convergencia) y de graficar los resultados (transitorios de presión, estimaciones sucesivas de caudal y errores en las estimaciones de caudal).

I.3. RESULTADOS ESPERADOS

Se esperan los siguientes resultados:

1. Simulador de transitorios en tuberías a presión - Simulador numérico que permita simular con una gran precisión -en particular, describiendo las pérdidas por fricción con el modelo de Brunone (1992)- los transitorios de presión producidos dentro de una tubería, cuando se cierra progresivamente una compuerta. Realización de pruebas con el mismo (por lo menos 4 casos simulados).

2. Simulador de tipo Monte Carlo - Simulador numérico que permita reproducir los tres principales problemas que se presentan, cuando se miden transitorios de presión con un transductor: tiempo de retraso, desfase del cero (offset) y ruido. Realización de pruebas con el mismo (por lo menos 4 x 4 = 16 casos simulados).

3. Algoritmo para determinar el caudal según el método de Gibson - Algoritmo iterativo que permita determinar el caudal según lo especificado en la norma IEC-60041 (1991), que de hecho solo explica cómo hacerlo con una técnica de planimetría. Realización de pruebas con el mismo (por lo menos 4 x 4 x 1,000 = 16,000 escenarios considerados).

II. METODOLOGÍA

II.1. TRABAJOS DE PROGRAMACION

Se llevaron a cabo las actividades que a continuación se describen con un equipo constituido por un Informático y dos Ingenieros en Hidráulica. Los trabajos de programación se hicieron en el ambiante MATLAB (vers. 6.0). Durante el mes de Marzo, se tuvieron varias reuniones con el personal del IMTA para definir los algorítmos necesarios para llevar a cabo las simulaciones deseadas:

1. Simulador de transitorios en tuberías a presión - Código basado en el esquema numérico de *Preissmann* y que utiliza el *modelo de Brunone* (1992) para describir las pérdidas por fricción. Se considera una tubería uniforme (diámetro constante). La función de cierre de la compuerta esta descrito por una *función spline*.

2. Simulador de tipo Monte Carlo - Código que utiliza la *función "randn.m"* (con una semilla dada) para simular un ruido blanco (Gausiano) y que simula el tiempo de retraso de un transductor de presión como si fuera una *función de primer orden* (utilizando una constante de tiempo).

3. Algoritmo para determinar el caudal según el método de Gibson - Código iterativo basado en lo especificado en la norma IEC-60041 (1991), en particular para definir *el tiempo final de integración* (t_F). Se considera la primera variante del método de Gibson, aplicada a un cierre total de compuerta (gasto de fuga nulo). El caudal Q_0 (m^3/s) es la integral: $Q_0 = \frac{A}{\rho L} \int_0^{t_F} \left(-\Delta P + \Delta p_f \right) dt$, donde A es el área de la sección de tubería (m^2), ρ la densidad del agua (1,000 kg/m^3), L la longitud del tramo de tuberia (m), t_F el tiempo final de integración (s), ΔP la diferencia de presión registrada durante una prueba de Gibson (Pa) y Δp_f la pérdida de presión por fricción (Pa), que se determina iterativamente.

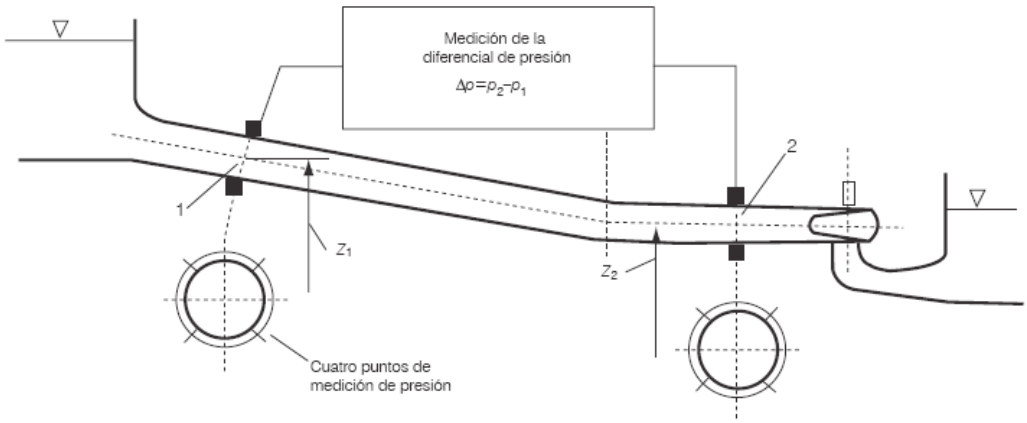

Ilustración 1. Los sitios de medición normalmente considerados cuando se aplica el método de Gibson (fuente: Urquiza *et al.*, 2007)

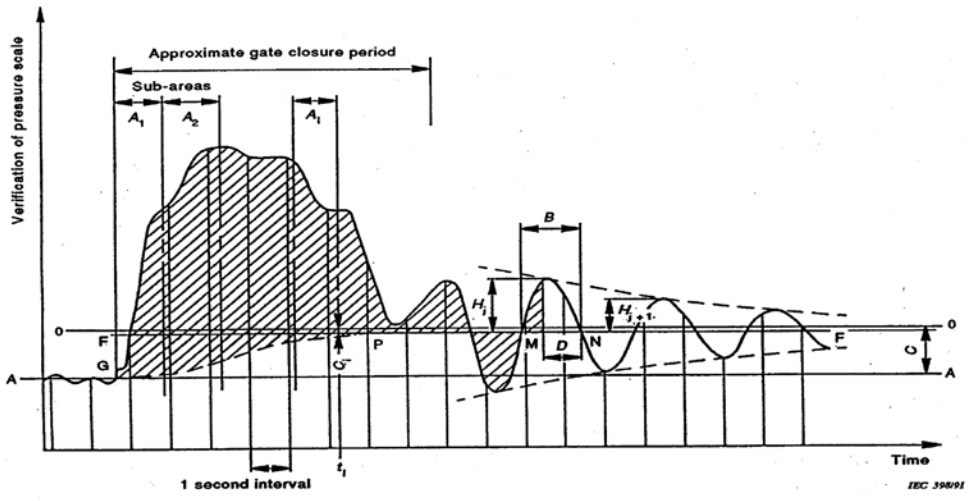

Ilustración 2. Resultado típico de una prueba de Gibson y área que se debe calcular para estimar el caudal (fuente: IEC-60041, 1991).

II.2. CONDICIONES PARA LAS SIMULACIONES

De común acuerdo con el personal del IMTA, se consideraron cuatro condiciones de flujo a presión. Estas condiciones corresponden a tubos de distintos diámetros que se han reportados en la literatura sobre el método de Gibson:

1. *Caso "Imtalab"* - Transitorio de presión en una tubería de PVC y de pequeño diámetro (0.1 m). Caso descrito en la Tesis de Maestría de Rafael Briseño (2011).

2. *Caso "Jonsson"* - Transitorio de presión en una tubería de acero y de pequeño diámetro (0.3 m). Caso descrito en el artículo de Jonnson *et al.* (2012).

3. *Caso "Bortoni"* - Transitorio de presión en una tubería de acero y de diámetro medio (3.2 m). Caso descrito en el artículo de Bortoni *et al.* (2008).

4. *Caso "Adamkowski"* - Transitorio de presión en una tubería de acero y de gran diámetro (6.5 m). Caso descrito en el artículo de Adamkowski *et al.* (2012).

II.3. REALIZACION DE LAS SIMULACIONES

Para las simulaciones, se considero el siguiente plan experimental:

1. *Cuatro tipos de tubería* - Casos "Imtalab", "Jonsson", "Bortoni" y "Adamkowski" (descritos anteriormente)

2. *Más de 500 escenarios de medición con el método de Gibson* - Por cada tipo de tubería, se generaron datos correspondientes a una prueba de Gibson para distintas posiciones (100) del sensor de presión "aguas arriba" y también varios espaciamientos (*L*) relativos al sensor de presión "aguas abajo".

3. *Cinco casos de ruido sobre los datos de presión* - Por cada escenario de medición, se consideraron cinco opciones para corromper los datos de presión, y de esta manera simular datos "ruidosos":

Clave	Datos de salida	Parámetros
0	Datos de presión sin ruido	
1	Datos con ruido aleatorio	Desviación estándar = 0.1 % de la Escala de Medición (*)
2	Datos de presión con error sistemático en el cero	Sesgo en el cero = 0.1 % de la Escala de Medición (*)
3	Datos con retraso	Constante de tiempo = 0.01 s
7	Datos con ruido, sesgo y retraso	Combina los casos 1, 2 y 3

(*) La Escala de Medición (EM) se calcula a cada vez con la formula de Jouguet

3. *Diez repeticiones (enfoque de Monte Carlo) cuando se simulan datos con ruido* - Por lo tanto, en el plan de simulación se consideraron: 4 tipos de tuberia x 500 escenarios x 4 tipos de ruido x 10 repeticiones, es decir más de 80,000 cálculos de Gibson.

III. RESULTADOS OBTENIDOS

III.1. SIMULADOR DE TRANSITORIOS EN TUBERIAS A PRESION

En base a la información recopilada de las publicaciones científicos es posible reconstruir cada una de sus pruebas y obtener resultados que permitan fundamentar que los transitorios simulados con el programa de cómputo desarrollado existen en condiciones reales. De igual manera se verifico gráficamente que los resultados plasmados en los diagramas presión–tiempo del programa son similares a los diagramas publicados por los autores aplicando sus características específicas (véase Ilustraciones 3 - 6).

El programa de simulación genera una tabla de datos calculados, la cual está ordenada en función del tiempo empleado para la prueba, así como del espacio (que son las secciones de análisis en la tubería); el primero representa el número de filas y el segundo el número de columnas de la tabla. Los datos contenidos son entonces, la evolución de la presión en metros de columna de agua para una prueba específica.

Para las pruebas se trabajó con 100 secciones de análisis y tiempos de simulación de 150 segundos en cada uno de los tipos de tubería (Imtalab", "Jonsson", "Bortoni" y "Adamkowski"). En base a lo anterior es posible generar un gran número de casos de análisis para la determinación del gasto posteriormente ya que basta relacionar una sección de análisis con otra para generar las diferencias de presión y posteriormente calcular el gasto, esto con el fin de tener diversas secciones ubicadas a lo largo de la conducción y con diferentes longitudes de análisis.

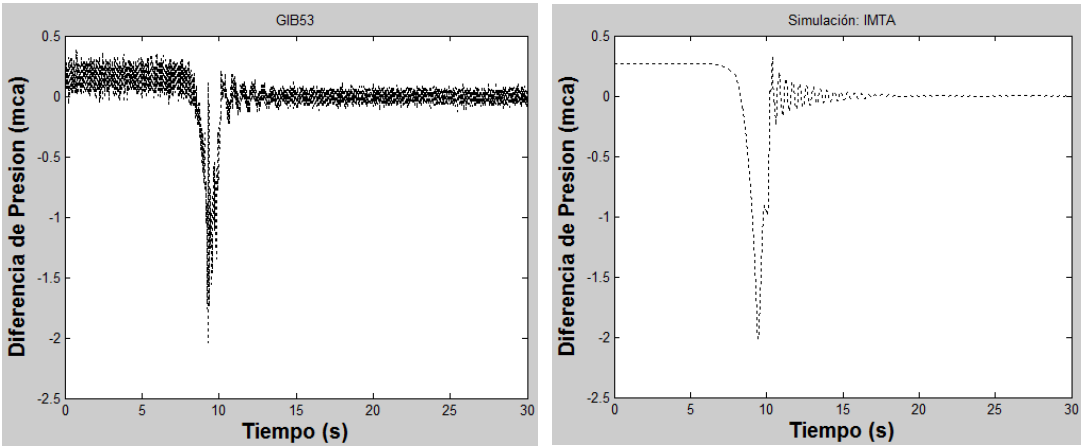

Ilustración 3. Comparación entre el diagrama presión-tiempo del IMTA
y el simulado con el código Preissman
(sensores ubicados al 79% y 97% de la longitud total, longitud entre sensores = 13 m)

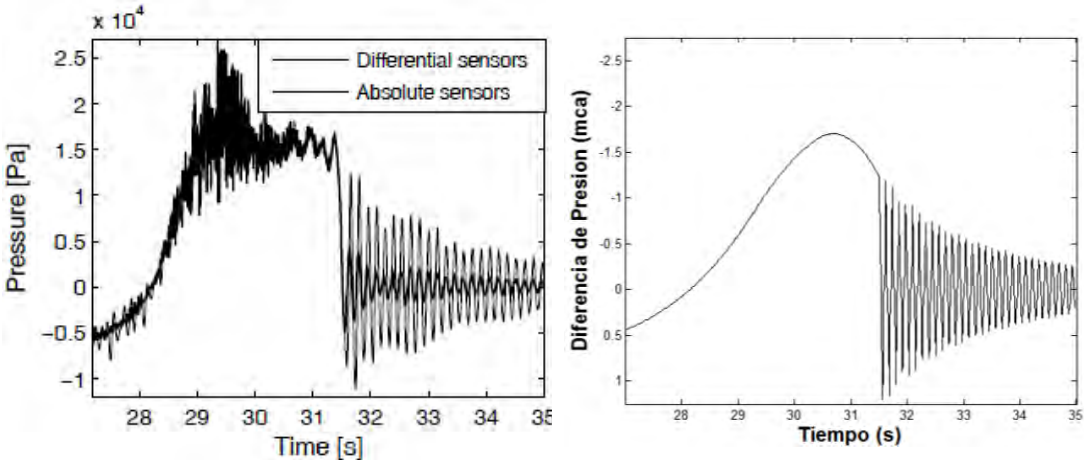

Ilustración 4. Comparación del diagrama presión-tiempo de Jonsson
y el simulado con el código Preissman
(sensores ubicados al 56% y 86% de la longitud total, longitud entre sensores = 8 m)

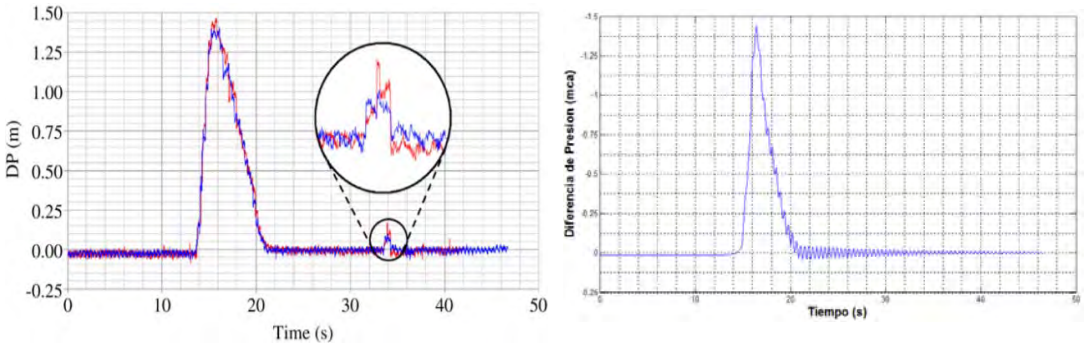

Ilustración 5. Comparación del diagrama presión-tiempo de Bortoni
y el simulado con el código Preissman
(sensores ubicados al 48% y 60% de la longitud total, longitud entre sensores = 12 m)

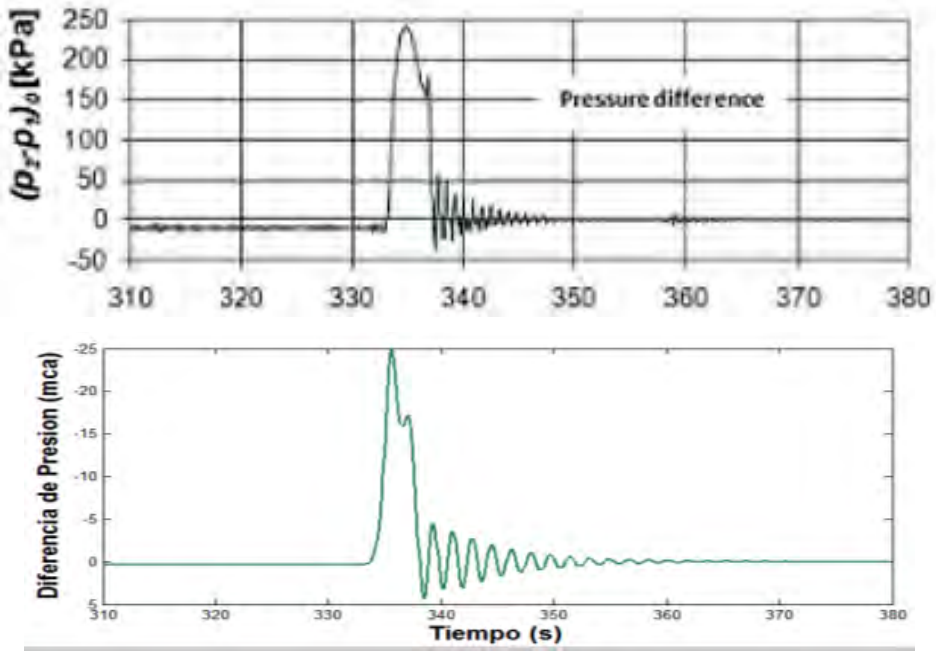

Ilustración 6. Comparación del diagrama presión-tiempo de Adamkowski
y el simulado con el código Preissman
(sensores ubicados al 5% y 47% de la longitud total, longitud entre sensores = 108 m)

III.2. SIMULADOR DE TIPO MONTE CARLO

Como se mencionó, el simulador de tipo Monte Carlo permite corromper los datos de presión simulados con el programa anterior de tres maneras (tiempo de retraso, ruido y/o sesgo), esto con el fin de reproducir los posibles datos que se obtendrían al utilizar un transductor de presión para una instrumentación real. Se dice que se corrompen los datos, ya que los transitorios que se obtienen del primer programa de cómputo están formulados en base a las leyes de conservación de masa, energía y cantidad de movimiento, por lo que se obtienen resultados teóricos en condiciones ideales (véase Ilustraciones 7 - 8).

1. El ruido aleatorio representa el primer caso que se añade en el programa utilizando una función para generar diferentes tablas de números aleatorios normalizados (distibución de probabilidad de Gauss), cada una de estas tablas con una semilla distinta de generación y que al multiplicarse por la precisión considerada por las características de la prueba y del transductor (*Escala de medición*) sumen un ruido aleatorio a cada uno de los datos ideales obtenidos.

2. El sesgo (*offset* del transductor) representa el segundo caso de análisis y a diferencia del ruido aleatorio descrito en el párrafo anterior, para el análisis se generan diferentes tablas con números aleatorios diferentes para cada posición pero que se mantienen constantes en el tiempo, para posteriormente sumarlos a los datos ideales; esto se hace con la finalidad de que el *offset* dependa del transductor y no de cada dato que éste registre.

3. El tiempo de respuesta representa la diferencia que existe entre el registro computacional realizado por el transductor en comparación al valor real, para lo anterior se utiliza un cinética de respuesta de primer orden para diferentes (ver Anexo V.2.1)

Además de lo anterior, el programa computacional desarrollado es capaz de combinar cada uno de los diferentes casos o dejar la información intacta para trabajar con los datos ideales.

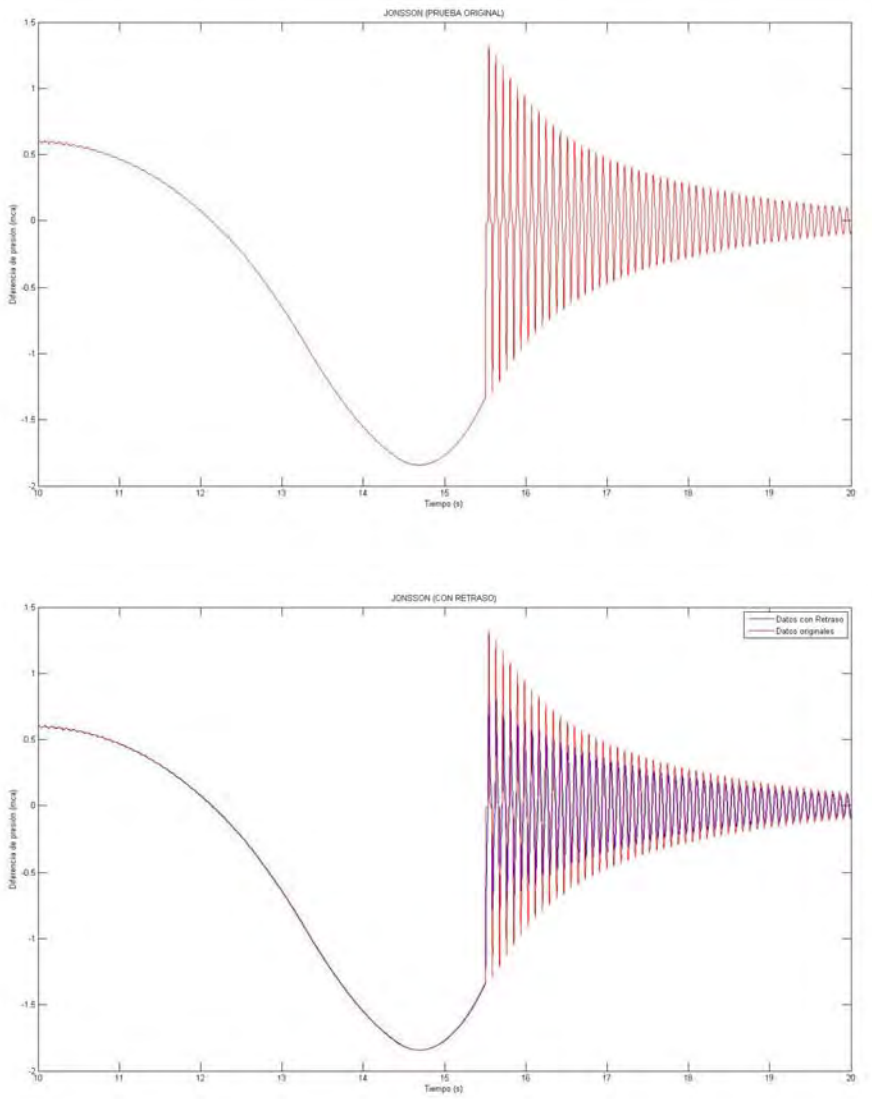

Ilustración 7. Simulación de un transitorio de presión (caso "Jonsson"): datos originales (arriba) y datos con tiempo de retraso (abajo)

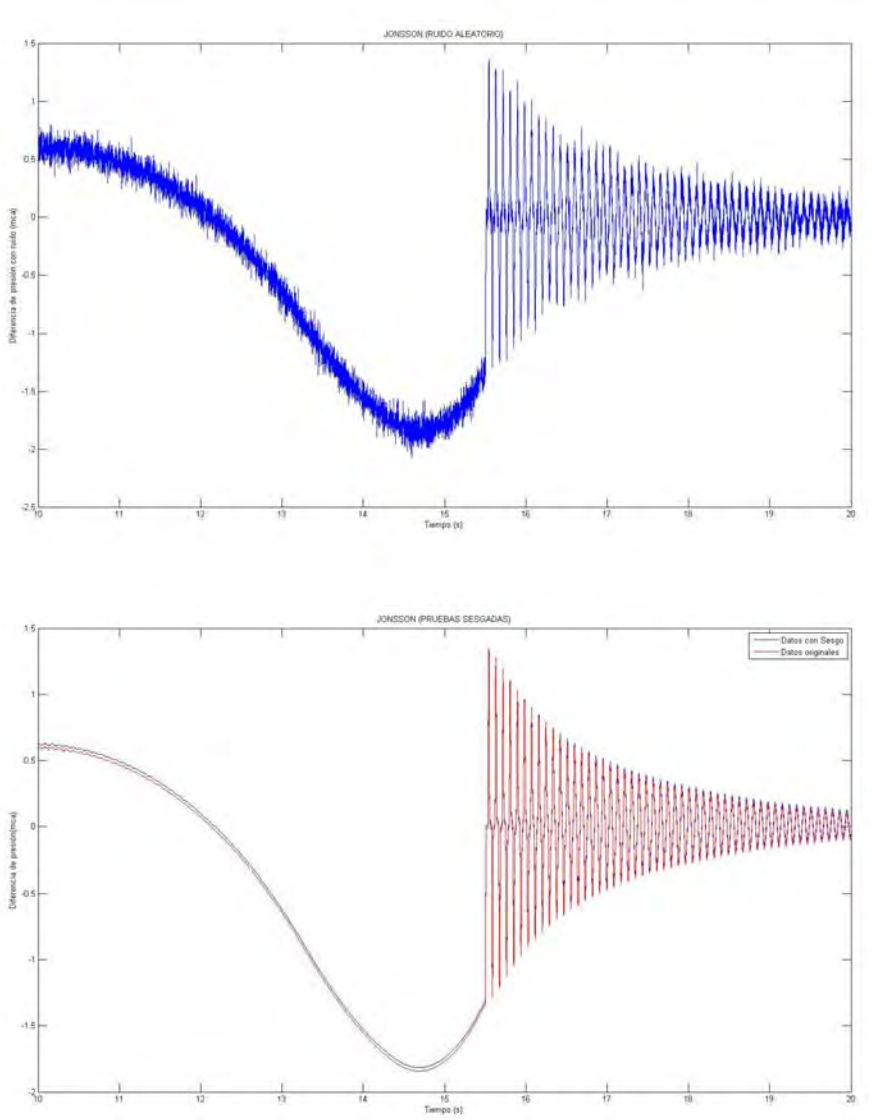

Ilustración 8. Simulación de un transitorio de presión (caso "Jonsson"): datos con ruido (arriba) y datos con error sistemático (abajo)

III.3. ALGORITMO PARA DETERMINAR EL CAUDAL

El algoritmo para determinar el caudal está basado en la norma IEC-60041 (1991) la cual describe el procedimiento a realizar en un conducto a presión en base a los datos de presión obtenidos por un transitorio de presión en dos secciones del conducto.

Del programa de Monte Carlo se selecciona el registro de presiones de dos secciones específicas y mediante un rastreo punto por punto de la información en el diagrama de diferencia de presión contra el tiempo se localizan los puntos donde las oscilaciones cruzan el eje creo en las abscisas así como el punto donde comienza el cierre de la compuerta.

Conociendo el inicio del transitorio y el del segundo o tercer cruce de la oscilación se genera una función de pérdidas por fricción. Ambas curvas al ser integradas proporcionan el gasto que posteriormente será corregido en base a las especificaciones de la norma para la estimación del gasto. Posteriormente se integra únicamente el resto de la curva transitoria; la suma de ambas representa el caudal de la prueba.

Además de eso se utiliza un modelo que describe al transitorio en base a una ecuación que relaciona la amplitud máxima, el periodo de las oscilaciones y el decaimiento del transitorio en la zona ubicada después de la línea de pérdidas por fricción, el cálculo de está función genera un modelo oscilador ideal que se integra y se suma al gasto obtenido por la integración de las curvas de pérdidas por fricción y diferencia de presión.

Se muestran a continuacioón algunos resultados obtenidos con el programa para la determinación del caudal según el método de Gibson cuando los datos de presión no son ruidosos (véase Ilustraciones 9 - 10) y cuando se agrega una componente de ruido a los datos (véase Ilustraciones 11 - 12).

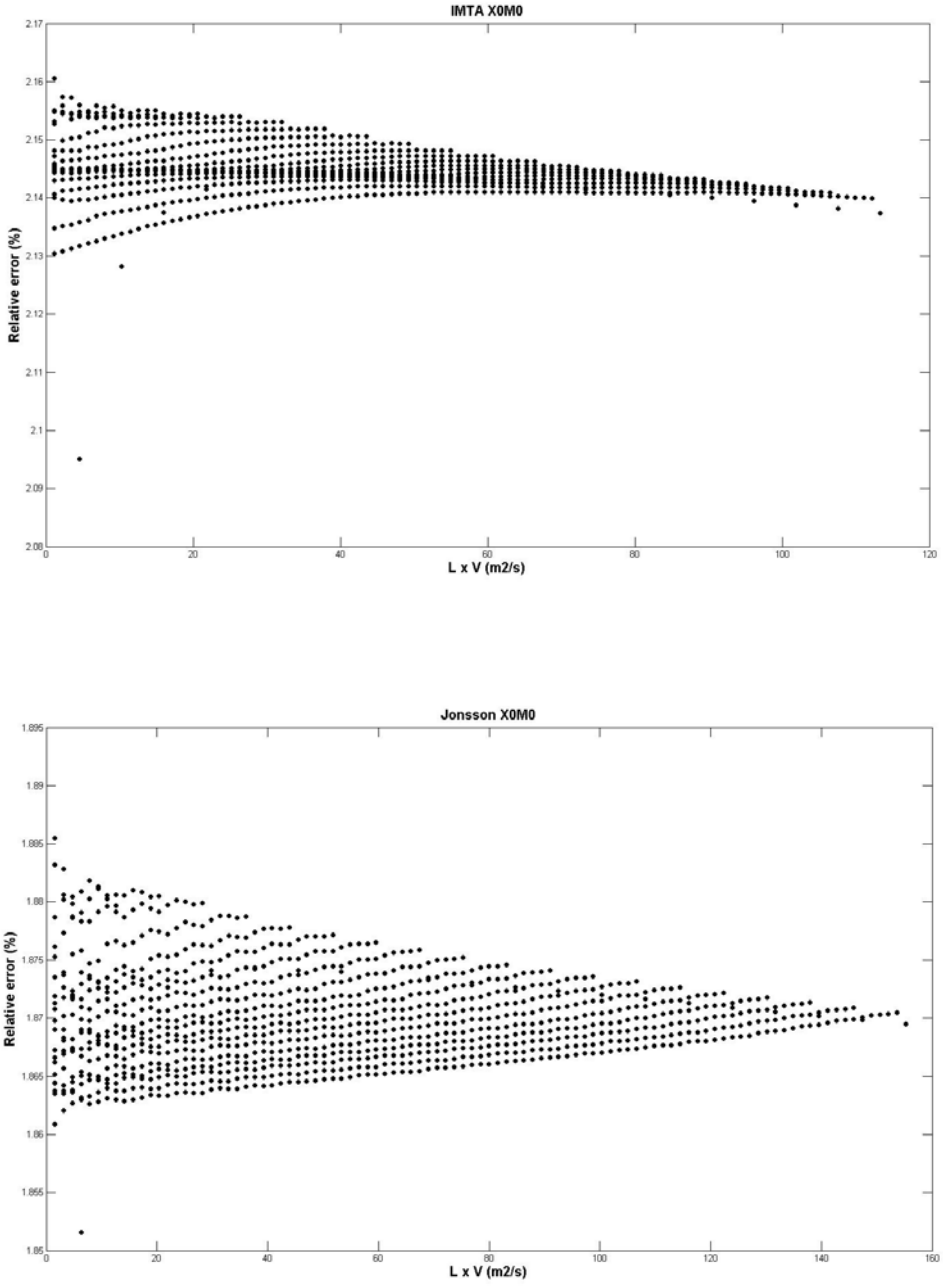

Ilustración 9. Evaluación del método de Gibson con datos sin ruido:
Casos "Imtalab" (arriba) y "Jonsson" (abajo)

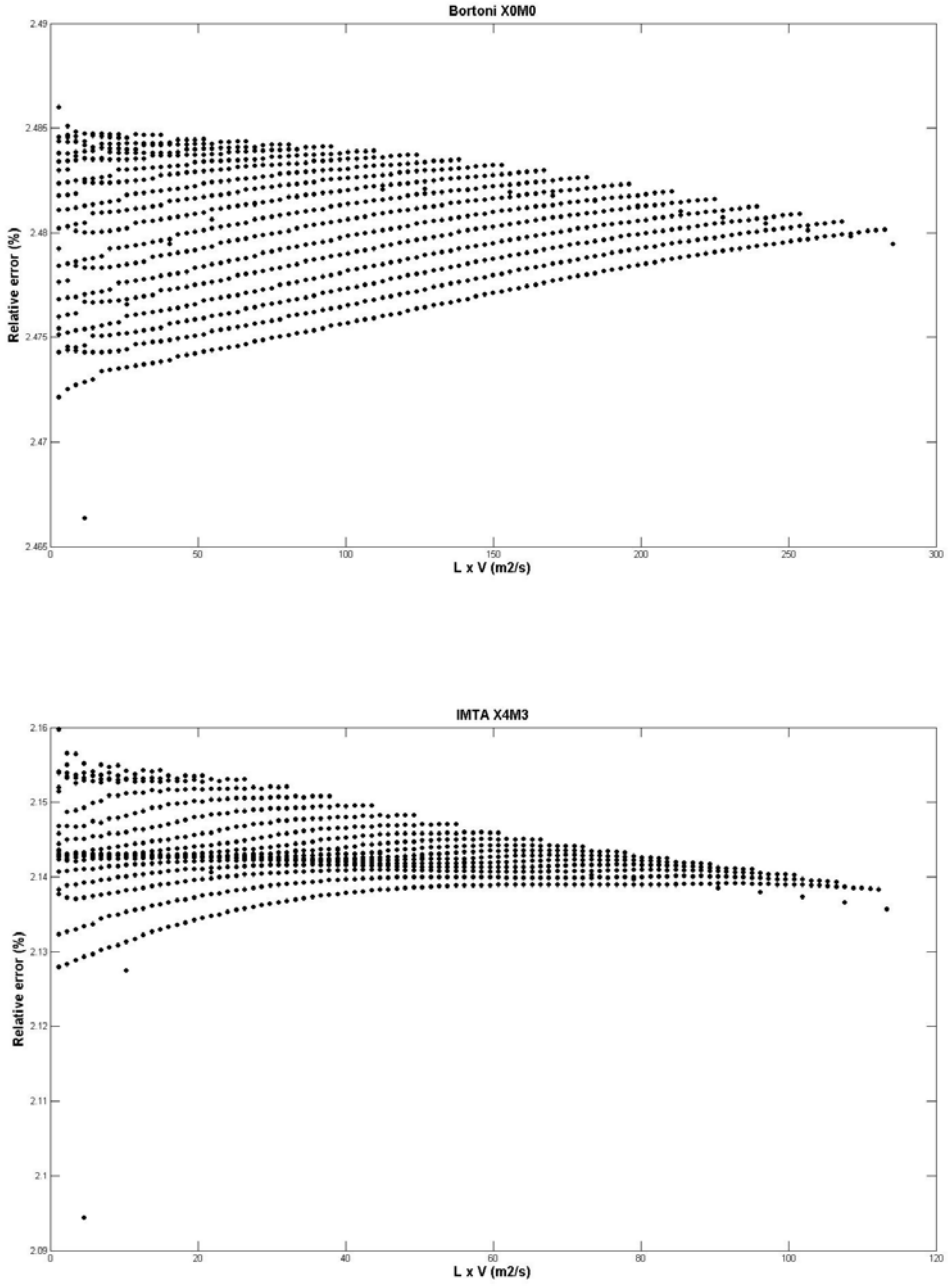

Ilustración 10. Evaluación del método de Gibson con datos sin ruido:
Casos "Bortoni" (arriba) y "Adamkowski" (abajo)

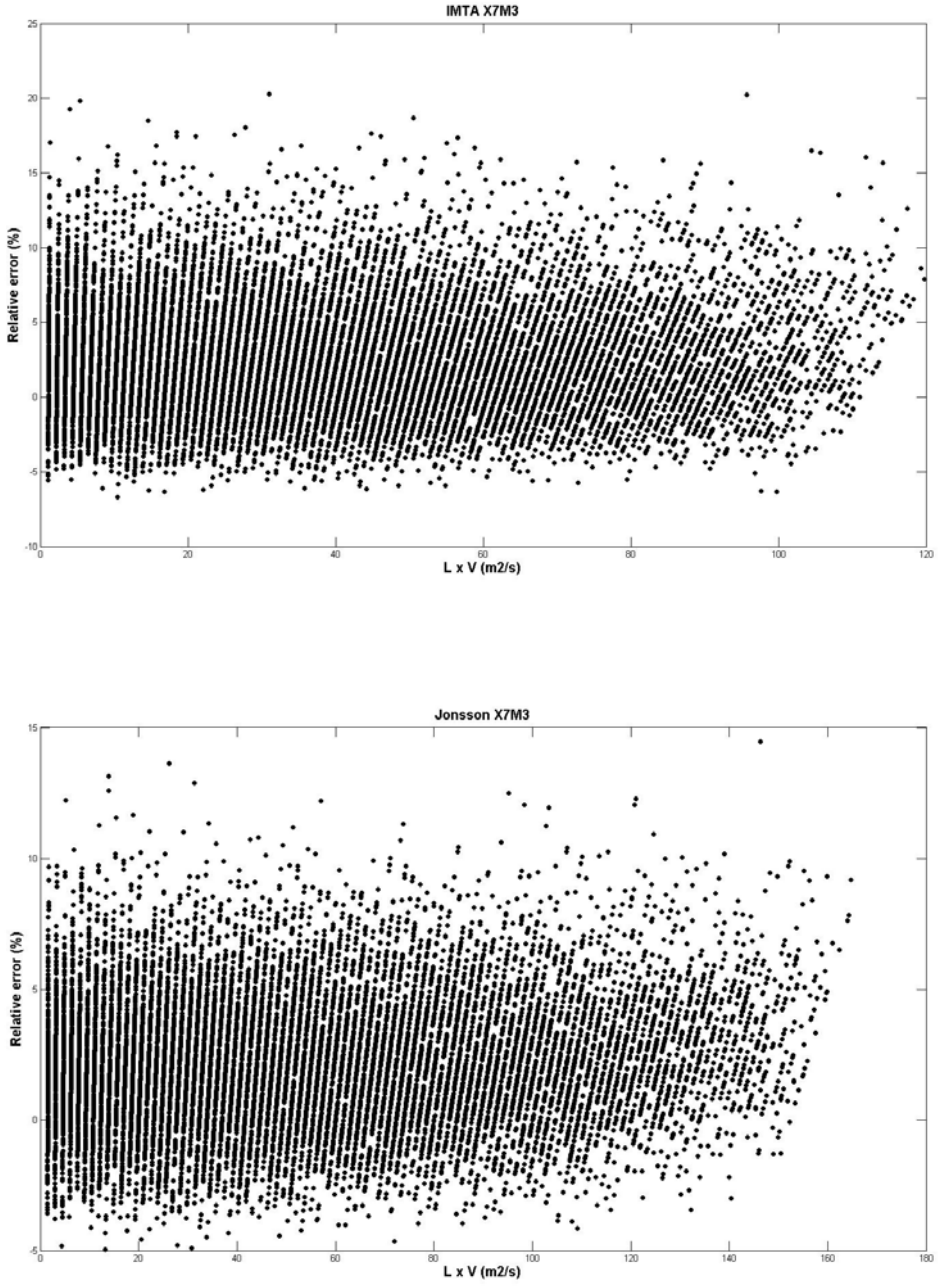

Ilustración 11. Evaluación del método de Gibson con datos con ruido:
Casos "Imtalab" (arriba) y "Jonsson" (abajo)

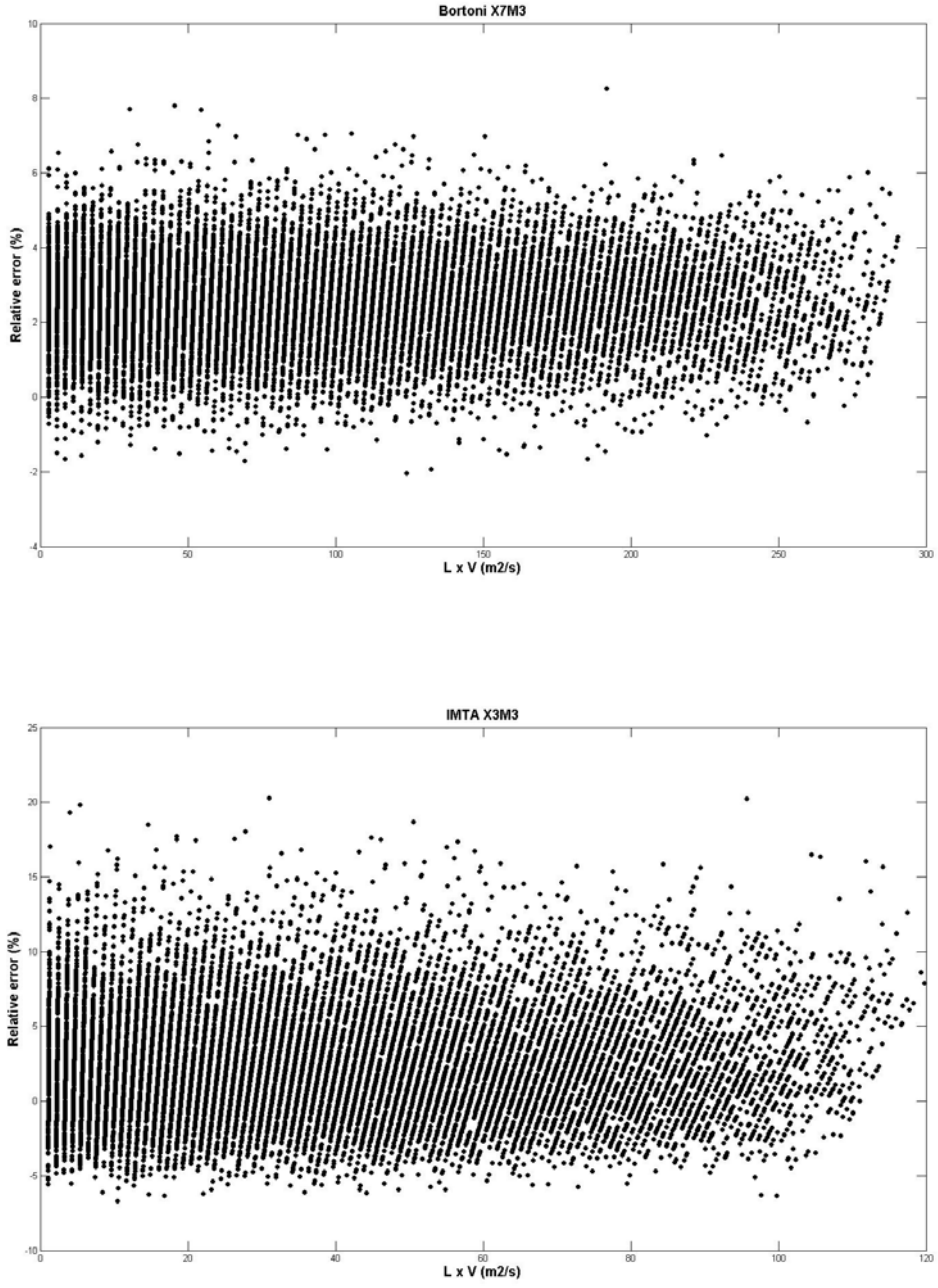

Ilustración 12. Evaluación del método de Gibson con datos con ruido:
Casos "Bortoni" (arriba) y "Adamkowski" (abajo)

IV. CONCLUSIÓN

Tal como se había solicitado en la orden de servicio, se brindo al personal del IMTA un apoyo en el desarrollo y la ejecución de tres códigos para poder evaluar numericamente el método de Gibson (1923) tal como esta descrito en la norma IEC-60041 (1991):

1. Simulador de transitorios en tuberías a presión - Simulador numérico que permita simular con una gran precisión los transitorios de presión producidos dentro de una tubería, cuando se cierra progresivamente una compuerta. Realización de pruebas con el mismo (4 casos simulados).

2. Simulador de tipo Monte Carlo - Simulador numérico que permita reproducir los tres principales problemas que se presentan, cuando se miden transitorios de presión con un transductor: tiempo de retraso, desfase del cero (offset) y ruido. Realización de pruebas con el mismo (16 casos simulados).

3. Algoritmo para determinar el caudal según el método de Gibson - Algoritmo iterativo que permita determinar el caudal según lo especificado en la norma IEC-60041 (1991). Realización de pruebas con el mismo (más de 80,000 escenarios considerados).

ELABORO:	ING. RAMON DANIEL SAMANIEGO MARTINEZ	CED. PROF. 1759491

V. ANEXOS

V.1. CÓDIGO PARA SIMULAR TRANSITORIOS EN TUBERIAS A PRESION

V.1.1. DATOS DE ENTRADA PARA LA SIMULACIÓN

Durante la simulación es importante tener información mínima específica de las pruebas, a continuación se presentan las variables que deben ser declaradas dependiendo de la información que se determine en la bibliografía:

1. Información mínima necesaria para realizar la simulación:

   Diámetro.
   Rugosidad.
   Pérdida local en la rejilla.
   Longitud.
   Altura del embalse.
   Tiempo de inicio de cierre de la válvula.
   Tiempo de cierre de la válvula.
   Tiempo de simulación.
   Número de intervalos de discretización.

2. Datos que pueden ser omitidos en el cálculo si se conoce la celeridad de onda:

   Espesor.
   Módulo de elasticidad de la tubería.
   Relación de Poisson.
   Módulo de compresibilidad del agua.
   Densidad del fluido.

3. Información que puede ser omitida si se conoce el caudal de la prueba:

   Altura de la descarga.
   Presión de la descarga.
   Coeficiente de descarga.
   Límite de convergencia en el cálculo del caudal (establecido por default).

4. Información declarada en las variables pero que puede pasarse por alto:

   Viscosidad cinemática a 20 °C.
   Tiempo de despliegue de gráfico.

5. Parámetros de convergencia y simulación (establecidos por default):

   Límite de convergencia no lineal en el cálculo de caudal.
   Límite de convergencia no lineal en el cálculo de nivel.
   Factor de peso temporal.
   Factor de peso espacial.
   Aceleración de la gravedad.

V.1.2. CÓDIGO NUMÉRICO

```
%**********************************************************************
% Solución del golpe de ariete en una tubería
% Aplicando un esquema de caja tipo Preissmann
% Adición del método de cálculo de fricción propuesto por Brunone
%**********************************************************************
clear
%**********************************************************************
% Datos de la tubería
%**********************************************************************
eval( 'D      =  0.3 '      );  % Diámetro de la tubería (m)
eval( 'ep     =  1e-5'      );  % Rugosidad (m)
eval( 'esp    =  1/4*0.0254' );  % Espesor de la tubería (m)
eval( 'E_elas =  200*1e9'     );  % Módulo de elasticidad de la tubería (m)
eval( 'v_poisson = 0.3'       );  % Relación de Poisson (adim)
%**********************************************************************
% Datos de la conducción
%**********************************************************************
eval( 'kl     =  0.5   ' );  % Pérdida local rejilla (admi.)
eval( 'L      = 26.67   ' );  % Longitud de la conducción (m)
eval( 'H_emb  = 9.75   ' );  % Carga total (m)
eval( 'z2     =  0.0   ' );  % Altura de la descarga (m)
eval( 'h2     =  0.0   ' );  % Sumergencia de la descarga (m)
eval( 'g      =  9.81  ' );  % Aceleración de la gravedad (m/s2)
eval( 'Cd     =  0.65  ' );  % Coeficiente de descarga de la válvula
%**********************************************************************
% Datos del fluido
%**********************************************************************
eval( 'K_elas =  2.19*1e9');  % Módulo de elasticidad del agua (m)
eval( 'nu     =  1e-6    ');  % Viscosidad cinemática (m2/s)
eval( 'rho    =  999     ');  % densidad del fluido (20 oC) (m/s2)
%**********************************************************************
% Tiempo de las condiciones de simulación
%**********************************************************************
eval( 'T_inicio     = 10.0  ' );  % Tiempo de inicio del cierre de la válvula (s)
eval( 'T_disp       =  0.1'); % Tiempo de despliegue de gráfico
eval( 'T_simulacion = 150.0  ' );  % Tiempo total de simulación (m/s2)
%**********************************************************************
% Condición de frontera al final de la tubería
%**********************************************************************
eval( 'Tcierre      =  5.5 ');  % Tiempo de cierra de la válvula
Tiempo=[0.0000 0.1250 0.8000 0.9500 0.9800 1.0000];% Política de cierre (tau vs t)
Tau   =[1.0000 0. 0.3750 0.0800 0.0300 0.0000];
%**********************************************************************
```

```
Tiempo=Tiempo*Tcierre+ T_inicio;
T_final=Tiempo(length(Tiempo));
Tiempo_i = T_inicio:(T_final-T_inicio)/100:T_final;
coef_val = spline(Tiempo,Tau);

figure(1)
clf
plot(Tiempo,Tau,'o',Tiempo_i,ppval(coef_val,Tiempo_i))
xlabel('Tiempo de apertura (s)')
ylabel('Apertura (admi)')
grid

%**********************************************************************
% Valores de discretización y convergencia
%**********************************************************************
eval( 'J        = 100    ' );  % Número de intervalos de discretización (entero)
eval( 'aq       = 1e-15  ' );  % Límite de convergencia en cálculo de caudal (m3/s)
eval( 'error_Q  = 1e-12  ' );  % Límite convergencia no lineal en cálculo caudal (m3/s)
eval( 'error_H  = 1e-12  ' );  % Límite convergencia no lineal en cálculo de nivel (m)
eval( 'theta    = 0.6    ' );  % Factor de peso temporal
eval( 'phi      = 0.5    ' );  % Factor de peso espacial
x=0:L/J:L;
ax=x(2);                        % Incremento espacial

%**********************************************************************
% Contrucción de la condición inicial ;  t=0
%**********************************************************************

% Condición de sujección de la tubería
psi=D/esp*(1-v_poisson^2);

% Valor de la celeridad de onda
celeridad=(K_elas/rho/(1+K_elas/E_elas*psi))^0.5;

% Condición de estabilidad
% at/ax <= 1/a;
at=1*ax/celeridad;
% NOTA: para este esquema at puede ser mayor a la condición Courant

%**********************************************************************
% Determinación del caudal máximo sin fricción
%**********************************************************************
A=(pi*D^2)/4;  % área de tubería
q1=A*(2*g*(H_emb-z2-h2))^0.5;

fprintf('El gasto sin fricción=  %12.5f \n', q1)
```

```
%*********************************************************************
% Determinación del caudal máximo con fricción
% incluye pérdidal local y
% pérdida por fricción ecuación de Darcy-Weisbach
%*********************************************************************
q0=0.00001;
while abs(q0-q1)/q0 > aq
    q0=q1;
    f1=DarcyWeis(q0/A,D,ep);
    q1=A*(2*g*(H_emb-z2-h2)/(1+f1*L/D+kl+1/Cd^2))^0.5;
end

% Carga aguas arriba de la válvula
H0=1/Cd^2*(q1/A)^2/2/g;
fprintf('El gasto con fricción=  %12.5f \n',q1)
fprintf('Carga aguas arriba de la válvula=  %12.5f \n',H0)

%*********************************************************************
% Armado de matrices para simulación transitoria
% *********************************************************************
%  Vectores de solución espacial y temporal
%  Q(1,:)       ;  Q(j,n      )
%  Q(2,:)       ;  Q(j,n+1,m  )
%  Q(3,:)       ;  Q(j,n+1,m+1)
Q=zeros(3,J+1);
%  H(1,:)       ;  H(j,n      )
%  H(2,:)       ;  H(j,n+1,m  )
%  H(3,:)       ;  H(j,n+1,m+1)
H=zeros(3,J+1);
%********************************** ********************************
%  Vectores auxialiares para la matriz de coeficientes

e1 = zeros(1,J);
b2 = zeros(1,J);
d2 = zeros(1,J);
e2 = zeros(1,J);
pi1= zeros(1,J);
pi2= zeros(1,J);
bb = zeros(1,2*J)';
%error_masa=zeros(1,J);
%error_momentum=zeros(1,J);
k=zeros(1,J);
dk=zeros(1,J);
fq=zeros(1,J);
Q_gib_Pr_Br=zeros(1,J);

%*********************************************************************
```

```
% ********************************************************************
% Vectores de la condición inicial t=0
% Q(x,0)= q0  caudal inicial en estado permanente
% H(x,0)= h(x), variación de la carga hidráulica desde el embalse hasta la válvula

Q(1,:)=q1;
H(1,1)=H_emb-q1^2/A^2/2/g*(1+kl);
for j=1:J
   H(1,j+1)=H(1,1)-q1^2/A^2/2/g*(f1*j*ax/D);
end
t=0;

%**************************************************************************
% Simulación transitoria t > 0
%**************************************************************************

a1=(1-phi)/at;
b1=-celeridad^2*theta/(g*A*ax);
c1=phi/at;
d1=-b1;
a2=-g*A/ax*theta;
c2=-a2;

a1i=zeros(1,J-1);
a1j=zeros(1,J-1);
a1v=zeros(1,J-1);
a2i=zeros(1,J-1);
a2j=zeros(1,J-1);
a2v=zeros(1,J-1);
b1i=zeros(1,J);
b1j=zeros(1,J);
b1v=zeros(1,J);
b2i=zeros(1,J);
b2j=zeros(1,J);
b2v=zeros(1,J);
c1i=zeros(1,J);
c1j=zeros(1,J);
c1v=zeros(1,J);
c2i=zeros(1,J);
c2j=zeros(1,J);
c2v=zeros(1,J);
d1i=zeros(1,J-1);
d1j=zeros(1,J-1);
d1v=zeros(1,J-1);
d2i=zeros(1,J-1);
d2j=zeros(1,J-1);
d2v=zeros(1,J-1);
```

```
% Coeficientes invariantes en la matriz de coeficientes
for j=1:J
   if j > 1
      a1i(j-1)=j*2-1;
      a1j(j-1)=j-2;
      a1v(j-1)=a1;
      a2i(j-1)=j*2;
      a2j(j-1)=j*2-2;
      a2v(j-1)=a2;
   end
   b1i(j)=j-1;
   b1j(j)=j*2-1;
   b1v(j)=b1;
   c1i(j)=j*2-1;
   c1j(j)=j*2;
   c1v(j)=c1;
   c2i(j)=j*2;
   c2j(j)=j*2;
   c2v(j)=c2;
   % índices para b2s
   b2i(j)=j*2;
   b2j(j)=j*2-1;
   if j < J
      d1i(j)=j*2-1;
      d1j(j)=j*2+1;
      d1v(j)=d1;
      %índice para d2s
      d2i(j)=j*2;
      d2j(j)=j*2+1;
   end
end
a1s=sparse(a1i,a1j,a1v,2*J,2*J);
a2s=sparse(a2i,a2j,a2v,2*J,2*J);
b1s=sparse(b1i,b1j,b1v,2*J,2*J);
c1s=sparse(c1i,c1j,c1v,2*J,2*J);
c2s=sparse(c2i,c2j,c2v,2*J,2*J);
d1s=sparse(d1i,d1j,d1v,2*J,2*J);
% Matriz porosa invariante
 AA1=a1s+a2s+b1s+c1s+c2s+d1s;

T_save=0.001;
T_data=T_save;
flag=1;
T_conta=0;
m=0;
```

```
while t < T_simulacion
    %fprintf('tiempo de simulación %8.4f  s \n',t)
   %*********************************************************************
   % Terminos de actualización para n y m (ecuación de masa)
   for j=1:J
      e1(j)=a1*H(1,j)+c1*H(1,j)-(1-theta)*celeridad^2/(g*ax)*(Q(1,j+1)-Q(1,j));
   end
   %*************************************************************************
   % Condición de frontera aguas abajo (Válvula)
   %*************************************************************************
   if t< T_inicio
       Q(3,J+1)=Tau(1)*q1;
   elseif t > T_final
       Q(3,J+1)=Tau(length(Tau))*q1;
   else
      % política de cierre de la válvula Cvn
      Q(3,J+1)=ppval(coef_val,t)*q1;
   end
   %*************************************************************************
   % Condición de frontera aguas arriba (Embalse)
   %*************************************************************************
   H(3,1)=H_emb-(1+kl*sign(Q(1,1)))*Q(1,1)^2/2/g/A^2;

   % Construcción de la iteración no lineal de Picard
   for j=1:J
      H(3,j+1)=H(1,j+1);
      H(2,j+1)=0;
      Q(3,j  )=Q(1,j  );
      Q(2,j  )=0;
   end
   dH=max(abs(H(2,:)-H(3,:)));
   dQ=max(abs(Q(2,:)-Q(3,:)));

   itera=0;
   while dH > error_H && dQ > error_Q
      Q(2,:)=Q(3,:);
      H(2,:)=H(3,:);
      for j=1:J+1
       re=abs(Q(1,j))/A*D/1e-6;
       if re<2300
           Cj=0.00476;
       else
           Cj=7.41/re^(log10(14.3/re^0.05));
       end
       k(j)=(Cj^0.5)/2.0;
       fq(j)=DarcyWeis(abs(Q(1,j))/A,D,ep);
      end
```

```
for j=1:J
     %*********************************************************************
     % Términos no lineales para n+1, m
     %*********************************************************************
     dk(j)=(1-phi)*k(j)+phi*k(j+1);
     pi1(j)=1/A*((1-theta)*((1-phi)*Q(1,j)+phi*Q(1,j+1))+...
                  theta *((1-phi)*Q(2,j)+phi*Q(2,j+1)))-...
                  dk(j)*celeridad;
   pi2(j)=fq(j)*sign(Q(1,j))/(2*D*A)*...
                  ((1-theta)*((1-phi)*Q(1,j)+phi*Q(1,j+1))+...
                      theta *((1-phi)*Q(2,j)+phi*Q(2,j+1)));
   b2(j)=(1-phi)/at*(1+dk(j)/2)-pi1(j)*theta/ax+pi2(j)*theta*(1-phi);
   d2(j)=   phi /at*(1+dk(j)/2)+pi1(j)*theta/ax+pi2(j)*theta*   phi;
   e2(j)=-g*A/ax*(1-theta)*(H(1,j+1)-H(1,j))+...
      ((1-phi)/at*(1+dk(j)/2)+ 1-theta)/ax-pi2(j)*(1-theta)*(1-phi))*Q(1,j  )+...
          (phi/at*(1+dk(j)/2)-pi1(j)*(1-theta)/ *(1-theta)*phi)*Q(1,j+1);
 end

 % construcción del arreglo matricial pentadiagonal,
 % b1 c1 d1                       Q1    e1,1-a1*g(tn)
 % b2 c2 d2                       H2    e2,1-a2*g(tn)
 %    a1 b1 c1 d1                 Q2    e1,2
 %    a2 b2 c2 d2                 H3    e2,2
 %          a1 b1 c1 d1           Q3  = e1,3
 %          a2 b2 c2 d2           H4    e2,3
 %                a1 b1 c1 d1     Q4    e1,4
 %                a2 b2 c2 d2     H5    e2,5
 %                      a1 b1 c1  Q5    e1,6-d1*f(tn)
 % El tamaño de la matriz de coeficientes es AA[J]X[J]=bb[J]
 for j=1:J
    b2v(j)=b2(j);
    if j < J
       d2v(j)=d2(j);
    end
    if j==1
       bb(2*j-1)=e1(j)-a1*H(3,1);
       bb(2*j  )=e2(j)-a2*H(3,1);
    elseif j==J
       bb(2*j-1)=e1(j)-d1   *Q(3,J);
       bb(2*j  )=e2(j)-d2(j)*Q(3,J);
    else
       bb(2*j-1)=e1(j);
       bb(2*j  )=e2(j);
    end
 end
```

```
      b2s=sparse(b2i,b2j,b2v,2*J,2*J);
      d2s=sparse(d2i,d2j,d2v,2*J,2*J);
      % Matriz porosa actualizada
       AA=AA1+b2s+d2s;
      %*************************************************************
      % Solución del sistema matricial
      % valores de H,Q para n+1,m+1
      %*************************************************************
      xx=AA\bb;
      for j=1:J
         H(3,j+1)=xx(2*j);
         Q(3,j)=xx(2*j-1);
      end
      dH=max(abs(H(2,:)-H(3,:)));
      dQ=max(abs(Q(2,:)-Q(3,:)));
      itera=itera+1;
    end

   % Guardo de información
   if t> T_data
       m=m+1;
        adp_p(m,1:J+1)=H(3,:);
        adp_q(m,1:J+1)=Q(3,:);
        time(m,1)=t;
        T_data=T_save;
        T_data=T_data+t;
   end
   % Actualización de (n+1,m+1) ->  (n)
   Q(1,:)=Q(3,:);
   H(1,:)=H(3,:);
   t=t+at
end

   TIEMPO  = [ D ; time ]            ;
   PRESION = [ x' adp_p' ]'    ;
   PRESION = [ TIEMPO  PRESION   ]     ;
   GASTO   = [ x' adp_q' ]'      ;
   GASTO   = [ TIEMPO   GASTO  ]       ;
   TOTAL   = [ PRESION ; GASTO ]       ;

save 'c:\Users\ \Desktop\PJ1.txt' TOTAL  -ascii
```

V.2. CÓDIGO PARA SIMULACIONES DE TIPO MONTE CARLO

V.2.1. TIEMPO DE RESPUESTA DE UN TRANSDUCTOR DE PRESIÓN

Para simular el tiempo de respuesta de un transductor de presión, se consideró una cinética de respuesta de primer orden.

1. Problemática

   Se tiene una serie discreta de datos (periodo de muestreo Δt) obtenidos con un transitorio de presión (t , P_o) y se pretende simular el efecto del tiempo de respuesta de un transductor de presión, es decir, generar lo que se hubiera "medido" en la realidad (t , P).

2. Determinación de la constante de tiempo del transductor

   Esto se puede hacer si se tiene la respuesta del transductor a un escalón; dicha respuesta se describe (al primer orden) por la siguiente función: $P(t) = P_{\max}\left(1 - e^{-t/\tau}\right)$, donde τ es la *constante de tiempo* del transductor (s)

Tiempo (s)	Proporción del escalón (Pa)
1 × τ	0.632 × Pmax
2 × τ	0.865 × Pmax
3 × τ	0.950 × Pmax
4 × τ	0.982 × Pmax
5 × τ	0.993 × Pmax

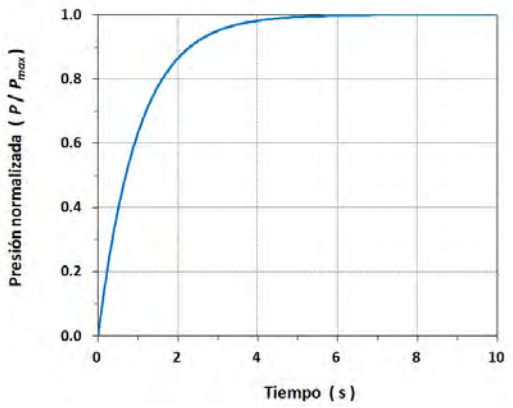

3. Simulación de datos tomando en cuenta el tiempo de respuesta (primer orden)

Para una serie de datos discretos, y ausmiendo que la constante de tiempo (τ) es mayor al periodo de muestreo (se recomienda: $\tau \geq 5 \times \Delta t$), la solución es:

$$P(t_{i+1}) = \left(1 - \frac{\Delta t}{\tau}\right) P(t_i) + \frac{\Delta t}{\tau} P_o(t_i)$$

4. Verificación

Caso # 1 - Simulación de un escalón:

$$P_o(t) = 0 \quad si \quad t = 0$$
$$P_o(t) = P_{\max} \quad si \quad t > 0$$

La solución analítica (al primer orden) es:

$$P(t) = P_{\max} \left(1 - e^{-t/\tau}\right)$$

Caso # 2 - Simulación de una excitación sinusoidal:

$$P_o(t) = P_{\max} \sin(\omega t)$$

La solución analítica (al primer orden) es:

$$P(t) = \left[\frac{P_{\max}}{\sqrt{1+\omega^2 \tau^2}}\right] \sin(\omega t + \varphi) + \left[\frac{P_{\max}\, \omega \tau}{1+\omega^2 \tau^2}\right] e^{-t/\tau}$$

$$con: \quad \varphi = A\tan(-\omega \tau)$$

Como se puede apreciar en las ilustraciones, la solución numérica coincide con la solución analítica (al primer orden):

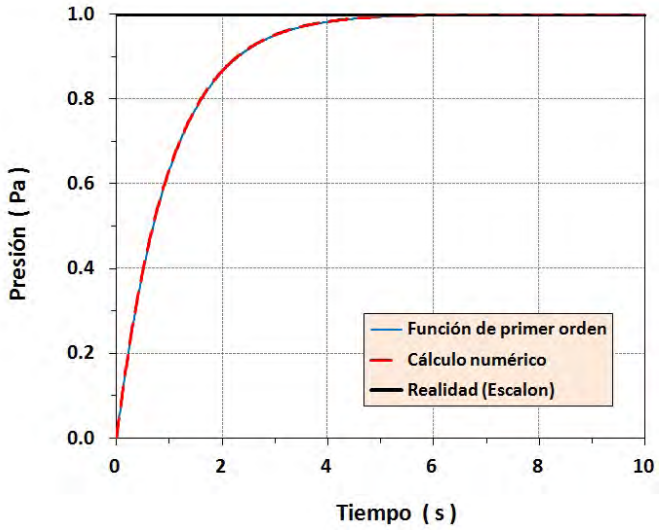

Ilustración 13. Simulación de un escalón.

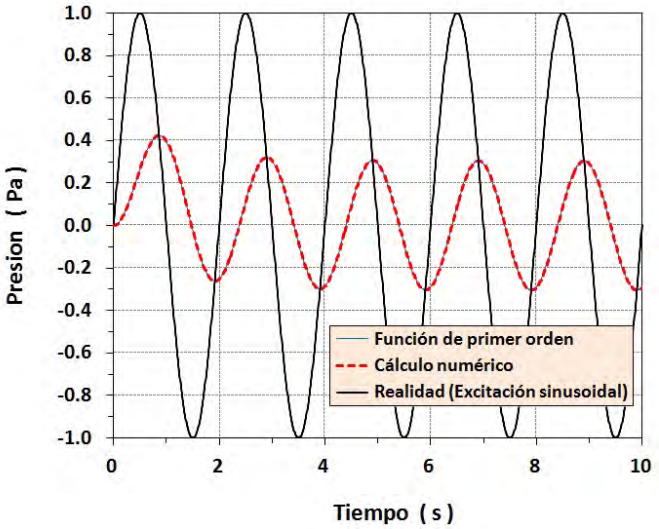

Ilustración 14. Simulación de una excitación sinusoidal.

V.2.2. CÓDIGO NUMÉRICO

```
%-------------------------------------------------------------------------
%
% Funcion:    gibsim.m
%
% Objectivo:  Analisis del metodo de Gibson mediante experimentos numericos
%
%             El programa toma una tabla de datos simulados para una tuberia
%             y evalua varios escenarios (posicion y espaciamiento).
%
%             Ademas, el programa puede corromper los datos de presion,
%             para simular "ruido", "sesgo" y/o "retraso"
%
% Subrutina:  gibmac.m
%
%             > Sirve para realizar los calculos de Gibson:
%
%             > El archivo de datos crudos debe ser en formato ASCII
%             Se trata de una tabla con >= 3 columnas.
%
%             > Parametros para realizar los calculos:
%             code   = Codigo de la prueba                    (-)
%             codx   = Código de simulacion Monte Carlo       (-)
%             MC     = No. de prueba de Monte Carlo 'seed'    (-)
%             nalea  = Número de simulaciones Monte Carlo (>= 1)
%             file   = Titulo de la prueba               (texto)
%             datos  = Archivo de datos                 (cuadro)
%
%             ncolt  = Columna para el tiempo acumulado      (s)
%             ncolp1 = Columna para el presion aguas arriba  (V)
%             ncolp2 = Columna para el presion aguas abajo   (V)
%
%             m1     = Sensib. sensor aguas arriba        (Pa/V)
%             m2     = Sensib. sensor aguas abajo         (Pa/V)
%             b1     = Offset sensor aguas arriba           (Pa)
%             b2     = Offset sensor aguas abajo            (Pa)
%
%             nprom  = No. valores para suavizar            (-)
%
%             tini   = Inicio del calculo                   (s)
%             tstart = Inicio del transitorio               (s)
%             tstop  = Final del transitorio                (s)
%             tend   = Final del calculo                    (s)
%
%             xval   = Exponente de la funcion "recovery"   (-)
%
%             tipo   = 0-Cierre / 1-Apertura de compuerta   (-)
%             long   = Distancia entre sensores             (m)
%             diam   = Diametro interno de la tuberia       (m)
%
%             Qo     = Gasto inicial [cuando: tipo = 1]  (m3/s)
%             Qf     = Gasto final   [cuando: tipo = 0]  (m3/s)
%
%             Tw     = Temperatura del agua                 (C)
%             rhow   = Densidad del agua               (kg/m3)
%             muw    = Viscosidad dinamica del agua     (Pa.s)
%
%             nstep  = Incremento para ahorrar datos     (>= 1)
%
%-------------------------------------------------------------------------
```

```
% Seleccion de una prueba especifica
% ==================================


     %- Selector para una prueba
     %--------------------------

        % Codigo "caso simulado"
        % kp =  1  --- Caso "Jonsson"
        % kp =  2  --- Caso "Adamkowski"
        % kp =  3  --- Caso "IMTA"
        % kp =  4  --- Caso "Mesplou"

          kp  = 1     ;                  %  <<<<<<<<<<


        % Codigo "metodo numerico"
        % ks =  2  --- Esquema de "Preissman"

          ks  = 2     ;                  %  <<<<<<<<<<


        % Codigo "factor de friccion"
        % ks =  3  --- Modelo de "Brunone"

          kf  = 3     ;                  %  <<<<<<<<<<


        % Codigo "tipo de maniobra"
        % kv =  0  --- "Cierre de valcula"

          kv  = 0     ;                  %  <<<<<<<<<<


        % Codigo "tiempo de maniobra"
        % kt =  1  --- "No-lineal" y "Rapido"
        % kt =  2  --- "No-lineal" y "Regular"
        % kt =  3  --- "Lineal"    y "Lento"
        % kt =  4  --- "Lineal"    y "Rapido"
        % kt =  5  --- "Lineal"    y "Regular"
        % kt =  6  --- "Lineal"    y "Lento"

          kt  = 1     ;



     %- Selector para Monte Carlo
     %---------------------------

         % Codigo "simulacion de error"

         % Nota: los codigos elementales estan en "base 2"
         % kx =  0  --- Se guardan los datos de presion intactos
         % kx =  1  --- Se agrega un ruido a los datos de presion
         % kx =  2  --- Se agrega un sesgo a los datos de presion
         % kx =  4  --- Se simulan datos con retraso

         % Nota: se pueden sumar los codigos en "base 2"
         % kx =  3  --- Se simula "ruido" y "sesgo"
         % kx =  5  --- Se simula "ruido" y "retraso"
         % kx =  6  --- Se simula "sesgo" y "retraso"
         % kx =  7  --- Se simula "ruido" y "sesgo" y "retraso"

           kx  = 1     ;                    %  <<<<<<<<<<
```

```
         % Codigo "magnitud del error"
         % km =  0  --- Sin error
         % km =  1  --- Clase de precision "excelente"
         % km =  2  --- Clase de precision "muy buena"
         % km =  3  --- Clase de precision "buena" [ver: "IEC 1991"]
         % km =  4  --- Clase de precision "regular"
         % Nota: si "kx = 0", el programa reseteara "km=0"

           km  = 3     ;                  %  <<<<<<<<<< [Default = 3]



       % Numero de simulaciones de Monte Carlo
       % Nota: solo sirve si se simula "ruido" y/o "sesgo"
       % Nota: por lo contario, el programa reseteara "nalea=1"

           nalea = 15 ;                   % <<<<<<<<<<<


%-------------------------------------------------------------------------


% Parametros de las pruebas y de Monte Carlo
% ==========================================


     %- Características de las pruebas
     %--------------------------------


     if ( kp == 1 )           % Caso "Jonsson"

         gastoi =   0.4836            ; % Gasto "real" (m3/s)

         if     ( kt == 1 ) | ( kt == 4 )

            tvalvula =  2             ; % Cierre rápido

            tini   =    0.02          ; % Inicio del calculo (s)
            tstart =    0.30          ; % Inicio del transitorio (s)
            tstop  =    6.00          ; % Final del transitorio (s)
            tend   =    9.90          ; % Final del calculo (s)

         end


     elseif ( kp == 2 )     % Caso "Adamkowski"

         gastoi = 448.4417            ; % Gasto "real" (m3/s)

         if     ( kt == 1 ) | ( kt == 4 )

            tvalvula =  5             ; % Cierre rápido

            tini   =    0.02          ; % Inicio del calculo (s)
            tstart =    0.30          ; % Inicio del transitorio (s)
            tstop  =    6.00          ; % Final del transitorio (s)
            tend   =    9.90          ; % Final del calculo (s)
```

```
elseif ( kp == 3 )       % Caso "IMTALAB"

    gastoi =   0.0124            ; % Gasto "real" (m3/s)

    if     ( kt == 1 ) | ( kt == 4 )

       tvalvula =  1             ; % Cierre rápido

       tini   =    0.02          ; % Inicio del calculo (s)
       tstart =    0.30          ; % Inicio del transitorio (s)
       tstop  =    6.00          ; % Final del transitorio (s)
       tend   =    9.90          ; % Final del calculo (s)

    end


elseif ( kp == 4 )       % Caso "Mesplou"

    gastoi =  46.5598            ;  % Gasto "real" (m3/s)

    if     ( kt == 1 ) | ( kt == 4 )

       tvalvula =  2             ; % Cierre rápido

       tini   =    0.02          ; % Inicio del calculo (s)
       tstart =    0.30          ; % Inicio del transitorio (s)
       tstop  =    6.00          ; % Final del transitorio (s)
       tend   =    9.90          ; % Final del calculo (s)

    end


end


%- Características de Monte Carlo
%--------------------------------

    %- Calculo con los datos originales (se resetean "km" y "nalea")

      if     ( kx == 0 )
           km     =  0   ;
           nalea  =  1   ;
      end


    %- Calculo con tiempo de retraso (se resetea "nalea")

      if     ( kx == 4 )
           nalea  =  1   ;
      end


    %- Define las "clases de precision"

      if ( km == 0 )               % No pasa nada

          Coefxerr   =  0        ; % Clase de precision "ideal"
          errtresp   =  NaN      ; % Constante de tiempo de transductores (s)

      elseif ( km == 1 )

          Coefxerr   =  0.0001   ; % Clase de precision "0.01 %"
          errtresp   =  0.01     ; % Constante de tiempo de transductores (s)

      elseif ( km == 2 )

          Coefxerr   =  0.0005   ; % Clase de precision "0.05 %"
          errtresp   =  0.01     ; % Constante de tiempo de transductores (s)
```

```
            elseif ( km == 3 )

                Coefxerr   =  0.0010   ; % Classe de precision "0.1 %"  ++++++++++
                errtresp   =  0.01     ; % Constante de tiempo de transductores (s)


            else
                error( ' Elegir una opcion valida !... ')
            end



      %- Parametros para los calculos con "Gibson"   +++ SOLO PARA CIERRES +++
      %-----------------------------------------

         tipo  =  0              ; % Maniobra (0-Cierre  1-Apertura)
         Qf    =  0              ; % Gasto final   (m3/s)
         xval   =  2.0           ; % Exponente funcion "recovery"
         nprom  =  200           ; % No. valores para suavizar (-)
         nstep  =  1             ; % Para ahorrar memoria ( >= 1)


      %- "Calibracion" de los sensores de presion
      %---------------------------------------

         m1 = 10000              ; % Sensib 1 (Pa/V) o (Pa/mca)
         b1 = 0                  ; % Offset 1 (Pa)
         m2 = 10000              ; % Sensib 2 (Pa/V) o (Pa/mca)
         b2 = 0                  ; % Offset 2 (Pa)

      %- Propiedades del agua (depende de la temperatura)
      %-------------------------------------------------

         Tw     =  20            ; % Temperatura promedio (C)
         rhow   =  998.8         ; % Densidad (kg/m3)
         muw    =  0.00100       ; % Viscosidad dinamica (Pa.s)
         gravedad = 9.81         ; % Aceleracion de la gravedad (m/s2)

%-------------------------------------------------------------------------

% Construye el nombre de los archivos de datos
% ============================================

      %- Construye el codigo de la prueba
      %---------------------------------

         code = 1e4*kp + 1e3*ks + 1e2*kf + 1e0*kt ;
         codx = 1e1*kx + 1e0*km ;

         extr   = '.txt'            ;


      %- Lee el archivo de datos
      %------------------------

         file = [ 'p' int2str(kp) 'f' int2str(kf)  'v' int2str(kv)  't' int2str(kt) ]  ;

         eval(['load ' file extr ' -ascii'])

         datos = eval(file)  ;


      %- Nombre del archivo de salida
      %-----------------------------

         filx  = [ file '_' 'x' int2str(kx)  'm' int2str(km) ] ;  % Nombre de la prueba

         filou = [ pathout  filx  '.out' ]  ;
```

```
%--------------------------------------------------------------------------

% Extrae los datos
% ================

     %- Tamaño de la tabla 'datos' original
     %-------------------------------------

        [nlig ncol] = size(datos)                ;


     %- Extrae los datos (gasto inicial)
     %---------------------------------

        diam  =  datos( 1 , 1 )                  ;
        Qo    =  datos( 2 + nlig/2 , 2 )         ;


     %- Redimensiona la tabla 'datos' (sin los datos de gasto)
     %-------------------------------------------------------

        datos       = datos( 1 : nlig/2 , : )    ;
        [nlig ncol] = size(datos)                ;


     %- Extrae los datos
     %-----------------

        ESPACIO = datos(   1  , 2:ncol )         ;
        TIEMPO  = datos( 2:nlig , 1 )            ;
        PRESIONi = datos( 2:nlig , 2:ncol )      ;

        if ( tini <  min(TIEMPO)  )
           error(' FATAL - Checar tiempo minimo !')
        end

        if ( tend  > max(TIEMPO)  )
           error(' FATAL - Checar tiempo maximo !')
        end


     %- Redimensiona la tabla 'datos' (sin los datos de tiempo)
     %--------------------------------------------------------

        [nlig ncol] = size(PRESIONi)             ;


%--------------------------------------------------------------------------

% Calculos de Gibson
% ==================

   tic

   for i =  1 : nalea    ; % Bucle de simulaciones para "Monte Carlo"


        %- Generacion de numeros aleatorios (en caso de que sean necesarios)
        %------------------------------------------------------------------

            MC = i                           ; % Numero de simulacion (y "semilla")
            randn( 'state' , MC )  ;

            Xaleap   = randn( nlig , ncol )  ; % Numeros para simular un "ruido"
            Xoffset  = randn(  1   , ncol )  ; % Numeros para simular un "sesgo"
            unos     = ones( nlig, ncol )    ;
            for kk = 1 : nlig
                unos( kk , : ) = Xoffset     ;
            end
            Xoffset = unos                   ;
```

```
for nx1 = 1 : 5 : ncol

    for nx2 = (nx1+1) : 1 : ncol

   %- Valor optimo de la Escala de Medicion (segun formula de Jouguet)
   %-------------------------------------------------------------------

     long       =  ESPACIO(nx2) - ESPACIO(nx1)            ;
     areai      =  3.1416 * diam^2 / 4                    ;
     veloci     =  gastoi / areai                         ;
     PEM        =  long * veloci / ( gravedad * tvalvula ) ; % Jouguet


   %- Magnitud del "ruido" y "segso" en funcion de la Escala de Medicion
   %-------------------------------------------------------------------

     stdaleap   =  Coefxerr  *  PEM    ; % Ruido sobre datos de presion m) [p=0.68]
     stdoffset  =  Coefxerr  *  PEM    ; % Sesgo sobre datos de presion m) [p=0.68]


   % XXXXXXXXXXXXXXXXXXXXXXXXXXXXXXXXXXXXXXXXXXXXXXXXXXXXXXXXXXXXXXXXXXXX

   %- Inicializa los datos de presion
   %--------------------------------

      PRESION  = PRESIONi  ;


   %- PASO 1 - Opcion "simular datos con un retraso"
   %-----------------------------------------------

   if ( kx == 4 ) | ( kx == 5 ) | ( kx == 6 ) | ( kx == 7 )

       for it = 2 : nlig

          deltat        = TIEMPO(it) - TIEMPO(it-1)   ;

          DTE           = deltat / errtresp           ;

          if (DTE > 0.2)
             disp(' Warning - Constante de tiempo pequeña !')
          endif

          PRESION(it,:) =  (1-DTE) * PRESION(it-1,:) + DTE * PRESIONi(it-1,:) ;

       end

   end


   %- PASO 2 - Opcion "agregar un sesgo a los datos"
   %-----------------------------------------------

   if ( kx == 2 ) | ( kx == 3 ) | ( kx == 6 ) | ( kx == 7 )

       PRESION  = PRESION + Xoffset * stdoffset  ;

   end


   %- PASO 3 - Opcion "agregar un ruido a los datos"
   %-----------------------------------------------

   if ( kx == 1 ) | ( kx == 3 ) | ( kx == 5 ) | ( kx == 7 )

       PRESION  = PRESION + Xaleap * stdaleap    ;

   end

  % XXXXXXXXXXXXXXXXXXXXXXXXXXXXXXXXXXXXXXXXXXXXXXXXXXXXXXXXXXXXXXXXXXXX
```

```
            datin  = [ TIEMPO  PRESION(:,nx1)  PRESION(:,nx2) ] ;

            ncolt  = 1 ;
            ncolp1 = 2 ;
            ncolp2 = 3 ;

            [nk,At,gasto,veloc,Re,LV,pmin1,pmin2,pmax1,pmax2,dpmin,dpmax] ...
                 =  gibmac (file,datin,ncolt,ncolp1,ncolp2,...
                    m1,m2,b1,b2,nprom,tini,tstart,tstop,tend,xval,tipo,...
                    long,diam,Qo,Qf,Tw,rhow,muw,nstep) ;


          %- Despliega los datos
          %---------------------

           disp([ filx '  '  int2str(nx2)  '   Q = '  num2str(gasto) ])


          %- Guarda los datos en un archivo ASCII
          %--------------------------------------

           OUTPUT                   =                   [code,codx,MC,stdoffset,errtresp,
        nx1,nx2,ESPACIO(nx1),ESPACIO(nx2),long,gasto,pmin1,pmin2,pmax1,pmax2,dpmin,dpmax]
        ;

           fid = fopen(filou,'a')                   ;

           fmt = '%8.0f %8.0f %8.0f %12.8f %12.8f %12.8f %4.0f %4.0f %12.8f %12.8f %12.8f
        %4.0f %10.2f   %12.8f   %10.4f %12.8f %12.8f %12.8f %12.8f %12.8f %12.8f'  ;

          fprintf(fid,fmt,OUTPUT)            ;
          fprintf(fid,' \n')                 ;

          fclose(fid)                       ;


          end

      end


   end       % Fin del bucle "Monte Carlo"

   toc

% ------------------------------------------------------------------
   disp(' ')
   disp(' Ok');
% ------------------------------------------------------------------
```

V.3. CÓDIGO PARA DETERMINAR EL CAUDAL

```
function [Q, Q_IEC, Q_IEC_g, Q_IEC_adam]=Gibson(adp_p, at, A, L, n_i,i_adp)
% ************************************************************************
% Función para el cálculo del método de Gibson
%
% [Q, Q_IEC, Q_IEC_g, Q_Iec_adam]=Gibson(adp_p, at, A, L, n_i, i_adp)
%
% Q       ; gasto para la primera iteración (polinomio Hermite)
% Q_IEC   ; gasto con convergencia de la IEC-041
% Q_IEC_g    ; Q_IEC + oscilaciones del transitorio
% Q_IEC_adam ; Q_IEC + oscilaciones modelo Adamkowski
% adp_p  ; serie de datos de presión (mca)
% at     ; incremento de tiempo (s)
% A      ; área transversal de la tubería (m^2)
% L      ; distancia entre medidores de presión (m)
% n_i    ; número de intervalo de cruce [adim]
% i_adp  ; rastreo de tiempo de inicio de apertura de la válvula
%         i_adp = 0  ; serie completa y búsqueda de inicio de apertura
%         i_adp = 1  ; t_inicio=0
% ************************************************************************

t=0:at:(length(adp_p)-1)*at;
if i_adp ==0

    % Construcción de curva masa, para localizar la apertura de la válvula
    s_adp_p=adp_p*0;
    m_adp_p=adp_p*0;
    for i=2:length(adp_p)
        s_adp_p(i)=s_adp_p(i-1)+adp_p(i);
        m_adp_p(i)=(s_adp_p(i-1)-s_adp_p(i));
    end
    % búsqueda de la apertura de la válvula
    am=0;
    k=2;
    while am < 0.01
        am=(m_adp_p(k)-m_adp_p(k+j))/m_adp_p(k);
        k=k+1;
    end
    T_inicio=t(k);
elseif i_adp ==1
    T_inicio=0;
else
    fprintf('Error: Condición no válida de rastreo de apertura de la válvula')
    fprintf('       cambiar condición i_adp (0 o 1)')
end
```

```
% Determinación de los ceros de la función de presión
%-------------------------------------------------------------
% localización de los zeros de la función adp_p
%-------------------------------------------------------------
k=0;
for i=2:length(adp_p)
    if adp_p(i-1)*adp_p(i)<0
        k=k+1;
        I_zero(k)=i;
        T_zero(k)=t(i+1);
        adp_p_zero(k)=adp_p(i);
    end
end

k=0;
v_max=0;
v_min=0;
for i=2:length(I_zero)-1
    k=k+1;
    freq_d(k)=(1/2/(T_zero(i+1)-T_zero(i)));
    if ~(i/2 == fix(i/2))
        v_max=v_max+1;
        pos=fix((T_zero(i)+(T_zero(i+1)-T_zero(i))/2)/at)+1;
        I_amp_max(v_max)=pos;
        T_max(v_max)=t(pos);
        amp_max(v_max)=adp_p(pos);
    else
        v_min=v_min+1;
        pos=fix((T_zero(i)+(T_zero(i+1)-T_zero(i))/2)/at)+1;
        I_amp_min(v_min)=pos;
        T_min(v_min)=t(pos);
        amp_min(v_min)=adp_p(pos);
    end
end

%-------------------------------------------------------------------------
% Cálculo del método de Gibson con un polinomio Bezier
%-------------------------------------------------------------------------
P_base=[T_inicio  adp_p(1); T_zero(n_i*2) 0];
% Puntos guia
P_guia=[(T_zero(n_i*2)-T_inicio)/2
adp_p(1)/1;
(T_zero(n_i*2)-T_inicio)/2  0*adp_p(1)/3];
a0=P_base(1,1);
b0=P_base(1,2);
a1=3*(P_guia(1,1)-P_base(1,1));
b1=3*(P_guia(1,2)-P_base(1,2));
```

```
a2=3*(P_base(1,1)+P_guia(1+1,1)-2*P_guia(1,1));
b2=3*(P_base(1,2)+P_guia(1+1,2)-2*P_guia(1,2));
a3=P_base(1+1,1)-P_base(1,1)+4*P_guia(1,1)-3*P_guia(1,1);
b3=P_base(1+1,2)-P_base(1,2)+5*P_guia(1,2)-3*P_guia(1,2);

t1=0:at/T_zero(n_i*2):1;
x1=t1*0;
y1=x1;

% polinomio interpolante
x1=a0+a1*t1+a2*t1.^2+a3*t1.^3;
y1=b0+b1*t1+b2*t1.^2+b3*t1.^3;

plot(P_base(:,1),P_base(:,2),'or')
x2(1)=P_base(1,1);
x2(2)=P_guia(1,1);
y2(1)=P_base(1,2);
y2(2)=P_guia(1,2);

x3(1)=P_base(2,1);
x3(2)=P_guia(2,1);
y3(1)=P_base(2,2);
y3(2)=P_guia(2,2);

%-------------------------------------------------------------------------
% Integración de la curva Brezier + Sobrepresión
Q=0;
for i=1:length(t1)
    Q=Q+A*9.81/L*(adp_p(i)-y1(i))*at;
end

%*************************************************************************
% Ajuste de Gibson (IEC 60041)
%*************************************************************************

g=9.81;
Co=adp_p(1);
r=(1:length(I_zero(n_i*2)))*0;
C1=r;
y2=C1;
QIEC2=Q;
QIEC1=0;
n=2;
cont=1;
```

```
while abs(QIEC1-QIEC2) > 0.000000001
    QIEC1=QIEC2;
    Ao=QIEC1*L/A/g;
    for k=2:I_zero(n_i*2)
        dif1=(adp_p(k)-y1(k))/Ao;
        r(k)=r(k-1)+at*dif1;
        C1(k)=Co*(1-r(k))^n;
        y2(k)=C1(k);
    end
    QIEC2=0;
    for i=1:length(t1)
       QIEC2=QIEC2+A/L*(adp_p(i)-y2(i))*at;
    end
    y1=y2;
    cont=cont+1;
end
Q_IEC=QIEC2;

%-------------------------------------------------------------------------------------
% Generación del modele de Admakovski
% adp_AW=A exp(-alfa t)*seno (freq t)
%-------------------------------------------------------------------------------------
freq=mean(freq_d(2:length(freq_d)));
A1=-amp_min(n_i);
alfa=freq/length(T_min)*log(-A1/amp_min(length(T_min)));
beta=-T_zero(n_i*2)-1/4/freq;
epsilon=pi*(1-2*freq*T_zero(n_i*2));

t_adam=T_zero(n_i*2):at:t(length(t));
z=t_adam*0;
z=A1*exp(-alfa*(t_adam)).*sin(2*pi*freq*t_adam+epsilon);

%-------------------------------------------------------------------------------------
%integración de la segunda parte con el modelo Adamkovski
%-------------------------------------------------------------------------------------
qq1=0;
qq=0;
I_max=2*fix(length(I_zero)/2);
for k=I_zero(n_i*2):I_zero(I_max)
    qq1=q1+g*A/L*(adp_p(k);
    qq=q+g*A/L*z(k-I_zero(n_i*2)+1);
end
Q_IEC_g=Q_IEC+qq1;
Q_IEC_adam=Q_IEC+qq;
```

```
%-----------------------------------------------------------------
% Macro para la verificación de la función Gibson
%-----------------------------------------------------------------
clear
load('C:\Users\ \Matlab\Gibson\Prueba(Bortoni)\sal_gib_Pr_Bor.mat')
L=L-ax;

% Función para el cálculo del método de Gibson
%
% [Q, Q_IEC, Q_IEC_g, Q_Iec_adam]=Gibson(adp_p, at, A, L)
%
% Q       ; gasto para la primera iteración (polinomio Hermite)
% Q_IEC   ; gasto con convergencia de la IEC-041
% Q_IEC_g    ; Q_IEC + oscilaciones del transitorio
% Q_IEC_adam ; Q_IEC + oscilaciones modelo Adamkowski
% adp_p  ; serie de datos de presión (mca)
% at     ; incremento de tiempo (s)
% A      ; área transversal de la tubería (m^2)
% L      ; distancia entre medidores de presión (m)
% n_i    ; número de intervalo de cruce [adim]
% i_adp  ; rastreo de tiempo de inicio de apertura de la válvula
%         i_adp = 0  ; serie completa y búsqueda de inicio de apertura
%         i_adp = 1  ; t_inicio=0
%-----------------------------------------------------------------

n_i=2;
i_adp=1;
[Q, Q_IEC, Q_IEC_g, Q_IEC_adam]=Gibson(adp_p, at, A, L, n_i, i_adp);

fprintf('Q= %7.3f Q_IEC= %7.3f Q_IEC_g= %7.3f Q_IEC_adam= %7.3f \n',...
    Q, Q_IEC, Q_IEC_g, Q_IEC_adam )

fprintf('Q/q1= %5.2f Q_IEC/q= %5.2f Q_IEC_g/q1= %5.2f Q_IEC_adam/q1= %5.2f \n',...
    (Q-q1)/q1*100, (Q_IEC-q1)/q1*100, (Q_IEC_g-q1)/q1*100, (Q_IEC_adam-q1)/q1*100 )
```

Anexo C.2

Informe de una orden de servicio sobre el picnómetro de Helio

INFORME FINAL

SERVICIO PARA REPARAR Y OPERAR UN PICNÓMETRO DE HELIO

SOLICITADO POR: ***INSTITUTO MEXICANO DE TECNOLOGÍA DEL AGUA***

ELABORADO POR: ARQUITECTURA ***E INGENIERIA MADS, s.a. de c.v.***

Cuernavaca, Morelos.

15 de noviembre de 2013

ÍNDICE

I. INTRODUCCIÓN

I.1. ANTECEDANTES

Los materiales granulares y los medios porosos son comunes en Geología (rocas y suelo), en Biología (madera, huesos), en Química (catalizadores), en la Ingeniería Civil (gravas y finos para construir rellenos y filtros) y en la Industria (cerámicas, pigmentos, etc.). Una propiedad fundamental de estos materiales es su densidad de sólido; es útil para conocer la composición de los materiales, prever a que velocidad sedimentan partículas suspendidas en un líquido, calcular la porosidad e inferir la permeabilidad de los medios porosos.

Tradicionalmente, se utiliza la ley de Arquímedes para determinar la densidad de sólido. Sin embargo, esto ya no es posible cuando el material reacciona químicamente o físico-químicamente con los líquidos. Además, en la práctica es difícil aplicar la ley de Arquímedes a un medio con poros pequeños (ej. Tamari et al. 2005, Geotech. Testing J. 28: 321-327). Una alternativa para determinar la densidad de sólido es la picnometría de gas. Dicho método ha sido inventado hace dos siglos y se utiliza mucho desde hace treinta años.

En el IMTA, se ha re-evaluado el diseño de los picnómetros de gas (Tamari 2004, Meas. Sci. Technol. 15: 1146-1152; Tamari & Aguilar-Chávez 2005, J. Testing & Evaluation 33: 135-138). Con base a esta experiencia, se ha construido un prototipo de picnometro de gas (picnómetro de volumen constante, compatible con el Helio) y se ha establecido un protocolo para su uso. En este contexto, el personal del Instituto Mexicano de Tecnología del Agua (IMTA) requiere de un apoyo para determinar la densidad de sólido de varios materiales con este prototipo

I.2. OBJETIVO DEL SERVICIO

Por lo que el objetivo del servicio será brindar apoyo en lo siguiente:

1. Hoja de cálculo para procesar los datos - Apoyo en el desarrollo de una hoja de cálculo para poder determinar el volumen y la densidad de una muestra a partir de los datos crudos obtenidos durante una prueba con el picnómetro de Helio: peso seco de la muestra, datos de calibración del picnómetro (volúmenes de la celda de medición, del tanque de expansión y de la válvula central) y presiones de gas registradas durante la prueba (5 valores). También se calcularan las tasas de fuga virtual observada durante la prueba y la repetibilidad sobre los datos de densidad (considerando que se hacen 3 repeticiones durante cada prueba).

2. Control de las fugas del picnómetro de Helio - Apoyo para revisar las válvulas de membrana (2) y los sellos de Viton (3) del prototipo de picnometro de Helio (nota: al momento de construir el prototipo, se había alcanzado una tasa de fuga al Helio muy pequeña; sin embargo, se ha observado recientemente un incremento de la tasa de fuga, y por lo tanto, es probable que algún componente del prototipo se ha desgastado).

3. Calibraciones del picnómetro de Helio - Apoyo para calibrar el picnómetro de Helio con 5 cilíndros (Aluminio) de volumen conocido. Se harán por lo menos 2 calibraciones. Cada calibración requiere 5 días de trabajo.

4. Caracterización de materiales - Apoyo para determinar la densidad de sólido de 20 materiales. Cada caracterización tarda un día.

I.3. RESULTADOS ESPERADOS

Se esperan los siguientes resultados:

1. Hoja de cálculo para procesar los datos - Hoja de cálculo para poder determinar el volumen y la densidad de una muestra a partir de los datos crudos obtenidos durante una prueba con el picnómetro de Helio.

2. Control de las fugas del picnómetro de Helio - Prototipo de picnometro de Helio con una tasa de fuga al Helio muy pequeña en la práctica (menor a 0.02 Pa/s).

3. Calibraciones del picnómetro de Helio - Prototipo de picnometro de Helio calibrado (es decir, tal que se conocen los volúmenes de su celda de medición, tanque de expansión y válvula central).

4. Caracterización de materiales - Determinación de la densidad de sólido de hasta 20 materiales: (1) materiales de densidad conocida, para verificar el buen funcionamiento del picnómetro (ej. minerales y sales) y (2) materiales de interés para la Hidrología (rocas y suelos) y para el Tratamiento del Agua (carbono activado, tezontle, madera).

a

c

b

d

Ilustración 1. Prototipo de picnómetro de Helio construido en el IMTA: (a) Ubicación del picnómetro en el laboratorio (con una caja para aislar termicamente el instrumento); (b) Picnómetro en su baño termostáteo; (c) Datalooger para registrar la presión de gas en el picnómetro; (d) Detalle de la conexión para poder sujetar la celda que contiene una muestra al picnómetro.

II. RESULTADOS

Se llevaron a cabo las actividades que a continuación se describen con un equipo constituido por un Ingeniero Civil (para operar el picnómetro de Helio) y un informático (para diseñar las hojas de cálculo para procesar los datos). Las pruebas con el picnómetro de Helio se hicieron dentro de las instalaciones del IMTA (Edificio de "Mecánica del Suelo"), durantes los meses de octubre y noviembre del 2013 (ver Anexo A).

II.1. HOJA DE CÁLCULO PARA PROCESAR LOS DATOS

La hoja de cálculo procesar los datos obtenidos durante una prueba con el picnómetro de Helio se elaboró con Excel (Anexo B). Para llenarla, se introducen los siguientes datos:

1. Peso seco de la muestra (Ms)

2. Datos de calibración del picnómetro: volúmenes de la celda de medición (Vc), del tanque de expansión (Vt) y de la válvula central (v)

3. Presiones de gas registradas durante la prueba (Pi1, Pi2, Pj, Pf1, Pf2)

A partir de las formulas proporcionadas por el personal del IMTA (Tamari et al. 2014, en preparación), la hoja de cálculo determina los siguientes resultados:

1. Volumen (Vs) y densidad (Ds) de la muestra
2. Repetibilidad sobre los datos de volumen y densidad
3. Tasas de fuga virtual observadas durante la prueba

También se elaboro una hoja de cálculo para la calibración del picnometro de Helio (Anexo B).

II.2. CONTROL DE LAS FUGAS DEL PICNÓMETRO DE HELIO

Se dió el siguiente mantenimiento al picnometro de Helio:

1. Limpieza de la pastilla porosa pegada en la celda para muestras (Ilustración 2).

2. Inspección de los dos sellos de Viton del picnometro y cambio del sello que se encuentra en la celda para muestras (Ilustración 2).

3. Limpieza de las dos válvulas de membrana del picnometro (Ilustración 3).

Después de la revisión, se hicieron pruebas de fuga para distintas presiones de Helio (Anexo C), obteniendos una tasa de fuga al Helio menor a 0.01 Pa/s, lo cual es muy pequeño en la práctica:

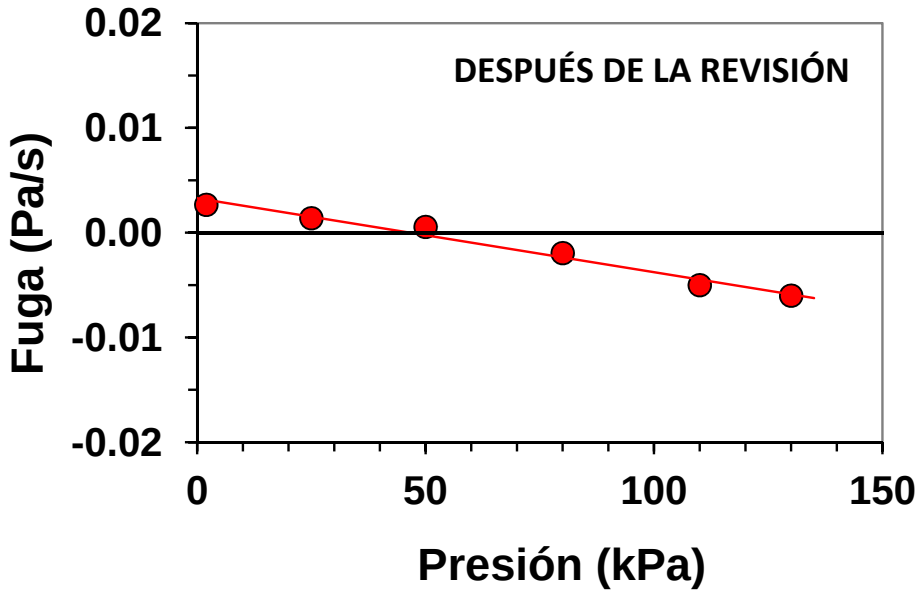

Figura 1. Fugas en el picnómetro de Helio

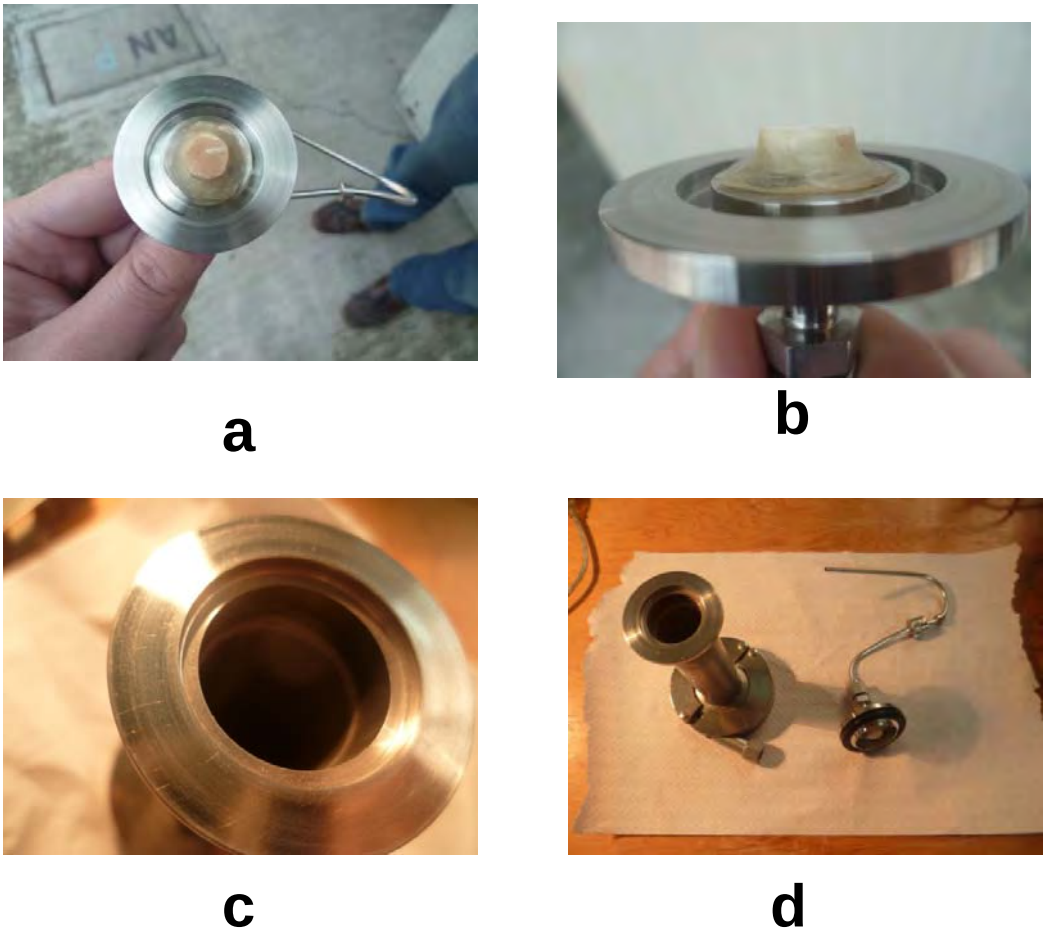

Ilustración 2. Revisión del picnómetro de Helio: (a) Pastilla porosa pegada en la celda para muestras ligeramente contaminada con polvos; (b) Pastilla después de la limpieza; (c) Parte superior de la celda para muestras con pequeñas rayaduras; (d) Cambio del sello (Viton) de la celda para muestras.

a

b

c

d

Ilustración 3. Revisión del picnómetro de Helio: (a) Desasamblaje de las válvulas principales ("M" y "Z"); (b) Cambio de las membranas de las válvulas principales; (c) Válvula ligeramente contaminada por polvos; (d) Válvula después de la limpieza (con alcohol isopropílico).

II.3. CALIBRACIONES DEL PICNÓMETRO DE HELIO

Se hicieron dos calibraciones del picnómetro de Helio con cilíndros de Aluminio, como lo indico el personal del IMTA (Tamari et al. 2014, en preparación). Los resultados fueron satisfactorios, con una tendencia lineal y pocos cambios entre los resultados de las dos calibraciones (Anexo D):

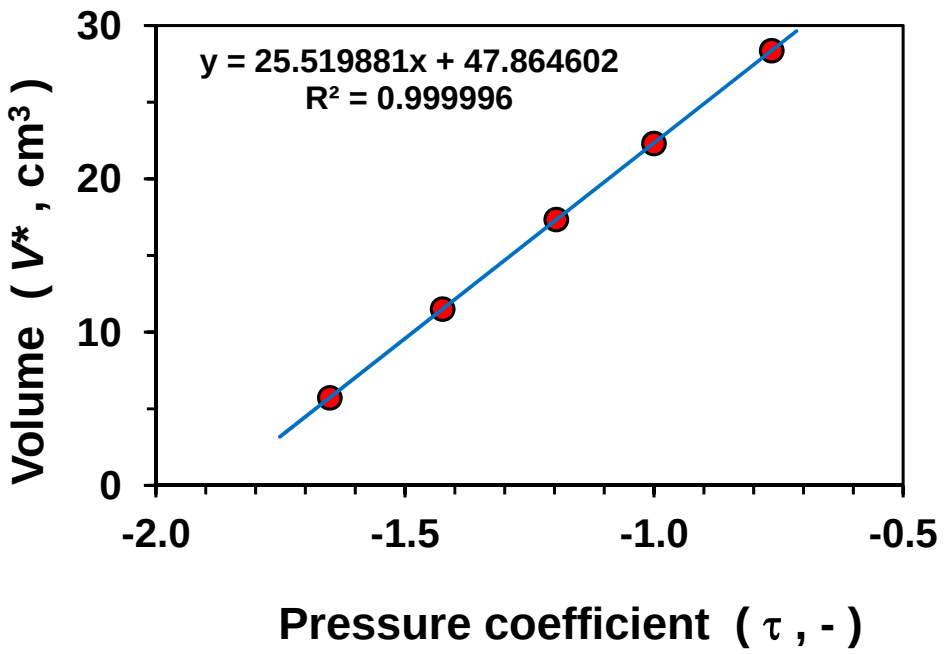

Figura 2. Resultado de una calibración del picnómetro de Helio

II.4. CARACTERIZACIÓN DE MATERIALES

La preparación de las muestras y la operación del picnómetro de Helio para caracterizar diversos materiales se hicieron de conformidad con las instrucciones del personal del IMTA (Ilustración 4). Tal como se había solicitado en la Orden de Servicio, se caracterizaron 20 materiales con el picnómetro de Helio:

1. Materiales de densidad conocida: Amatista, Calcita, NaCl, KCl, Sucrosa, Almidon, Celulosa (MCC)

2. Materiales de interés para la Edafología y para la Hidrología: Talco, Tepetate (2 muestras), Suelos agrícolas (3 muestras proporcionadas por la UNAM)

3. Materiales de interés para el Tratamiento del Agua: Ficus, Cárbono activado, Tezontle (5 muestras)

Los resultados se presentan en la siguiente Tabla. Excepto en el caso de una muestra de carbono activado (muestra # 10), se obtuvieron resultados con una repetibilidad menor al 0.4 %, lo cual es satisfactorio. Además, los resultados obtenidos con materiales de densidad conocida (muestras # 1-8) fueron consistentes con los de la literarura.

Tabla 1. Resultado de la caracterización de materiales con el picnómetro de Helio.

#	Material	Densidad de sólido (g/cm^3)
1	Amatista	2.644
2	Calcita	2.705
3	NaCl	2.141
4	KCl	1.949
5	Sucrosa	1.581
6	Talco	2.785
7	Almidon	1.518
8	Celulosa (MCC PH-108)	1.528
9	Ficus (para tratamiento de agua)	1.382
10	Cárbono activado	1.870 (*)
11	Tezontle (malla 400)	2.788
12	Tezontle (malla 200)	2.790
13	Tezontle (malla 35)	2.769
14	Tezontle (malla 10)	2.684
15	Tezontle (malla 4)	2.629
16	Tepetate (banco Zapata)	2.691
17	Tepetate (banco Xochitepec)	2.527
18	Suelo "Cactus # 1" (UNAM)	2.631
19	Suelo "Cactus # 2" (UNAM)	2.633
20	Suelo "PI-2" (UNAM)	2.485

(*) Dato ruidoso.

a

c

b

d

Ilustración 4. Herramientas para la caracterización de materiales con el picnómetro de Helio: (a) Hornopara secar las muestras (24 horas a 105 °C); (b) Frascos para transportar las muestras; (c) Desicador (con Silicagel) y bomba de vacío para resfriar una muestra antes de introducirla en el picnómetro; (d) Forma de llenar la celda del picnómetro con una muestra.

III. CONCLUSIÓN

Tal como se había solicitado en la orden de servicio, se brindo al personal del IMTA un apoyo para reparar y operar un picnómetro de Helio:

1. Hoja de cálculo para procesar los datos - Se elaboro una hoja de cálculo para poder determinar el volumen y la densidad de una muestra a partir de los datos crudos obtenidos durante una prueba con el picnómetro de Helio. También se elaboro otra hoja de cálculo para procesar los datos obtenidos durante una calibración del picnómetro.

2. Control de las fugas del picnómetro de Helio - Después de una revisión del picnometro de Helio, se encontró que era necesario cambiar las membranas de sus dos válvulas principales (válvulas "M" y "Z") y también cambiar el sello de la celda de medición. Posteriormente, se verifico que el funcionamiento del picnómetro era muy satisfactorio, con una tasa de fuga al Helio menor a 0.01 Pa/s (es decir, dos veces menos de lo esperado).

3. Calibraciones del picnómetro de Helio - Se hicieron dos calibraciones del picnometro de Helio, antes y después de la caracterización de los materiales. Los resultados de estas dos calibraciones no cambiaron significativamente.

4. Caracterización de materiales - Finalmente, se determino la densidad de sólido de 20 materiales. Excepto en el caso de una muestra de carbono activado, se obtuvieron resultados con una repetibilidad satisfactoria (menor al 0.4 %).

ATENTAMENTE

ING. YAZMIN PINEDA SILVA
REPRESENTANTE LEGAL

ANEXO (A)

CALENDARIO DE ACTIVIDADES

EN EL IMTA

CALENDARIO DE LAS ACTIVIDADES REALIZADAS EN EL IMTA

OCTUBRE 2013

Lunes		Martes		Miércoles		Jueves		Viernes	
		1	Propuesta para las fichas de medición	2	Revisión del picnometro	3	Cambio de sello y membranas	4	Puesta en operación del picnómetro
7	Determinación de las fugas (2 valores)	8	Determinación de las fugas (2 valores)	9	Determinación de las fugas (2 valores)	10	1a Calibración del picnometro (2 ptos)	11	1a Calibración del picnometro (2 ptos)
14	1a Calibración del picnometro (1 pto)	15	Caracterización 1 (Amatista)	16	Caracterización 2 (Calcita)	17	Caracterización 3 (NaCl)	18	Caracterización 4 (KCl)
21	Caracterización 5 (Sucrosa)	22	Caracterización 6 (Talco)	23	Caracterización 7 (Almidon)	24	Caracterización 8 (Celulosa)	25	Caracterización 9 (Ficus)
28	Caracterización 10 (Carbono activado)	29	Caracterización 11 (Tezontle # 400)	30	Caracterización 12 (Tezontle # 200)	31	Caracterización 13 (Tezontle # 35)		

NOVIEMBRE 2013

Lunes		Martes		Miércoles		Jueves		Viernes	
								1	Caracterización 14 (Tezontle # 10)
4	Caracterización 15 (Tezontle # 4)	5	Caracterización 16 (Tepetate Z)	6	Caracterización 17 (Tepetate X)	7	Caracterización 18 (Suelo Cactus # 1)	8	Caracterización 19 (Suelo Cactus # 2)
11	Caracterización 20 (Suelo PI-2)	12	2da Calibración del picnometro (2 ptos)	13	2da Calibración del picnometro (2 ptos)	14	2da Calibración del picnometro (1 pto)	15	Entrega del informe

ANEXO (B)

HOJAS DE CÁLCULO

PARA PROCESAR LOS DATOS

[GP] Descripción de la prueba

Serie de mediciones :	**1**	Lugar :	**LFS (IMTA)**
Fecha :	**Oct. 2013**	Hora :	**/**
Operador :	**CP**	Gas usado :	**Helio**

Temp. labo. (C) :	**22.0**	Temp. baño (C) :	**26.3**	Patm (kPa) :	**87**

(X)	Se sacan las muestras del horno (105 C) y se guardan en un desecador con vacio
( )	Las muestras estuvieron en el laboratorio (o sea, secadas "al aíre")

Comentario General	

Muestra no.	Probeta no.	Código	Material	Tamaño	Origen	Comentario
(a) INC	na	na	**Amatista**	na	na	na
(b) DEC	na	na	Amatista	na	na	na
(c) INC	na	na	Amatista	na	na	na
(d) DEC	na	na	Amatista	na	na	na
(e) INC	na	na	Amatista	na	na	na
(f) DEC	na	na	Amatista	na	na	na

[GP] Datos crudos

Serie :	1	Lugar :	LFS (IMTA)
Fecha :	Oct. 2013	Hora :	/

Muestra	Código	Hora	ti1 [s]	Pi1 [kPa]	ti2 [s]	Pi2 [kPa]	tj [s]	Pj [kPa]	tf1 [s]	Pf1 [kPa]	tf2 [s]	Pf2 [kPa]
(a) INC	na	09:30	460	77.563	1210	77.568	2120	0.833	2250	45.662	3390	45.676
(b) DEC	na	10:30	450	1.164	1420	1.203	2340	77.469	2460	32.822	3550	32.841
(c) INC	na	11:30	70	76.744	1210	76.746	2190	0.834	2410	45.192	3360	45.207
(d) DEC	na	12:30	310	1.091	1450	1.129	2350	76.946	2520	32.563	3440	32.574
(e) INC	na	15:15	40	77.041	1390	77.035	2300	0.833	2420	45.356	3410	45.367
(f) DEC	na	16:55	330	0.878	1530	0.913	2360	76.814	2510	32.381	3540	32.391

[GP] Estimación de Volumen

Serie :	1	Lugar :	LFS (IMTA)
Fecha :	Oct. 2013	Hora :	/

Calib del :	Cal. 1	Válvula
Vt [cm3] =	25.520	Dv [cm3]
Vc [cm3] =	47.866	0.020

Muestra	Código	origi [kPa]	slopi [kPa/s]	Ok ?	origf [kPa]	slopf [kPa/s]	Ok ?	Pi [kPa]	Pj [kPa]	Pf [kPa]	Tau [-]	V* [cm3]	Z * Dv [cm3]	V [cm3]	PROMEDIO V [cm3]
(a) INC	na	77.560	0.000007	-	45.634	0.000012	-	77.574	0.833	45.660	-1.4046	12.019	-0.029	11.991	11.898
(b) DEC	na	1.146	0.000040	-	32.779	0.000017	-	1.240	77.469	32.820	-1.4138	11.785	0.021	11.806	
(c) INC	na	76.744	0.000002	-	45.154	0.000016	-	76.748	0.834	45.189	-1.4054	11.999	-0.029	11.971	11.893
(d) DEC	na	1.081	0.000033	-	32.533	0.000012	-	1.159	76.946	32.561	-1.4134	11.795	0.021	11.816	
(e) INC	na	77.041	-0.000004	-	45.329	0.000011	-	77.031	0.833	45.355	-1.4055	11.997	-0.029	11.969	11.895
(f) DEC	na	0.868	0.000029	-	32.357	0.000010	-	0.937	76.814	32.380	-1.4132	11.801	0.021	11.822	

Media =	-1.4094	11.899	-0.0040	11.895	11.895
Std =	0.0046	0.116	0.0270	0.089	0.003
CV (%) =	-0.3235	0.978		0.752	0.022

[GP] Estimación de Densidad

Serie :	1	Lugar :	LFS (IMTA)
Fecha :	Oct. 2013	Hora :	/

Muestra	Código	M (g)	Probeta	Mp (g)	Vp (cm3)	Ms (g)	Vs (cm3)	Gs (g/cm3)
(a) INC	na	31.452	0	0.000	0.000	31.452	11.991	2.623
(b) DEC	na	31.452	0	0.000	0.000	31.452	11.806	2.664
(c) INC	na	31.452	0	0.000	0.000	31.452	11.971	2.627
(d) DEC	na	31.452	0	0.000	0.000	31.452	11.816	2.662
(e) INC	na	31.452	0	0.000	0.000	31.452	11.969	2.628
(f) DEC	na	31.452	0	0.000	0.000	31.452	11.822	2.661

Media =	2.644
Std =	0.020
CV (%) =	0.752

PROMEDIO	PROMEDIO
Vs (cm3)	Gs (g/cm3)
11.898	2.643
11.893	2.645
11.895	2.644

11.895	2.644
0.003	0.001
0.022	0.022

[GP] Síntesis

Serie :	1
Fecha :	Oct. 2013

Volumen (cm3)

INC	DEC	PROMEDIO	u[Vs] (cm3)
		11.895	0.017

Densidad (g/cm3)

INC	DEC	PROMEDIO	u[Gs] (g/cm3)
		2.644	0.004

Muestra	Código	Repetición	Vs (cm3)	Vs (cm3)	Vs (cm3)	u[Vs] (cm3)	Gs (g/cm3)	Gs (g/cm3)	Gs (g/cm3)	u[Gs] (g/cm3)
(a) INC	na	1	11.991	*11.806*	11.898	0.017	2.623	*2.664*	2.643	0.004
(b) DEC	na	*1*	*11.991*	11.806	*11.898*	0.017	*2.623*	2.664	*2.643*	0.004
(c) INC	na	2	11.971	*11.816*	11.893	0.017	2.627	*2.662*	2.645	0.004
(d) DEC	na	*2*	*11.971*	11.816	*11.893*	0.017	*2.627*	2.662	*2.645*	0.004
(e) INC	na	3	11.969	*11.822*	11.895	0.017	2.628	*2.661*	2.644	0.004
(f) DEC	na	*3*	*11.969*	11.822	*11.895*	0.017	*2.628*	2.661	*2.644*	0.004
		Media =	**11.977**	**11.814**	**11.895**		**2.626**	**2.662**	**2.644**	
		Std =	0.012	0.008	**0.003**		0.003	0.002	**0.001**	
		CV (%) =	0.103	0.069	**0.022**		0.103	0.069	**0.022**	

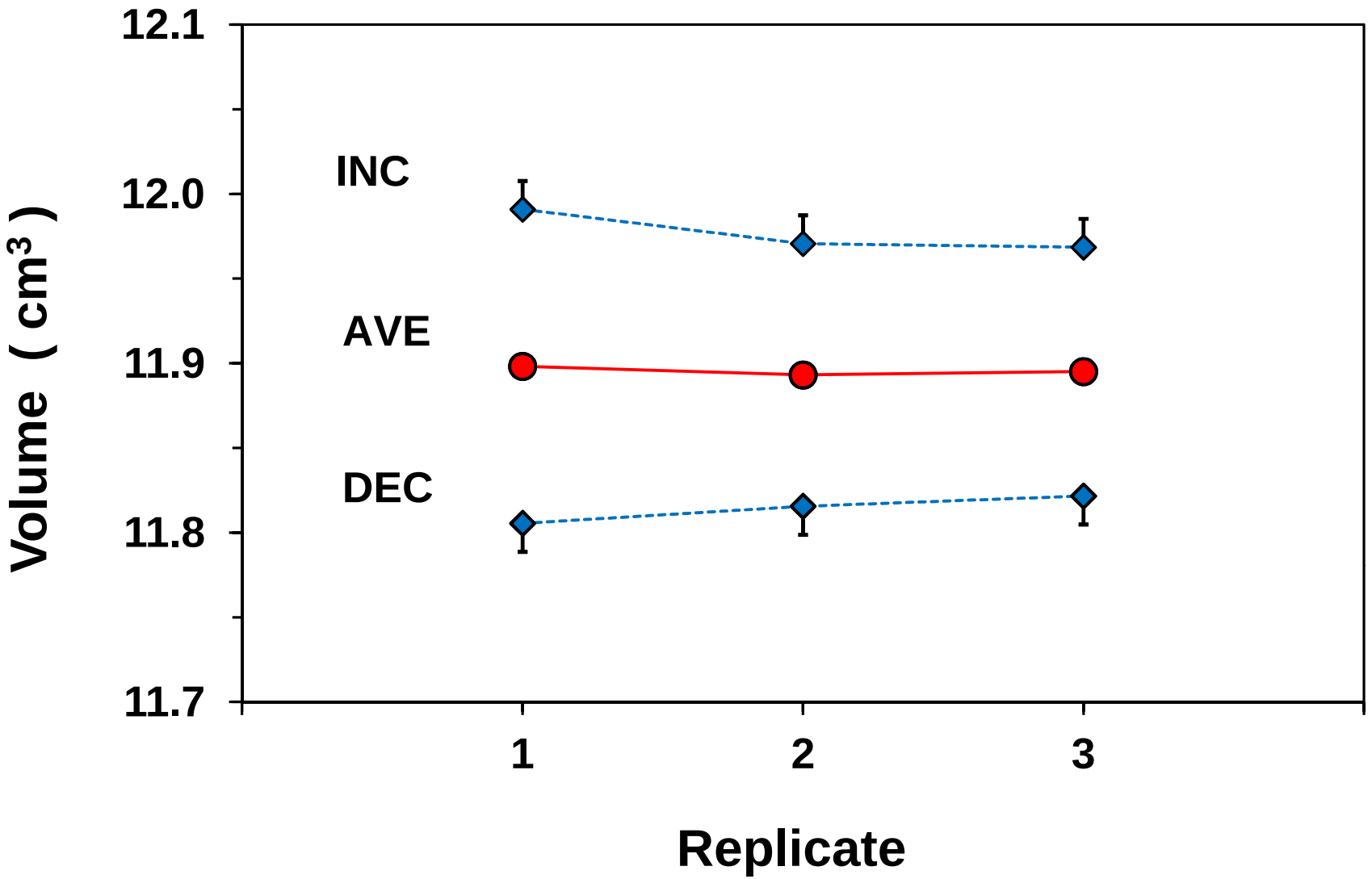
12.1
12.0
11.9
11.8
11.7
Volume (cm³)
INC
AVE
DEC
1
2
3
Replicate

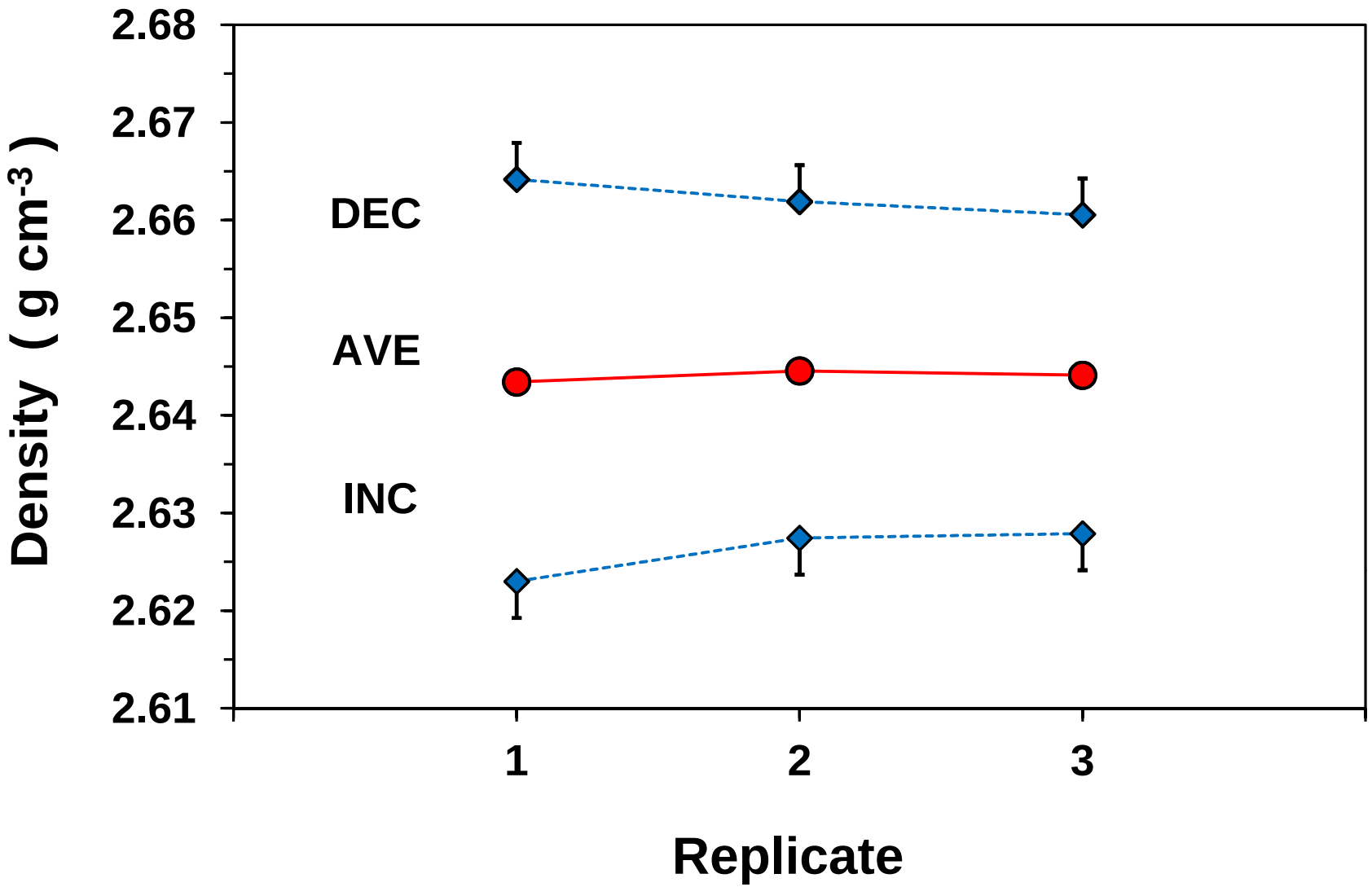
Density (g cm-3)
2.68
2.67
2.66
2.65
2.64
2.63
2.62
2.61
DEC
AVE
INC
1
2
3
Replicate

Vers. 2013 Hoja 1/1

GP - Calibración con cilíndros de aluminio

No tocar	
1	*1*
1	*2*
3	*1*
3	*2*
4	*1*
4	*2*
2	*1*
2	*2*
5	*1*
5	*2*

Vt [pendiente "m"] =	**25.5199**
Vc [intersecion ""b"] =	**47.8646**
Coeficiente de determinación [r2] =	**0.9999965**
Error típico para la estimación y [sey] =	**0.019**
Valor F observado [F] =	854464
Grados de libertad [df] =	3
Error típico de Vt [sem] =	**0.028**
Error típico de Vc [seb] =	**0.034**
Suma de regresión de cuadrados [ssreg] =	314.997
Suma residual de cuadrados [ssresid] =	0.001

CV [Vt] =	0.11%	**Ok**
CV [Vc] =	0.07%	**Ok**

				CENAM @ 26 °C	Promedio	Promedio
No.	Operator	#	Cylindre	Vs (cm3)	Tau [-]	Z * Dv [cm3]
1	**CP**	**Cal. 1**	**ALU 1**	**5.713**	**-1.65115**	**-0.0064**
2	**CP**	**Cal. 1**	**ALU 2**	**11.505**	**-1.42468**	**-0.0041**
3	**CP**	**Cal. 1**	**ALU 3**	**17.352**	**-1.19652**	**-0.0018**
4	**CP**	**Cal. 1**	**ALU 4**	**22.312**	**-1.00047**	**0.0001**
5	**CP**	**Cal. 1**	**ALU 5**	**28.372**	**-0.76400**	**0.0024**

Promedio	Promedio	Promedio	Promedio
Tau [-]	**V* [cm3]**	V* est [cm3]	**Résidual (%)**
-1.651	5.719	5.727	0.14
-1.425	11.509	11.507	-0.02
-1.197	17.354	17.329	-0.14
-1.000	22.312	22.333	0.09
-0.764	28.370	28.367	-0.01

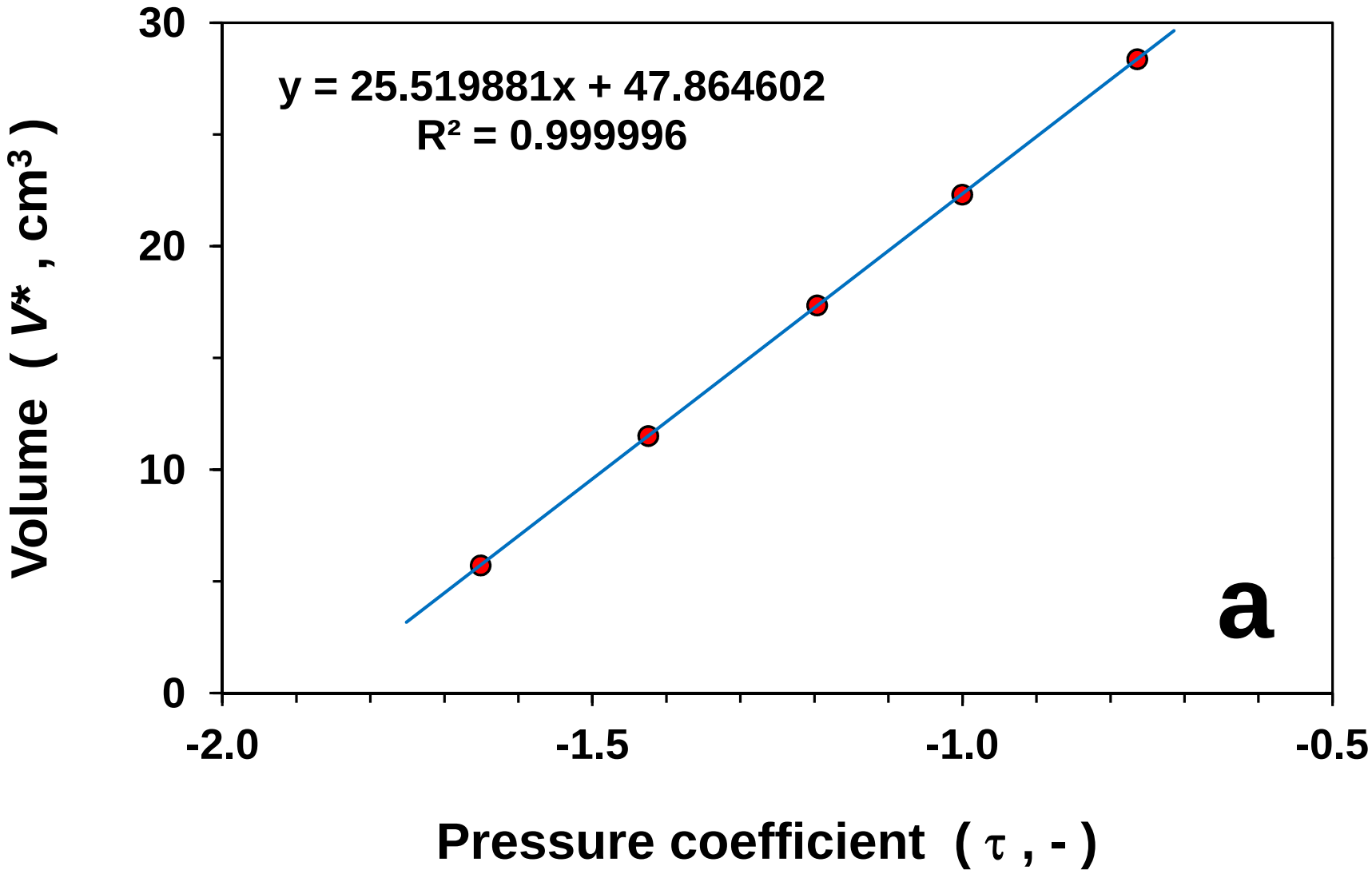
y = 25.519881x + 47.864602
R² = 0.999996
30
20
10
0
-2.0
-1.5
-1.0
-0.5
Volume (V* , cm3)
Pressure coefficient (τ , -)
a

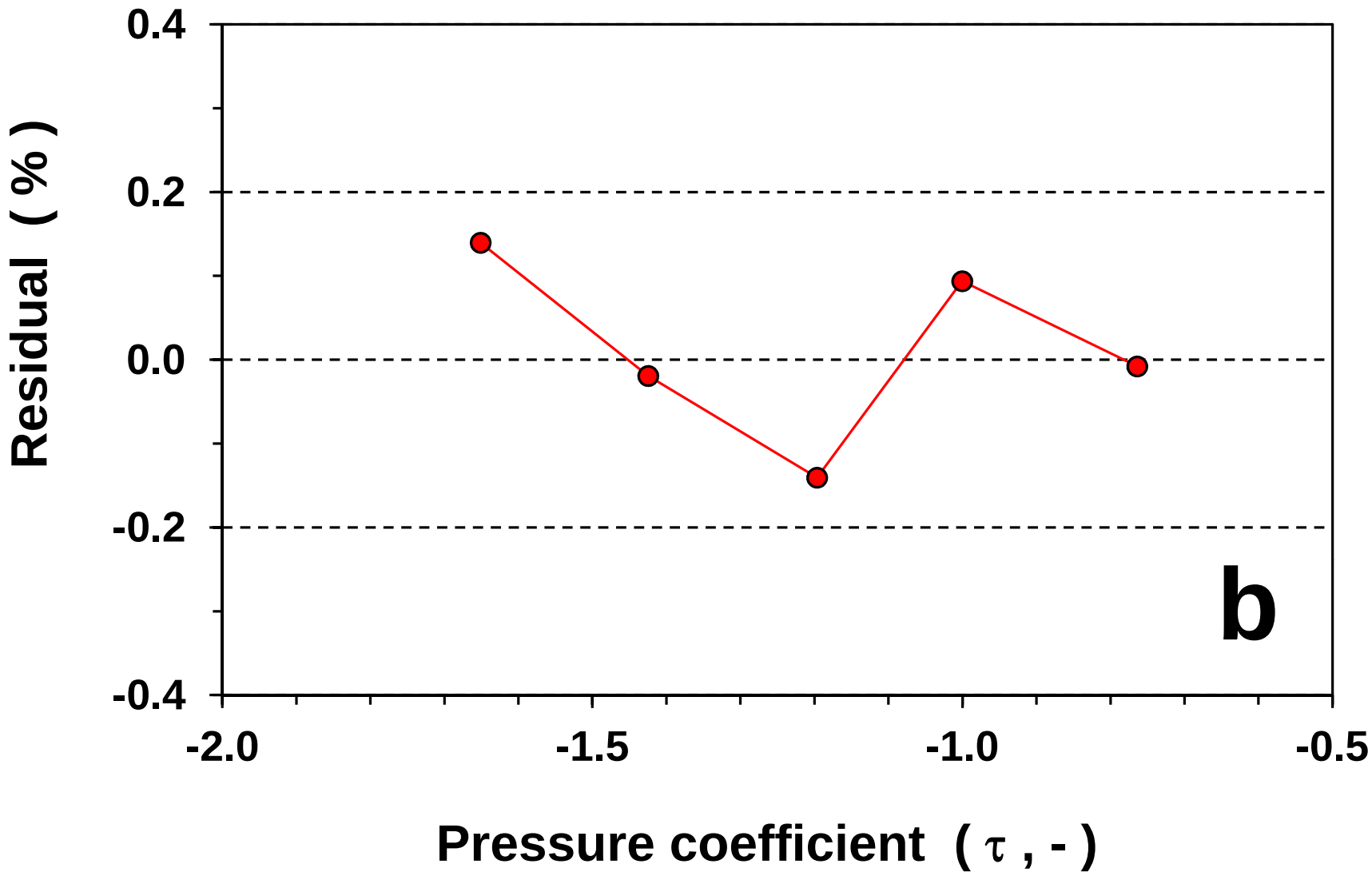
0.4
0.2
0.0
-0.2
-0.4
Residual (%)
-2.0
-1.5
-1.0
-0.5
Pressure coefficient (τ , -)
b

ANEXO (C)

FUGAS EN EL PICNÓMETRO

ANTES Y DESPUES DE LA REVISIÓN

FUGAS EN EL PICNOMETRO DE GAS

Fugas calculadas después de 12 horas de espera

ANTES DE LA REVISION (Feb. 2013)

Presion (kPa)	Fuga (Pa/s)
4	0.005
77	-0.008
131	-0.018
28	0.001
46	-0.003

DESPUES DE LA REVISION (Oct. 2013)

Presion (kPa)	Fuga (Pa/s)
2	0.003
25	0.001
50	0.001
80	-0.002
110	-0.005
130	-0.006

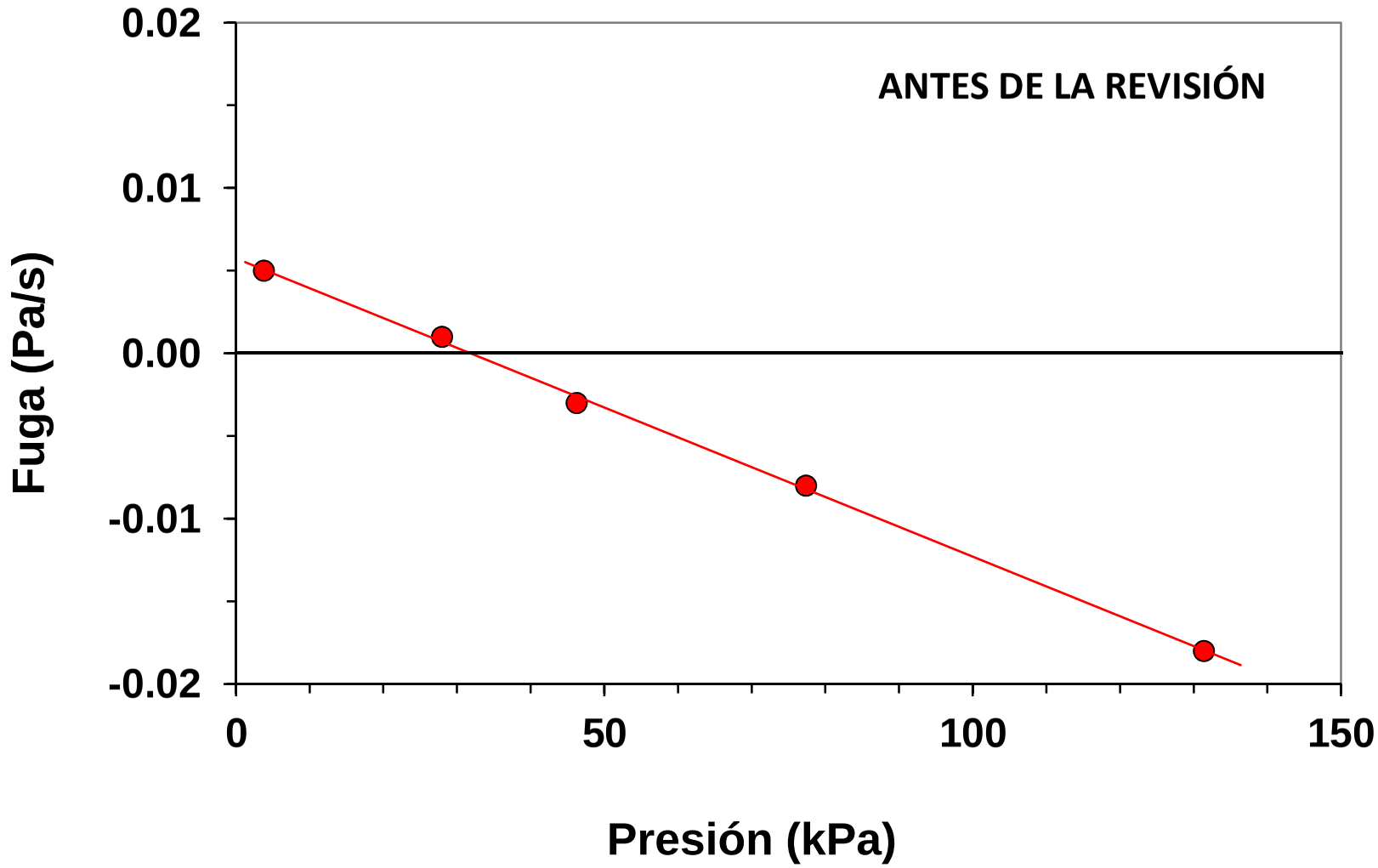
ANTES DE LA REVISIÓN
0.02
0.01
0.00
-0.01
-0.02
Fuga (Pa/s)
0
50
100
150
Presión (kPa)

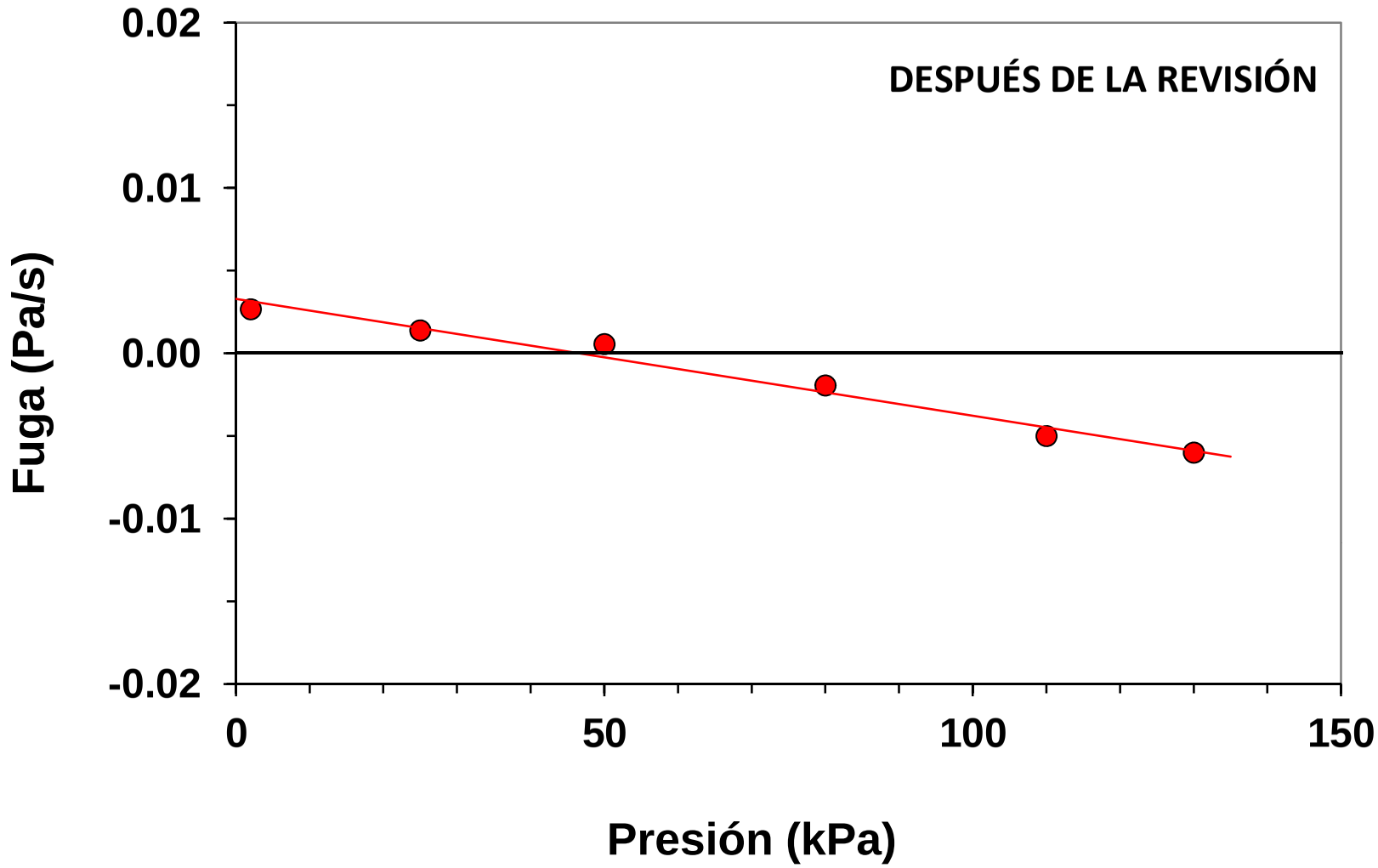
DESPUÉS DE LA REVISIÓN
0.02
0.01
0.00
-0.01
-0.02
Fuga (Pa/s)
0
50
100
150
Presión (kPa)

ANEXO (D)

CALIBRACIONES DEL PICNÓMETRO

Vers. 2013 Hoja 1/1

GP - Calibración con cilíndros de aluminio

No tocar !	
1	*1*
1	*2*
3	*1*
3	*2*
4	*1*
4	*2*
2	*1*
2	*2*
5	*1*
5	*2*

Vt [pendiente "m"] =	**25.5199**
Vc [intersecion ""b"] =	**47.8646**
Coeficiente de determinación [r2] =	**0.9999965**
Error típico para la estimación y [sey] =	**0.019**
Valor F observado [F] =	854464
Grados de libertad [df] =	3
Error típico de Vt [sem] =	**0.028**
Error típico de Vc [seb] =	**0.034**
Suma de regresión de cuadrados [ssreg] =	314.997
Suma residual de cuadrados [ssresid] =	0.001

CV [Vt] =	0.11%	**Ok**
CV [Vc] =	0.07%	**Ok**

				CENAM @ 26 °C	Promedio	Promedio
No.	Operator	#	Cylindre	Vs (cm3)	Tau [-]	Z * Dv [cm3]
1	**CP**	**Cal. 1**	**ALU 1**	**5.713**	**-1.65115**	**-0.0064**
2	**CP**	**Cal. 1**	**ALU 2**	**11.505**	**-1.42468**	**-0.0041**
3	**CP**	**Cal. 1**	**ALU 3**	**17.352**	**-1.19652**	**-0.0018**
4	**CP**	**Cal. 1**	**ALU 4**	**22.312**	**-1.00047**	**0.0001**
5	**CP**	**Cal. 1**	**ALU 5**	**28.372**	**-0.76400**	**0.0024**

Promedio	Promedio	Promedio	Promedio
Tau [-]	**V* [cm3]**	V* est [cm3]	**Résidual (%)**
-1.651	5.719	5.727	0.14
-1.425	11.509	11.507	-0.02
-1.197	17.354	17.329	-0.14
-1.000	22.312	22.333	0.09
-0.764	28.370	28.367	-0.01

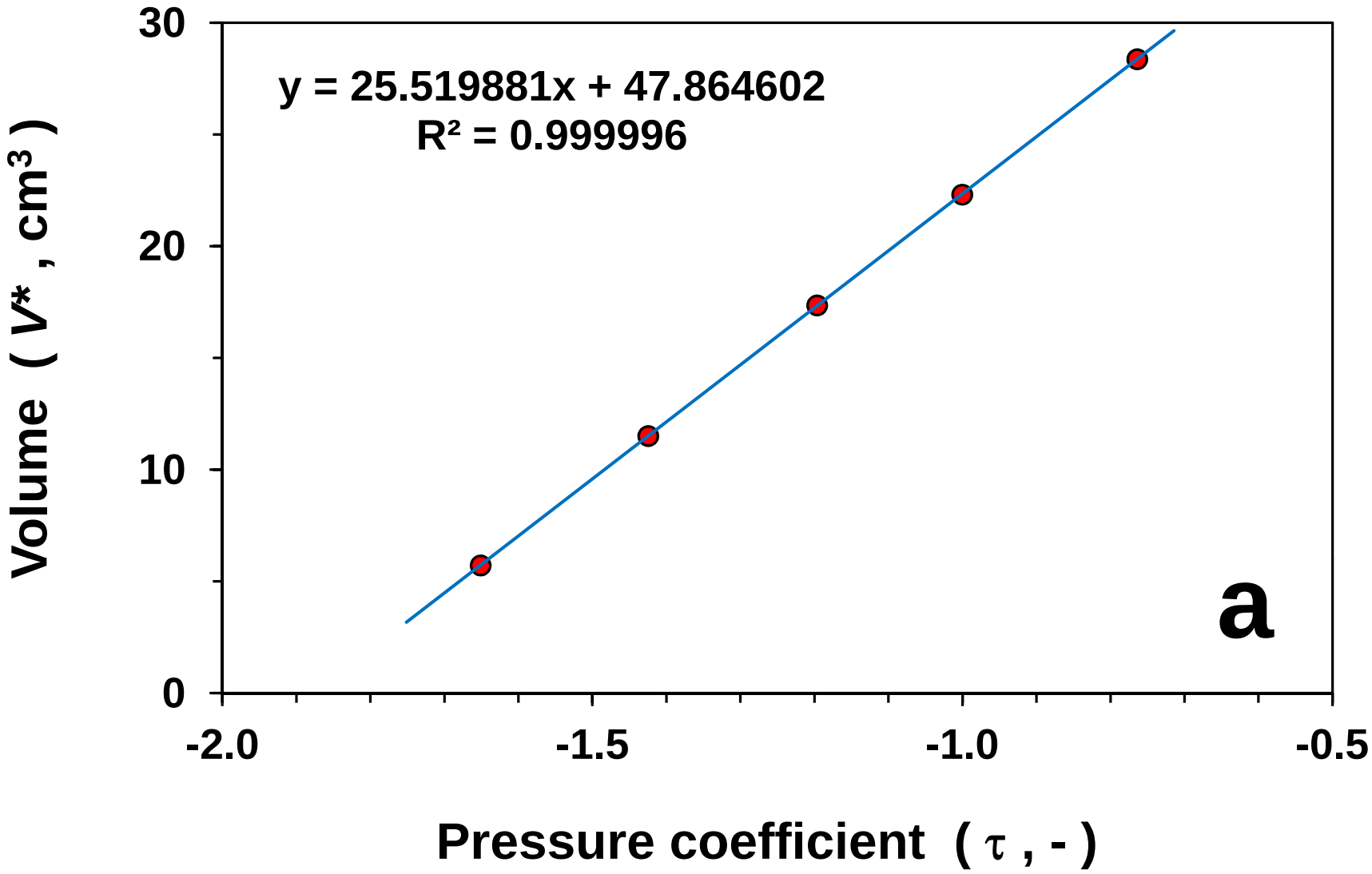
y = 25.519881x + 47.864602
R² = 0.999996
a
Volume (V* , cm3)
Pressure coefficient (τ , -)
30
20
10
0
-2.0
-1.5
-1.0
-0.5

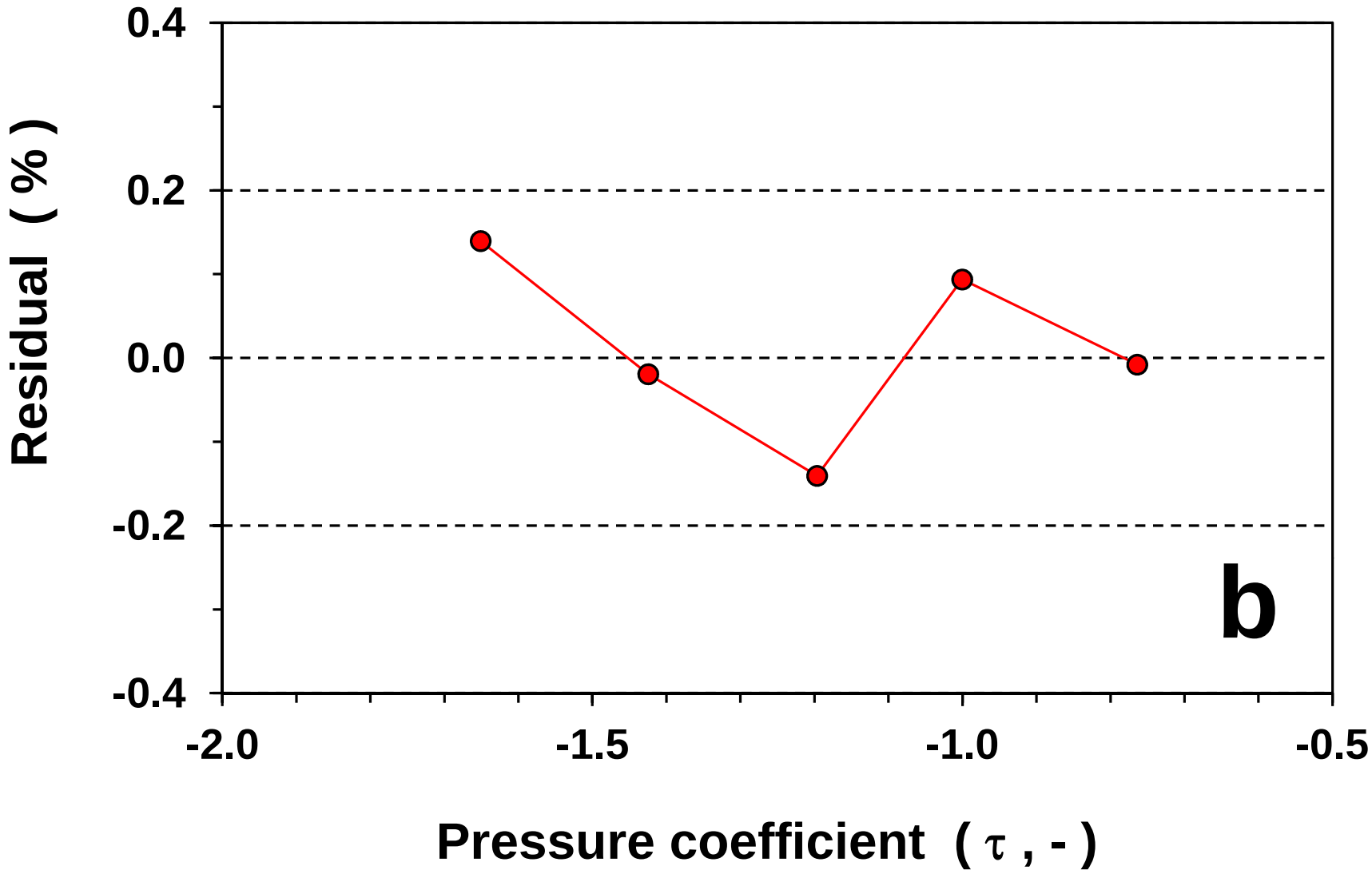
0.4
0.2
0.0
-0.2
-0.4
Residual (%)
-2.0
-1.5
-1.0
-0.5
Pressure coefficient (τ , -)
b

Vers. 2013 Hoja 1/1

GP - Calibración con cilíndros de aluminio

No tocar !	
1	*1*
1	*2*
3	*1*
3	*2*
4	*1*
4	*2*
2	*1*
2	*2*
5	*1*
5	*2*

Vt [pendiente "m"] =	**25.5408**
Vc [intersecion ""b"] =	**47.7627**
Coeficiente de determinación [r2] =	**0.9999954**
Error típico para la estimación y [sey] =	**0.022**
Valor F observado [F] =	654717
Grados de libertad [df] =	3
Error típico de Vt [sem] =	**0.032**
Error típico de Vc [seb] =	**0.039**
Suma de regresión de cuadrados [ssreg] =	314.999
Suma residual de cuadrados [ssresid] =	0.001

CV [Vt] =	0.12%	**Ok**
CV [Vc] =	0.08%	**Ok**

				CENAM @ 26 °C	Promedio	Promedio
No.	Operator	Date	Cylindre	Vs (cm3)	Tau [-]	Z * Dv [cm3]
1	**CP**	**Cal. 2**	**ALU 1**	**5.713**	**-1.64671**	**-0.0062**
2	**CP**	**Cal. 2**	**ALU 2**	**11.505**	**-1.41946**	**-0.0040**
3	**CP**	**Cal. 2**	**ALU 3**	**17.352**	**-1.18946**	**-0.0014**
4	**CP**	**Cal. 2**	**ALU 4**	**22.312**	**-0.99631**	**0.0001**
5	**CP**	**Cal. 2**	**ALU 5**	**28.372**	**-0.76001**	**0.0025**

Promedio	Promedio	Promedio	Promedio
Tau [-]	**V* [cm3]**	V* est [cm3]	**Résidual (%)**
-1.647	5.719	5.704	-0.26
-1.419	11.509	11.508	0.00
-1.189	17.353	17.383	0.17
-0.996	22.312	22.316	0.02
-0.760	28.370	28.351	-0.06

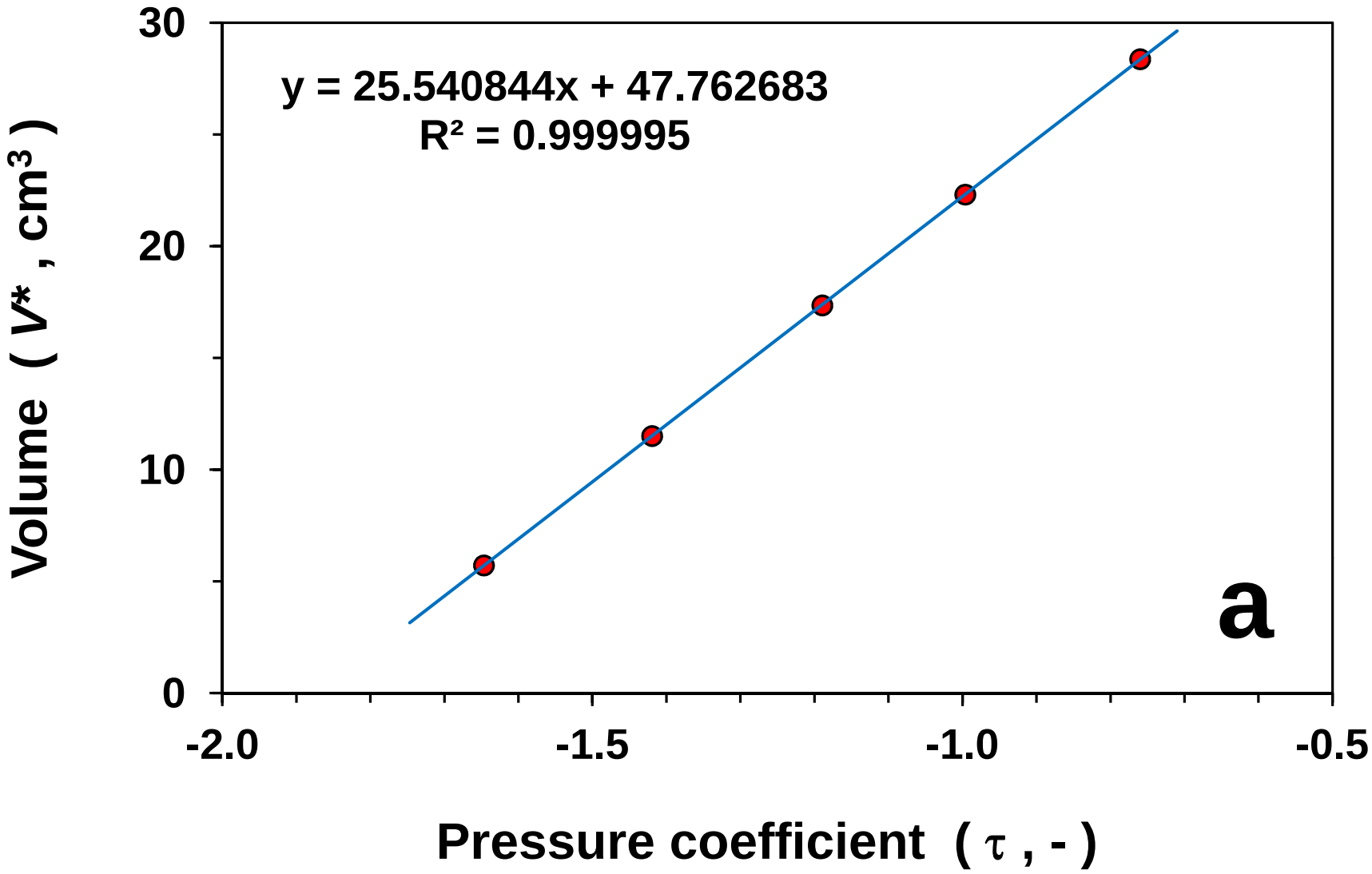
y = 25.540844x + 47.762683
R² = 0.999995
a
Volume (V* , cm3)
Pressure coefficient (τ , -)
30
20
10
0
-2.0
-1.5
-1.0
-0.5

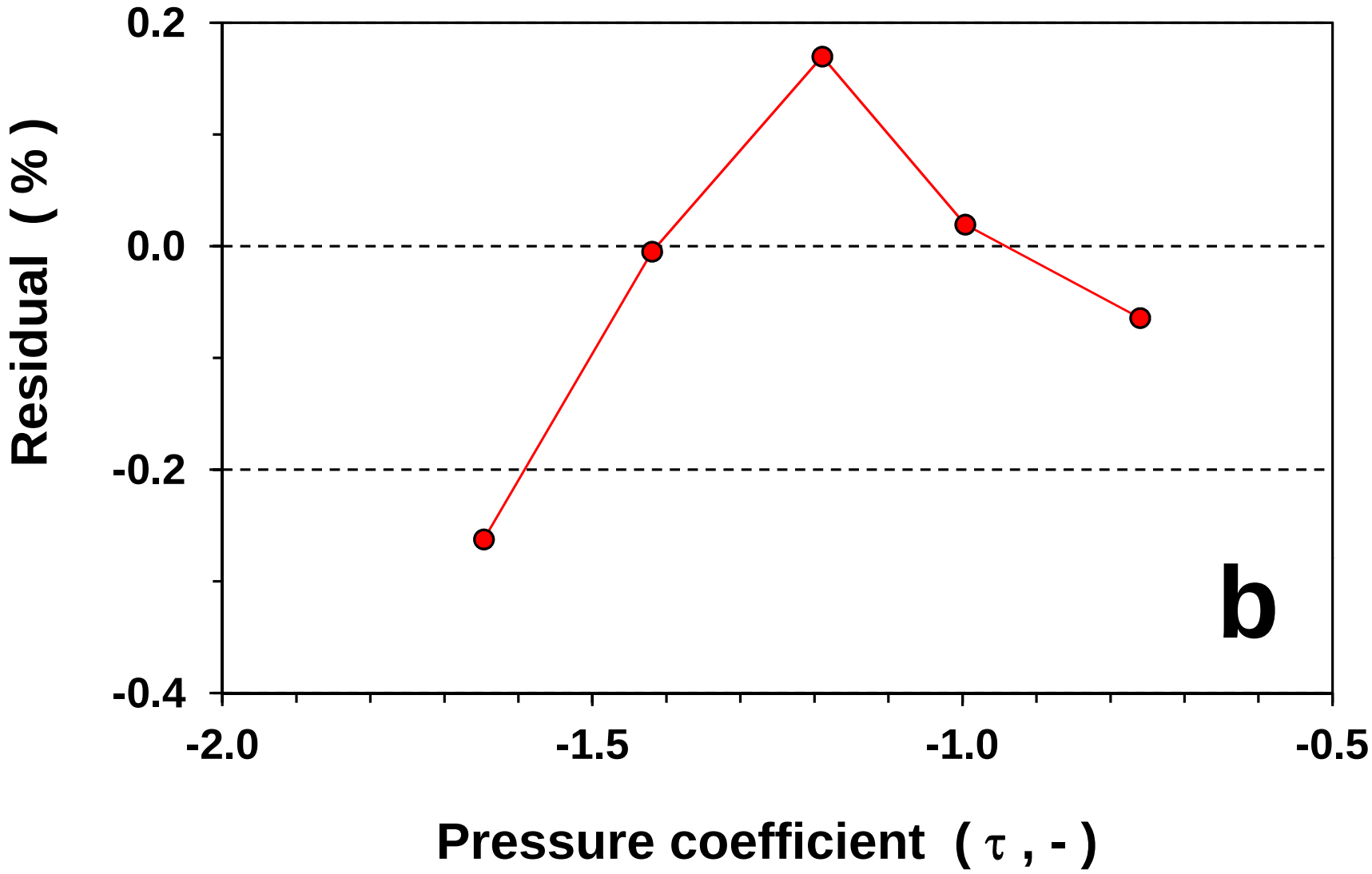
0.2
0.0
-0.2
-0.4
Residual (%)
-2.0
-1.5
-1.0
-0.5
Pressure coefficient (τ , -)
b

ANEXO (E)

CARACTERIZACIÓN DE MATERIALES

[GP] Descripción de la prueba

Serie de mediciones :	**1**	Lugar :	**LFS (IMTA)**
Fecha :	**Oct. 2013**	Hora :	**/**
Operador :	**CP**	Gas usado :	**Helio**

Temp. labo. (C) :	**22.0**	Temp. baño (C) :	**26.3**	Patm (kPa) :	**87**

(X)	Se sacan las muestras del horno (105 C) y se guardan en un desecador con vacio
( )	Las muestras estuvieron en el laboratorio (o sea, secadas "al aíre")

Comentario General	

Muestra no.	Probeta no.	Código	Material	Tamaño	Origen	Comentario
(a) INC	na	na	**Amatista**	na	na	na
(b) DEC	na	na	Amatista	na	na	na
(c) INC	na	na	Amatista	na	na	na
(d) DEC	na	na	Amatista	na	na	na
(e) INC	na	na	Amatista	na	na	na
(f) DEC	na	na	Amatista	na	na	na

[GP] Datos crudos

Serie :	1	Lugar :	LFS (IMTA)
Fecha :	Oct. 2013	Hora :	/

Muestra	Código	Hora	ti1 [s]	Pi1 [kPa]	ti2 [s]	Pi2 [kPa]	tj [s]	Pj [kPa]	tf1 [s]	Pf1 [kPa]	tf2 [s]	Pf2 [kPa]
(a) INC	na	09:30	**460**	**77.563**	**1210**	**77.568**	**2120**	**0.833**	**2250**	**45.662**	**3390**	**45.676**
(b) DEC	na	10:30	**450**	**1.164**	**1420**	**1.203**	**2340**	**77.469**	**2460**	**32.822**	**3550**	**32.841**
(c) INC	na	11:30	**70**	**76.744**	**1210**	**76.746**	**2190**	**0.834**	**2410**	**45.192**	**3360**	**45.207**
(d) DEC	na	12:30	**310**	**1.091**	**1450**	**1.129**	**2350**	**76.946**	**2520**	**32.563**	**3440**	**32.574**
(e) INC	na	15:15	**40**	**77.041**	**1390**	**77.035**	**2300**	**0.833**	**2420**	**45.356**	**3410**	**45.367**
(f) DEC	na	16:55	**330**	**0.878**	**1530**	**0.913**	**2360**	**76.814**	**2510**	**32.381**	**3540**	**32.391**

[GP] Estimación de Volumen

Serie :	1	Lugar :	LFS (IMTA)
Fecha :	Oct. 2013	Hora :	/

Calib del :	Cal. 1	Válvula
Vt [cm3] =	25.520	Dv [cm3]
Vc [cm3] =	47.866	0.020

Muestra	Código	origi [kPa]	slopi [kPa/s]	Ok ?	origf [kPa]	slopf [kPa/s]	Ok ?	Pi [kPa]	Pj [kPa]	Pf [kPa]	Tau [-]	V* [cm3]	Z * Dv [cm3]	V [cm3]	PROMEDIO V [cm3]
(a) INC	na	77.560	0.000007	-	45.634	0.000012	-	77.574	0.833	45.660	-1.4046	12.019	-0.029	11.991	11.898
(b) DEC	na	1.146	0.000040	-	32.779	0.000017	-	1.240	77.469	32.820	-1.4138	11.785	0.021	11.806	
(c) INC	na	76.744	0.000002	-	45.154	0.000016	-	76.748	0.834	45.189	-1.4054	11.999	-0.029	11.971	11.893
(d) DEC	na	1.081	0.000033	-	32.533	0.000012	-	1.159	76.946	32.561	-1.4134	11.795	0.021	11.816	
(e) INC	na	77.041	-0.000004	-	45.329	0.000011	-	77.031	0.833	45.355	-1.4055	11.997	-0.029	11.969	11.895
(f) DEC	na	0.868	0.000029	-	32.357	0.000010	-	0.937	76.814	32.380	-1.4132	11.801	0.021	11.822	

Media =	-1.4094	11.899	-0.0040	11.895	11.895
Std =	0.0046	0.116	0.0270	0.089	0.003
CV (%) =	-0.3235	0.978		0.752	0.022

[GP] Estimación de Densidad

Serie :	1	Lugar :	LFS (IMTA)
Fecha :	Oct. 2013	Hora :	/

Muestra	Código	M (g)	Probeta	Mp (g)	Vp (cm3)	Ms (g)	Vs (cm3)	Gs (g/cm3)
(a) INC	na	31.452	0	0.000	0.000	31.452	11.991	2.623
(b) DEC	na	31.452	0	0.000	0.000	31.452	11.806	2.664
(c) INC	na	31.452	0	0.000	0.000	31.452	11.971	2.627
(d) DEC	na	31.452	0	0.000	0.000	31.452	11.816	2.662
(e) INC	na	31.452	0	0.000	0.000	31.452	11.969	2.628
(f) DEC	na	31.452	0	0.000	0.000	31.452	11.822	2.661

Media =	2.644
Std =	0.020
CV (%) =	0.752

PROMEDIO	PROMEDIO
Vs (cm3)	Gs (g/cm3)
11.898	2.643
11.893	2.645
11.895	2.644

11.895	2.644
0.003	0.001
0.022	0.022

[GP] Síntesis

Serie :	1
Fecha :	Oct. 2013

Volumen (cm3)

INC	DEC	PROMEDIO	u[Vs] (cm3)
		11.895	0.017

Densidad (g/cm3)

INC	DEC	PROMEDIO	u[Gs] (g/cm3)
		2.644	0.004

Muestra	Código	Repetición	Vs (cm3)	Vs (cm3)	Vs (cm3)	u[Vs] (cm3)	Gs (g/cm3)	Gs (g/cm3)	Gs (g/cm3)	u[Gs] (g/cm3)
(a) INC	na	**1**	11.991	*11.806*	11.898	0.017	2.623	*2.664*	2.643	0.004
(b) DEC	na	*1*	*11.991*	11.806	*11.898*	0.017	*2.623*	2.664	*2.643*	0.004
(c) INC	na	**2**	11.971	*11.816*	11.893	0.017	2.627	*2.662*	2.645	0.004
(d) DEC	na	*2*	*11.971*	11.816	*11.893*	0.017	*2.627*	2.662	*2.645*	0.004
(e) INC	na	**3**	11.969	*11.822*	11.895	0.017	2.628	*2.661*	2.644	0.004
(f) DEC	na	*3*	*11.969*	11.822	*11.895*	0.017	*2.628*	2.661	*2.644*	0.004
		Media =	**11.977**	**11.814**	**11.895**		**2.626**	**2.662**	**2.644**	
		Std =	0.012	0.008	**0.003**		0.003	0.002	**0.001**	
		CV (%) =	0.103	0.069	**0.022**		0.103	0.069	**0.022**	

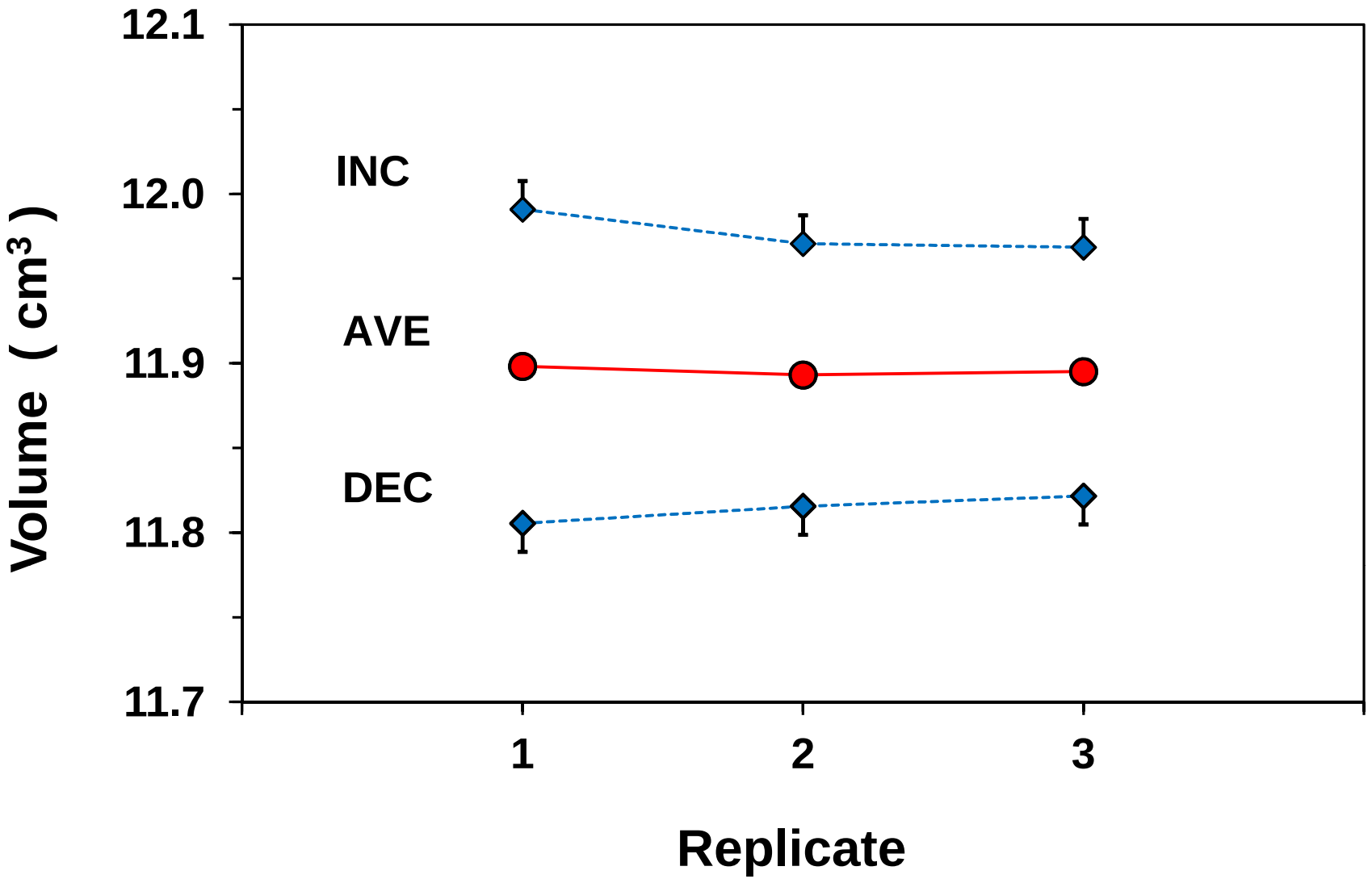
12.1
12.0
11.9
11.8
11.7
Volume (cm³)
INC
AVE
DEC
1
2
3
Replicate

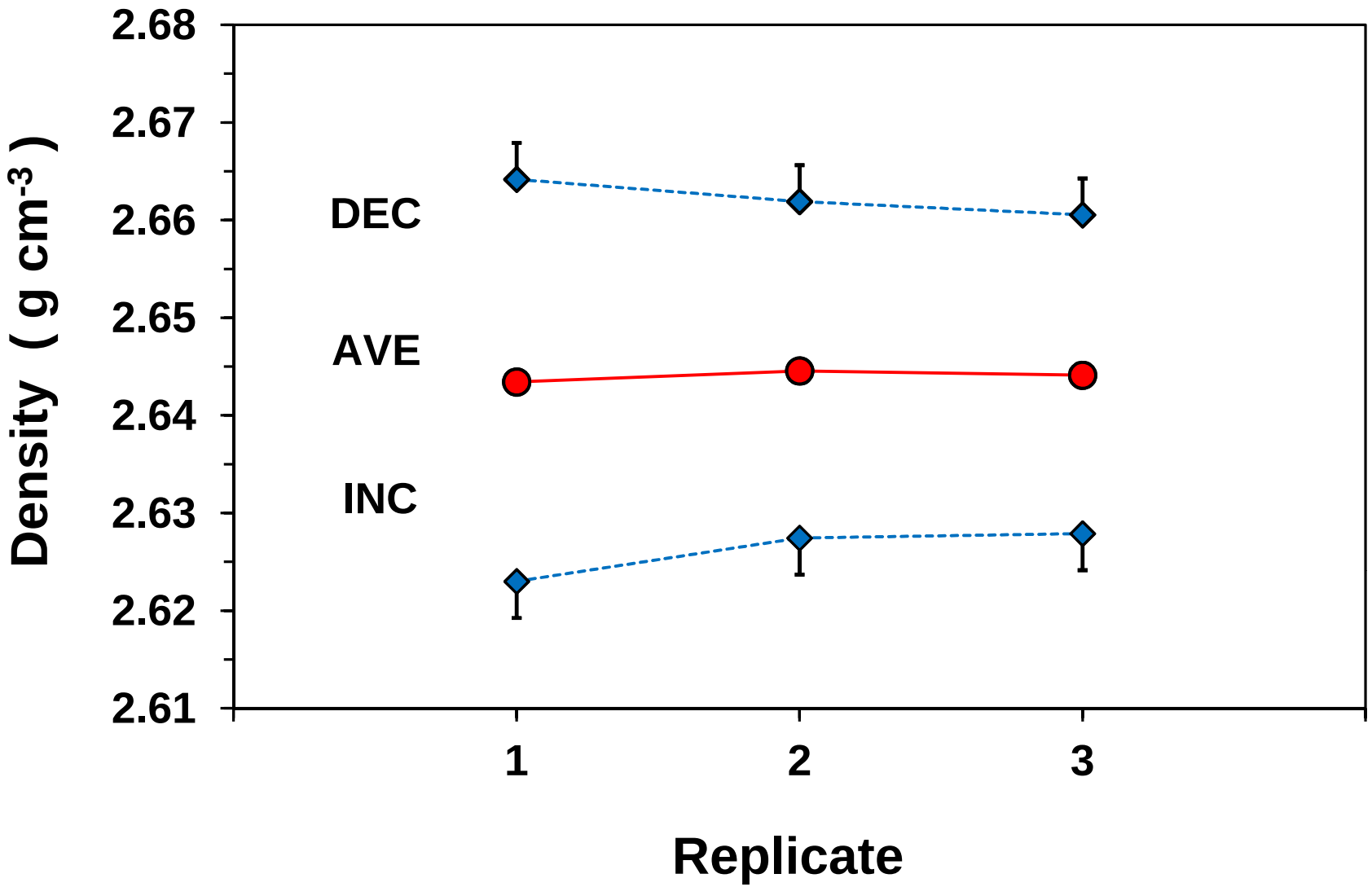
2.68
2.67
2.66
2.65
2.64
2.63
2.62
2.61
Density (g cm-3)
DEC
AVE
INC
1
2
3
Replicate

[GP] Descripción de la prueba

Serie de mediciones :	**1**	Lugar :	**LFS (IMTA)**
Fecha :	**Oct. 2013**	Hora :	**/**
Operador :	**CP**	Gas usado :	**Helio**

Temp. labo. (C) :	**22.0**	Temp. baño (C) :	**26.3**	Patm (kPa) :	**87**

(X)	Se sacan las muestras del horno (105 C) y se guardan en un desecador con vacio
( )	Las muestras estuvieron en el laboratorio (o sea, secadas "al aíre")

Comentario General	

Muestra no.	Probeta no.	Código	Material	Tamaño	Origen	Comentario
(a) INC	na	na	**Calcita**	na	na	na
(b) DEC	na	na	Calcita	na	na	na
(c) INC	na	na	Calcita	na	na	na
(d) DEC	na	na	Calcita	na	na	na
(e) INC	na	na	Calcita	na	na	na
(f) DEC	na	na	Calcita	na	na	na

[GP] Datos crudos

Serie :	1	Lugar :	LFS (IMTA)
Fecha :	Oct. 2013	Hora :	/

Muestra	Código	Hora	ti1 [s]	Pi1 [kPa]	ti2 [s]	Pi2 [kPa]	tj [s]	Pj [kPa]	tf1 [s]	Pf1 [kPa]	tf2 [s]	Pf2 [kPa]
(a) INC	na	08:45	310	76.916	1240	76.907	2150	0.827	2370	43.610	3350	43.620
(b) DEC	na	09:45	330	1.159	1250	1.197	2170	76.983	2420	34.278	3430	34.300
(c) INC	na	10:45	260	76.637	1260	76.642	2280	0.834	2460	43.460	3560	43.469
(d) DEC	na	11:45	380	1.000	1220	1.031	2160	76.731	2320	34.061	3460	34.070
(e) INC	na	12:45	50	76.853	1480	76.866	2380	0.833	2560	43.599	3810	43.613
(f) DEC	na	13:45	290	1.071	1230	1.100	2160	76.639	2340	34.066	3450	34.080

[GP] Estimación de Volumen

Serie :	1	Lugar :	LFS (IMTA)
Fecha :	Oct. 2013	Hora :	/

Calib del :	Cal. 1	Válvula
Vt [cm3] =	25.520	Dv [cm3]
Vc [cm3] =	47.866	0.020

Muestra	Código	origi [kPa]	slopi [kPa/s]	Ok ?	origf [kPa]	slopf [kPa/s]	Ok ?	Pi [kPa]	Pj [kPa]	Pf [kPa]	Tau [-]	V* [cm3]	Z * Dv [cm3]	V [cm3]	PROMEDIO V [cm3]
(a) INC	na	76.919	-0.000010	-	43.586	0.000010	-	76.898	0.827	43.608	-1.2851	15.071	-0.026	15.045	14.970
(b) DEC	na	1.145	0.000041	-	34.225	0.000022	-	1.235	76.983	34.273	-1.2928	14.874	0.021	14.895	
(c) INC	na	76.636	0.000005	-	43.440	0.000008	-	76.647	0.834	43.459	-1.2843	15.090	-0.026	15.064	14.973
(d) DEC	na	0.986	0.000037	-	34.043	0.000008	-	1.066	76.731	34.060	-1.2933	14.861	0.021	14.882	
(e) INC	na	76.853	0.000009	-	43.570	0.000011	-	76.874	0.833	43.597	-1.2851	15.071	-0.026	15.045	14.971
(f) DEC	na	1.062	0.000031	-	34.036	0.000013	-	1.129	76.639	34.064	-1.2927	14.876	0.021	14.897	

Media =	-1.2889	14.974	-0.0028	14.971	14.971
Std =	0.0045	0.114	0.0257	0.088	0.002
CV (%) =	-0.3455	0.759		0.588	0.011

[GP] Estimación de Densidad

Serie :	1	Lugar :	LFS (IMTA)
Fecha :	Oct. 2013	Hora :	/

Muestra	Código	M (g)	Probeta	Mp (g)	Vp (cm3)	Ms (g)	Vs (cm3)	Gs (g/cm3)
(a) INC	na	40.502	0	0.000	0.000	40.502	15.045	2.692
(b) DEC	na	40.502	0	0.000	0.000	40.502	14.895	2.719
(c) INC	na	40.502	0	0.000	0.000	40.502	15.064	2.689
(d) DEC	na	40.502	0	0.000	0.000	40.502	14.882	2.722
(e) INC	na	40.502	0	0.000	0.000	40.502	15.045	2.692
(f) DEC	na	40.502	0	0.000	0.000	40.502	14.897	2.719

Media =	2.705
Std =	0.016
CV (%) =	0.588

PROMEDIO	PROMEDIO
Vs (cm3)	Gs (g/cm3)
14.970	2.706
14.973	2.705
14.971	2.705

14.971	2.705
0.002	0.000
0.011	0.011

[GP] Síntesis

Serie :	1
Fecha :	Oct. 2013

Volumen (cm3)

INC	DEC	PROMEDIO	u[Vs] (cm3)
		14.971	0.021

Densidad (g/cm3)

INC	DEC	PROMEDIO	u[Gs] (g/cm3)
		2.705	0.004

Muestra	Código	Repetición	Vs (cm3)	Vs (cm3)	Vs (cm3)	u[Vs] (cm3)	Gs (g/cm3)	Gs (g/cm3)	Gs (g/cm3)	u[Gs] (g/cm3)
(a) INC	na	1	15.045	*14.895*	14.970	0.021	2.692	*2.719*	2.706	0.004
(b) DEC	na	*1*	*15.045*	14.895	*14.970*	0.021	*2.692*	2.719	*2.706*	0.004
(c) INC	na	2	15.064	*14.882*	14.973	0.021	2.689	*2.722*	2.705	0.004
(d) DEC	na	*2*	*15.064*	14.882	*14.973*	0.021	*2.689*	2.722	*2.705*	0.004
(e) INC	na	3	15.045	*14.897*	14.971	0.021	2.692	*2.719*	2.705	0.004
(f) DEC	na	*3*	*15.045*	14.897	*14.971*	0.021	*2.692*	2.719	*2.705*	0.004
		Media =	**15.051**	**14.891**	**14.971**		**2.691**	**2.720**	**2.705**	
		Std =	0.011	0.008	**0.002**		0.002	0.002	**0.000**	
		CV (%) =	0.075	0.056	**0.011**		0.075	0.056	**0.011**	

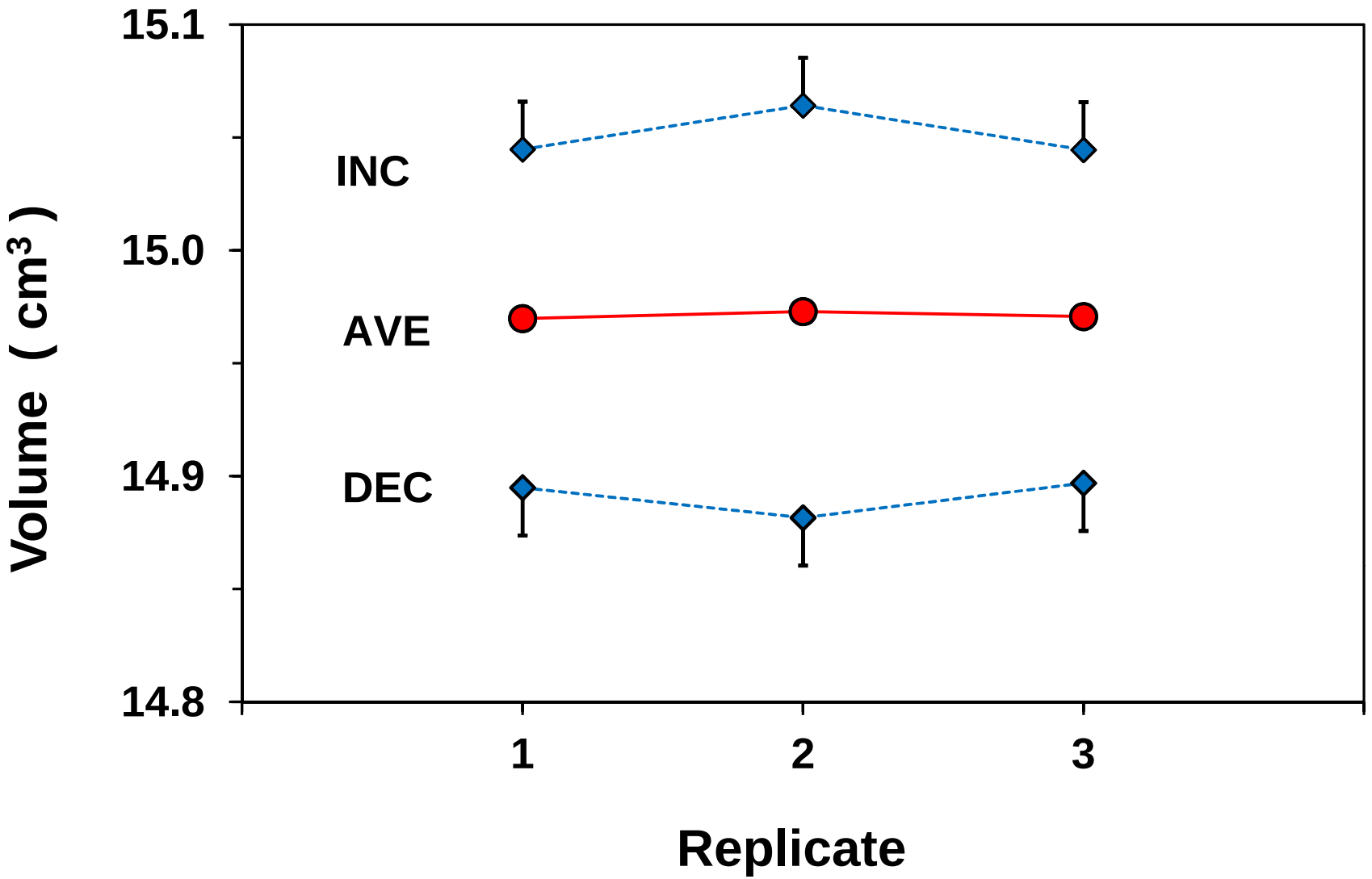
15.1
15.0
14.9
14.8
Volume (cm³)
INC
AVE
DEC
1
2
3
Replicate

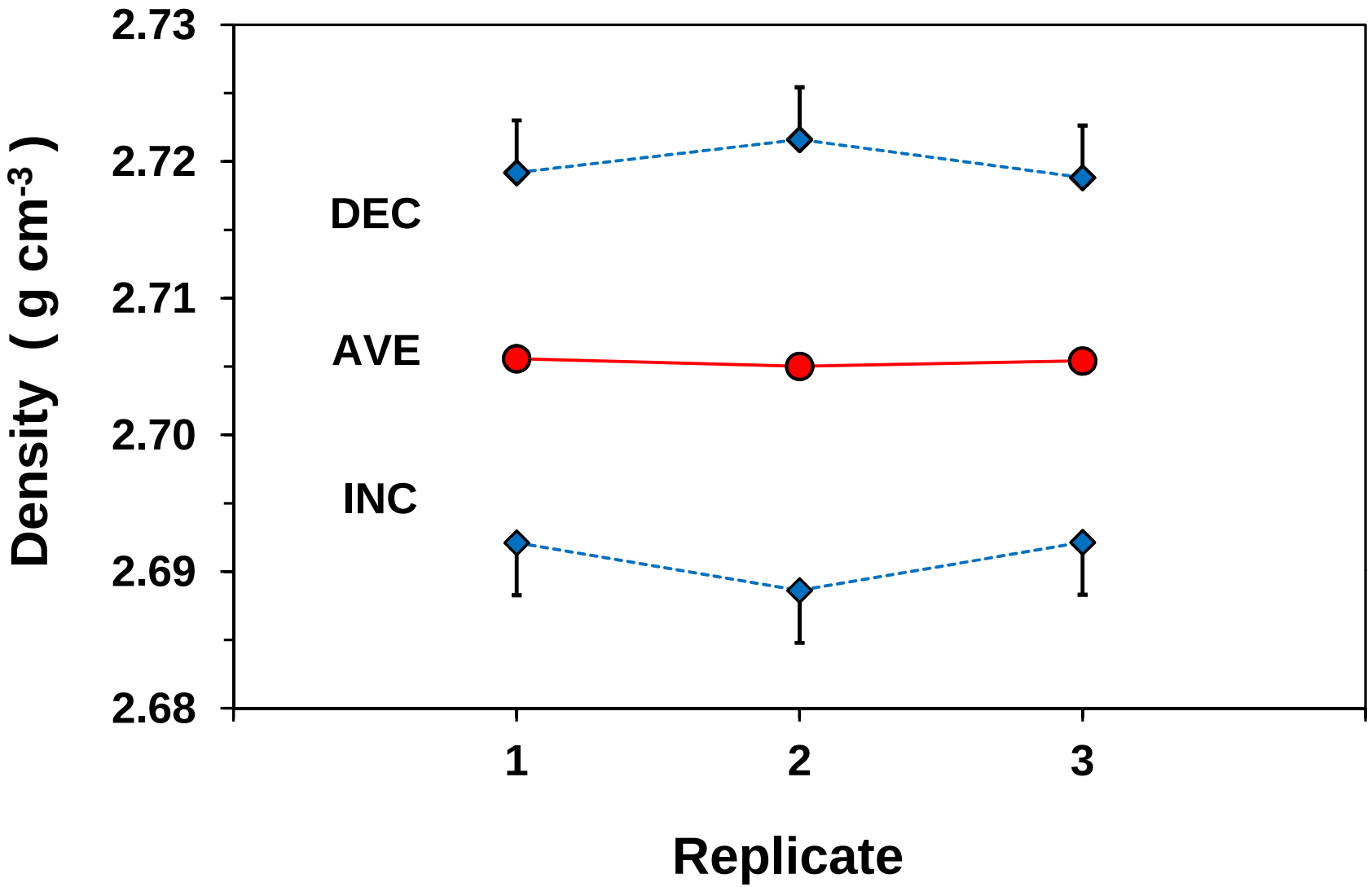
2.73
2.72
2.71
2.70
2.69
2.68
Density (g cm-3)
DEC
AVE
INC
1
2
3
Replicate

[GP] Descripción de la prueba

Serie de mediciones :	**1**	Lugar :	**LFS (IMTA)**
Fecha :	**Oct. 2013**	Hora :	**/**
Operador :	**CP**	Gas usado :	**Helio**

Temp. labo. (C) :	**22.0**	Temp. baño (C) :	**26.3**	Patm (kPa) :	**87**

(X)	Se sacan las muestras del horno (105 C) y se guardan en un desecador con vacio
( )	Las muestras estuvieron en el laboratorio (o sea, secadas "al aíre")

Comentario General	

Muestra no.	Probeta no.	Código	Material	Tamaño	Origen	Comentario
(a) INC	na	na	**NaCl**	na	Baker	na
(b) Dec	na	na	NaCl	na	Baker	na
(c) Inc	na	na	NaCl	na	Baker	na
(d) Dec	na	na	NaCl	na	Baker	na
(e) Inc	na	na	NaCl	na	Baker	na
(f) Dec	na	na	NaCl	na	Baker	na

[GP] Datos crudos

Serie :	1	Lugar :	LFS (IMTA)
Fecha :	Oct. 2013	Hora :	/

Muestra	Código	Hora	ti1 [s]	Pi1 [kPa]	ti2 [s]	Pi2 [kPa]	tj [s]	Pj [kPa]	tf1 [s]	Pf1 [kPa]	tf2 [s]	Pf2 [kPa]
(a) INC	na	09:30	770	76.554	1580	76.564	2990	0.631	3190	36.545	3610	36.556
(b) Dec	na	10:30	730	0.908	1330	0.950	2180	75.736	2620	40.286	3600	40.294
(c) Inc	na	11:40	180	75.465	1250	75.564	2220	0.635	2660	36.019	3610	36.035
(d) Dec	na	12:40:00	460	0.747	1220	0.801	2150	75.515	3780	40.122	6980	40.152
(e) Inc	na	13:50	480	75.379	1140	75.376	2140	0.624	2450	35.969	3140	35.978
(f) Dec	na	14:50	630	0.700	1340	0.741	2190	75.192	2450	39.904	3610	39.914

[GP] Estimación de Volumen

Serie :	1	Lugar :	LFS (IMTA)
Fecha :	Oct. 2013	Hora :	/

Calib del :	Cal. 1	Válvula
Vt [cm3] =	25.520	Dv [cm3]
Vc [cm3] =	47.866	0.020

Muestra	Código	origi [kPa]	slopi [kPa/s]	Ok ?	origf [kPa]	slopf [kPa/s]	Ok ?	Pi [kPa]	Pj [kPa]	Pf [kPa]	Tau [-]	V* [cm3]	Z * Dv [cm3]	V [cm3]	PROMEDIO V [cm3]
(a) INC	na	76.544	0.000012	-	36.461	0.000026	-	76.581	0.631	36.540	-0.8968	24.980	-0.018	24.962	24.905
(b) Dec	na	0.857	0.000070	-	40.265	0.000008	-	1.010	75.736	40.282	-0.9027	24.828	0.021	24.848	
(c) Inc	na	75.448	0.000093	-	35.974	0.000017	-	75.654	0.635	36.012	-0.8924	25.092	-0.018	25.074	24.966
(d) Dec	na	0.714	0.000071	-	40.087	0.000009	-	0.867	75.515	40.107	-0.9024	24.838	0.020	24.858	
(e) Inc	na	75.381	-0.000005	-	35.937	0.000013	-	75.371	0.624	35.965	-0.8968	24.979	-0.018	24.961	24.910
(f) Dec	na	0.664	0.000058	-	39.883	0.000009	-	0.790	75.192	39.902	-0.9023	24.840	0.020	24.860	

Media =	-0.8989	24.926	0.0011	24.927	24.927
Std =	0.0042	0.108	0.0212	0.089	0.034
CV (%) =	-0.4702	0.433		0.356	0.136

[GP] Estimación de Densidad

Serie :	1	Lugar :	LFS (IMTA)
Fecha :	Oct. 2013	Hora :	/

Muestra	Código	M (g)	Probeta	Mp (g)	Vp (cm3)	Ms (g)	SAMPLE Vs (cm3)	SAMPLE Gs (g/cm3)
(a) INC	na	53.367	0	0.000	0.000	53.367	24.962	2.138
(b) Dec	na	53.367	0	0.000	0.000	53.367	24.848	2.148
(c) Inc	na	53.367	0	0.000	0.000	53.367	25.074	2.128
(d) Dec	na	53.367	0	0.000	0.000	53.367	24.858	2.147
(e) Inc	na	53.367	0	0.000	0.000	53.367	24.961	2.138
(f) Dec	na	53.367	0	0.000	0.000	53.367	24.860	2.147

	SAMPLE Vs (cm3)	SAMPLE Gs (g/cm3)
Media =	24.927	2.141
Std =	0.089	0.008
CV (%) =	0.356	0.355

SAMPLE PROMEDIO Vs (cm3)	SAMPLE PROMEDIO Gs (g/cm3)
24.905	2.143
24.966	2.138
24.910	2.142
24.927	2.141
0.034	0.003
0.136	0.135

[GP] Síntesis

Volumen (cm3)

Densidad (g/cm3)

Serie :	1
Fecha :	Oct. 2013

INC	DEC	PROMEDIO	u[Vs] (cm3)
		24.927	0.035

INC	DEC	PROMEDIO	u[Gs] (g/cm3)
		2.141	0.003

Muestra	Código	Repetición	Vs (cm3)	Vs (cm3)	Vs (cm3)	u[Vs] (cm3)	Gs (g/cm3)	Gs (g/cm3)	Gs (g/cm3)	u[Gs] (g/cm3)
(a) INC	na	1	24.962	*24.848*	24.905	0.035	2.138	*2.148*	2.143	0.003
(b) Dec	na	*1*	*24.962*	24.848	*24.905*	0.035	*2.138*	2.148	*2.143*	0.003
(c) Inc	na	2	25.074	*24.858*	24.966	0.035	2.128	*2.147*	2.138	0.003
(d) Dec	na	*2*	*25.074*	24.858	*24.966*	0.035	*2.128*	2.147	*2.138*	0.003
(e) Inc	na	3	24.961	*24.860*	24.910	0.035	2.138	*2.147*	2.142	0.003
(f) Dec	na	*3*	*24.961*	24.860	*24.910*	0.035	*2.138*	2.147	*2.142*	0.003
		Media =	**24.999**	**24.856**	**24.927**		**2.135**	**2.147**	**2.141**	
		Std =	0.065	0.006	**0.034**		0.006	0.001	**0.003**	
		CV (%) =	0.260	0.025	**0.136**		0.260	0.025	**0.135**	

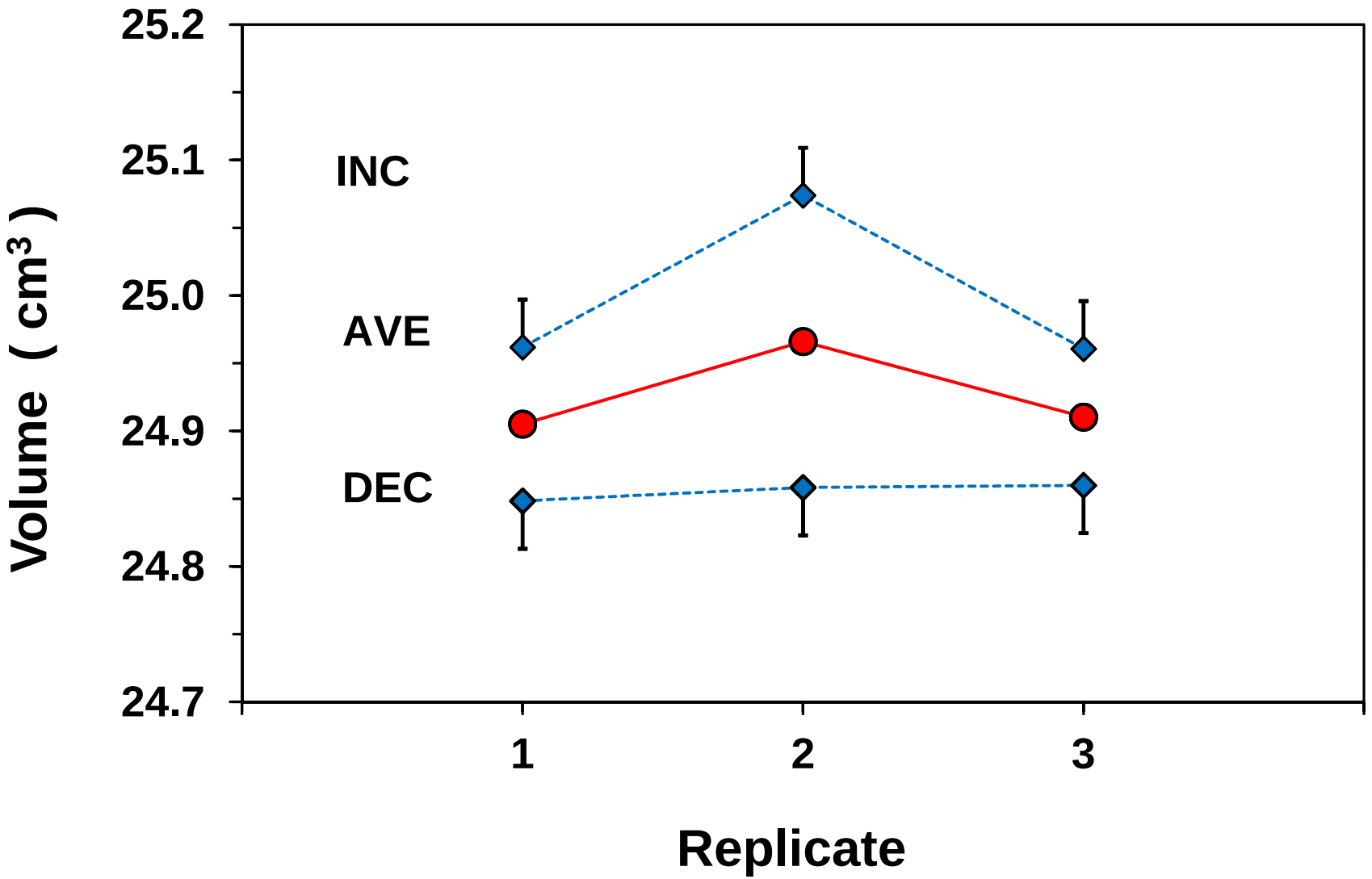
25.2
25.1
25.0
24.9
24.8
24.7
Volume (cm³)
INC
AVE
DEC
1
2
3
Replicate

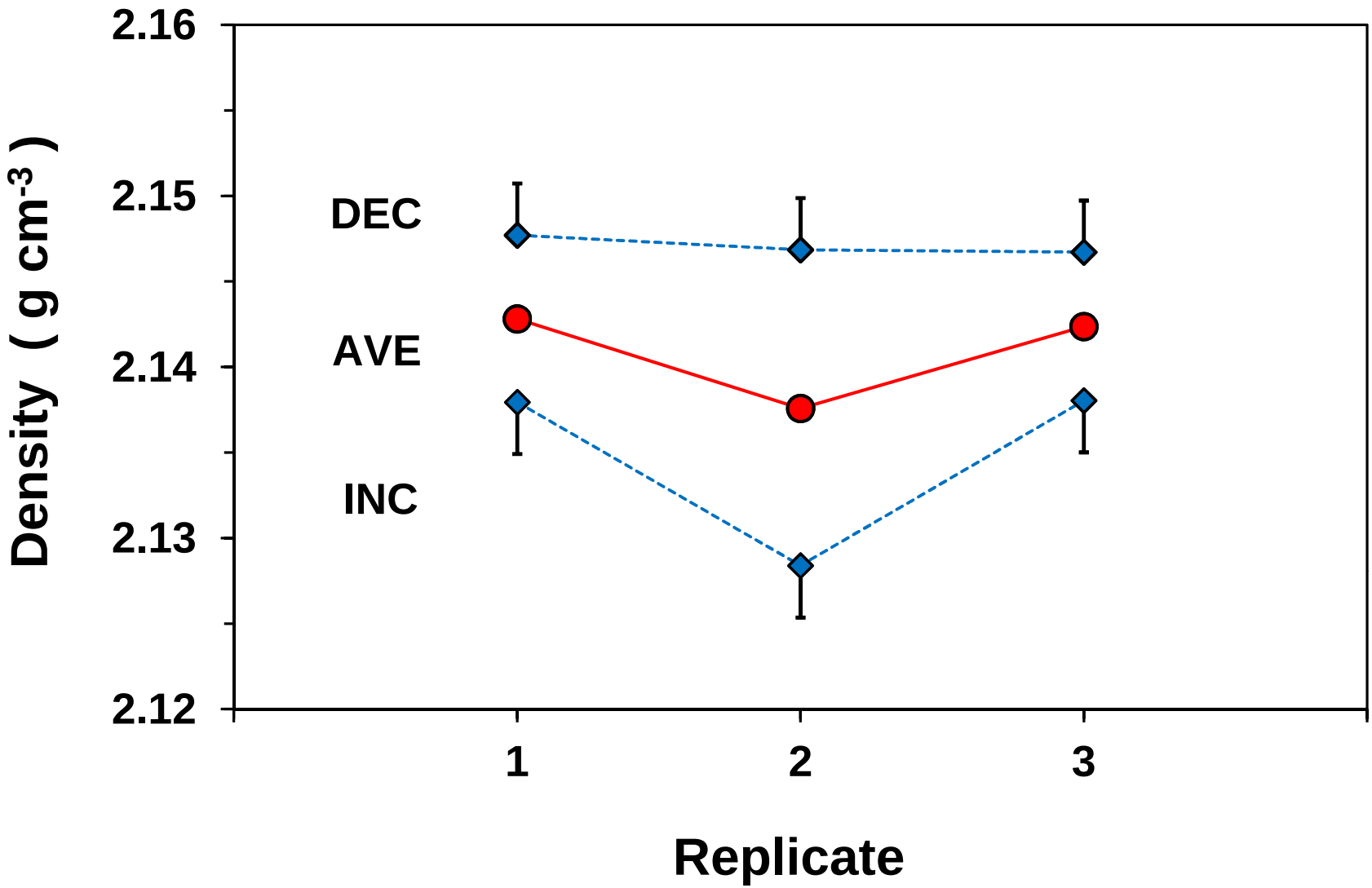
2.16
2.15
2.14
2.13
2.12
Density (g cm-3)
DEC
AVE
INC
1
2
3
Replicate

[GP] Descripción de la prueba

Serie de mediciones :	**1**	Lugar :	**LFS (IMTA)**
Fecha :	**Oct. 2013**	Hora :	**/**
Operador :	**CP**	Gas usado :	**Helio**

Temp. labo. (C) :	**21.0**	Temp. baño (C) :	**26.00**	Patm (kPa) :	**86.6**

(X)	Se sacan las muestras del horno (105 C) y se guardan en un desecador con vacio
	Las muestras estuvieron en el laboratorio (o sea, secadas "al aíre")

Comentario General	

Muestra no.	Probeta no.	Código	Material	Tamaño	Origen	Comentario
(a) Inc	**0**		**KCl**		**Baker**	
(b) Dec	0	0	KCl	0	Baker	0
(c) Inc	0	0	KCl	0	Baker	0
(d) Dec	0	0	KCl	0	Baker	0
(e) Inc	0	0	KCl	0	Baker	0
(f) Dec	0	0	KCl	0	Baker	0

[GP] Datos crudos

Serie :	1	Lugar :	LFS (IMTA)
Fecha :	Oct. 2013	Hora :	/

Muestra	Código	Hora	ti1 [s]	Pi1 [kPa]	ti2 [s]	Pi2 [kPa]	tj [s]	Pj [kPa]	tf1 [s]	Pf1 [kPa]	tf2 [s]	Pf2 [kPa]
(a) Inc	0	09:30	**270**	**77.101**	**1260**	**77.075**	**2180**	**0.645**	**2480**	**39.687**	**3460**	**39.697**
(b) Dec	0	10:30	**570**	**0.752**	**1220**	**0.800**	**2210**	**76.466**	**2490**	**37.744**	**3390**	**37.754**
(c) Inc	0	11:40	**500**	**76.498**	**1230**	**76.499**	**2280**	**0.628**	**2470**	**39.357**	**3450**	**39.371**
(d) Dec	0	12:40:00	**600**	**0.799**	**1190**	**0.833**	**2220**	**76.269**	**2520**	**37.681**	**3270**	**37.689**
(e) Inc	0	13:50	**460**	**76.394**	**1230**	**76.391**	**2140**	**0.624**	**2350**	**39.294**	**3420**	**39.308**
(f) Dec	0	14:50	**690**	**0.704**	**1260**	**0.730**	**2150**	**76.176**	**2410**	**37.576**	**3500**	**37.587**

[GP] Estimación de Volumen

Serie :	1	Lugar :	LFS (IMTA)
Fecha :	Oct. 2013	Hora :	/

Calib del :	Cal. 1	Válvula
Vt [cm3] =	25.520	Dv [cm3]
Vc [cm3] =	47.866	0.020

Muestra	Código	origi [kPa]	slopi [kPa/s]	Ok ?	origf [kPa]	slopf [kPa/s]	Ok ?	Pi [kPa]	Pj [kPa]	Pf [kPa]	Tau [-]	V* [cm3]	Z * Dv [cm3]	V [cm3]	V [cm3]
(a) Inc	0	77.108	-0.000026	-	39.662	0.000010	-	77.051	0.645	39.684	-1.0447	21.204	-0.021	21.183	21.132
(b) Dec	0	0.710	0.000074	-	37.716	0.000011	-	0.873	76.466	37.741	-1.0504	21.060	0.020	21.081	
(c) Inc	0	76.497	0.000001	-	39.322	0.000014	-	76.500	0.628	39.354	-1.0425	21.260	-0.021	21.239	21.177
(d) Dec	0	0.764	0.000058	-	37.654	0.000011	-	0.892	76.269	37.678	-1.0491	21.093	0.020	21.114	
(e) Inc	0	76.396	-0.000004	-	39.263	0.000013	-	76.387	0.624	39.291	-1.0424	21.265	-0.021	21.244	21.181
(f) Dec	0	0.673	0.000046	-	37.552	0.000010	-	0.771	76.176	37.573	-1.0489	21.098	0.020	21.118	

Media =	-1.0463	21.164	-0.0004	21.163	21.163
Std =	0.0036	0.091	0.0228	0.069	0.027
CV (%) =	-0.3402	0.429		0.327	0.129

PROMEDIO

[GP] Estimación de Densidad

Serie :	1	Lugar :	LFS (IMTA)
Fecha :	Oct. 2013	Hora :	/

Muestra	Código	M (g)	Probeta	Mp (g)	Vp (cm3)	Ms (g)	SAMPLE Vs (cm3)	SAMPLE Gs (g/cm3)
(a) Inc	0	41.249	0	0.000	0.000	41.249	21.183	1.947
(b) Dec	0	41.249	0	0.000	0.000	41.249	21.081	1.957
(c) Inc	0	41.249	0	0.000	0.000	41.249	21.239	1.942
(d) Dec	0	41.249	0	0.000	0.000	41.249	21.114	1.954
(e) Inc	0	41.249	0	0.000	0.000	41.249	21.244	1.942
(f) Dec	0	41.249	0	0.000	0.000	41.249	21.118	1.953
Media =							21.163	1.949
Std =							0.069	0.006
CV (%) =							0.327	0.327

SAMPLE PROMEDIO Vs (cm3)	SAMPLE PROMEDIO Gs (g/cm3)
21.132	1.952
21.177	1.948
21.181	1.947
21.163	1.949
0.027	0.003
0.129	0.129

[GP] Síntesis

Serie :	1
Fecha :	Oct. 2013

Volumen (cm3)

INC	DEC	PROMEDIO	u[Vs] (cm3)
		21.163	0.030

Densidad (g/cm3)

INC	DEC	PROMEDIO	u[Gs] (g/cm3)
		1.949	0.003

Muestra	Código	Repetición	Vs (cm3)	Vs (cm3)	Vs (cm3)	u[Vs] (cm3)	Gs (g/cm3)	Gs (g/cm3)	Gs (g/cm3)	u[Gs] (g/cm3)
(a) Inc	0	**1**	21.183	*21.081*	21.132	0.030	1.947	*1.957*	1.952	0.003
(b) Dec	0	*1*	*21.183*	21.081	*21.132*	0.030	*1.947*	1.957	*1.952*	0.003
(c) Inc	0	**2**	21.239	*21.114*	21.177	0.030	1.942	*1.954*	1.948	0.003
(d) Dec	0	*2*	*21.239*	21.114	*21.177*	0.030	*1.942*	1.954	*1.948*	0.003
(e) Inc	0	**3**	21.244	*21.118*	21.181	0.030	1.942	*1.953*	1.947	0.003
(f) Dec	0	*3*	*21.244*	21.118	*21.181*	0.030	*1.942*	1.953	*1.947*	0.003
		Media =	**21.222**	**21.104**	**21.163**		**1.944**	**1.955**	**1.949**	
		Std =	0.034	0.020	**0.027**		0.003	0.002	**0.003**	
		CV (%) =	0.160	0.097	**0.129**		0.161	0.097	**0.129**	

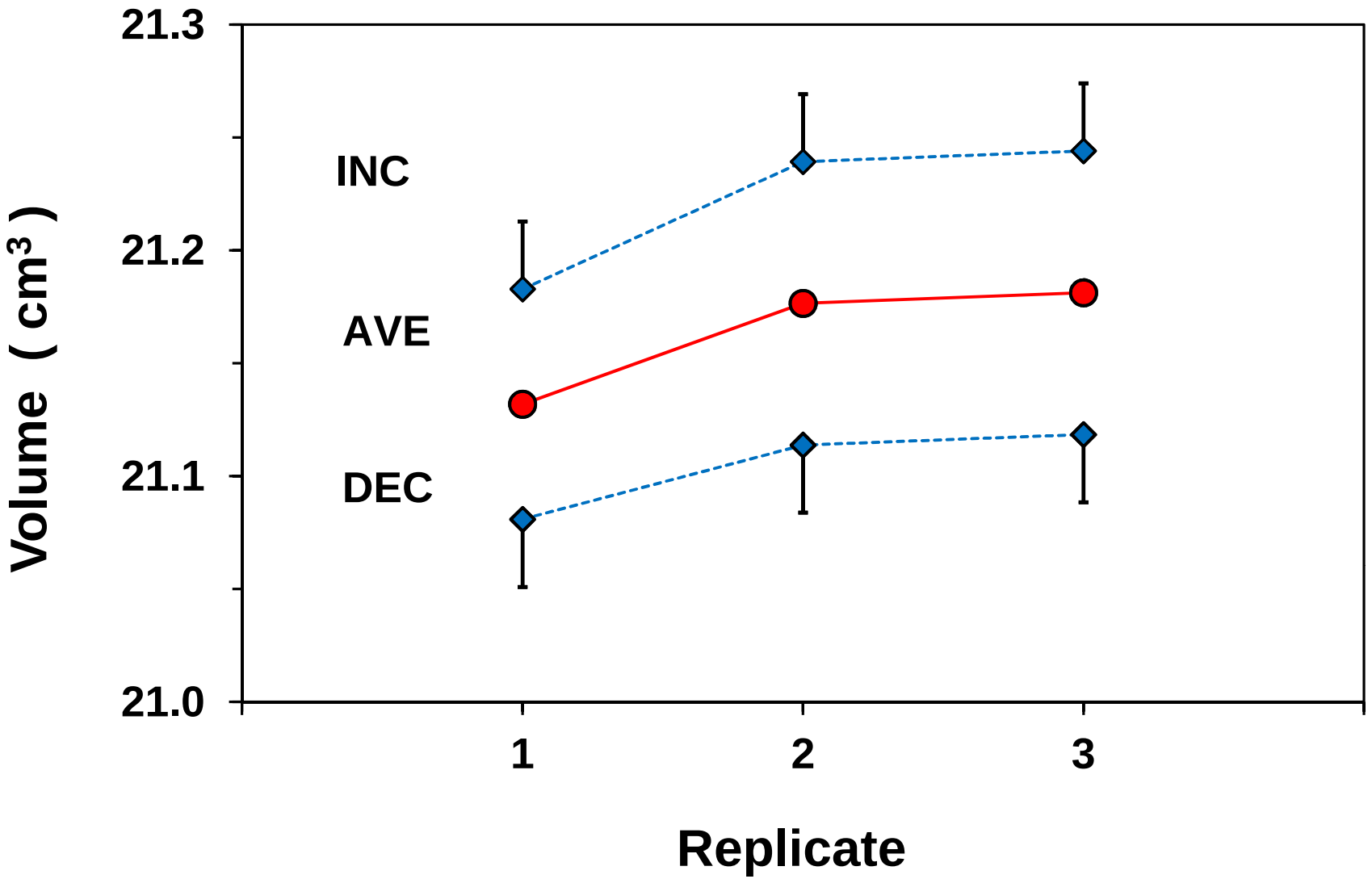
21.3
21.2
21.1
21.0
Volume (cm³)
INC
AVE
DEC
1
2
3
Replicate

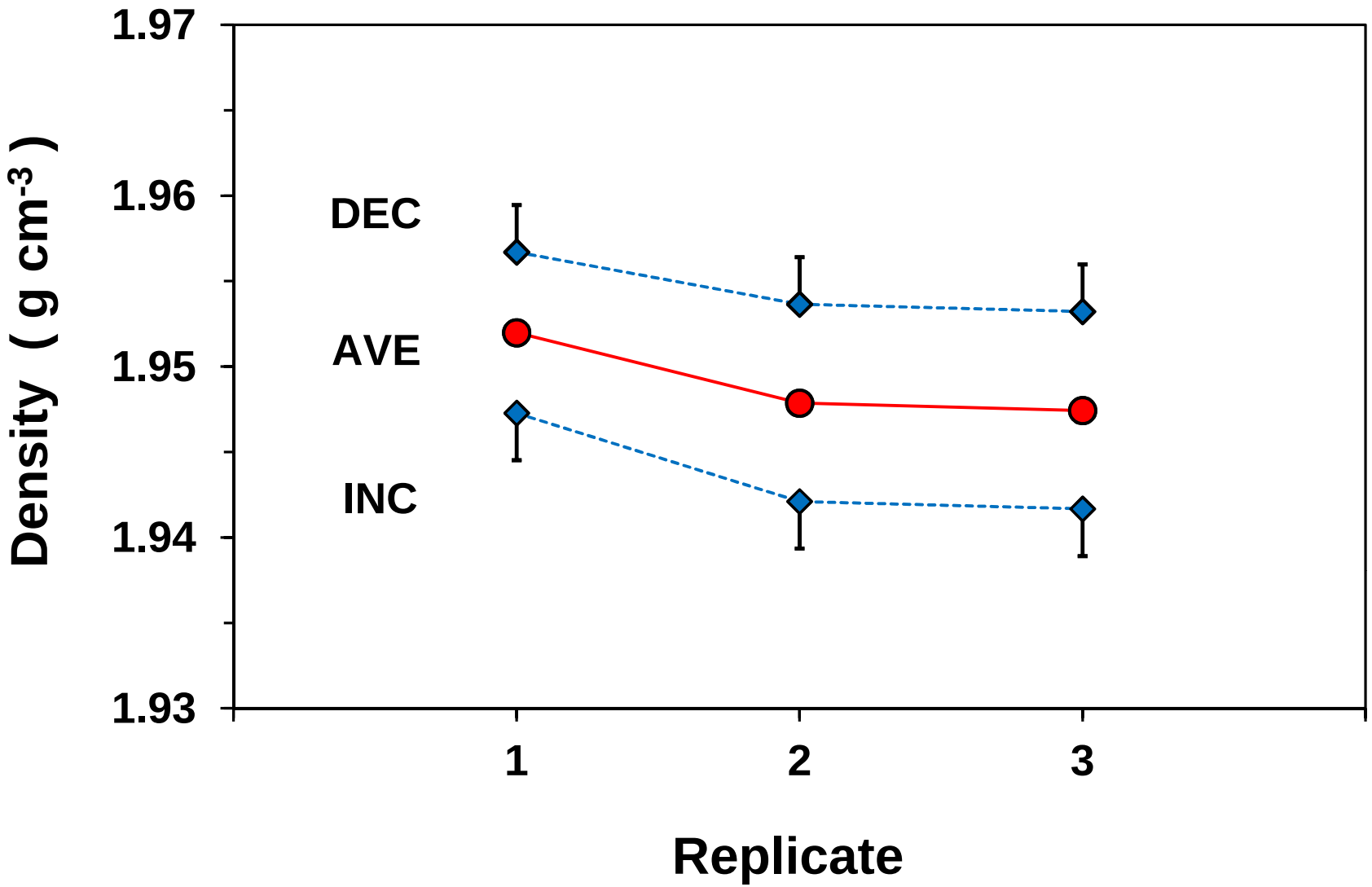
1.97
1.96
1.95
1.94
1.93
Density (g cm-3)
DEC
AVE
INC
1
2
3
Replicate